Copyright is owned by the Author of the thesis. Permission is given for a copy to be downloaded by an individual for the purpose of research and private study only. The thesis may not be reproduced elsewhere without the permission of the Author.

ROADS

First class
Second class
Unsealed road
Vehicle track
Foot track
Road Surface: sealed / metalled / unmetalled
National State Highway
Provincial State Highway
Tunnel
Bridge, two lane
Bridge, one lane
Footbridge

WATER FEATURES

Coastal rocks
Sand and mud
Sand
Shingle
Swamp
Dam, waterfall
Cold spring; hot spring
Watercourse; drain
Stream disappearing into ground

RELIEF FEATURES

Index contours
Intermediate contours
Supplementary contour
Depression contours
Shallow depressions
Trig station beaconed; unbeaconed
Elevation in metres ·130 △130m
Cliff, terrace
Rock outcrop
Stopbank
Cutting
Embankment
Sandhills
Subsidence

RAILWAYS

Double or multiple track
Single track
Station
Railway yard
Level crossing
Road over railway
Railway over road
Tramway

VEGETATION FEATURES

Native forest
Exotic forest
Scrub
Scattered scrub
Shelter belt
Trees
Orchard
Mangroves
Burnt and fallen timber

MISCELLANEOUS

Residential area
Large buildings
Building
Homestead
Church
Cemetery
Historic sites:
Monument
Pa site or stronghold
Maori Pa
Redoubt
Wind machine (windmill, windpump)
Lighthouse; beacon
Wreck
Fence (selection only)
Power line on pylons (at least pylons in built areas only)
Power line on poles
Telephone line
Masts: radio, T.V.; microwave
Mine: underground; opencast
Cave
Buried gas pipeline

The representation on this map of a road or track does not necessarily indicate a public right of way

MAGNETIC NORTH on this map is 21½°(382 mils) EAST of GRID NORTH during 1988 increasing at the rate of approx. ½° (9 mils) over 6 years.

GRID NORTH — G–M Angle — MAG. NORTH

TO GIVE A GRID REFERENCE ON THIS MAP
(To nearest 100 metres)

Disregard the smaller figures of corner grid numbers. They are for finding full coordinates.

SAMPLE POINT ▲ Huiarangi

East		North	
Locate first VERTICAL grid line to LEFT of point and read figures labelling the line in either the top or bottom margin or across the centre of the map.	16	Locate first HORIZONTAL grid line BELOW point and read figures labelling the line in either the left or right margin or up the centre of the map.	29
Estimate tenths eastward from grid line to point.	2	Estimate tenths northward from grid line to point	4
	162		294

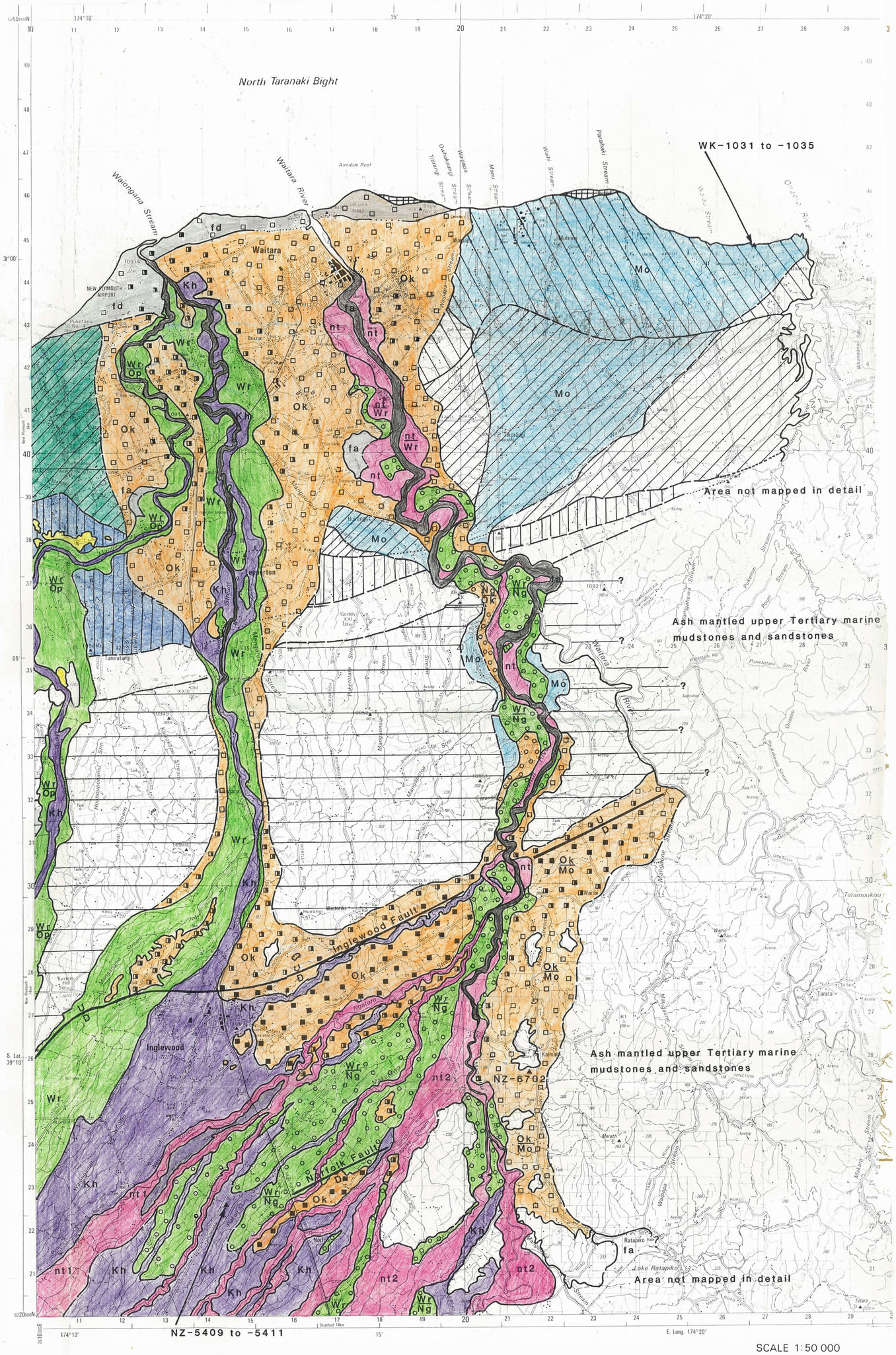
SAMPLE REFERENCE (Quote sheet number first): QI8 162294

THE VERTICAL INTERVAL BETWEEN THE CONTOURS IS 20 METRES HEIGHTS ARE ABOVE MEAN SEA LEVEL

Contours and spot elevations in forest and snow areas may be less accurate
Geodetic Datum 1949
International Spheroid
New Zealand Map Grid Projection
Date of compilation June 1984

Users noting errors, omissions or changes since the above date are urged to mark hereon and forward to the Department of Survey and Land Information, P.O. Box 170, Wellington
Maps so forwarded will be returned.
Recreational users should seek the latest information on huts and tracks from rangers or other authorities

Topomap WAITARA
Infomap 260 Q19
Edition 1 1988



GEOLOGICAL LEGEND

Tephra Deposits

Kyrs B.P

- Manganui tephra
- Inglewood Tephra
- Korito Tephra
- Mangatoki Tephra
- Tariki Tephra
- Waipuku Tephra
- Kaponga Tephra
- Konini Tephra
- Mahoe Tephra
- Kaihouri tephra
- Paetahi Tephra
- Poto Tephra
- Tuikonga Tephra
- Koru Tephra
- Pukeiti Tephra
- Waitepuku Tephra
- Mangapotoa tephr
- Waitui tephra
- Araheke tephra
- Te Arei Tephra
- Epiha Tephra
- Ninia tephra

Laharic Deposits

- nt NGATORO FORMATION
  - nt1 north-east lobe
  - nt2 east lobe
- Kh KAHUI FORMATION
- Wr WAREA FORMATION
- Ng NGAERE FORMATION
  - Axial a facies (●)
  - Axial b facies (◑)
  - Marginal facies (○)
- Op OPUNAKE FORMATION CORRELATIVES
- OKAWA FORMATION
  - Ok Axial a facies
  - Axial b facies
  - Marginal facies
- Mo Motunui lahar deposit
- unnamed lahar deposits
- MAITAHI LAHARS
- ELTHAM LAHARS

kyrs B.P

Sediments and Uplifted Marine Terraces

- Alluvium and Peat Deposits
- fd Fixed and active dune sand
- KATIKARA FORMATION
- NT1
- NT2
- NT3
- NT4
- NT5

GEOLOGICAL SYMBOLS

Contact concealed

Fault Trace with direction of movement (U / D)

MAP 1: Stratigraphy and distribution of coverbeds in relation to uppermost laharic deposits of North-eastern and Central Taranaki

Reference Only



CHAPTER 5
AEOLIAN SANDS

5.0 Katikara Formation
(Neall 1975; redefined this study)

5.1 Introduction

This Formation was formally named by Neall (1975) after Katikara Stream which originates in the Pouakai Range at 1377m altitude and flows north-westwards to the coastline between Okato and Oakura. Katikara Formation was first defined to "... encompass all the redeposited tephras between the Oakura Tephra and the Koru Tephra, ... and restricted to ring plain surfaces graded to the Pouakai Range".

In this study, Katikara Formation is here redefined to include all last-glacial (O^{18} stage 2) saltated andesitic material which exhibits a percentage decrease of fresh 15-bar water between 0 and 30%. This redefinition avoids confusion with medial material of localised aeolian origin which exhibit a higher percentage (>30%) decrease of fresh 15-bar water.

In the eastern and north-eastern sectors of the Egmont ring plain localised wedge shaped deposits of massive to laminar bedded andesitic sands are recognised and correlated to Katikara Formation (Plate 4.06). In North Taranaki, Katikara Formation is more widespread and forms prominent dunes and mounds which are conspicuous upon the Eltham Surface and within deeply dissected stream and river valleys between the Egmont ring plain and the coastal plain (Plate 5.01).

5.2 Type Section

The holostratotype was designated by Neall (1975) as a 5m high and 35m long exposure on a sharp corner to the south side of

Saunders Road, between the junctions of Wiremu and Carrington Road, at N118/510698. This section has since been removed by road straightening. A lectostratotype is here defined as:

> South-facing road cutting, Egmont Road 5.5km north of junction with State Highway 3 (Q19/101329) (See **Section 17** of Appendix 1; Plates 3.04 and 5.02).

5.3 Criteria

Katikara Formation comprises millimetre to centimetre, laminar to weakly cross stratified, well to very well sorted alternating beds of yellowish brown (10YR 5/6 - 5/8) friable, sandy loam and heavy mineral-rich (ferromagnesian and titanomagnetite minerals) loamy sand to sand (Plate 3.04). Moderately well sorted to well sorted pebble lenses are discernible at some sites. In outcrop, Katikara Formation is either massive or weakly developed, coarse to very coarse blocky structured.

5.4 Age

Katikara Formation in north-eastern Taranaki, appears to have been intermittently deposited between c.13 and 23kyr B.P. An uppermost Kaihouri tephra, dated (NZ5411A) at 12,900 +/- 200 years B.P., immediately overlying a thin wedge of Katikara Formation (Plate 4.06), provides an upper age limit. A probable cessation in the deposition of Katikara Formation during late last glacial time is supported by palynological evidence from the same vicinity (see Chapter 11), which indicates widespread expansion of podocarp - broadleaf forest on the Egmont ring plain in response to rapid climatic amelioration. There is no evidence in north-eastern and central Taranaki to suggest that localised deposition of Katikara Formation continued into the post-glacial, unlike higher areas of north-western Taranaki where deposits may be as young as 7000 years (Neall 1975).

Until recently the age of Katikara Formation was considered probably less than 20kyr B.P. (Neall 1975). However the



Plate 5.01: Andesitic sand dunes of **Katikara Formation** upon the **Eltham Laharic Planeze** (left) and within an inter-fluve of a Mangaoraka Stream tributary (right).



Plate 5.02: Andesitic sand dune of **Katikara Formation** exposed on Egmont Road at its lectostratotype (Section 17; Q19/101329). Note interbedded **Aokautere Ash**.

occurrence of the c.22.5kyr **Aokautere Ash** interbedded midway within a Katikara dune on the Eltham Surface (Plate 3.04) suggests that deposition of the formation commenced earlier than previously thought. The absence of Katikara Formation and erosional unconformities in the stratigraphic succession beneath **Tuikonga Tephra** indicates that widespread erosion in the north-eastern and central Taranaki landscape commenced c.23kyr B.P. (e.g. Plates 2.32 and 4.08).

5.5 Correlation

Katikara Formation closely correlates to **Mokai Sands** found in the Central North Island (Vucetich and Pullar 1969).

5.6 Origin

The occurrence of unconformities without associated fluvial deposits in the stratigraphic succession above **Tuikonga Tephra** suggests that Katikara Formation is largely derived from pedospheric stripping of pre-existing hydrous, medial and lapilli materials under the influence of wind deflation. Katikara Formation is also considered to be derived in part from wind deflation of aerially exposed, water sorted volcaniclastic deposits (Plate 5.03).

The conspicuous absence of inter-bedded tephras within most Katikara dunes suggest that as the formation was being deposited, any tephra erupted at the time was rapidly saltated and redeposited as a Katikara Formation deposit.

Areas most susceptible to wind deflation appear to be those associated with fluvial systems draining Egmont Volcano and Pouakai Range. On the Pouakai ring plain, where Katikara Formation is particularly prevalent, dendritic drainage channels are wider and deeper than the radial channels on the Egmont ring plain. On the Egmont ring plain where Katikara



Plate 5.03: Water-sorted volcaniclastic sediment of Last glacial age derived from underlying lahar deposit. Aerially exposed, these sediments provide an additional source material for **Katikara Formation**.

Formation is comparatively localised, the extent of surficial fluvial dissection is limited by numerous, often thick, near surface Egmont-source laharic units.

To facilitate wind deflation, colder, drier and possibly windier climatic conditions would be neccessary compared with those conditions which prevailed in post-glacial times. Thus, it is suggested that pedospheric stripping and dune formation occurred in the period from c.23 to 13kyr B.P. when there is ample evidence for severe climate. Evidence for climate change of this order is supported by changes in the TQC and QAR (see Chapter 6).

5.7 Reference Localities

The following two reference localities are designated for Katikara Formation.

1. East-facing embankment at the Toetoe Well Site, Mangaone Road extension, 1.8km north from the junction with Mangaone Road (Q19/246316).

2. West-facing embankment, Farm Quarry 0.2km east of Kaimata Road, 1.1km north from junction with Junction Road (Q19/218268) (Plate 4.06).

CHAPTER 6

6.0 LABORATORY STUDIES

6.1.0 An Attempt to Confirm the Identification of Selected Andesitic Tephra Marker Beds by Microprobe Analysis of their Titanomagnetites.

6.1.1 Introduction

Fe - Ti oxide compositions determined in various ways, have proved useful in tephra correlation studies in New Zealand and overseas (e.g. Kohn 1970, 1973; Topping and Kohn 1973; Westgate and Fulton 1975). Titanomagnetites were chosen as a particularly suitable oxide mineral because (a) it is a common accessory mineral in most volcanic rocks, (b) it can be easily extracted by a magnet in a reasonably pure form, (c) it has a considerable range in chemical composition and thermomagnetic properties (Ewart 1967; Mormose et al.1968; Duncan and Taylor 1968) and (d) it has been shown by Aomine and Wada (1962) and Ruxton (1968) to be relatively stable during weathering.

In Taranaki, Kohn and Neall (1973) attempted to distinguish twelve Taranaki tephras by titanomagnetite chemistry as measured by emission spectrographic analysis. Results of analyses indicate that the tephra fall into five groups based on similarity of elemental abundances. No systematic differences in titanomagnetite composition occurred with time from tephras above the New Plymouth Ashes.

In this study Fe - Ti oxides were extracted from thirteen selected andesitic marker beds and analysed by a JEOL-733 electron microprobe in an attempt to distinguish between individual eruptives pertaining to Egmont Volcano and determine whether there were any distinctive compositional differences with time. The electron microprobe has limited capabilities for

time. The electron microprobe has limited capabilities for measuring elements other than major elements and certain transition or heavy metals. Thus vanadium was not analysed, and measurements of nickel are of little value, since they are almost always below the accurate detection limits of the probe. The major element chemistry and statistical analyses of titanomagnetites are lodged in the Department of Soil Science and available upon request.

6.1.2 Results and Discussion

Based on electron microprobe analyses, the Fe - Ti oxides comprise mostly titanomagnetite with rare magnetite and ilmenite. Very few grains exhibit exsolution features, although inclusions are relatively common. Core to rim traverses across individual titanomagnetite grains indicate compositional homogeneity with respect to all major elements. Thus discrete grain analyses may be spatially independent and represent the whole mineral composition.

Initially, General Linear Models procedure was used to determine whether there were any significant differences between tephras, as measured by titanomagnetite elemental composition. The statistical model was in the form Y = X; where Y (dependent variable) is the titanomagnetite element and X is the tephra. The site from which the tephra was sampled was the replication for each tephra. For each element significant differences existed between tephras, but no logical grouping of tephras was observed e.g. on the basis of age.

The number of tephras being examined made comparisons unwieldy so another statistical procedure was used (Principal Component Analysis). This procedure is a multivariate approach which accounts for variability in data by giving a linear combination of correlated variables (in this case - elements) that maximises the ratio of between group variance to within group variance. For

example - Principal Components will give a combination of elements that will allow titanomagnetite measurements from one tephra to cluster together and be readily distinguished from another tephra.

Principal Component Analysis was made on three groups of tephra, grouped on the basis of age. The first group of tephras (1 - 7) needed three principal components to explain 80 percent variability in titanomagnetite data, and six principal components to explain 99 percent variability. The first principal component (Prin1) explained 52 percent of variability in data. The plot of Prin1 and Prin2 (Figure 6.01) shows some grouping of tephra, however there is sufficient overlap between each tephra group to suggest that measurement of Prin1 and Prin2 would not allow clear distinction between some tephra (e.g. tephra 3 & 4, tephra 5 & 6).

Interpretation of Prin1 and Prin2 is also difficult since Prin1 is a linear combination of four components (i.e. Al, Ti, Mg and Fe/Mg ratio) and Prin2 of two components (i.e. Fe and sum of total major elements). Results for Group 2 (tephras 8 and 9) (Figure 6.01) and Group 3 (tephras 10 - 13) (Figure 6.01) have similar difficulties -some grouping of tephra occurs when Prin1 and Prin2 are plotted, but interpretation of the two principal components is difficult and of little practical use.

The elemental composition of titanomagnetites therefore does not provide a ready means for confirming the identification of different Egmont-sourced tephras. This finding is similar to that of Lowe (1988) who was unable to distinguish between eight distal Egmont-sourced tephras based on elemental composition of titanomagnetites. Although elemental differences do occur and each tephra has a restricted compositional range, no workable pattern is observed and finding a combination of two or more elements that will group tephras but be of practical use has

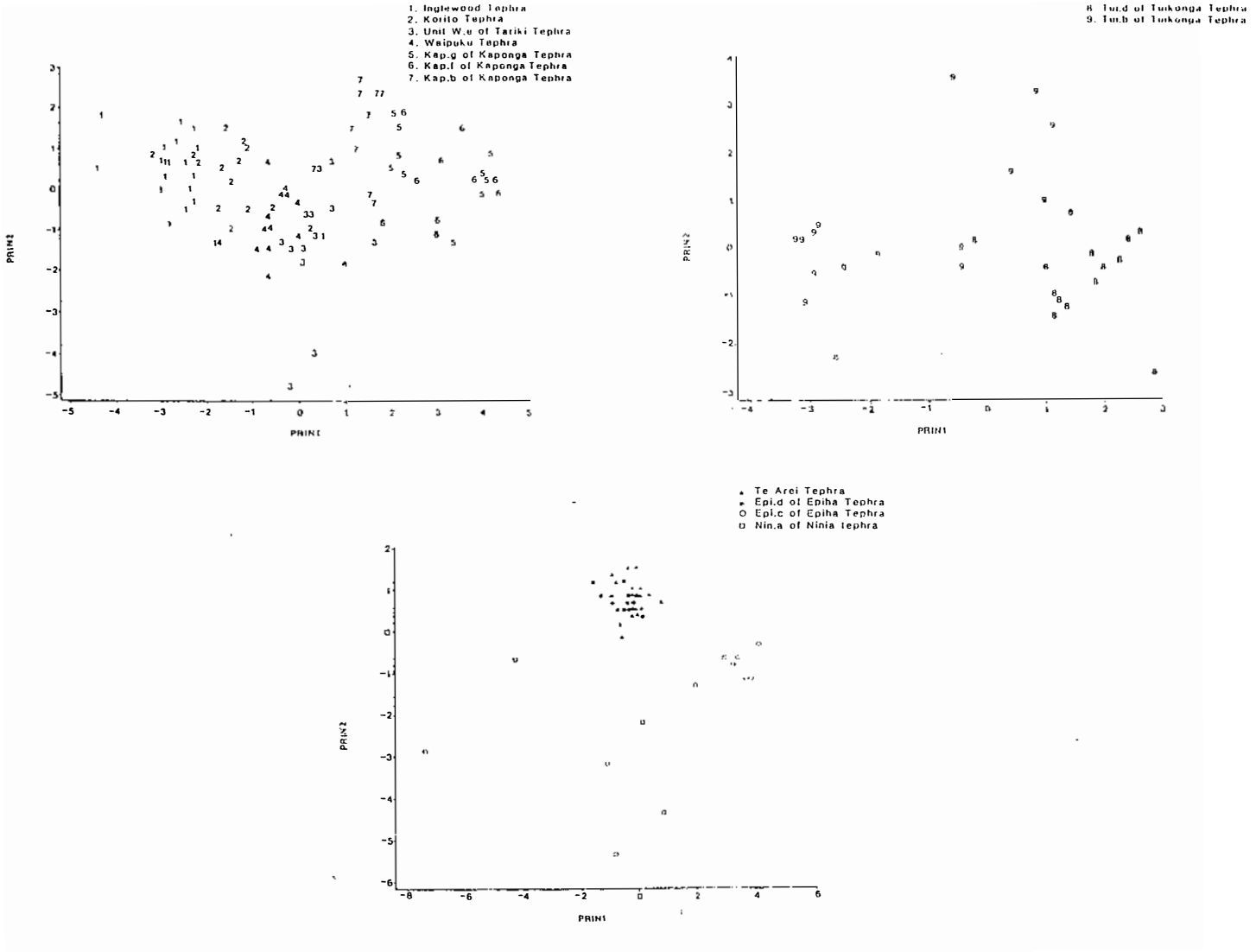


FIG. 6.01 **PRINCIPAL COMPONENT ANALYSIS** OF TITANOMAGNETITES FROM SELECTED ANDESITIC MARKER BEDS

proved difficult. It maybe that other less time consuming measurements are of better use in distinguishing between tephras.

6.2.0 LABORATORY STUDIES CONDUCTED ON MEDIAL MATERIAL.

6.2.1 Introduction

Most of the early laboratory studies on the volcanic ash soils (Andisols) of Taranaki have been concerned with the unusually high allophane content of the soil and its associated physical and chemical properties (Birrell 1951; Birrell and Fieldes 1952; Saunders 1956, 1963; New Zealand Soil Bureau 1968). More recently, studies have also used mineralogical and grain size variations to determine the age and provenance of coverbeds that post-date deposition of the Aokautere Ash (Stewart et al. 1977).

The thinning pattern and morphological characteristics of S- and L-units indicate formation under differing climatic episodes of the Late Quaternary. By using a variety of physical and chemical techniques, this study attempts to identify characteristics that can help to distinguish between S- and L-units and confirm the climatostratigraphy inferred from the medial cover bed sequence.

Two well preserved and representative exposures were selected for detailed studies. At both sites, stratigraphic control was provided by andesitic and rhyolitic tephra marker beds. The first site was at the Waitui drill-site, bordering the Egmont ring plain on the Eltham Laharic Planeze (Section 19 of Appendix 1). This site has since been recontoured and the exposure removed. The site consisted of a c.5.5m high embankment in which the stratigraphic relationships of S1 to uppermost L3 were clearly displayed. At Waitui, samples were collected from beneath 0.20m

depth below ground surface (above this level being disturbed by ploughing), to the base of the section. Between 0.20m and 1.0m depth samples were collected every 0.10m interval and below 1.0m depth, samples were collected at every 0.05m interval.

The second site is a prominent road cut through a flat terrace site adjacent to the Onaero River (**Section 30** of Appendix 1). Here a c.9.5m thick cover-bed sequence overlies andesitic sands and the NT2 wave cut surface (Chappell 1975). The stratigraphic relationships of **S1** to **L5** at this site, are clearly displayed. Samples were collected at 0.10m intervals from beneath 0.20m depth to the andesitic sands.

6.3.0 Particle Size Analyses

6.3.1 Introduction

In the Rotorua district, Benny (1982) demonstrated the usefulness of grain size studies in providing an accurate means of differentiating tephra from 'tephric loess'. In north and north-east Taranaki, particle size analyses of the highly allophanic material proved difficult because of allophane flocculating, preventing complete particle dispersion. Dispersion treatments such as using deflocculants, followed by mechanical agitation proved ineffective.

Japanese studies on the dispersion of Andisols have been summarised by Kobo (1964), and an extensive series of tests on the dispersion of similar soils in the Antilles and Latin America have been reported by Colmet-Daage et al. (1972). From these results it appears that there is no single method which applies to all Andisols, since different allophanes react differently to various dispersion treatments. The most promising dispersion method currently available involves the treatment at pH 10 (NH_4OH or NaOH) or pH 4 (HCl) after peroxidation and washing in water (Wada and Harward 1974). Wada (1978) suggested that an alkaline

medium be used for soils containing allophane with SiO_2/Al_2O_3 ratio of 2 or higher, whereas an acidic medium is best for those soils containing imogolite or allophane with a SiO_2/Al_2O_3 ratio lower than 2.

For the medial material being investigated in this study considerable time was spent in order to identify the most satisfactory dispersion treatment. Neither an acidic or alkaline pretreatment proved effective, so an entirely new procedure was implemented. This involved chemical dissolution of the short range order clays and organic complexes (hereafter referred to as **SROCO**), after which particle size analyses of the residue were determined. This selective chemical dissolution could not only be used for the determination of non-crystalline clay constituents but also enables quantitative determination of the residual sand, silt and crystalline clay constituents following dissolution treatment.

In this study, the acid-oxalate extraction method (Tamm 1932) has been employed as a pre-treatment procedure. This particular extraction method selectively dissolves short range order materials that are composed of allophane or ferrihydrite materials (Schwertmann 1964; Higashi and Ikeda 1974; Wada and Wada, 1977). If conducted in the dark, dissolution of crystalline oxides and layer silicates is regarded as very limited (Tamm 1932; Higashi and Ikeda 1974; Fey and Le Roux 1975, 1977; Wada 1977; Wada and Wada 1977).

6.3.2 Sample Preparation

The samples were air dried and gently disaggregated so as to pass through a 2mm seive. Sub-samples of c.10 gram weight were weighed to a thousandth of a gram, then added to 1 litre of 0.2M acid oxalate (pH 3.0 - 3.5) and shaken end on end in the dark at 20°C overnight. The sub-sample was then centrifuged at 5000 rpm for c.5 minutes. The clear supernatant is then carefully, but

completely decanted off. A further 1 litre of 0.2M acid oxalate is added to the sub-sample, which is shaken in the dark for a further 24 hours. Following selective dissolution, the sub-sample was then wet seived through a 30um mesh. The >30 micron fraction was oven dried, sieved into respective size fractions and weighed. The material passing through the 30 micron mesh was retained and centrifuged at 2500 rpm. The clear supernatant liquid was decanted off, while the <30 micron fraction was retained, oven dried and weighed. Grain size was then calculated for the residuum on a short range order clay and organic material-free (SROCO-free) basis.

A major limitation of this technique is the large volume (2l) of acid-oxalate required to treat relatively small quantities of sample (c.10g). The quantity of treated <30um sediment residue is therefore too small (<3gm) for accurate pipette or sedigraph grain size determinations to be undertaken.

6.3.3 Results

Textural Classes

Grain size data expressed as percentage of total sample (Air dry, <2mm) is plotted on a **modified** U.S.D.A textural ternary diagram (Figure 6.02). Grain size data of samples from Waitui and Onaero are shown in Appendix 3.1 and 3.2, respectively.

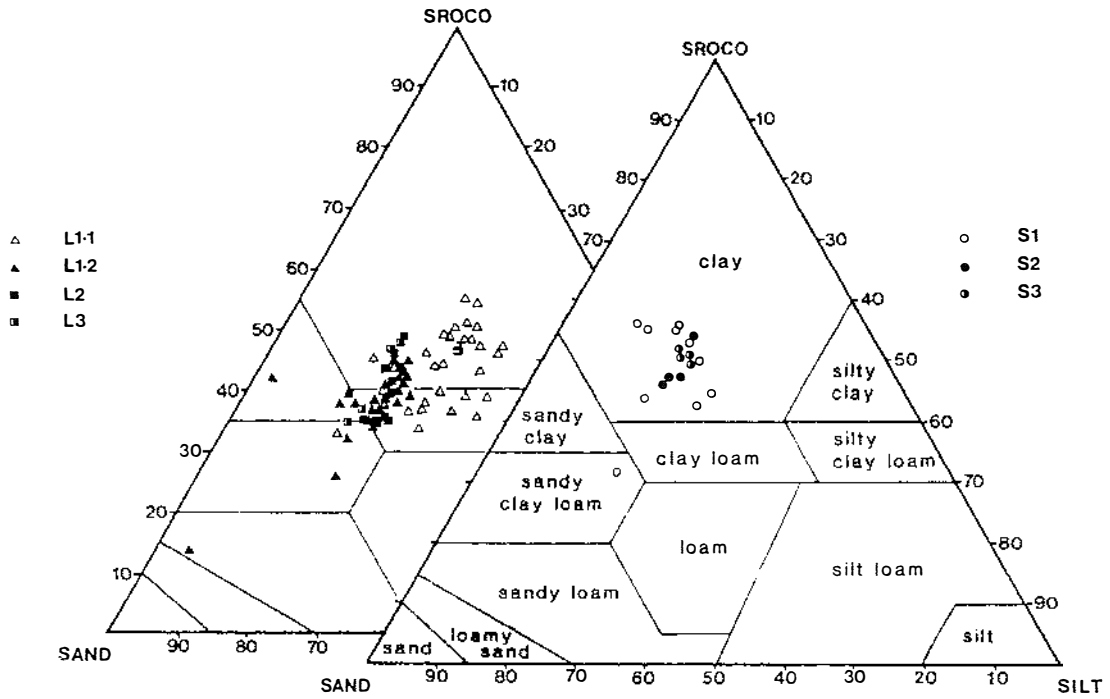
i) Waitui

Most samples, with the exception of tephra units, plot within the clay and clay loam textural fields. The most uniquely distinguishing feature at Waitui is the high (16 - 35%) silt and crystalline clay content in **L1.1.** Other units (**S1, L1.2, S2, L2** and **S3**) contain notably less (11 - 27%) silt and crystalline clay.

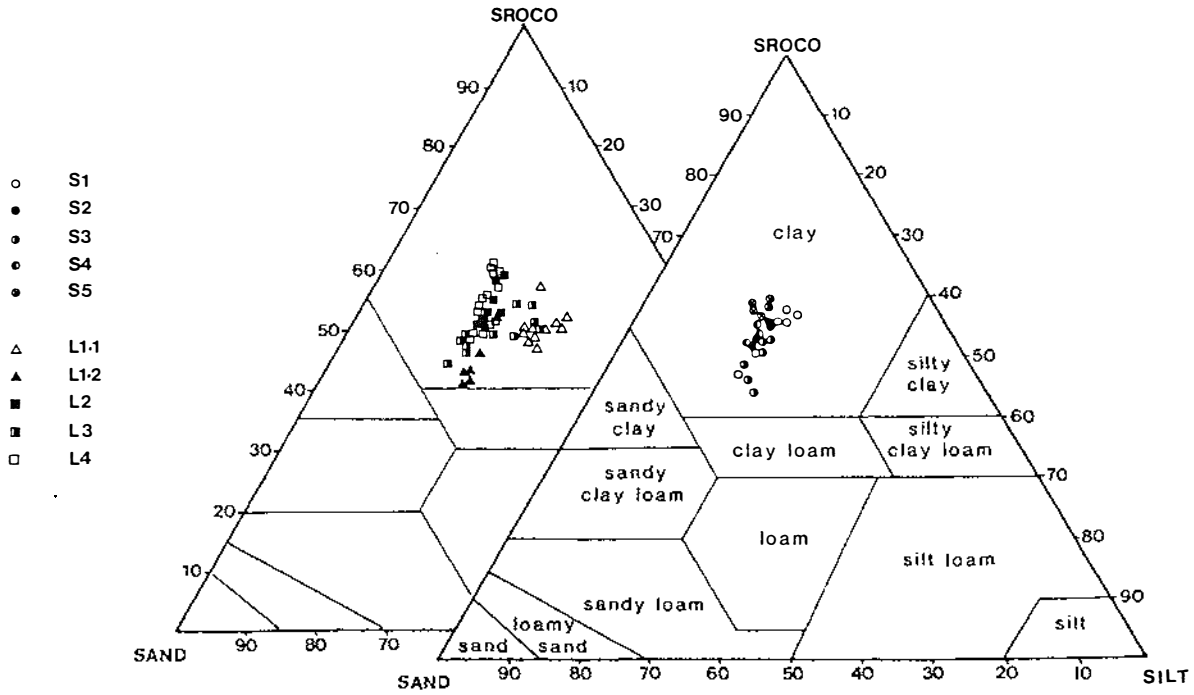
FIG. 6.02

Modified U.S.D.A Textural Ternary Diagram

Waitui grain size data expressed as a percentage of total sample
(Air dry : less than 2 mm)



Onaero grain size data expressed as a percentage of total sample
(Air dry : less than 2 mm)



S1, **S2** and **S3** plot within a narrow field on the ternary diagram and are distinguished by high (44 - 56%) SROCO and low (25 - 34%) sand content. **L1.2** and **L2** are coarser grained than **S**-units, with less (31 - 45%) SROCO and a greater (34 - 49%) sand content.

ii) Onaero

All samples plot within the clay textural field. High silt and crystalline clay content distinguishes **L1.1** (24 - 30%) and lower **L3** (22 - 27%) from other units which contain notably less (16 - 24%) silt and crystalline clay.

Lower **S1**, **L1.1** and lower **L3** is characterised by low sand (18 - 25%) and high SROCO (49 - 58%) content, whereas other units (upper **S1**, **S2**, **L2**, **S3**, upper **L3**, **S4**, **L4**, **S5** and **L5**) contain greater sand and less SROCO. With the exception of **L1.1** and lower **L3**, **L**-units cannot be differentiated from **S**-units.

6.4.0 Quartz Content

6.4.1 Introduction

Quartz is common in New Zealand soils formed from parent materials ranging from volcanic ash to sediments (New Zealand Soil Bureau 1968). Quartz in soils formed from basic and intermediate volcanic ash has been shown to be of eolian origin (Campbell 1971; Mokma et al. 1972; Stewart et al. 1977, 1986). However in soils formed from rhyolites the quartz may also be a primary constituent (Mokma et al. 1972). This study attempts to determine if variations of quartz content with depth in the dominantly andesitic cover-beds of north and north-east Taranaki provide a record of Late Quaternary climate change.

A previous investigation of a single representative Egmont loam profile, found that variations in quartz content within the soil profile reflected climatic change from glacial (post-Aokautere Ash) to post-glacial conditions (Stewart et al. 1977). The amount of quartz was shown to be greater in the lower 'tephric loess' unit than the upper, andesitic tephra unit. Stewart et al. (1977) postulated that this was due to the presence of a land bridge extending from north-west Nelson to western Taranaki during the last glacial (Lewis and Eade 1974). The subsequent rapid post-glacial rise in sea level at c.11,000 years B.P. (Cullen 1967) covered this source, resulting in a rapid decline in quartz accumulation in the upper part of the Egmont soil.

6.4.2 Method of Quartz Determination

Methods available for quartz determinations in sediments fall into two groups. Firstly, chemical methods which are usually precise but time consuming, and secondly X-ray diffraction methods which are usually more rapid but less precise.

The widely used method of Trostel and Wynne (1940) for free silica involves a pyrosulphate fusion, dissolution of the fusion by alkalis, leaving free silica for gravimetric estimation. The method is precise, with a coefficient of variation of c.1 per cent.

Alternatives to the above method in the past were mainly X-ray diffraction techniques. Till and Spears (1969) described a rapid and precise method for quartz determination in sediments, with a coefficient of variation of 1.9 per cent. Boehmite (y-alumina monohydrate) was used as an internal standard and the 4.26A (I/I_1 35) reflection of quartz was measured.

In this study, a standard quartz curve was prepared using the method of Johnson and Beavers (1959). This method is similar to that of Till and Spears (1969) but sodium fluoride (NaF) is used

as an internal standard and the strongest quartz line at 3.34A (I/I_1 100) is used.

Quartzose sand of Kapuni Formation was HCl washed, then mechanically ground in a Tema ring-grinder to c.15 microns. The purity of the ground quartz sample was monitored by X-ray diffraction. A $MgO/CaCO_3$ matrix was prepared with a calculated mass adsorption coefficient (CoK) similar to that for bulked standard chemical analyses of Egmont sourced andesites (Neall et al. 1986). Standard quartz mixtures were prepared by mixing varying amounts of quartz (hereafter abbreviated to Qtz) with the $MgO/CaCO_3$ matrix to make a total of 1 gram. A constant amount of 0.25gm of NaF was then added as an internal standard to each Qtz - $MgO/CaCO_3$ sample.

Acid-oxalate treated samples were ground by hand to a talc-like consistency in a agate mortar. Great care was taken to ensure reproducibility of grinding. The mixture was placed in a plastic tube with a ball bearing, and homogenised by end on end shaking for 1 hour. The standard samples were then packed into a hollow aluminium sample holder and scanned in a Phillips 1840 X-ray diffraction diffractometer unit under the following conditions:

CoK - Fe filtered radiation
Slit - 0.2mm, T.C - 1.0 seconds, Range - 2.10^4cs
40kV, 40mA.

A maximum chart speed of 100mm/^{0}2θ and a scan rate of 1.2/^{0} 2θ/min. was employed to spread the peaks for accurate area measurements. The magnitude of the 3.34A reflection of Qtz and the 2.32A reflection of NaF in counts per second were then obtained. The intensity of the background in counts was determined for each 2θ positions and subtracted from the total average counts for the Qtz and NaF reflections. By dividing the net counts per second for the 3.34A by the net counts per second for 2.32A NaF reflection the Qtz/NaF ratio for each standard

mixture was obtained. The average Qtz/NaF ratio of x determinations for each mixture was plotted against the percent quartz in the mixture and the regression line which best fits these points was determined (Figure 6.03). A linear fit was found to be satisfactory for these samples:

$$y = 0.0211 + 0.028x$$

where x = quartz percentage
y = Qtz (3.34A)/Sodium Fluoride (2.32A) peak area

The quartz content of unknown samples (63-30um and <30um fractions) was then determined by the same procedure, using the working regression line. Table 6.01 shows the results of three replicate determinations of each original sample. The coefficient of variation obtained ranges between 2.5 and 11 per cent.

The total quartz content (TQC) of SROCO-free samples with depth was determined using this XRD procedure and working regression line. Quartz content of samples from Waitui and Onaero are shown in Appendix 3.1 and 3.2, respectively.

6.4.3 Determination of Quartz Accumulation Rate

Once TQC was determined, the quartz accumulation rate (QAR) was then calculated:

TQC/100 x 1 = gm Quartz/gm Soil

gm Qtz/gm Soil x Average Bulk Density (gm per cm^3) x Sedimentation Rate (cm per kyr) = QAR ($gm/cm^2/kyr$).

In calculating QAR, the sedimentation rate of coverbed units down a profile varies significantly in response to the periodicity and magnitude of tephra-fall accretion from Egmont Volcano. Under such conditions, a constant sedimentation rate cannot be assumed as is done in deep sea or Antarctic ice cores. Sedimentation rates for these cover-bed units were calculated using the deep sea oxygen isotope timescale (Shackleton et al. 1983) and the

chronology of two Central North Island silicic tephra inter-beds (Aokautere Ash and Rotoehu Ash).

The grain size distribution of quartz in the acid-oxalate treated samples exhibiting peak TQC values, were also determined. Grain size fractions of the SROCO-free samples were separated by decantation and centrifugation (Jackson 1956) and the quartz content for each size fraction was quantitatively determined by XRD.

6.4.4 Results

i) Waitui (Figures 6.04 and 6.05)

At Waitui, TQC and QAR values throughout S1 remain at trace levels (<1% and <0.04gm cm^2 kyr, respectively). In L1.1, low TQC's and QAR's values persist to 1.40m depth but below this depth there is a significant increase at 1.80m depth to maximum values of 7.34% and 0.82gm/cm^2/kyr, respectively. From this depth, TQC and QAR decrease to minimum values of 0.32% and 0.03gm/cm^2/kyr at 2.00m depth coincident with **Pae.a** of **Paetahi Tephra** being preserved between 1.90-2.00m depth. Below **Paetahi Tephra**, TQC and QAR values increase to 5.38% and 0.60gm/cm^2/kyr respectively at 2.10m depth, then rapidly decrease to 1.24% and 0.14gm/cm^2/kyr at 2.35m depth. This minimum value is coincident with an unnamed unit of **Poto Tephra** preeserved within the stratigraphic sucession between 2.30-2.35m depth. Below **Poto Tephra**, TQC and QAR fluctuate from 3.46% and 0.39gm/cm^2/kyr at 2.40m to 2.86% and 0.34gm/cm^2/kyr at 2.90m depth. Across the L1.1/L1.2 boundary at 2.95m depth TQC and QAR values continue to decrease to 1.37% and 0.16gm/cm^2/kyr at 3.10m depth. TQC and QAR values of L1.2 between 3.10m and 4.05m depth are consistently low (<1% and <0.09gm/cm^2/kyr). From 4.05m to 5.40m depth, TQC and QAR values of **S2**, **L2** and **S3** are at trace levels (<1% and <0.03gm/cm^2/kyr).

FIG. 6.03 Quartz Standard Regression Line

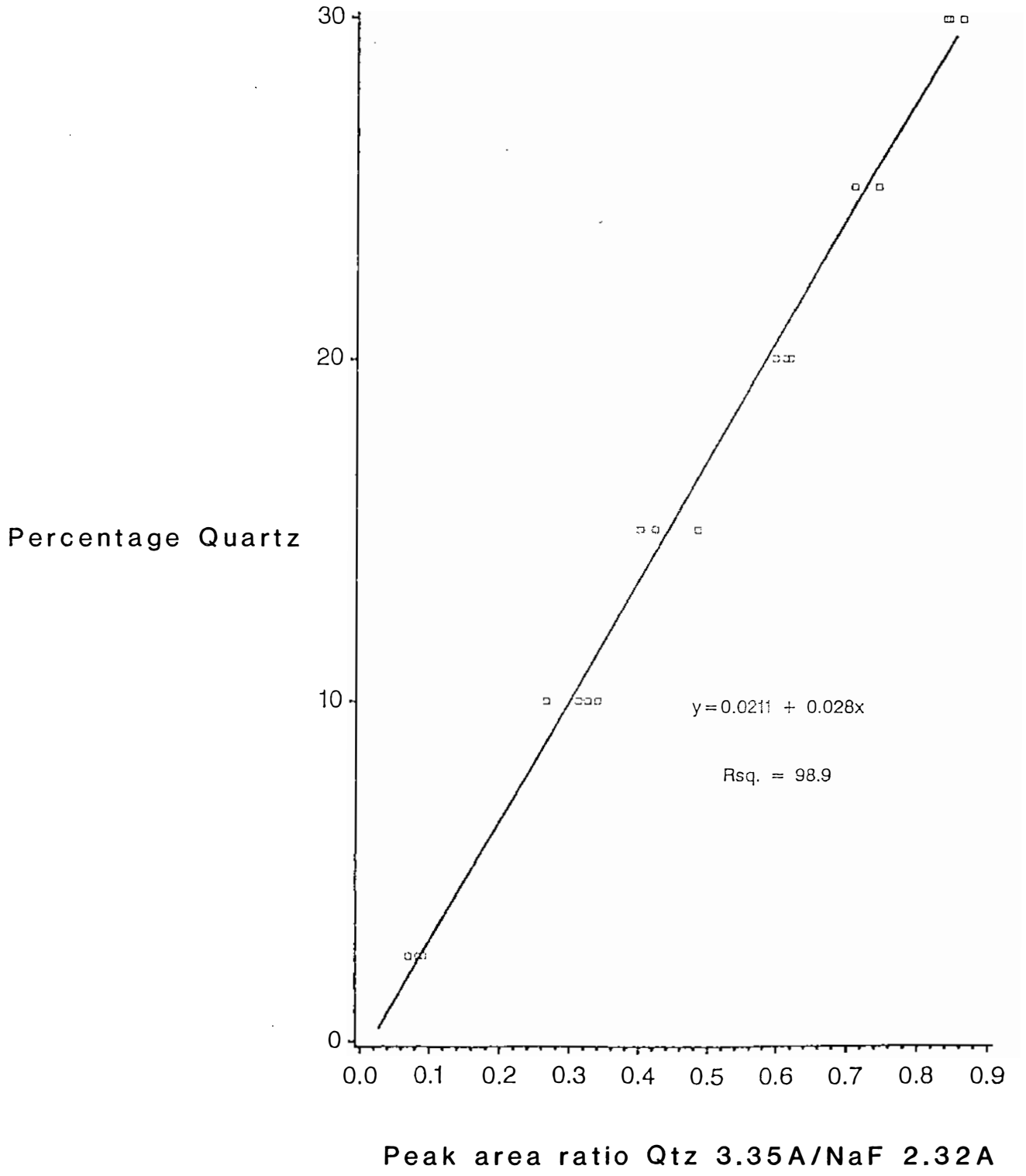
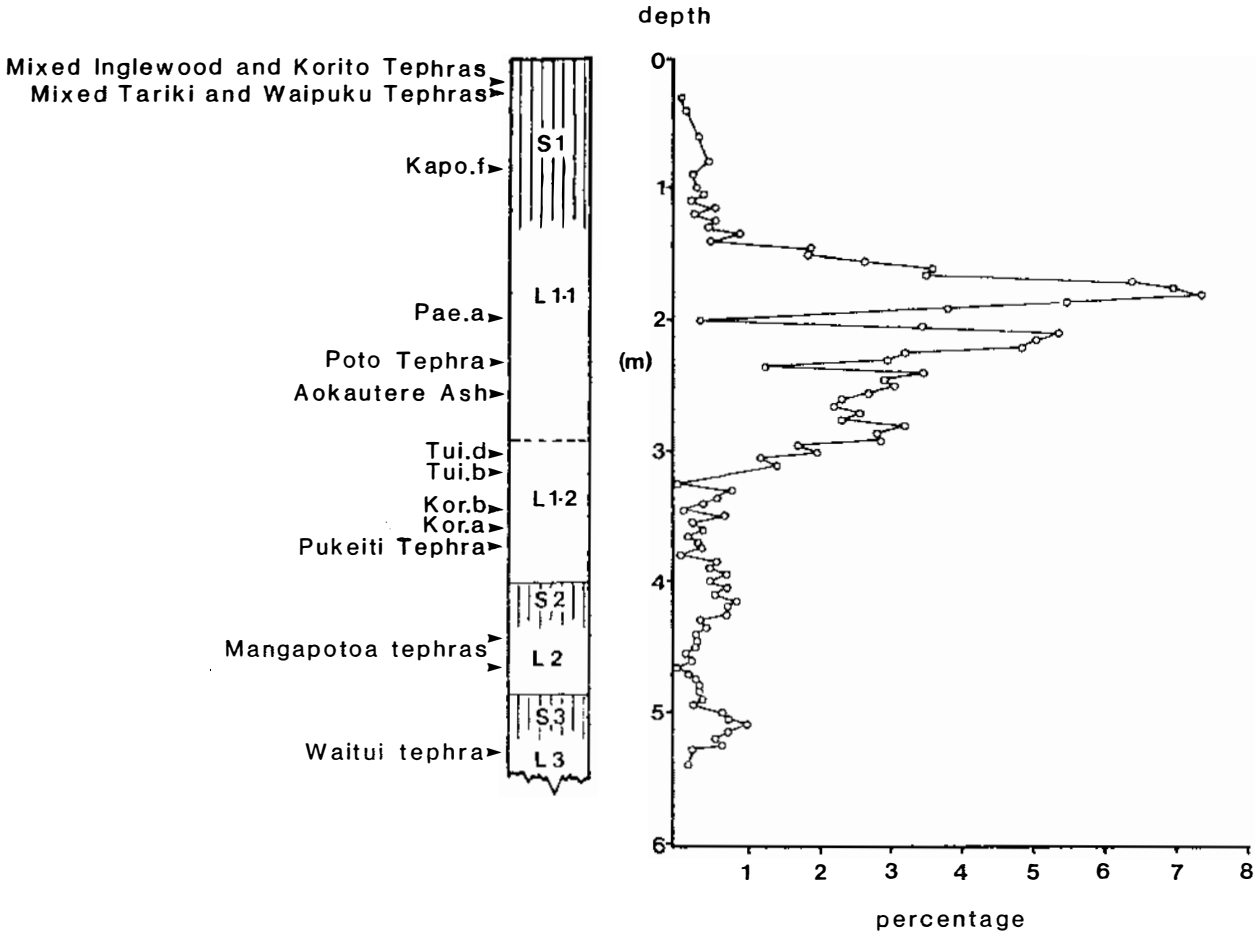


TABLE 6.01: REPLICATE QUARTZ DETERMINATIONS ON AN UNKNOWN USING THE XRD METHOD.

	Quartz (%)	
	19.95	
	20.22	Standard error = 0.50 per cent
	19.24	Coefficient of variation = 2.5 per cent
Mean	19.80	

	3.45	
	2.87	Standard error = 0.36 per cent
	3.53	Coefficient of variation = 10.97 per cent
Mean	3.28	

FIG. 6.04 **Total Quartz Content** Waitui Section 19



Onaero Section 30

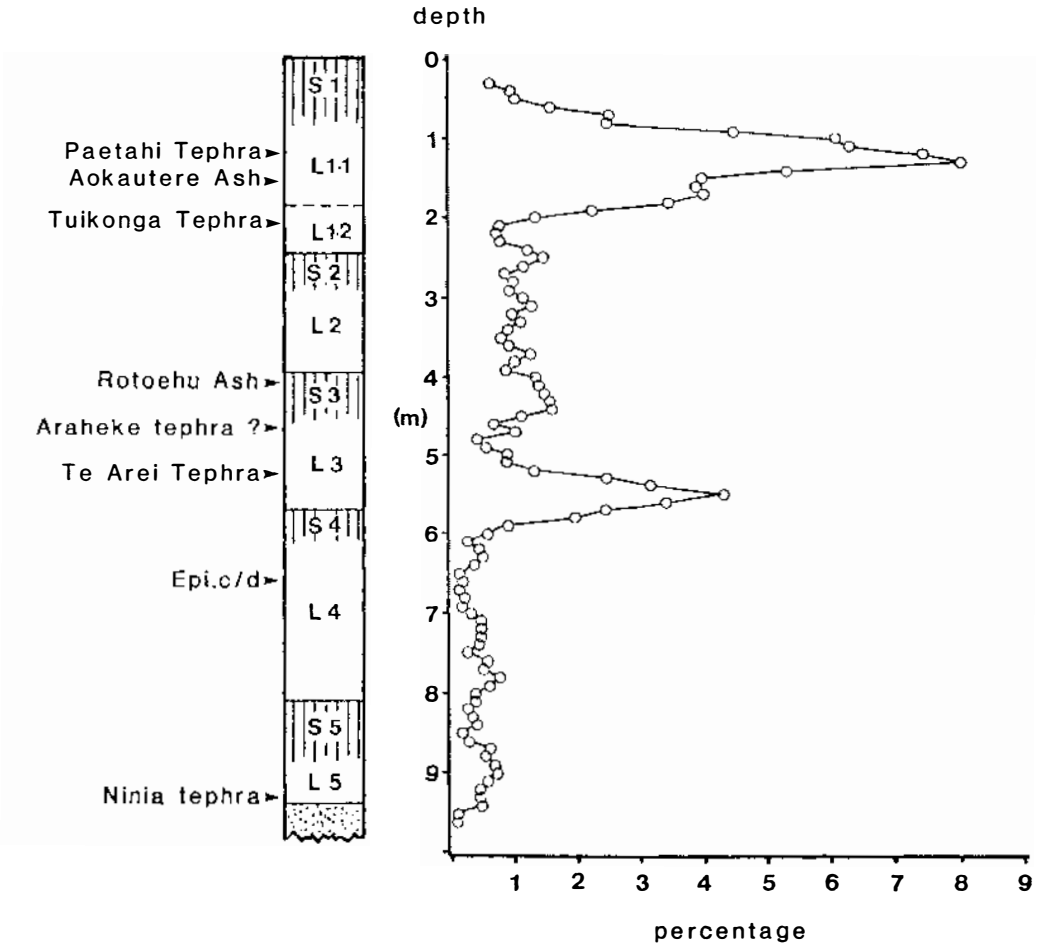
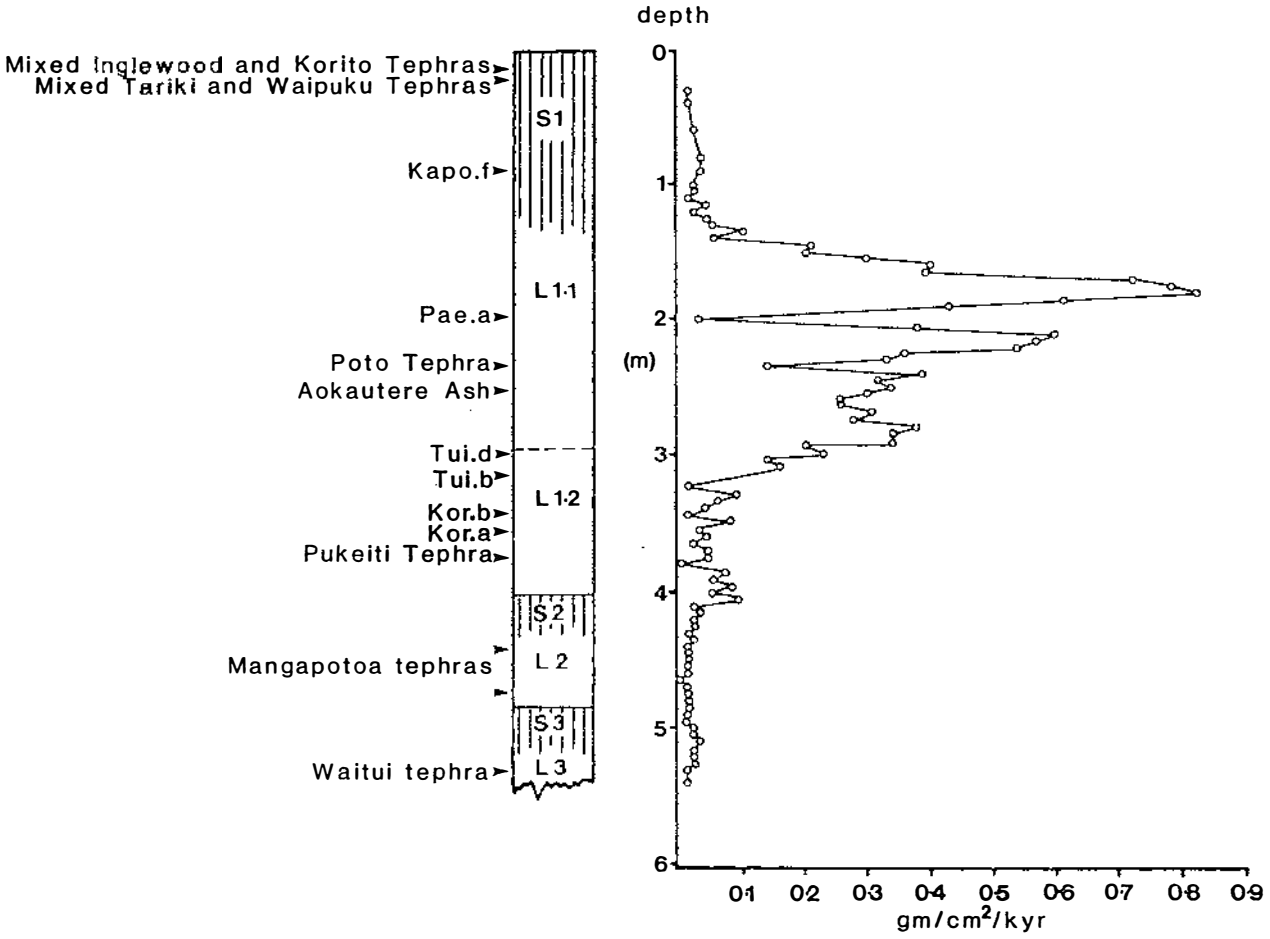
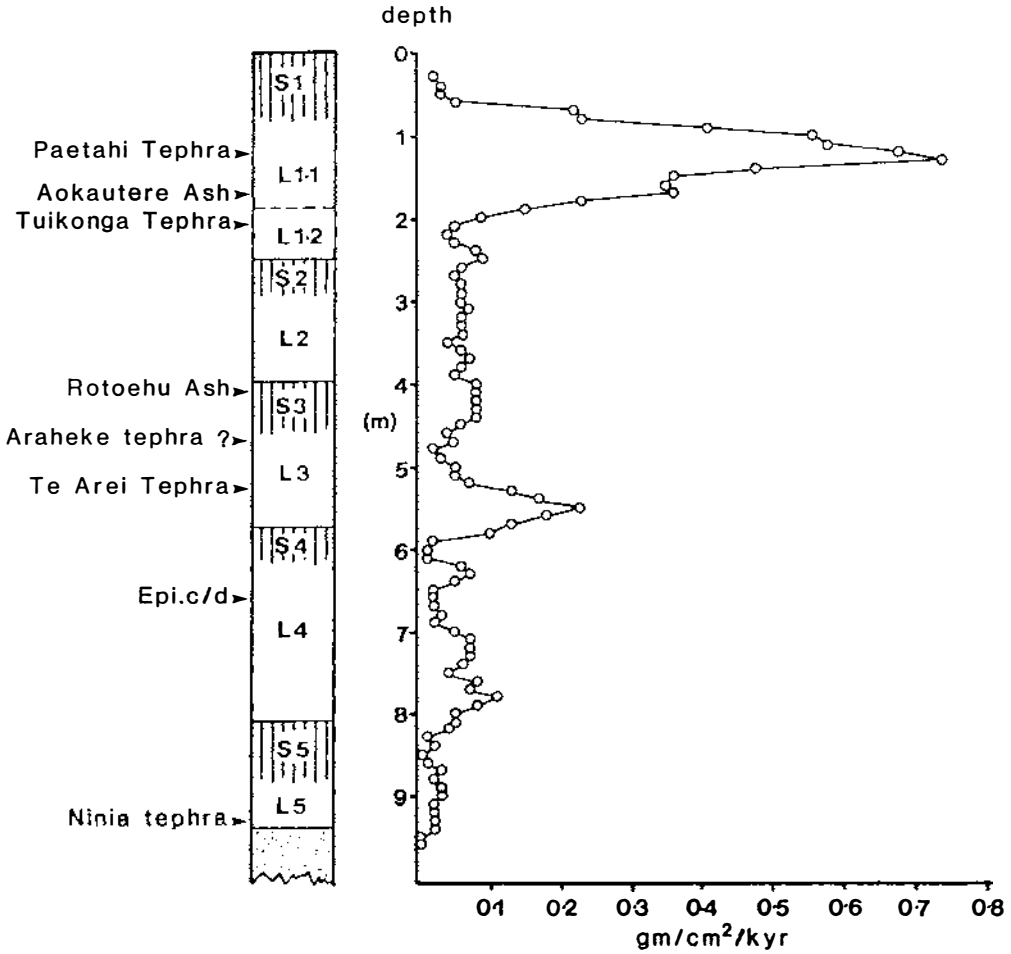


FIG. 6.05 **Quartz Accumulation Rate** Waitui Section 19



Onaero Section 30



ii) Onaero (Figures 6.04 and 6.05)
At Onaero, two major peaks in TQC and QAR values are recognised between 0.70 - 2.00m depth and 5.20 - 5.80m depth, respectively. The first peak coincides with deposition of lower **S1** and **L1.1** with a maximum TQC of 8.06% and a QAR of 0.74gm/cm^2/kyr at 1.30m depth. This maximum value closely coincides with **unit Pae.a** of **Paetahi Tephra** in the stratigraphic sucession between 1.30 - 1.40m depth. TQC and QAR values are trace in the interval between 2.00m - 2.40m depth, which coincides with the deposition of **Tuikonga Tephra** and **L1.2**.

The second peak coincides with deposition of lower **L3** with a maximum TQC of 4.29% and a QAR of 0.23gm/cm^2/kyr at 5.50m depth. TQC and QAR values in **S2**, **L2**, upper **L3**, **S4**, **L4**, **S5** and **L5** remain low to trace levels (<1% and <1gm/cm^2/kyr respectively). A slight increase in TQC and QAR values was recorded between 4.00 - 4.40m depth and coincides with the deposition of **S3**.

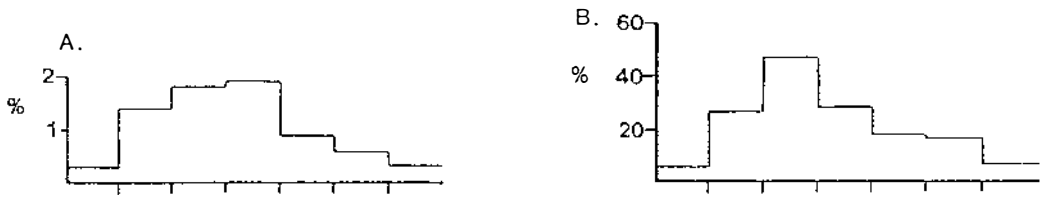
Quartz Grain size Distribution
The grain size distribution of the quartz is consistent with both loessial and tropospheric dust origin. Quartz is largely restricted to <125 um in size and mostly occurs in the <63um fraction (Figure 6.06). The size distribution of the **L1.1** TQC maximas from Onaero and Waitui are near identical with a broad mode (75% of total quartz) between 63 and 10 microns. The highest percentage of total quartz (c.28%) occurs in the 20 - 10um fraction, with 20 to 25% of total quartz occurring in the <10um fractions. The grain size distribution of the **L3** quartz maxima is similar to that of **L1.1**.

FIG. 6.06 Quartz Grain Size Distribution

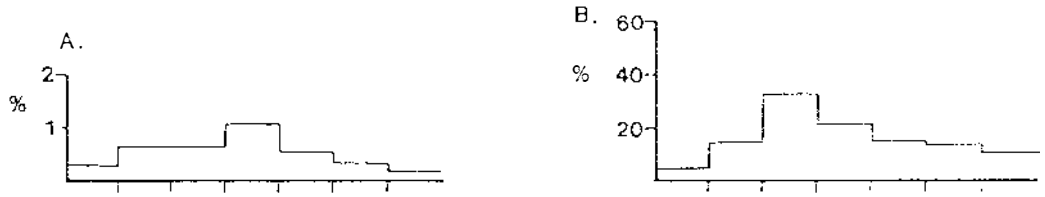
A. Quartz in Size Fractions as percentage total quartz

B. Quartz content percentage of size fractions

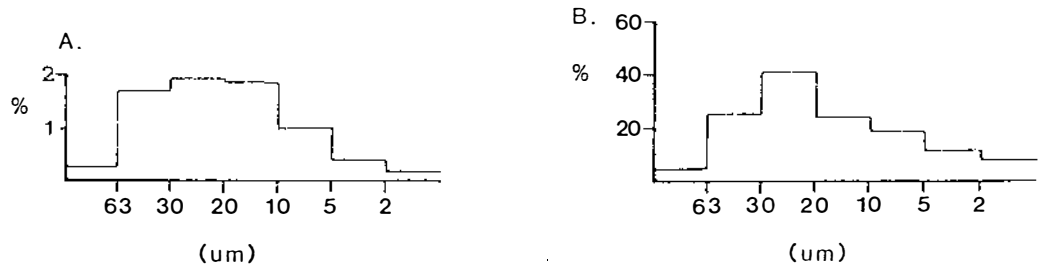
Onaero (Section 30) L1.1 Quartz Maxima



Onaero (Section 30) L3 Quartz Maxima



Waitui (Section 19) L1.1 Quartz Maxima



6.5.0 15-Bar Water Retention

6.5.1 Introduction

The high water retentivity of previously undried medial material and the large irreversible change in water retentivity on air-drying are important characteristics of Andisols. The large specific surface area of allophane and its high proportion of micropores (50 - 80% <10um diameter) are the properties which determine its ability to retain large amounts of water even at high suctions. At a suction of 15-bars, which is equivalent to the permanent wilting point of a soil, Andisols may have gravimetric water contents of over 100% (Maeda et al. 1977).

Differences in the 15-bar water retention of both field moist and air dry samples were determined as a measure of the previous drying history of a deposit. Data from field moist and air dried samples taken from Waitui and Onaero are shown in Appendix 3.3.

6.5.2 Sample Preparation

Water retention at 15-bars was determined on a ceramic plate extractor. Air dried and field moist samples were held in plastic rings approximately 40mm in diameter and 10mm high, and were wetted to saturation on the ceramic plates using a fine mist spray. Complete saturation was effected after 24 hours in an air tight container. The plates were then placed in the apparatus and a pressure of 15-bars was applied. The pressure was maintained for 7 days, after which time it was considered that equilibrium had been reached, and then the water contents were determined gravimetrically on an oven dry (105°C) basis.

6.5.3 Results

i) Waitui

A total of six samples of similar textured medial materials were obtained from within **S1** and **L1.1**. The field moist samples in **S1** and **L1.1** is similar and presumably indicates a similar content of

allophane. However, the percentage decrease of fresh 15-bar water (hereafter referred to as d-15 bar) of samples from **L1.1** is notably lower (45 - 53%) than those samples obtained from **S1** (64 - 68%). This difference in d-15 bar values appears to indicate some degree of irreversible drying during allophane formation in **L1.1.**

ii) Onaero

Following preliminary investigation of 15-bar water content of selected samples from **S1** and **L1.1** at Waitui, a more detailed investigation was conducted on the 15-bar water content of the upper c.2.6m of the Onaero Profile. The d-15 bar of samples in **L1.1** was found to be notably lower (49 - 33%) than for **S1** (56 - 64%). These difference in values appear to relate to coarser texture with some degree previous drying in the former case.

In **L1.1** a sharp increase in d-15 bar to 65% occurs between 1.3m and 1.4m depth, and is coincident with the deposition of **unit Pae.a of Paetahi Tephra.** This sudden increase of d-15 bar relates to a lower sand and higher SROCO content compared to that of the enclosing sediment. Lower d-15 bar values of between 33 and 40% in **L1.1** between 1.7m and 1.4m depth, relates to an increase in silt and sand content and is coincident with the occurrence of dispersed silicic glass of Aokautere Ash.

Unit L1.2 which is notably coarser grained than **L1.1** has lower d-15 bar (9 - 33%). These lower d-15 bar values appear to relate to the large increase in sand content (c.<15%) and corresponding decrease in SROCO. A sharp increase in d-15 bar values occur in **S2** at 2.40m depth and occurs in spite of similar textural values to upper L1.1. This suggests that this increase is attributed to *in situ* allophane formation without drying.

6.6.0 Al/Si Ratio of Allophane

6.6.1 Introduction

Andesitic glass, with an intrinsically greater Al/Si ratio than rhyolitic glass, weathers much more rapidly and with marked loss of SiO_2 and mobile cations (Neall 1977; Kirkman and McHardy 1980). Kirkman and McHardy (1980) and Kirkman (1981a) concluded that the structure and chemical composition of allophane, and hence its behavior and persistence, are governed chiefly by the chemical composition and bonding characteristics of the parent glass.

A weathering sequence for andesitic glass suggests that under humid temperate conditions, allophane and possibly imogolite are stable for periods in excess of 100kyr B.P (Kirkman 1978, 1980b, 1981, 1981a; Kirkman and McHardy 1980; Parfitt et al. 1982).

A weathering scheme emphasising leaching (rainfall) and Si concentration more than time has been proposed in clay mineral transformations of andesitic tephra (<20Kyr B.P.) in Taranaki (Parfitt et al. 1983). The range of Al/Si ratios for the allophanes may therefore, reflect the effects of environmental conditions (ie. climate), rather than time.

6.6.2 Sample Preparation

The Al/Si ratio of allophane is determined using acid-oxalate extractable Al (Al_o) and Si (Si_o), and pyrophosphate extractable Al (Al_p) which gives an estimation of Al in Al-humus complexes. Two samples of equivalent age and similar texture were collected from lower **S1** at Waitui (0.90 - 1.00m depth) and at Onaero (0.60m - 0.70m depth). Similarly two samples of equivalent age were also collected from **L1.1** at Waitui (2.70 - 2.80m depth) and at Onaero (1.70 - 1.80m depth). Al, Si and Fe extraction was conducted on these two samples (air dry; <2mm) by K.M.Giddens of New Zealand Soil Bureau in June 1987. The methods outlined by Parfitt and Henmi (1982) and Farmer et al. (1983) were used. The Al/Si ratio

for a sample is obtained from $(Al_o-Al_p)/Si_o$. Chemical data of samples taken from Waitui and Onaero are shown in Appendix 3.4.

6.6.3 Results

The Al/Si ratio of the samples obtained from **S1** at Waitui and Onaero are similar (2.02 and 2.03 respectively). The Al/Si ratios of the samples from **L1.1** at the two sites also agree (1.53 and 1.66 respectively) but they are lower than those from **S1**. If the Al/Si ratio of allophane relates to mean annual rainfall as suggested by Parfitt et al. (1983), these results indicate that allophane formation in **L1.1** at Onaero and Waitui, probably occurred during an interval which received lower mean annual rainfall than the interval of allophane formation in **S1**. This interpretation is supported by independent palynological data presented in this study (see Chapter 10). Further detailed research is required to test whether or not Al/Si ratios of allophane can be effectively used as a paleoclimatic indicator.

6.7 Discussion

Particle size analyses of the cover-beds at Waitui and Onaero reveal that **L1.1** and lower **L3** contain significantly higher silt than all other **S**- and **L**-units. The silt content of **L1.1** at Onaero and Waitui is similar but slightly higher than the silt content of lower **L3** at Onaero.

Grain-size variation is greatest at Waitui closer to Egmont Volcano. Here, the texture of **S1**, **S2** and **S3** is similar and can be clearly differentiated from **L1.2** and **L2** which contain lower SROCO and higher sand.

However at Onaero, there is less distinctive grain size variation, with the texture of **S**-units resembling that of **L1.2**, **L2**, upper **L3**, **L4** and **L5**. **L**-units at Onaero are finer grained than

equivalent units at Waitui but **S**-units remain of similar fine texture.

The high silt in **L1.1** and lower **L3** is found to closely correspond with high TQC and QAR values. Values of quartz are higher within **L1.1** and lower **L3** than all other medial units with values for **L1.1** significantly higher than lower **L3**.

The grain size distribution of quartz from the two investigated sites is similar and probably indicates derivation from a similar source area. The most likely quartzose source area is the exposed continental shelf of the southern North Island. Quartz of Australian provenance may also be represented by the finer grain fractions (<30um). This possibility cannot be discounted since concentrations of fine grained, aeolian quartz have been mapped in last glacial maximum sediments in the Tasman Sea (Thiede 1979), and historic dust storm events when clay and quartz from Australia were deposited over large areas of New Zealand following jet stream transport (Marshall 1903; Marshall and Kidson 1929; Healy 1970).

The influx of silt and crystalline clay with a significant quartz component to the coverbed sequence records two major peaks in **L1** and **L3**, which are correlated to O^{18} stages 2 and 4 (see **Chapter 4**).

In **L1** at both sites, the initial increase in TQC and QAR values occurs at c.23.4kyr following the deposition of **Tuikonga Tephra.** TQC and QAR values gradually increase to a small broad peak at c.22.5kyr which is coincident with the deposition of the Aokautere Ash. TQC and QAR values dramatically increase from c.22.5 kyr to a maximum at c.20kyr which closely coincides with the deposition of Pae.a of **Paetahi Tephra.** At Waitui, TQC and QAR values rapidly decline from c.20kyr to consistently low values at c.13kyr B.P. TQC and QAR values in the interval between c.13kyr

and the present day, remains at low to trace values. However for **S1** at Onaero, the apparently higher TQC and QAR values at its base can be explained by its downward development into **L1** below. In contrast, the airfall accretionary rate at Waitui is considerably higher, so that **S1** accuumulated faster than any downward development into **L1**.

The TQC and QAR maximum in **L3** at Onaero, is considered to be indirectly dated between 60 and 78kyrs B.P. based on the occurrence of the **c**.50kyr **Rotoehu Ash** (Kennedy 1987) within **S3** and extrapolated accumulation rates.

The trends in quartz content in Taranaki Andisols over the last c.130kyr B.P show strong similarity to recently reported trends of Al and Na aerosol concentrations within an Antarctic ice core (De Angelis *et al*. 1987). Excellent correlation exists between the quartz and Al accumulation rate maxima in O^{18} stage 2. However an offset of 5 - 8kyr occurs between the **L3** QAR maxima and the late Stage 4 Al accumulation rate maximum in the ice core. The reason for this offset may be due to a) regional differences in climatic response, or b) eruptive activity and higher sedimentation rates of tephric material between the Rotoehu Ash and the **L3** QAR maxima.

The TQC and QAR results support the argument for O^{18} stages 2 and 4 being the only two cold episodes in which full glacial conditions occurred in the Taranaki Region since c.130kyr B.P. Results obtained in this study indicate that 15-bar water contents and Al/Si ratios are useful in distinguishing between **S**- and **L**-units, and thus provide evidence of past environmental depositional conditions. Consistent differences in the 15-bar water contents of **S1** and **L1.1** at Waitui and Onaero, suggest that allophane formed during the **L1.1** depositional interval was subjected to some irreversible drying. In contrast the 15-bar water contents suggest that allophane formed during the **S1** and **S2**

depositional intervals were not subjected to the same drying conditions.

If the Parfitt et al. (1983) theory is accepted then the low Al/Si ratios of selected samples from **L1.1** suggest allophane formation occurred during an interval of lower mean annual rainfall than the present. In contrast, the higher Al/Si ratios of selected samples from **S1** suggest allophane formation occurred during an interval of higher mean annual rainfall than that persisting during the accumulation of **L1.1.**

The 15-bar water contents and Al/Si ratios are consistent with evidence for drier climatic conditions during the accumulation of L1 than the intervals in which S1 and S2 accumulated. It is suggested these two methods have considerable potential in differentiating between L-and S-units that lack unique distinguishing grain size and mineralogical properties. Al/Si ratios could prove an extremely useful parameter in the Wanganui district where, at present, there is difficulty in distinguishing between andesitic tephra inter-beds in loess and paleosols separating loess accumulation episodes.

CHAPTER 7

7.0 LAHAR STRATIGRAPHY

7.1 Introduction

The word 'Lahar' is Indonesian for "volcanic breccia transported by water" (Van Bemmelen 1949, p.191). Subsequent definitions have expanded the term to include torrential waterflows (Schieferdecker 1959), hyperconcentrated streamflows (Fisher and Schmincke 1984), or an origin on the flank of a volcano (Crandell 1971).

The term 'lahar' is used here to refer to " .. an event comprising a rapid flowing mixture (other than normal stream-flow) of rock debris and water from a volcano .. ". The term "lahar" has often been conveniently used to encompass both volcanic debris flows and volcanic mudflows, as well as for their resultant deposits. This usage has tended to avoid terminology problems and subjective distinctions based on depositional texture. However in Taranaki, two categories of lahar deposits are recognised on the lower flanks of Egmont Volcano and can be clearly differentiated on the basis of depositional texture: 1) rare deposits in which mud (the total of silt- and clay-size sediment) is a significant part of the deposit and dominates in the inter-clast matrix (mudflows) and 2) common deposits that contain negligible medial material and clay in the inter-clast matrix (debris flows).

Mudflow deposits on the lower flanks of Egmont Volcano, are readily distinguishable from debris flow deposits on the basis of substantially higher proportions of medial material and clay within the inter-clast matrix and to a lesser extent - lithologic heterogeneity of clasts. Mudflow deposits are typically unstratified and exhibit very poor sorting (Plate 7.01). Clasts

are dispersed randomly in the matrix range from rounded to angular. The basal contact is occasionally erosional with clasts of underlying tephric and medial material incorporated within the deposit during flowage (Plate 7.01). Mudflow deposits are texturally similar to those deposits mapped as marginal facies of a debris avalanche but fragmental rock clasts and an associated hummocky surface are apparently absent. Weakly consolidated clasts in mudflow deposits exhibit features indicative of plastic deformation and progressive disaggregation during flowage.

Debris flow deposits are poorly sorted, and comprise angular to sub-rounded clasts either clast- or matrix- supported with silty sand of similar composition (Plate 7.02). The top surface of debris flow are near planar often with a boulder strewn upper surface. Debris flows generally lack vertical grain size variations and are usually poorly stratified, except for an occasional, texturally distinct, thin, basal sub-layer (Plate 7.03). Some debris flow deposits may exhibit crude reverse-to-normal grading or reverse grading throughout the thickness of the depositional unit. The basal contact of debris flows confined to channel areas is usually erosional with underlying deposits incorporated during flowage (Plates 7.04 and 7.05). However the basal contact of debris flow deposits on marginal inter-fluve areas is seldom erosional. In these areas vertical tree moulds are often observed (Plate 7.06) but wood is rarely preserved.

Debris flows demonstrate proximal-to-distal transformations to "hyperconcentrated" flows - a transport mode intermediate between debris flow and normal stream-flow, and characterised by suspensions in the volume concentration range of 20-60% (40-80% by weight) (Beverage and Culbertson, 1964).



Plate 7.01: Mudflow deposit of **Kahui Formation** exposed near Norfolk Road on State Highway 3 (Q19/164214). Note the poor sorting, lack of stratification and rip-up clasts of medial material.

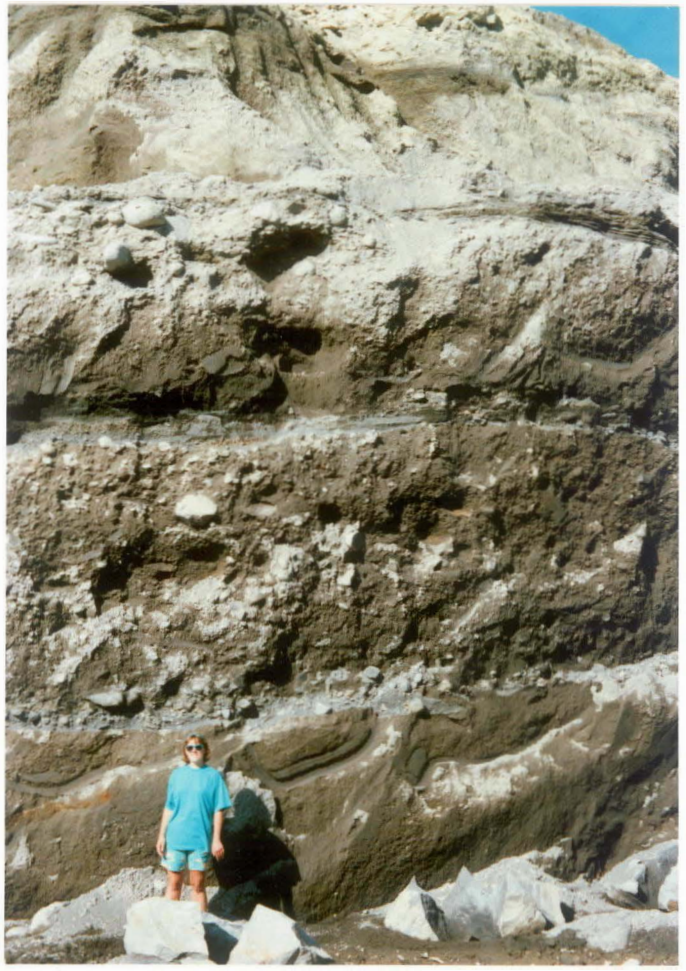


Plate 7.02: Debris flow deposits of **Warea Formation** separated by fluvial deposits at Bell Block Quarry on Manutahi Road (Q19/106376). Note the textural variation but similar lithological composition.



Plate 7.03: Textural distinct, thin, basal sub-layer of **Ngatoro Formation** exposed at Q20/171208 in effluent pond near Section 12. Note flame dewatering structure and **Inglewood Tephra** below sub-layer.



Plate 7.04: Erosion and incorporation of fluvial deposits by overlying debris flow deposits of **Warea Formation** in the Waiongana Stream catchment at Bell Block Quarry, on Manutahi Road (Q19/106376).



Plate 7.05: Erosion of hyperconcentrated flow deposit by overlying debris flow deposit of **Warea Formation** in the Manganui River catchment at Everett Road Quarry (Q19/205299).



Plate 7.06: Tree Mould in marginal area of **Ngatoro Formation**. Note underlying **Inglewood Tephra**.

Hyperconcentrated flow deposits, well documented at Mt. St. Helens (e.g. Pierson and Scott 1985), are best distinguished from the debris flow deposits from which they evolved by their massive or crudely stratified appearance with sometimes an inversely graded sub-unit in the basal part of each depositional unit (Plate 7.07). The most definitive characteristic of hyperconcentrated flow deposits is their elongate clasts developing an a-axis parallel-to-flow orientation in well sorted deposits. This improvement in sorting is reflected by the lack of dispersed clasts and grain supported matrix which is usually granular, non-cohesive and with greater void space. The upper surface of hyperconcentrated flow deposits is usually planar.

Deposits that represent a transitional flow regime between debris flow and hyperconcentrated flow are also recognised. These deposits in a vertical sequence are often characterised by a stratified very fine to coarse sand unit overlain by an unstratified gravelly sand unit, which upwardly grades to a faintly stratified coarse sand (Plate 7.08). These units were presumably deposited sequentially by a single flood wave that was in the process of transforming from debris flow to hyperconcentrated flow. The vertical contact between the two deposit types in each flow unit is transitional and downstream the debris flow unit thin progressively.

The most striking feature of debris/hyperconcentrated flow deposits in Taranaki, is their similarity in lithology, texture and fabric. This leads to problems in mapping and correlating separate flow events because they lack individual diagnostic properties (Plate 7.09) and are currently mapped collectively.

7.2 Te Popo debris flows
(new informal formation)

Te Popo debris flows are named after Te Popo Stream that flows eastwards from Egmont Volcano, crossing State Highway 3 just north of Midhurst. On the upper eastern flanks of Egmont Volcano, Te Popo debris flows comprises at least two units that are separated by up to 0.15m of humic, ashy or medial material.

Upper and Lower Contacts

The upper contact of the uppermost Te Popo debris flow unit is separated from **Mg.d** of **Manganui tephra** above, by up to 0.10m of ashy or medial material (**Section** 3 of Appendix 1 and Figure 2.05; Plate 7.10). **Mg.c** of **Manganui tephra** interstratifies the ashy/medial material intervening between the two debris flow units. The lowermost Te Popo debris flow unit is directly underlain by **Mg.b** of **Manganui tephra.**

Age

Te Popo debris flows are considered to closely correspond in age to **Manganui tephra,** since both formations are closely associated in the stratigraphic succession. On this basis both debris flow units are considered to have an age between c.2.9kyr and c.3.1kyr B.P.

Type Section

An informal type section is here designated in a deep drain parallel to a farm track, 0.54km north of Denbigh Road and 6.1km west of the junction with State Highway 3 at Q20/129112. (**Section 3** of Appendix 1 and Figure 2.05). Here Te Popo debris flow deposits are exposed as follows:

Maketawa tephra

0.24m ---------- Distinct and wavy boundary ----------

0.04m	Yellowish-brown (10YR 5/4), friable, weakly developed, medium nut structured medial material. Distinct and wavy boundary.
0.04m **Mg.d**	Many, moderately sorted, grey (10YR 5/1 - 3/1), coarse ash and fine lapilli dispersed in yellowish brown (10YR 5/4) ashy material. Indistinct and wavy boundary.
0.09m	Yellowish-brown (10YR 5/4), friable, weakly developed fine granular structured ashy material with common dirpersed grey fine lapilli throughout. Distinct and wavy boundary.
1.82m	1.80m of very poorly sorted, unstratified, light greyish brown to grey (10YR 6/2 to 5/1) angular to sub-rounded gravels dispersed in a very firm matrix of pebbly sand. Sharp and wavy boundary to
sub-layer	0.02m of moderately well sorted, brown (10YR 5/3) fine sand. Sharp and wavy boundary. (**upper Te Popo debris flow**)
0.02m	Very dark brown (10YR 2/2), firm, massive structured humic material. Sharp and wavy boundary.
0.07m	Dark brown (10YR 4/3 - 3/3), firm, massive structured humic material with discontinuous pockets of moderately well sorted, dark brown and red coated, grey, fine to medium lapilli of **unit Mg.c**. Clear and wavy boundary.
0.37m	0.32m of very poorly sorted, faint reverse to normal graded, light greyish brown to grey (10YR 6/2 to 5/1) angular to sub-rounded gravels abundantly dispersed in a very firm, sub-ordinate matrix of pebbly sand. Abrupt and wavy boundary to
sub-layer	0.05m of moderately sorted coarse to very coarse grey sand. Sharp and wavy boundary. (**lower Te Popo debris flow**)

0.07m **Mg.b**	Profuse, moderately well sorted, red (2.5YR 4/6 - 4/8), dark grey (10YR 4/1), fine to medium lapilli. Sharp and wavy boundary.
0.31m	0.13m thick layer of dark brown (7.5YR 4/4) humic material with small tree stumps in growth position. Indistinct and wavy transition to 0.12m thick layer of dark brown (7.5YR 3/4) carbonaceous, slightly gravelly clayey material. Sharp and wavy transition to 0.06m layer of very dark grey (5YR 3/1) humic material with protruding tree stumps.
3.07m ----------	Distinct and wavy boundary ----------

Il.b of **Inglewood Tephra**

Distribution

On the eastern flanks of Egmont Volcano, Te Popo debris flows occur as a broad lobe between Patea River in the south and Mangamawhete Stream in the north. In the vicinity of the National Park boundary, the units appear to have overtopped the channels and laterally spread onto the extensive planar inter-fluve surfaces. In the vicinity of Te Popo Stream, either side of Denbigh Road, debris mounds of Ngaere Formation protrude from beneath the debris flow units. Both units of Te Popo debris flows together with the closely underlying Ngatoro Formation often occur distributed within the inter-mound areas. Further south, the elevated hummocky terrain of Ngaere Formation, has formed a topographic obstruction for Te Popo debris flow deposits. In this terrain, both debris flow units were principally confined within the channels of Waingongoro River and Mangatoki Stream. The debris flow units, further east, become confined within Piakau, Te Popo, Waipuku and Mangamawhete Stream channels as well as the Manganui and Patea Rivers.



Plate 7.07: Hyperconcentrated flow deposit of **Warea Formation** at Bell Block Quarry, on Manutahi Road (Q19/106376). Note crude stratification of well sorted deposit and elongate clasts with a-axis parallel to flow orientation.



Plate 7.08: **Unnnamed lahar deposit** exposed at Q20/167202 (Section 10) on Bains Farm. This deposit represents the transitional flow phase between debris flow and hyperconcentrated flow.



Plate 7.09: Debris flow and hyperconcentrated flow deposits of **Warea Formation** at Bell Block Quarry, on Manutahi Road (Q19/106376). These deposits are mapped collectively since they generally lack individual and readily identifiable diagnostic properties.



Plate 7.10: **Te Popo debris flow deposit** (upper unit) at Q20/129112 (Section 3) between Denbigh and York Roads. Position of **Maketawa tephra** (black arrow) and **Mg.d** of **Manganui tephra** (white arrow) is indicated. Note unnamed debris flow deposit truncating **Maketawa tephra**.

7.3 Ngatoro Formation (after Neall 1979)

This Formation was formally named by Neall (1979) after Ngatoro Stream that drains the north-east flanks of Egmont Volcano. The type locality is the area within 0.4km to the north and east of Bedford Road and south of Norfolk Road junction (Q20/138187). On the lower eastern flanks of Egmont Volcano, Ngatoro Formation comprises a single debris flow unit (Plate 7.11) which downstream sequentially transforms to a hyperconcentrated flow unit (Plate 7.12) and then a normal stream flow unit (Plate 7.13).

Upper and Lower Contact

The upper contact of Ngatoro Formation is separated from **Manganui tephra** above, by <0.20m of medial or hydrous material. The lower contact is separated from **Il.b** of **Inglewood Tephra** below, by <0.10m of medial or hydrous material (Plates 7.06 and 7.11).

Age

A radiocarbon date (NZ3353A) from wood beneath the Ngatoro Formation, at Q19/156210, gave a maximum age of 3,610 +/- 80 years B.P. (Neall 1979). Another radiocarbon date (Wk-1031A) of 3,690 +/- 80 years B.P. from peat immediately beneath Inglewood Tephra confirms the maximum age for the closely overlying Ngatoro Formation. On the basis of the above radiometric dates, Ngatoro Formation is here considered to have an age of between c.3.5 and c.3.6kyr B.P.

Reference Locality

In addition to the two reference sections already designated by Neall (1979), a new reference section is chosen in this study. This section occurs at a prominent west-facing road cut on State Highway 3 at Tariki Railway overpass, opposite the junction with

Johns Road at Q20/167202. (**Section 10** of Appendix 1 and Figure 2.05). Here the following section is exposed:

Manganui tephra

0.26m ---------- Indistinct and wavy boundary ----------

0.13m	Brownish yellow (10YR 6/6), firmly friable, weakly developed, fine to medium blocky structured medial material. Distinct and wavy boundary.
c.1.45m **Ngatoro Formation**	Moderately to poorly sorted, massive (upper portion) to stratified (lower portion), inversely graded sub-units of light greyish brown to greyish brown (10YR 6/2 to 5/2) angular to sub-rounded gravels supported in a very firm matrix of pebbly sand of similar lithology. Common pumice layers occur near base of unit which exhibits planar, as well as low angle X-stratification. Sharp and irregular boundary to
sub-layer	<0.20m of firm, well sorted fine sand with flame dewatering structures evident. Sharp and irregular boundary.
0.07m	Brownish yellow (10YR 6/6), firmly friable, massive structured medial material.

1.91m ---------- Distinct and wavy boundary ----------

Il.b of Inglewood Tephra

Distribution

Ngatoro Formation can be subdivided into a c.1km wide, north-east (**nt1**) lobe and a c.3km wide, eastern (**nt2**) lobe. The eastern lobe in the vicinity of Egmont National Park, occurs between the Maketawa Stream in the north and Mangatengehu Stream in the south. Between Mangamawhete Stream and the mapped southern boundary, the **nt2** lobe is buried beneath Te Popo debris flow units. Ngatoro Formation is likely to be distributed further south beneath Te Popo debis flow units. Further mapping in this vicinity is required.

The north-east lobe (**nt1**) is preserved on the inter-fluve surfaces between the channels of tributaries to the Ngatoro Stream. At c.15.2km north-east of the present Egmont summit, **nt1** becomes channelised into the Ngatoro and the Ngatoro-iti Stream channels. At this point, the two channelised deposits of **nt1** are separated by a <0.4km wide inter-fluve surface of Kahui Formation. The channelised deposits of **nt1** combine a further c.5.4km north-east and enter the Manganui River at c.26.1km north-east of the present Egmont summit.

The eastern lobe (**nt2**) at c.14.6km from the Egmont summit, forms two small sub-lobes separated by an 0.7km wide inter-fluve surface of Kahui Formation. The northern sub-lobe is distributed on the inter-fluve surfaces between Maketawa Stream and a tributary of Waitepuku Stream, and becomes principally confined within these stream channels at c.16.6km north-east of the Egmont summit. The south sub-lobe is extensively distributed in the area between Waitepuku and Mangatengehu Streams and continues to be distributed on the inter-fluve surfaces between the two streams north-east of the State Highway 3. However an elevated area of Tertiary siltstone located c.2km east of State Highway 3, near the end of Rugby Road, appears to have caused the flow to bifurcate. A portion of the southern sub-lobe followed the Mangamawhete and Mangatengehu Streams before entering the Manganui River catchment c.3.8km further eastward, whereas the other portion followed tributaries of Waitepuku Stream before entering Manganui River, further north.

At the Manganui River and Ngatoro Stream junction, where **nt1** and **nt2** lobes merge, Ngatoro Formation can be mapped c.17km further north towards the coast within the confines of the Manganui River valley. Over this distance, Ngatoro Formation appears to progressively transform from a hyperconcentrated flow deposit to a normal stream flow deposit.

7.4 Unnamed lahar deposit

A single debris flow unit has been recognised within the confines of Waipuku Stream and its tributaries, north-east of State Highway 3 in the vicinity of Tariki (Plate 7.08). The distribution of this unit south-west of State Highway 3 is presently unknown.

The upper contact of this unit is clear and irregular, and separated from **W.a** of **Tariki Tephra** above, by c.<0.30m of medial material. The lower contact is sharp and wavy, and is separated from **Waipuku tephra** below, by up to 0.15m of medial material (Plate 2.11). This debris flow unit, is therefore estimated to have an age range of between c.4.6kyr and c.5.2kyr B.P.

A reference section for this debris flow unit is designated at a farm cutting within a stream valley, c.0.15km south-east of a milking shed on Bains Property, Tariki Road at Q20/192194. (**Section 12** of Appendix 1 and Figure 2.09). Here the debris flow unit is transitional to a hyperconcentrated flow unit.

7.5 Kahui Formation

(after Neall 1979; redefinition this study)

The formation was formally named Kahui Debris Flows by Neall (1979) after Kahui Hill (P20/972119) and comprises at least eight debris flow units deposited in West Taranaki between c.7kyr and c.12.5kyr B.P. Similar aged debris flow units were also recognised along the Waiwakaiho River in north-east Taranaki. The type section was designated in the northern bank of the Waiweranui Stream at P20/912194, 1.45km due north of the eastern end of Newall Road. As Kahui Debris Flows have proved a useful lithostratigraphic unit in both west and north-east Taranaki they are here defined as Kahui Formation.

In describing the lithology of this formation, Neall (1979; pg.20) remarks that "smaller debris flow units were deposited as fine sands across the landscape, in a similar manner to floods observed in historic times". This comment intimates that some debris flow units of the Kahui Formation underwent progressive proximal-to-distal transformation to normal stream flow units.

On the north-eastern lower flanks of Egmont Volcano, a succession of at least **three** debris flow units and one mudflow unit are recognised. The debris flow units are mapped collectively, since poor exposure and lack of diverse lithology, precludes individual mapping.

Upper and Lower Contact

On the lower north-eastern flanks of Egmont Volcano, the upper contact of the uppermost debris flow unit is separated from **Waipuku Tephra** above, by c.<0.25m of medial material. The lowermost unit is separated from **Konini Tephra** below, by c.<0.60m of medial material. The debris flow units of Kahui Formation are

frequently interstratified by constituent units of **Kaponga Tephra** (e.g. **Sections 8** and **12** of Figure 2.12; Plate 2.11).

Age

Kahui Formation in north-eastern Taranaki is closely associated in the stratigraphic succession with Kaponga Tephra. On this basis the Formation is here considered to have an age range between c.6.0kyr and c.10kyr B.P.

Distribution

Kahui Formation is extensively distributed on the inter-fluve surfaces of **Warea Formation correlatives** between State Highway 3 and the National Park boundary. In the vicinity of Inglewood, Kahui Formation has partially inundated the inter-mound areas of Okawa Formation and is frequently buried by units of Ngatoro Formation. In the vicinity of Waipuku Stream, Kahui Formation is buried by an unnamed debris flow unit.

North and north-east of State Highway 3, debris flow units of Kahui Formation generally become channelised within the confines of major stream tributaries. Exposures within most of these valleys are generally limited, due to subsequent widespread burial by the flow unit of Ngatoro Formation deposited down the same channels. However, within and adjacent to the present course of the Waiongana Stream channel, the uppermost debris flow unit of Kahui Formation is the youngest laharic deposit in the catchment and can be mapped to the coast. This uppermost unit appears to have progressively transformed from debris flow to normal stream flow.

The mudflow unit of Kahui Formation (Figure 7.01), forms the uppermost lahar deposit on the inter-fluve surfaces between the Maketawa and Waitepuku tributaries, between Durham and Johns Road. In this vicinity, the unit is without a hummocky surface

topography and has inundated small debris mounds tentatively correlated to the Okawa Formation. From State Highway 3, the unit can only be traced a further c.3km north-east along Norfolk Road before it is concealed beneath Ngatoro Formation.

Reference Localities

In north-east Taranaki eight reference localities are designated for units of Kahui Formation.

1. Farm cutting in contoured stream valley, right of farm race, c.0.15km south-east of milking shed, Bains Property, Tariki Road at Q20/192194. (**Section 12** of Appendix 1 and Figure 2.11).

2. Prominent drain, south side of Durham Road, c.1.85km south-west of the junction of Durham Road and State Highway 3 at Q19/144226. (**Section 8** of Appendix 1 and Figure 2.11).

3. Driveway cutting immediately adjacent to Ngatoro Stream on Burgsteden's property, near Reservoir on Dudley Road (Q19/119226).

4. Drain running diagonally across paddock into Ngatoro-iti Stream (Q19/155249).

5. Silage Pit adjacent Ngatoro Stream, Nichols Property, Bristol Road (Q19/187277).

6. Drain adjacent boundary of Everett Reserve in paddock at the junction of Bristol and Everett Roads, (Q19/208298).

7. Cutting alongside paddock, near Ngatoro Stream, 0.4km north of Junction Road, (Q19/183272).

8. Prominent west facing road cut on State Highway 3, c.0.2km south-east from Norfolk School at Q19/164214.



Plate 7.11: Debris flow deposit of **Ngatoro Formation** with protruding Dacrydium cupressinum (rimu) stumps in position of growth at York Road Quarry (Q20/119119). Spade (1m length) rests on stump in centre of plate. Arrow indicates position of **Il.b** of **Inglewood Tephra** in peat below debris flow deposit.

7.6 Warea Formation Correlatives (after Neall, 1979)

On the eastern and north-eastern lower flanks of Egmont Volcano, a closely spaced succession of at least five debris and hyperconcentrated flow units are recognised. These units, appear to have a similar age range to the Warea Formation but differ in depositional texture and lack associated mounds with fragmental rock clasts. The lack of readily identifiable, diverse lithologic character of individual units and the absence of interbedded tephra markers between the units, precludes sub-division of the succession and downstream mapping and correlation of individual events (Plate 7.09). On this basis, it therefore seems appropriate to collectively term these units as **Wr correlatives** (after Neall 1979).

Upper and Lower Contacts

The uppermost **Wr correlative** is separated from the **S1** above, by c.<0.20m of **L1.1** medial material and uppermost Kaihouri tephra (**Section 10** of Appendix 1 and Figure 2.16; Plate 2.20). Near source the basal contact of the lowermost unit is rarely exposed. However, distally this lowermost contact is occasionally separated from **Aokautere Ash** below, by **L1.1** of variable thickness. **Wr correlatives** intercalate with **L1.1** or andesitic sands of the Katikara Formation (Plate 7.14).

Reference Localities

Five reference sections are designated for units of **Wr correlatives** in north and north-east Taranaki.

1. Everett Road Quarry, 7km north-east of Inglewood Borough at junction of Everett and Bristol Roads, (Q19/205299).

2. Road cutting on Konini Road, Inglewood Borough at Q19/136276.

3. Bell Block Quarry, Manutahi Road at Q19/106376.

4. Quarry, 0.1km north of State Highway 3 and 0.8km west of junction of State Highway 3 and 3A (Q19/125418).

5. Silage pit on Howes Property, 0.1km north of saw mill situated at the Waiongana Stream bridge, State Highway 3 (Q19/141423).

Distribution

Deposits of **Wr correlatives** are extensively distributed on the north and north-east lower flanks of Egmont Volcano but are often buried beneath a thick (c.>3.0m) succession of laharic, medial, ashy and lapilli deposits. On the lower flanks there are only two extensive areas where **Wr correlatives** form the uppermost laharic deposit. Here they comprise debris flow units. In the vicinity of Inglewood, these debris flows units have partially surmounted small aeolian-modified debris mounds of Okawa Formation (e.g. at Q19/136275 on Konini Road).

Extending to the north of Inglewood, **Wr correlatives** can be mapped within the confines of north trending drainage channels that connect the Egmont ring plain to the North Taranaki coastal plain. Within the confines of the Mangaoraka Stream Valley at least five, dominantly debris flow units can be collectively mapped. These units appear to have obstructed natural drainage from the Umutekai swamp and partially surmounted intra-valley aeolian dunes of Katikara Formation of Neall (1975) (Plate 7.14). These debris flow units exhibit minimal proximal-to-distal transformation to hyperconcentrated flow units but appear to become better sorted and finer grained with distance from source.

Within the confines of the Waiongana Stream valley, at least two debris flow transitional units can be mapped collectively.

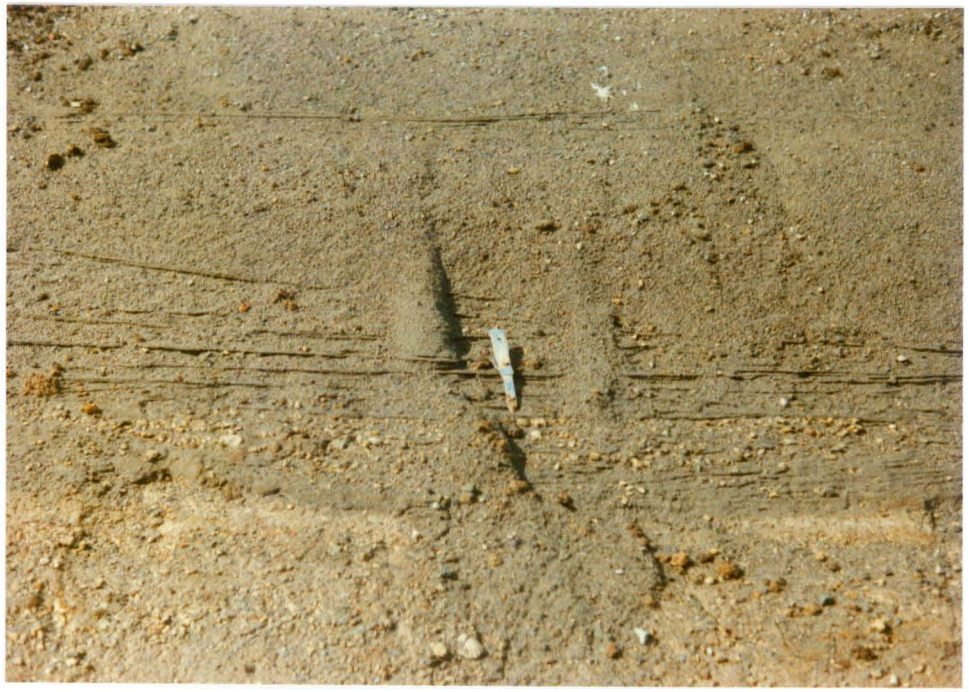


Plate 7.12: Hyperconcentrated flow deposit of **Ngatoro Formation** exposed at Q20/171208 in effluent pond on Rugby Road near Section 12.



Plate 7.13: Debris-flow related stream flow deposit of **Ngatoro Formation** exposed in drain at Q19/208208.



Plate 7.14: Debris flow deposits of **Warea Formation** intercalating andesitic sand dune of **Katikara Formation** at Q19/102347. Arrow indicates position of **Aokautere Ash**.



Plate 7.15: Vertical tree moulds in marginal area of **Warea Formation** adjacent Waiongana Stream near Lepperton. Note sharp and vertical boundary between **Warea Formation** and **Kahui Formation** (indicated by large arrows - far left).

Further north, on the coastal plain, these units occur on the inter-fluve areas directly adjacent to the present stream courses. Near Lepperton, the uppermost debris flow unit appears to have overtopped the channel and spilled over into a forest, indicated by the numerous tree moulds (Plate 7.15). Further north towards the coast, prominent debris mounds of Okawa Formation protrude from beneath the debris flow units whilst smaller mounds were inundated.

Within the Manganui River valley, at least five debris and hyperconcentrated flow units form an extensive intra-valley laharic aggradation surface. This surface has been subsequently dissected, to leave small planar remnants along the river valley to just south of Waitara. The units that comprise these small remnant surfaces are poorly exposed.

Age

A radiocarbon date (NZ6702A) of 21,500 +/- 300 years B.P. was obtained from wood immediately beneath a lowermost Wr correlative in the Waiongana Stream valley (Q19/144314).

7.7 Opunake Formation Correlatives

Opunake Formation correlatives have so far been observed at only three sites in north and north-east Taranaki. From this meagre data, the extent of these deposits is extremely difficult to ascertain. Two debris flow units closely underlying **Aokautere Ash**, appear to have been channelised down the Waiwhakaiho River. These units are exposed in a prominent road cut on State Highway 3, 0.1km west of the Waiwhakaiho River Bridge at P19/084285 (Plate 4.02). Two further debris flow units, also closely underlying **Aokautere Ash**, appear to have been channelised down the Waiongana Stream. These units, separated by a thin tephra bed

provisionally correlated to **Tuikonga Tephra**, are exposed in a silage pit adjacent to Waiongana Stream on the coastal plain (Q19/142424).

A further debris flow unit overlying the c.28kyr Waitepuku tephra is identified on the ring plain in the vicinity of Inglewood at Q19/171259 (**Section 16** of Appendix 1 and Figure 2.28; Plate 2.38). This debris flow unit is exposed beneath a thick overlying succession that includes units of **Wr correlatives**, as well as **Ngaere Formation.**

7.8 Motunui Lahar Deposit
(new informal formation)

A single c.4.25m thick, dominantly unstratified, heterolithologic mudflow unit is near continuously exposed in coastal cliffs that extend from just east of Waitara to the Onaero River (Plate 7.16). The mudflow unit comprises abundant angular to well rounded rock clasts and common plastically deformed soil and tephra rip-up clasts dispersed in a clay rich inter-clast matrix. At some exposed sections clasts are concentrated towards the basal portions of the mudflow unit. Fragmental rock clasts have not been observed within the unit.

Upper and Lower Contacts
Along the North Taranaki coast, the lower contact of Motunui Lahar deposit is sub-horizontal, sharp and wavy and separated from the wave-cut surface of NT2 terrace below, by a thin carbonaceous paleosol developed directly in variably thick, planar to low angle cross-stratified, well sorted andesitic sands and gravels (Plate 7.16). At the same section the upper contact is separated from Ni.a of Ninia tephra by <0.30m of lignitic material (Plate 2.39). The sub-horizontal upper surface of the

mudflow unit, along isolated sections of the coast, is directly overlain by prominent dunes comprising steep angled cross-stratified, well sorted andesitic sands.

Further inland the mudflow unit is seldom exposed. However at two sections adjacent to the Waitara River on the NT3 terrace, the mudflow unit is well exposed. In a stream gully on Honor's Property at Q19/173399, the deposit is separated from Okawa Formation above, by c.6.70m of lignitic material and gyttja interbedded by at least thirty-four ash and lapilli units of Ninia tephra. Here the base of the unit is not exposed but has a minimum thickness of c.12m.

In a cliff section at Osborne's Property c.2.5km further south-east at Q19/187383, the Motunui laharic deposit is unconformably separated from Okawa Formation above, by 0.8m of lignite. The base of the Motunui laharic deposit is exposed unconformably resting upon a c.5m thickness of planar to low angled cross-bedded well sorted sands which abruptly grade downwards to c.8m of gyttja containing wood and lignitic lenses overlying a gravel unit above the NT3 wave cut surface, below.

Further inland, Motunui laharic deposit is only tentatively correlated to a section along Mangaone Road extension at Q19/244306, c.10.5km north-east from Inglewood. Here, the upper 2m of the mudflow unit is exposed just above road level and is separated from the overlying Okawa Formation by c.3.7m of gyttja with at least 45 lapilli and ash inter-beds of Ninia tephra.

Age

The Motunui laharic deposit closely post-dates the cutting of the NT2 terrace and therefore has an age of c.115kyr based on the correlation of the closely underlying NT2 wave cut surface (Hay 1967; Chappell 1975) to the Rapanui Formation of Wanganui



Plate 7.16: **Motunui lahar deposit** within the cover-beds of NT2 terrace in the vicinity of Titirangi Stream mouth along the North Taranaki coast (Q19/197458). Here the lahar deposit is overlain by cross-bedded sand dune and underlain by laminated sand and gravel above the NT2 wave cut surface. Note the wave cut fragmental rock clast.

(Fleming 1953; subsequently redefined and indirectly dated at c.130kyrs B.P.).

Distribution

The mudflow unit is widely distributed on the North Taranaki coastal plain based on its near continuous occurrence within the cover-beds of NT2 terrace along the coast. The thickening of the unit at sites adjacent to the Waitara River further inland suggest it was channelised down the Waitara River Valley. Small isolated remnants of the highest laharic aggradation surface within the portion of the Waitara River Valley that dissects the Eltham surface, probably relate to the Motunui laharic depostional event.

Due to meagre outcrop data, it remains unclear whether the Motunui laharic deposit originated from a youthful ancestral Egmont Volcano or an actively degrading Pouakai Volcano. It also remains uncertain whether or not the mudflow resulted from lateral transformation of a large volume debris avalanche deposit because no fragmental rock clasts or remnants of a hummocky surface physiography have been identified.

7.9 Discussion

At least eleven debris flow units post-dating the c.22.5kyr Aokautere Ash have been recognised in northern and north-eastern Taranaki, whereas only two mudflow units have been recognised. Both categories of lahar deposits originating from Egmont Volcano, are either confined within radial drainage channels or have spilled over onto the inter-fluve surfaces of the ring-plain. Most units extend from the Egmont ring plain to the North Taranaki coastline after having been completely or partially channelised within prominent north trending drainage paths. Most

debris flows underwent proximal-to-distal transformation to hyperconcentrated flows and normal stream flows.

As both categories of lahar deposits appear to be markedly different in morphology, it is therefore reasonable to suggest that the mechanisms of generation were also quite different. An understanding of the mechanisms of debris flow formation has been obtained from numerous studies of the recent eruptions at Mt.St.Helens. Here a deflating pyroclastic surge has been observed to rapidly move downslope under the influence of gravity and to become transformed from a highly dispersed, air- and gas-mobilised state to a water-mobilised state (Janda et al. 1981; Pierson, 1985; Scott, 1985). Smaller debris flows were also generated by the transformation from eruption-induced snowmelt surges. In Taranaki, the generation of prehistoric debris flows by either transformation is strongly suggested by the dominantly homogeneous lithology of the deposits and the occurrence of synchronous tephra deposits which indicate concurrent eruptive activity. The occurrence of lava bombs enclosed within some lithologically similar debris flows further support the suggestion that debris flows were eruption-induced. The sorting of debris flows and their minor clay content, also suggests that they formed mainly from volcanic materials previously subject to progressive or selective sorting. This could have been by the winnowing of elutriated fines from a deflating air-moblised pyroclastic surge and/or subsequent fluvial sorting in stream channels.

The main source of water for downstream dilution of debris flows was probably eroded snow and ice, which was incorporated by turbulent mixing into the flow along with associated slope talus. Ground water expelled together with the rock debris during an initiating eruptive event may have also contributed to the water content of some flows.

Mudflows with a high clay component are considered to be derived from volcanic materials not selectively sorted. How mudflows were generated at Egmont Volcano and how water and clay were incorporated into the flows in a manner that clearly differs from that of debris flows remains at this stage speculative.

CHAPTER 8

8.0 DEBRIS AVALANCHE DEPOSITS

8.1 Introduction

Deposits of fragmental debris at the base of Egmont Volcano display a surface of numerous hills and small mounds. In early geological surveys these "conical hills" were considered to be a series of small independent volcanic vents (de Clarke, 1912; Morgan and Gibson, 1927). Bossard (1928) later suggested that these hills were blisters on lava flows. It was Grange (1931) who was first to argue that they were remnants of a huge lahar flow based on their similarity to other volcanic mudflow deposits, a view that attained general acceptance (Cotton, 1969; MacDonald, 1972; Williams and McBirney, 1979).

Neuman van Padang (1939) and van Bemmelen (1949) attributed the hills at the base of several Indonesian volcanoes to "landsliding or avalanching" of a sector of the volcanic cone, and the deposits were described as laharic breccias. In Japan, research prior to the 1980 Mt. St. Helens eruption suggested that these deposits differed from lahars. Murai (1961) used the term "dry mudflow" to discuss debris avalanches emplaced by "gravitational forces without the agency of water". Mizuno (1964) also distinguished fragmental deposits of "avalanche type" from those of "flow type". Then in 1975, Ando and Yamagishi concluded that many of the "mudflow hills" at the base of Japanese volcanoes actually formed by either cold or hot avalanches. Nakamura (1978) emphasised that the 1888 Bandai deposit was not water saturated, and introduced the term "volcanic dry avalanche" to distinguish deposits of such avalanches from lahars. The 1980 Mt.St.Helens eruption was the first instance in which details of a large volcanic debris avalanche were documented at the time of emplacement and this has provided a model for interpretation of

similar deposits elsewhere. The incompletely water saturated 1980 Mt.St.Helens deposit (Voight et al. 1981) was termed a "rockslide avalanche" (Voight et al. 1983) or a "rockslide-debris avalanche" (Glicken et al. 1981). These two terms accurately describe the emplacement processes, whereas "debris avalanche" has been increasingly used for the resulting deposits (Soya and Katsui, 1981; Aramaki et al., 1981; Mimura et al. 1982); Newhall, 1982; Crandell et al., 1984).

In Taranaki, Neall (1979) mapped three Late Quaternary laharic breccia deposits extending west and south-west from Egmont Volcano. These deposits, showing development of mounds or "conical hills" (Morgan and Gibson, 1927), were named Pungarehu, Warea and Opua formations (Neall 1979) and later identified as debris avalanche deposits. The most spectacular of these three avalanche deposits is the Pungarehu Formation with an estimated minimum volume of 6 - 7.5km^3 (Neall, 1979; Ui et al., 1986). This deposit was mapped from 10 to 27km away from the present summit and covers an area of approximately 200 - 250km^2.

On the eastern and north-eastern lower flanks of Egmont Volcano, two further Late Quaternary deposits (Ngaere and Okawa Formations) are identified in this study and interpreted to have formed from debris avalanches which laterally transformed into mudflows. In this study, Okawa Formation has been mapped, however, further mapping is required to more fully elucidate the extent of Ngaere Formation in central and south-eastern Taranaki.

8.2 Nomenclature

The main internal structures of both deposits can be sub-divided into two major components: 1) fragmental rock clasts (hereafter referred to as 'FRC'), and 2) matrix.

A FRC is here defined as a fragmented or deformed piece of lava or layered volcaniclastic material commonly preserving stratification and/or intrusive contacts formed within the original volcanic edifice. In eastern Taranaki the most commonly recognised FRC is andesitic lava which is usually brecciated, forming a diamicton of homogeneous composition. The scheme of Sundell and Fisher (1985) has been used to define the FRC's i.e.. **boulder** (0.256 - 10m), **megaboulder** (10 - 100m), **block** (100 - 1000m) and **megablock** (1 - 10km). In addition, a **gravel** sized class of FRC's (0.002 - 0.256m) is recognised. In this study the matrix is here referred to as - **inter-clast matrix** for all the material within the deposit surrounding the FRC's and less than 0.002m in diameter. It should not be confused with the matrix of a FRC which is here termed **intra-clast matrix**. Inter-clast matrix includes all blended, unsorted and unstratified parts of the deposit comprising material ranging in size from clay to very coarse sand. Incorporated within the inter-clast matrix are clasts of plastically distorted soil, lignite and tephra layers, clasts of variable degrees of rounding and wood fragments derived from the terrain beneath. Inter-clast matrix is more abundant in inter-mound areas and is predominant in the distal and lateral margins of the deposit.

The area of a deposit where FRC's are predominant and a hummocky surface develops, was mapped as an **axial facies** by Neall (1979) and as a **block** facies by Crandell et al. (1984). In contrast the area where inter-clast matrix is predominant was mapped as **marginal facies** by Neall (1979), as **matrix facies** by Crandell et al. (1984), as **main** facies by Mimura and Kawachi (1981) and **matrix mixture** by Ui (1983).

The lithology and relative proportions of inter-clast matrix to FRC's varies not only throughout each debris avalanche deposit but between the deposits as well. These variations are influenced

by the composition of the original volcanic edifice, type and scale of the initial volcanic event, and also the occurrence of nearby ridges, channel systems and lowlands.

In mapping prehistoric debris avalanche deposits in eastern Taranaki, an adaptation of axial and marginal facies nomenclature introduced by Neall (1979) is preferred as an alternative to block and matrix facies. Usage of this nomenclature is considered more appropriate since it distinguishes the mapping units from being confused with sedimentological descriptions.

Both avalanche deposits on the eastern Egmont ring plain can be sub-divided into three facies: axial a, axial b and marginal facies, on the basis of lateral variations between the FRC's and inter-clast matrix (Figure 8.01).

Axial a facies is here defined as those mappable areas where fragmental rock clasts dominate with <30% inter-clast matrix and the surface physiography is dominated by a concentrated area of steep sloped hills and mounds with large basal diameters and smaller inter-mound areas.

Axial b facies is defined as those areas where the proportion of inter-clast matrix is sub-dominant to dominant (30-90%) relative to FRC's and the surface physiography is dominated by sparsely distributed mounds and hills of small basal area with more extensive inter-mound areas. This facies corresponds with the **mixed block and matrix facies** of Glicken (1986).

Marginal facies is defined as those areas where the proportion of inter-clast matrix is dominant (>90%) relative to FRC's and the surface physiography is planar without mounds or hills.

FIG. 8.01 Debris Avalanche Facies

Axial a Facies



Axial b Facies



Marginal Facies



8.3.0 Ngaere Formation
(new formation)

The Formation is named after the east Taranaki farming community of Ngaere situated on State Highway 3, 4km south of Stratford Borough.

8.3.1 Upper and Lower Contacts

In areas of the south-eastern sector dominated by mounds and hills (axial a facies), the upper contact of Ngaere Formation varies from sharp to diffuse and usually separates megaboulders and blocks below, from **Pot.c** of **Poto Tephra**, above (Plate 8.01). The lower contact of Ngaere Formation in these areas has not been observed.

In the extensive inter-mound areas of the south-eastern sector (axial b facies), the lower contact is usually sharp and planar, directly overlying **Pot.b** of **Poto Tephra** (Plates 2.25 and 2.26).

In areas of the marginal facies, the upper contact of Ngaere Formation is distinct and separated from **Aokautere Ash** above, by <c.0.08m of medial material (Plate 3.03). Here the lower contact of Ngaere Formation is sharp and separated from **Tui.d** of **Tuikonga Tephra** by <c.0.40m of medial material (Plate 2.31).

8.3.2 Morphology

The most conspicuous feature of Ngaere Formation on the south-eastern lower flanks of Egmont Volcano, is the extensive hummocky landscape between Manaia Road and Pembroke Road (Plate 8.02). This landscape can be sub-divided into two physiographic types - (a) clustered hummocks with large basal areas and small inter-mound areas (occupied by axial a facies), and (b) scattered



Plate 8.01: Upper contact of **Ngaere Formation** at its best section in the vicinity of Mahoe (Q20/108037). Here **Ngaere Formation** is overlain by units of **Poto Tephra**. The position of **Aokautere Ash** intercalating **Poto Tephra** is indicated by arrows.



Plate 8.02: Subdued surface physiography of **Ngaere Formation** (Axial a facies) vicinity of upper Palmer Road in the south-east sector.

hummocks with variable basal diameters and extensive inter-mound areas (occupied by axial b facies). In this sector, a thick succession of airfall mantle has reduced the physiographic expression of these hummocks to such an extent that only the largest FRC's have surface expression.

Clustered hummocks (axial a facies), extend eastward from the Egmont National Park Boundary to State Highway 3, in the vicinities of Stratford and Midhurst (c.18 - 20km east of the present Egmont summit). Scattered hummocks (axial b facies) have also been identified along State Highway 3 between Eltham and Stratford, c.23km south-east of the present summit. The most distal mounds correlating with Ngaere Formation are located just north of Matapu c.25km south-east from the present summit.

On the eastern lower flanks of Egmont Volcano, north of Pembroke Road, individual mounds and mound clusters of Ngaere Formation protrude from beneath surficial deposits of **Te Popo debris flows** and **Ngatoro Formation** which are confined to the flat, tephra mantled inter-mound areas. Further north, hummocks of Ngaere Formation occur on elevated terrain in the vicinity of Waipuku and Croydon Roads (c.18km east from the present Egmont summit).

The density of mounds per km^2 as determined from aerial photographs, decreases with increasing distance from Egmont Volcano. Distally in the vicinity of Ngaere, mound densities are generally very low seldom exceeding c.35 per km^2 but nearer to Egmont Volcano mound densities exceed 135 per km^2 in small areas between Kaponga and Cardiff.

8.3.3 Lithology

Fragmental rock clasts are the most distinctive component of Ngaere Formation. They most commonly occur as elongate or tabular, grey to very dark grey, andesitic breccia with an intra-

clast matrix of identical composition and may preserve stratification formed within the original volcanic edifice (Plate 8.03).

The contacts between FRC's are often sharp and irregular. With increasing distance from Egmont Volcano, the proportion of fragmental rock clasts steadily decreases relative to the inter-clast matrix. Similarly with increasing distance from source, progressive disaggregation and plastic deformation reduces the average diameter of FRC's to **gravel** size (Plate 8.04). A corresponding increase in the overall sphericity of some FRC's was also observed.

The most variable and heterogeneous component of Ngaere Formation is inter-clast matrix. This is recognised by lack of bedding and heterolithologic composition. The dominant colour of the inter-clast matrix is generally yellowish brown (10YR 5/4 to 5/8) being very similar to the medial material underlying Ngaere Formation (e.g. Plate 2.30). Pale brown, yellow, grey and reddish yellow colours predominate in the FRC and pumice fragments. Variations of these colours appear to be influenced by the relative proportions of the original source materials, attrition of FRC's and material incorporated from units underlying the formation. In the north-eastern sector, a wedge of Ngaere Formation is exposed unconformably overlying a progressively older sequence of medial inter-beds and tephra beds along a road cut adjacent to the Manganui River (e.g. **Section 22** of Appendix 1 and Figure 2.22). Here a 0.70m sequence comprising the uppermost tephra bed (Tuikonga Tephra) has been locally incorporated and plastically deformed within the Formation (Plate 3.03).



Plate 8.03: Orange pumiceous lapilli beds preserved within a fragmental rock clast of **Ngaere Formation** at Q20/220057, near Stratford Borough. These beds appear to represent stratification formed within the original volcanic edifice.



Plate 8.04: A boulder-sized fragmental rock clast within **Ngaere Formation** exhibiting dissagregation during flowage. Reference section on Eltham Road (Q20/114969).

8.3.4 Distribution

Following initiation of the avalanche the constituent materials were broken up, mixed and dispersed throughout a minimum area of 320km^2 on the eastern and south-eastern lower flanks of Egmont Volcano. East of State Highway 3 the Formation has yet to be mapped. However, the occurrence of hummocks in this vicinity and outcrops of Ngaere Formation exposed near the junction of Standish and Ahuroa Roads (**Section 21**) (c.27km east from the present summit) suggest that the Formation extends considerable distances further east towards the Tertiary hill country. It seems probable that the Formation was also channelled down the Patea River valley.

Further south, in the vicinity of Eltham Borough, the distribution of Ngaere Formation appears to have been influenced by the Eltham Lahar planeze. Ngaere Formation was channelled between Eltham Lahar remnants, down the Waingongoro River where it appears to have obstructed natural drainage from Eltham Swamp just south of Eltham Borough. Eltham Lahar remnants further south-west appear to have been buried beneath Ngaere Formation.

Hummocks and debris of Ngaere Formation border the western margin of Ngaere Swamp but their extent further east is unknown. A narrow ridge of Tertiary mudstone (along Rawhiti Road) separates Ngaere Swamp from Eltham Swamp. On the north side of this narrow ridge, the ground surface of Ngaere Swamp is notably higher in elevation than the surface of Eltham Swamp. This elevation difference may be due to greater disruption of drainage outlets by Ngaere Formation and differential infilling of Ngaere Swamp compared to Eltham Swamp.

The extent of Ngaere Formation north of Waipuku Stream is extremely difficult to ascertain, because the Formation is buried

beneath thick deposits of younger lahars and tephra. Ngaere Formation is exposed in the vicinity of Inglewood (e.g. **Section 16** of Appendix 1; Plate 2.30) and along the Manganui River (e.g. **Section 22** of Appendix 1). Ngaere Formation can be recognised within the confines of the Waitara River valley further north at Q19/207364 (Plate 2.31) and at Q19/194390.

The extent of Ngaere Formation is extremely difficult to ascertain west of Manaia Road, and south of a line extending between Kaponga and Matapu. In these areas adequate exposure is severely lacking. A >4m thick mudflow deposit is exposed at the junction of Skeet and Upper Glenn Road, c.12km south-west of Kaponga (**Section 15**), which is here correlated with Ngaere Formation since it closely underlies **Pot.c** to **Pot.e** of **Poto Tephra**, as well as **Aokautere Ash** (Plate 2.29).

Also, near the South Taranaki coast (c.35km south-east of the present summit) a thin (<0.3m) mudflow deposit is exposed at a site c.1km east of Ohawe Beach Road (Plate 8.05). This mudflow deposit, closely underlies **Aokautere Ash** and overlies Last-glacial grey, massive sands and is thus here correlated to Ngaere Formation.

From this meagre outcrop data it appears that Ngaere Formation is also extensively distributed over the north-east, south-east and south portions of the Egmont ring plain. It also appears that Ngaere Formation was channelled down the Manganui/Waitara River valley to the North Taranaki coast (Plate 8.06). The 320km^2 areal extent of Ngaere Formation is therefore considered a minimum estimate, and a maximum estimate may total 500km^2. At present, Ngaere Formation is calculated to have a minimum volume of 5.85km^3.



Plate 8.05: **Ngaere Formation** (mapped as marginal facies) exposed near Ohawe Beach, at the south Taranaki coast. The position of the trowel indicates the location of **Aokautere Ash**. Note the enthralled stance of the field assistant.



Plate 8.06: **Ngaere Formation** (mapped as marginal facies) exposed at Q19/207364, near Manganui Road, in the Waitara River Valley. **Tuikonga Tephra** underlies the Formation at the level of the white marker card.

8.3.5 Age

Ngaere Formation is estimated to have an age range of between c.22.5 and 23kyr B.P. This estimate is based on its closely underlying position with respect to the c.22.5 kyr **Aokautere Ash.**

8.3.6 Type Section

The type section of Ngaere Formation is designated at a prominent north facing road cut opposite Cardiff Road Walkway Carpark, 100m west of the Waingongoro River Bridge, on Opunake Road (**Section 7** of Appendix 1 and Figure 2.22; Plate 2.26). This type section has been chosen because it is the same as that designated for Mahoe Tephra, Paetahi Tephra, Poto Tephra and Kaihouri tephra, and shows clearly their stratigraphic relationships. A detailed description of Ngaere Formation at this section is given in Chapter 2.

8.3.7 Best Locality

A best locality is designated here at an east-facing road cut just south of Mangatoki Stream bridge on Upper Palmer Road at Q20/108037. Here, **Pot.c** to **Pot.e** of **Poto Tephra**, as well as, **Aokautere Ash**, are the lowermost tephric deposits that directly mantle the Ngaere Formation (Plate 8.01).

8.3.8 Correlation

Initially, deposits of Ngaere Formation were tentatively correlated with those of Pungarehu Formation (Neall 1979). The andesitic tephra beds most useful in identifying Ngaere Formation into the eastern sector of Egmont Volcano are not well preserved to the west due to limited westward distribution. Since wood fragments within Pungarehu Formation were dated (NZ1623A) at 22,100 +/- 600 years B.P. and closely correspond in age with deposits of Ngaere Formation, provisional correlation was then based upon equable age.

However, recent fieldwork in Western Taranaki suggests that the Pungarehu Formation immediately post-dates deposition of the Aokautere Ash (Neall pers.comm. 1988), whereas, the Ngaere Formation closely pre-dates deposition of Aokautere Ash. From this evidence, it appears that Ngaere and Pungarehu Formations represent two similar but chronologically distinct deposits that relate to the same eruptive episode.

8.3.9 Reference Localities

A total of **ten** reference localities throughout the eastern Taranaki Region are designated for the Ngaere Formation. The location of these sites are as follows:

1. North-west facing road cut on Opunake Road 0.5km west of Mangatoki Stream Bridge and 0.9km east of the junction of Opunake Road with Upper Palmer Road, (**Section 6**), (Q20/119027).

2. Prominent south facing road cut on Opunake Road, 0.1km east of Tuikonga Stream Bridge and c.2.6km east of Cardiff Road junction, (**Section 7**), (Q20/158043).

3. North-facing road cutting between corner of Glenn and Skeet Roads, and stream bridge 0.1km further westward, (**Section 15**), (P20/042908) (Plate 2.29).

4. West-facing farm cut behind milking shed, Browns Property, Durham Road, c.2.6km north-east from State Highway 3, (**Section 16**), (Q19/171259) (Plate 2.30).

5. South-west facing road cutting <0.1km south-east of Standish and Ahuroa Road junction, (**Section 21**) (Q20/272094).

6. Prominent road cut either side of Bristol Road, 0.1km east of Manganui River Bridge, (**Section 22**), (Q19/213296) (Plate 3.03).

7. Prominent east-facing road cut on State Highway 3, 0.1km north of junction with Croydon Road, (Q20/182153) (Plate 4.03).

8. North-facing road cut, 0.1km west of disused Dairy Factory on Finnerty Road, (Q20/215009) (Plate 8.07).

9. Prominent south-facing road cut, 0.2km west of State Highway 3 on Climie Road, (Q20/218025) (Plate 8.08).

10. Prominent Road cut either side of Eltham Road, 0.1km east of Kapuni Stream, (Q20/114969) (Plate 8.09).

8.3.10 Associated Air-fall Deposits

Directly underlying Ngaere Formation at its type section (c.15km south-east of the present summit) is a c.0.06m thick, very well sorted, reverse graded, dark grey, monolithologic, medium to coarse sandy ash (**Pot.b** of **Poto Tephra**) (Plate 2.27). This unit is exposed at two other sites (Q20/218025 and Q20/215009) located c.23km south-east from the present summit (Plates 8.07 and 8.08 respectively). Here, **Pot.b** comprises a c.<0.03m thick, discontinuous ash. It is clear that the texture and sorting characteristics of **Pot.b** compared to representative samples of deposits from the May 1980 eruptions of Mt. St Helens (Figures 8.02, 8.03 and 8.04), represents a tephra-fall eruptive that immediately preceded the onset of the avalanche. This unit is not associated with an equivalent '**pyroclastic density current**' (an informal term encompassing both pyroclastic flow and surge; Siebert et al. 1987). The mineralogy of this tephra comprises plagioclase, clinopyroxene, titanomagnetite, hornblende and minor olivine, typical of many Egmont eruptives (Stewart pers. comm. 1989). Particles are predominantly holohyalline, ranging to hollocrystalline, and silica contents of glass fall in a narrow range of 57 - 60 wt % suggesting derivation from a magma rather than fragmentation of pre-existing lavas during an explosive event. This tephra represents a pulse of new magma entering the volcano and leading to a new cycle of activity.

This new cycle of activity is represented by a sequence of thirteen, very closely spaced pumiceous and scoriaceous tephra-fall beds (**Pot.c** to **Pot.o**) that directly overlie Ngaere Formation in the south-east lower flanks (see Plate 2.25).

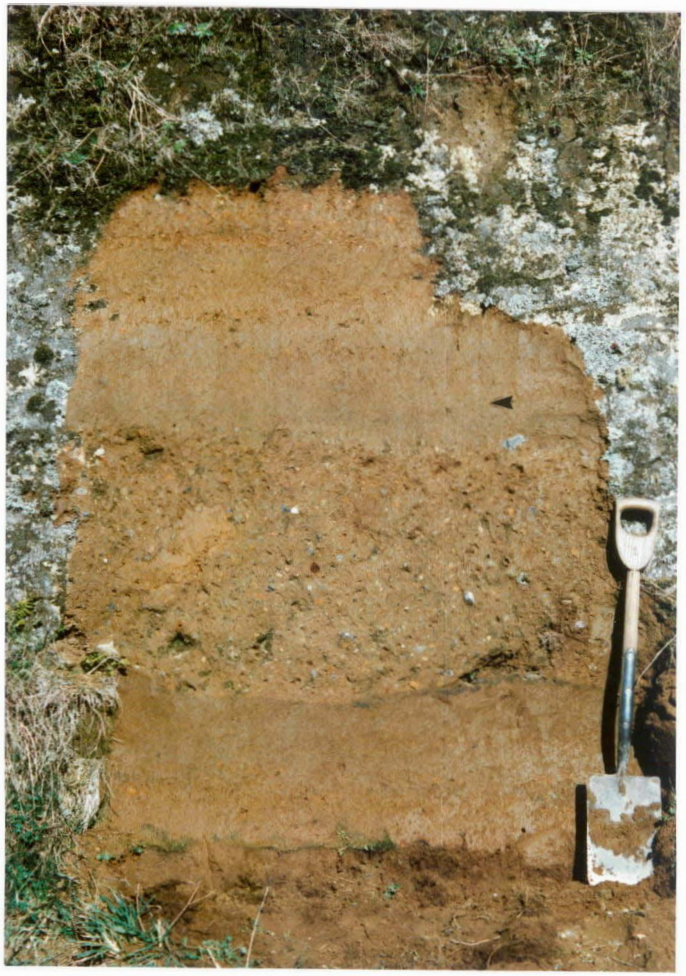


Plate 8.07: **Ngaere Formation** with underlying precursory eruptive (**Pot.b**) at reference section on Finnerty Road (Q20/215029). The position of **Aokautere Ash** in the section is indicated by an arrow.



Plate 8.08: **Ngaere Formation** with underlying precursory eruptive (**Pot.b**) at reference section on Climie Road (Q20/218025). The position of **Aokautere Ash** intercalating prominent units of **Poto Tephra** is indicated by an arrow.



Plate 8.09: **Ngaere Formation** at reference section on Eltham Road (Q20/114969). Note the absence of the **Pot.b** at this section.

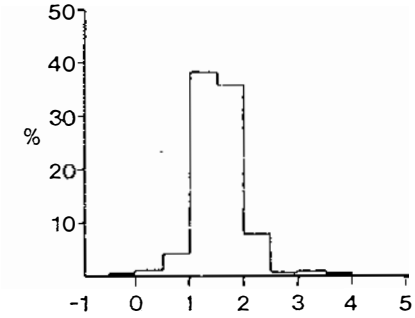
These units, clearly represent a post-avalanche phase of high frequency eruptive activity and active reconstruction of a lava dome or central cone. It was during this post-avalanche eruptive phase that another large volumed debris avalanche deposit (Pungarehu Formation) was initiated from the western side of the reconstructing Egmont Volcano.

The association of air-fall tephra deposits with Ngaere Formation is consistent with **Bezymianny-type** eruptive activity (Seibert 1984; Siebert et al. 1987).

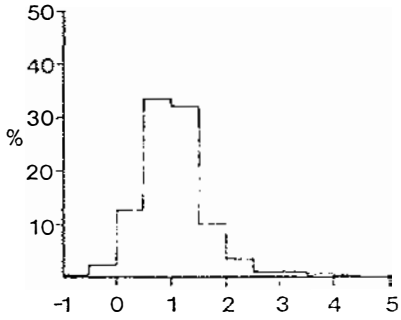
FIG. 8.02 **Grain Size Distribution of Unit Pot.b**

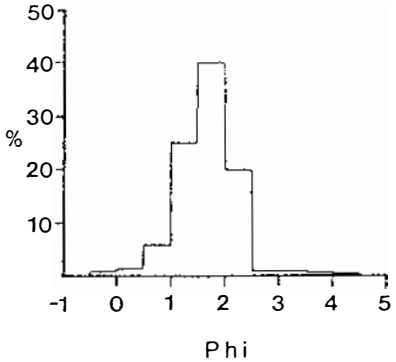
Section 7 (Q20/158043)
c. 14 km from Egmont Volcano Summit

A. Lower layer of Unit Pot.b



B. Upper layer of Unit Pot.b





Climie Road (Q20/218025)
c. 23 km from Egmont Volcano Summit

FIG. 8.03 Cumulative percent curves of Unit Pot.b compared to representative samples of deposits from the 1980 eruptions of Mt. St. Helens (Kuntz et al 1981)

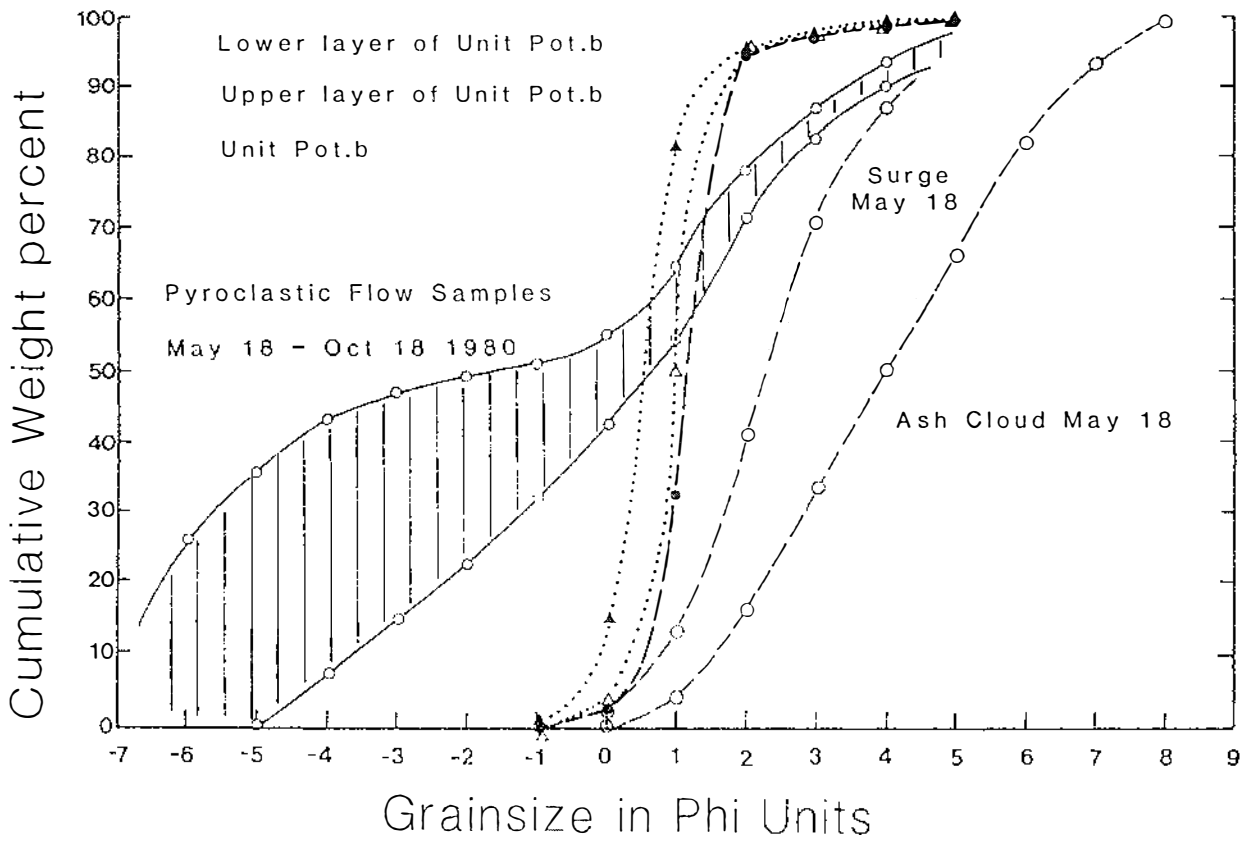
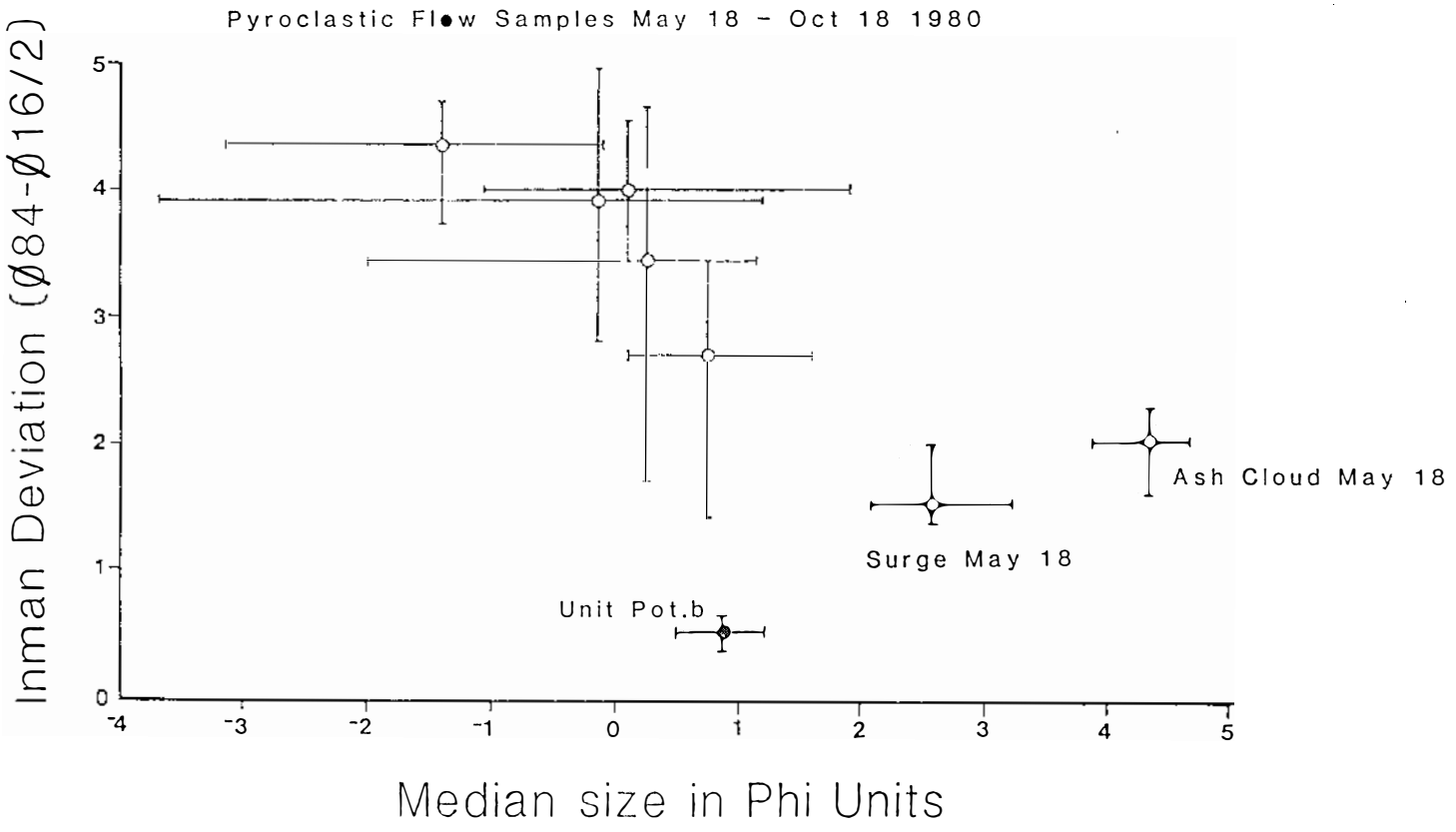


FIG. 8.04 Inman deviation versus Median Phi size of Unit Pot.b compared to representative samples of deposits from the 1980 eruptions of Mt. St. Helens (Kuntz et al 1981)



8.4.0 Okawa Formation
(new formation)

Okawa Formation is named after Okawa XX Trig (Q19/200366), 0.8km north-west of the Te Arei and Everett Road junction and c.2km west of the Manganui and Waitara River junction.

8.4.1 Type Section
The type section of **Okawa Formation** is here designated as a prominent north-facing cliff exposure at Airedale Reef, 1.4km east of Waitara River Mouth (Q19/178461) (**Section 27** of Appendix 1 and Plate 8.10). The **Okawa Formation** type section is also the type section for the **Epiha Tephra** described in Chapter 2.

8.4.2 Upper and Lower Contacts
Along the North Taranaki coastline, Okawa Formation is separated from lowermost **Epiha Tephra** by <0.20m of peaty muds and lignite above (Plate 8.11). At the type section Okawa Formation is separated from a thin unnamed pumiceous fine lapilli below by <0.01m of lignitic material (Plate 8.12). Further inland towards Egmont Volcano, this unnamed lapilli and **Epi.a** and **Epi.b** overlying the Okawa Formation cannot be identified because they are not enclosed within lignite and appear to have been subject to post-depositional soil mixing and weathering. Hence only **Epi.c, Epi.d** and **Epi.e** of **Epiha Tephra** are preserved in medial material overlying Okawa Formation. In the vicinity of Lepperton (e.g. **Section 18** of Appendix 1), the **Okawa Formation** is separated from **Epi.c/d** and **Epi.e** of **Epiha Tephra** above, by medial material of **S5.** Here the lower contact of the mudflow deposit is distinct and wavy, unconformably overlying **L5.**

At two sites near Inglewood, the upper contact of Okawa Formation is an unconformity which separates boulder to block sized FRC's from the overlying c.23.5 kyr Tuikonga Tephra. The lower contact of Okawa Formation has not been so far observed in this vicinity.

8.4.3 Age

Although not dated directly, the Okawa Formation is indirectly dated at c.100kyr B.P. This estimate is based on the position of the Okawa Formation interbedded with S5. This unit is correlated to the global warm period and high sea level transgression of oxygen isotope sub-stage 5c as shown from the deep sea oxygen isotope record (Shackleton et al. 1983) (see Chapter 4). The deposition of Okawa Formation during this warm interval of the Last Interglacial is supported by palynological evidence obtained from the lignitic material enveloping Okawa Formation at its type section (see Chapter 11).

8.4.4 Morphology

Three principal areas are identified where mounds are concentrated in clusters. The first of these occurs in the vicinity of Inglewood Borough on the north-eastern margin of the Egmont ring plain (20km from the present Egmont summit). Here mounds are principally concentrated within a c.2.5km wide belt, that extends north-east, parallel with Bristol Road along the downthrown side of the Inglewood Fault, to just west of the Waitara River (c.33km from the present Egmont summit) (Plate 8.13). Hummocky mounds are also conspicuous on a small area of elevated and dissected terrain of the Eltham Lahar planeze immediately north-east of Inglewood where the Okawa Formation surmounts the Inglewood Fault scarp. Mounds are also present on either side of the Waiongana Stream valley entrance immediately to the north. South-east of Inglewood, scattered mounds protrude from beneath thick surficial deposits of Warea Formation

correlatives and Ngaere Formation. Further towards Egmont Volcano, mounds have little or no surface expression, because they have been buried beneath a thickening succession of younger volcaniclastic material.

The second area where mounds are concentrated, occurs on the north Taranaki coastal plain, immediately north of the Eltham Lahar planeze. Here mounds form a distinct hummocky belt c.1km either side of Waiongana Stream, that extends north of Lepperton to the present coastline (38km from the present Egmont summit). A third area of scattered mounds is conspicuous in the area between the Waitara River and Ngatimaru Road, just south-east of State Highway 3 (c.42km from the present Egmont summit). These mounds are situated just seaward of a high fossil cliff that separates NT2 terrace from NT3 terrace further inland (this study; see Chapter 9). They appear to present the point where the original avalanche changed from being confined within the Waitara River channel to being unconfined on the coastal plain.

Mound dimensions are extremely difficult to ascertain. On the Egmont ring plain, irregular and elongate mounds of Okawa Formation are usually mantled by a very thick (>8m) succession of medial beds. Mound heights and basal diameters may be further accentuated by aeolian wedges of either sands (Katikara Formation) or localised overthickened medial material. With increasing distance north from the ring plain, the mounds gradually become equidimensional in shape, are mantled by a progressively thinner sequence of cover beds, and progressively decrease in basal diameter and height. Immediately north-east of Inglewood, some mounds were measured with basal diameters as much as 350m across and heights of 45m above the inter mound areas, whereas at the north coast, most mounds have basal diameters less than 25m and heights less than 10m.

In the first two hummocky mound belts, the largest mounds appear to be concentrated near the centre, with mound basal diameter and density steadily decreasing either side of the 'axis'. In the other mound area south-east of Waitara, there appears to be no spatial differentiation of mounds according to basal diameter across the deposit.

Within the Waitara/Manganui River valley as well as the Waiongana Stream valley, a prominent terrace remnant is preserved from the Okawa avalanche event. Rapid emplacement of this deposit appears to have been followed by a lengthy interval of river degradation. Preservation of the terrace remnant was dependant on no subsequent larger volume, aggradational events.

8.4.5 Lithology

Okawa Formation is predominantly exposed in quarry sites located in areas mostly mapped as axial a facies. At these sites the most conspicuous component of the deposit is fragmental rock clasts; inter-clast matrix is usually sub-ordinate and seldom observed. The most frequently exposed FRC's are tabular or elongate blocks and megaboulders composed of indurated, grey to very dark grey andesitic breccia. Occasionally observed are elongate and sometimes plastically deformed megaboulders and boulders, comprising intensely altered hydrothermal and solfataric debris. Slightly deformed, unconsolidated, stratified blocks that retain their primary bedding appear to be also common in this facies (Plate 8.14). Mounds in axial a facies often contain many megaboulder to block sized FRC's which are usually in sharp and irregular contact with each other (Plate 8.14). However in the same facies near the North Taranaki coast, most mounds appear to be cored by a single boulder-sized FRC (Plate 8.15).



Plate 8.10: **Okawa Formation** type section at Airedale Reef (Section 27; Q19/178461). Here the Formation directly overlies highly carbonaceous muds with rata-rimu tree stumps in position of growth (also exposed at low tide in foreground of photo). Note the lignite deposit in the depression upon the upper surface of the Formation.



Plate 8.11: Woody lignite and interbedded units of **Epiha Tephra** overlying **Okawa Formation** at Q19/121445 (Section 25), near the Waiongana Stream mouth.



Plate 8.12: Woody lignite with thin, unnamed pumiceous coarse ash and fine lapilli beds underlying **Okawa Formation** at its type section (Section 27; Q19/178461).



Plate 8.13: View of Egmont Volcano from the vicinity of Section 19 in the north-east sector. Hummocky surface physiography of **Okawa Formation** (mapped as axial a facies) visible in foreground.



Plate 8.14: Block-sized FRC's in sharp and irregular contact with each other at Fredricksons Quarry, adjacent to Bristol Road (Q19/193293). Note deformed tephra interbeds in far right of photo.



Plate 8.15: Mound of **Okawa Formation** cored by a single megaboulder-sized FRC near the Waiongana Stream mouth at Q19/125448.

Smaller FRC's of gravel and boulder size, retaining primary bedding are sometimes exposed suspended in the inter-clast matrix as far north as the coast. The primary stratification of these unconsolidated and layered FRC's may sometimes be offset along small planes normal to bedding (Plate 8.16). This deformation is interpreted to have resulted from local compressional stresses exerted on the clast during transport. In the axial b facies, gravel sized FRC's are often found in very close proximity to boulder sized FRC's of identical lithology and similar texture of intra-clast matrix (Plate 8.17). This suggests the FRC's were continually disaggregating and plastically deforming until all the intra-clast constituents were dispersed as discrete clasts within the inter-clast matrix.

In areas of axial b and marginal facies, fractured and partially offset gravel clasts (Plate 8.18), as well as a 'rock flour' rim enclosing larger clasts were noted within the intra-clast matrix of FRC's (Plate 8.19). These features suggest that grinding and fracturing of intra-clast constituents took place as the FRC's were plastically deformed during transport.

The average diameter of suspended clasts in Okawa Formation decreases towards the distal edge of the marginal facies. Okawa Formation in areas mapped as marginal facies, generally contains abundant angular to well rounded rock clasts, many plastically deformed rip-up clasts of lignitic (Plate 8.20) and medial material, and scattered wood fragments. Coarse grained pumiceous fragments are relatively uncommon. Stratified clasts of Tertiary siltstone are occasionally observed and exhibit features indicative of plastic deformation (Plate 8.21).



Plate 8.16: Primary stratification of an unconsolidated and layered FRC offset along small planes normal to bedding.



Plate 8.17: Gravel-sized FRC in close proximity to boulder-sized FRC of identical lithology and similar texture of intra-clast matrix.



Plate 8.18: Offset gravels within intra-clast matrix of boulder-sized FRC.



Plate 8.19: Rock-flour rim enclosing a large clast of identical lithology within intra-clast matrix of an FRC.



Plate 8.20: Plastically deformed rip-up clasts of lignite containing tephra inter-beds, near Airedale Reef.

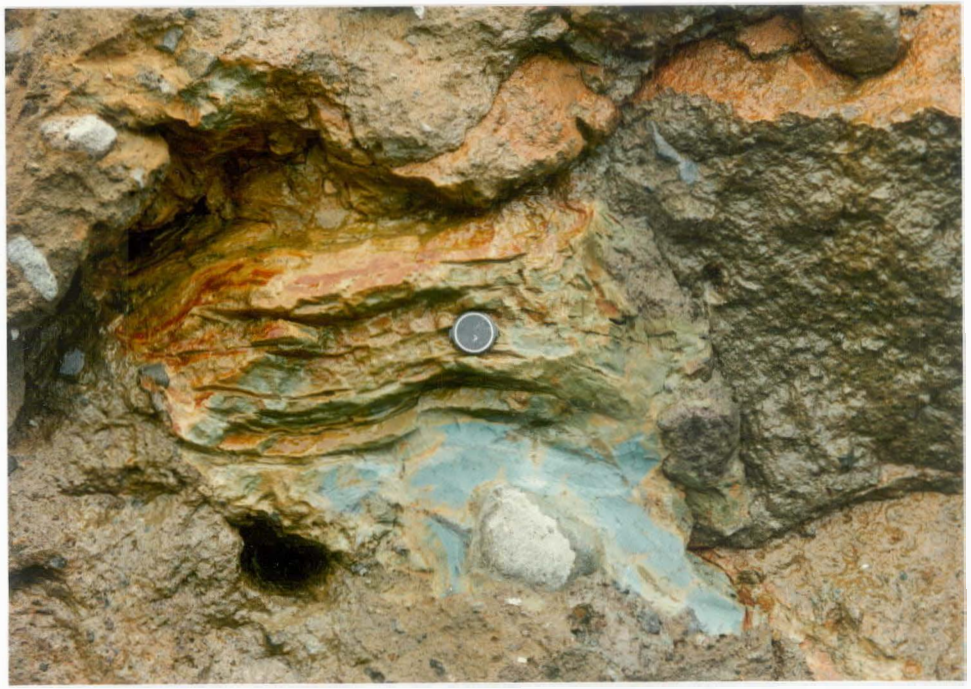


Plate 8.21: Rip-up clast of stratified Tertiary siltstone enclosing andesitic cobble.

8.4.6 Distribution

Okawa Formation has been mapped over a minimum area of 255km^2 in northern and north-eastern Taranaki and has a calculated minimum volume of 3.62km^3. Following initiation, the collapsing flank disaggregated to become a debris avalanche that initially travelled in a north-eastern direction from an ancestral Egmont Volcano. On encountering the Eltham Lahar planeze, just north-east of Inglewood (c.11km from the present Egmont summit) the avalanche had sufficient kinetic energy to partially surmount the planeze to the north of the Inglewood Fault scarp.

The major portion of the avalanche was then deflected north-east for c.7km along the Inglewood Fault scarp, before the main bulk entered the Manganui River valley and become channelled for a further c.18km northwards to the coast. That portion which did not flow down the Manganui River valley continued north-eastwards for a further 4km along the fault scarp to the present course of the Waitara River.

A subsidiary portion of the avalanche that surmounted the fault scarp at Inglewood, became channelled northwards along the Waiongana Stream valley. This valley, provided a closer and more direct route to the northern coastline than the main flow path down the Manganui/Waitara River valley.

When the avalanche emerged from the confines of the Waiongana valley, it spread laterally as a broad lobe across three extensive marine terraces. The two fossil cliffs separating these terraces were buried, subduing their surface physiographic expression. The axis of the avalanche remained parallel to the Waiongana Stream valley and is defined by a hummocky belt of prominent mounds that extend to near the Waiongana Stream mouth. A cross-section of this distal portion of the avalanche from axis

to margin, is continuously exposed in the coastal cliffs for c.2km southwest from the Waiongana Stream mouth. In this vicinity Okawa Formation drapes over a fossil cliff bounded at the inner edge of NT2 terrace and partially surmounts Last Interglacial sand dunes on the NT3 terrace. Here, the avalanche deposit is mostly enveloped by lignitic and carbonaceous clayey materials with numerous tephra inter-beds (Plate 8.22).

The other avalanche confined within the Manganui/Waitara River valley, appears to have only partially surmounted the higher marine terraces on the coastal plain. As it emerged from the confines of the valley it spread laterally to form an area of scattered debris mounds, just seaward of the fossil cliff cut by the NT2 marine transgression. This portion of the avalanche does not appear to extend further east than Otaraoa Road on the NT2 terrace.

8.4.7 Associated Air-fall Deposits

Closely underlying Okawa Formation at its type section is a c.0.01m thick, moderately sorted, yellow, dominantly pumiceous coarse ash and fine lapilli bed in lignitic material (Plate 8.12). This tephra bed provides a distal record of pre-avalanche magmatic activity at the ancestral Egmont Volcano.

Closely overlying Okawa Formation at its type section, is a sequence of at least seven, dominantly pumiceous units of **Epiha Tephra** (Plate 2.38). These units serve as a well preserved distal record of post-avalanche eruptive activity. The distal association of air-fall tephra deposits with Okawa Formation is consistent with **Bezymianny-type** eruptive activity (Seibert 1984; Siebert et al. 1987). However, at present there is no evidence nearer to source area that indicates an eruptive event either directly triggered the Okawa avalanche or immediately followed from the collapse. Hence, the possibility of seismically induced gravitational sliding of the ancestral cone cannot be discounted.

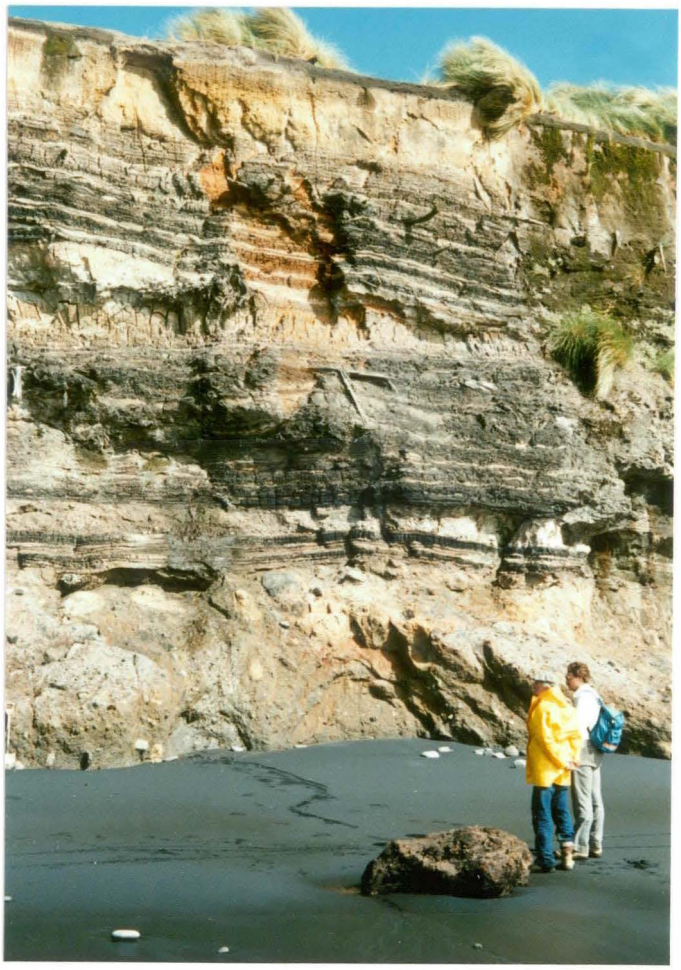


Plate 8.22: **Okawa Formation** mapped as marginal facies wedging out within the dominantly lignitic cover-beds of NT3 terrace mid-way between the Waiongana Stream mouth and Bell Block Beach along the North Taranaki coast.

Earthquakes generated by either volcanism, tectonism or sedimentary loading may have triggered the gravitational collapse.

8.5 Discussion

Both Ngaere and Okawa Formations appear to have originated from ancestral edifices of Egmont Volcano as large volume avalanches which distally developed into mudflows at c.23 and c.100kyrs B.P., respectively. In each instance, initial sliding of the ancestral cone appears to have been by rapid en masse movement. Both sliding masses began breaking up on the lower flanks of the ancestral volcano and spread laterally. The avalanche that emplaced the Okawa Formation was probably slowed by the physiographic barrier of the Eltham Lahar planeze causing the mass to bifurcate and become channelised northwards to the coastal plain. Ngaere Formation, on the other hand, was emplaced virtually unconstrained on the ring plain.

As sections of the ancestral cone initially slid, they broke into many rigid, heterogeneous large fragmental rock clasts. Many of these are relatively undeformed and appear to have only rotated slightly. Indurated andesite lavas and volcaniclastics remained as large fragmental rock clasts supported by other FRC's and a minor inter-clast matrix. Others were surrounded by a mobile inter-clast matrix enabling them to fracture, deform and distintegrate into smaller FRC's.

As the mass flowed seawards, additional inter-clast matrix was generated by the progressive deformation and disaggregation of FRC's and by the incorporation of medial material and other poorly consolidated sediments from beneath the moving body of the avalanche. The dominant mode of transport probably changed from

slide to flow as the ratio of inter-clast matrix to FRC's increased. The inter-clast matrix probably behaved as a high yield strength material supporting and hence transporting the FRC's away from source.

The overall size of the two deposits, distance of transport and thickness of material appears to have been controlled by the total volume of the material involved in the initial slide. The combined effects of increasing friction at the base, physiographic barriers, loss of high pore-fluid pressures and the lack of further material from source probably initiated cessation of motion. Rapid burial of the debris avalanche deposits by tephra and lahar deposits has resulted in minimal post-depositional modification of their upper surfaces.

CHAPTER 9

9.0 STRATIGRAPHY OF THE MARINE TERRACES

9.1 Previous Work

In 1953, Fleming classified the late Pleistocene terrace deposits of the Wanganui district into Rapanui, Brunswick and Kaiatea Formations. When Rapanui Terrace was first mapped in Wanganui district its polygenetic character was recognised by the use of the term "sub-Rapanui terrace" (Fleming 1953, p.42). During geological mapping of Taranaki for the Geological Map of New Zealand 1:250,000 (Sheet 7), Grant-Taylor (1964a) found there was an additional marine terrace between terraces that he correlated with the Rapanui and Brunswick Terraces. The name Rapanui then became restricted to the lower seaward terrace and the higher terrace was named Ngarino. This nomenclature was published by Grant-Taylor (1964a; 1964b) who used the terms Kaiatea, Brunswick, Ngarino and Rapanui for terraces in Western Taranaki which he correlated with those of Wanganui. These names were also used on the geological map of the area (Hay 1967). The basis upon which these correlations were made is unclear but they were accepted in a later study of North Taranaki terraces by Chappell (1975).

In Chappell's later study, two terraces, which he informally named NT2 and NT3, were mapped below c.50m elevation, north of Urenui and were correlated to the Rapanui and Ngarino Terraces of Wanganui described in an earlier publication by Dickson et al. (1974). NT2 terrace dominates the coastal plain north of Whitecliffs. However, in the Urenui area immediately to the south, the terraces were interpreted to broaden with NT2 terrace becoming subordinate to NT3. Uplift rates based on these terraces were calculated to be essentially constant at 0.3mm/yr.

In this study, five uplifted marine terraces are mapped immediately south of Urenui, on the North Taranaki coastal plain. The stratigraphy of individual terraces is presented in this section, in chronological order from youngest to oldest.

9.2 NT1 TERRACE

NT1 terrace is a newly identified terrace, first recognised in two coastal sections between Waitara and Turangi Road. NT1 extends <c.0.2km inland and is bounded on its inner edge by a prominent linear topographic rise which separates it from the higher NT2 terrace (Plate 9.01). This rise separating two sub-horizontal land surfaces, is interpreted as the surface expression of a buried sea cliff. In a coastal cliff section 0.2km south-east of Turangi Road, the NT1 strandline is exposed c.2.5m above HWL with the wave cut platform gently dipping northwards (Plate 9.02).

Overlying this platform are two 1.0 - 1.5m thick gravel units comprising sub-rounded to rounded cobbles and boulders in a sandy pebble matrix separated by up to 0.2m of andesitic planar to weak cross-bedded sands (Plate 9.03). Lack of suitable exposure at this section precludes elucidation of the stratigraphy above the gravel units. However further westwards, the gravel units upwardly grade to well cemented iron stained sands unconformably overlain by Holocene grey andesitic beach sands with charcoal and heat fractured cobbles (umu stones).

The absence of Okawa Formation within the cover of NT1 terrace suggests an age of less than c.100kyrs. Similarly the occurrence of iron cemented sands within its cover, suggest an age that pre-dates the post-glacial period. On this basis, NT1



Plate 9.01: NT1 terrace and fossil cliff at Q19/185458 near Airedale Reef. Arrow indicates NT1 terrace remnant in the vicinity of Turangi Road.



Plate 9.02: NT1 strandline exposed at Q19/238460 along the coast near Turangi Road. Note wave cut surface of NT2 terrace.



Plate 9.03: NT1 formation exposed at Q19/238460 along the coast near Turangi Road.

terrace may correlate with either the c.60kyr or c.81kyr marine terrace of the the Wanganui district (Pillans 1983).

In correlating the NT1 terrace, the linear regression equation of Pillans (1983) has been used in which Y = C + AX, where Y = strandline height (m), A = age (kyrs), X = uplift (0.3mm/yr) and C = paleo-sea level relative to the present (m). In predicting the height of the 60ka and 81ka strandlines in North Taranaki, this equation was solved for each. The 60ka strandline is estimated at -6m (Y= -24 + 60 (0.3)) and the 81ka strandline at +4m (Y= -20 + 81 (0.3)).

The height of the NT1 strandline (+2m) more closely approaches the c.81kyr strandline (+4m) and is thus correlated with the Hauriri Marine Terrace of Wanganui (Pillans 1983).

9.3 NT2 TERRACE

The seaward margin of NT2 terrace between Waitara and Onaero is mostly marked by an active coastal cliff which exposes an uplifted wave cut surface and associated cover-bed deposits. However, in two sections of the coast between Waitara and Turangi Road, the seaward margin of the terrace is occasionally marked by a prominent fossil cliff which separates the NT2 terrace from the lower NT1 marine terrace (Plate 9.01).

The NT2 terrace extends between 2.0 - 4.5km inland from the coast, and is bounded on its inner edge by a conspicuous fossil cliff at c.60m elevation (Plate 9.04) which separates it from the older NT3 marine terrace further inland. On the coastal plain the NT2 cliff can be mapped between the Waitara River and Urenui, and in some sections has been partially buried by Motunui laharic

deposit. Further west of the Waitara River, the cliff has been completely buried by Okawa Formation and Motunui laharic deposit resulting in the uncertain distribution of the terrace.

The NT2 wave-cut surface is almost continuously exposed in cliffs along the coast. From Airedale Reef to the vicinity of Otarao Road the cut surface rises up from below sea level to a height c.6m +/- 1m above high water mark. The cut surface approximately maintains this height to Turangi Road, 4km further eastward. The cut surface between Turangi Road and Waiau Stream then gradually rises to c.9m +/- 1m and maintains a similar height for a further c.3km to just east of the Onaero River.

An abrupt change in the lithology underlying the wave-cut surface occurs in the vicinity of Waiau Stream. Eastwards, bluish-grey mudstones and sandstones of Urenui Formation comprise the NT2 wave cut platform. However, west of Waiau Stream, the platform comprises a laterally extensive, massive, c.8m thick laharic unit containing fragmental rock clasts (Plate 7.16). The reason for this abrupt lithological change is unclear but may possibly relate to a faulted Tertiary block whose surface expression across this boundary was removed by the NT2 marine trangression.

A c.0.5m thick gravel unit comprising angular to rounded cobbles and boulders in a sandy pebbly matrix overlies the wave-cut lahar platform west of Waiau Stream. The gravels were eroded from the laharic unit below (Plate 9.05). Locally an unusually high proportion of angular clasts occur. These are derived from fragmental rock clasts directly underlying the wave-cut platform. The gravel unit grades upward to a variably thick unit of weakly cross-laminated grey andesitic sands with minor sub-rounded to rounded pebbles.

The Tertiary wave-cut platform east of Waiau Stream is overlain by planar to weakly cross-bedded andesitic sands containing wood and uncommon gravel clasts. The wood and underlying wave-cut platform shows visible signs of marine worm borings.

Overlying the grey andesitic sands is a massive c.4m thick laharic diamicton correlated to the Motunui laharic deposit (Plate 7.16). This unit can be traced nearly continuously from the Waitara River to the Onaero River.

This laharic unit is often conformably overlain by a c.9m sequence of medial beds (Plate 7.16) and occasional steeply cross-bedded sand dunes of Last Interglacial age. Represented within this sequence are five L-units which are interpreted to have been deposited during the Last Glacial and Last Interglacial (see Chapter 4). Along sections of the coast the laharic unit is also overlain by up to c.7m of lignites and carbonaceous muds which grade upward to medial units deposited during the Last Glacial (Plate 9.05). The top of this lignitic and carbonaceous mud sequence can be directly correlated to the lignite at Airedale Reef, where a detailed late Last Interglacial record of vegetation and paleoclimate change in North Taranaki has been elucidated (see Chapter 11).

An older wave cut-platform is exposed beneath the NT2 wave-cut laharic platform in a vertical cliff section 0.8km southeast of Turangi Road (Section 28) (Plate 9.05). Here, the wave cut laharic unit is underlain by a prominent c.0.2m thick carbonaceous paleosol and separated from the older cut platform below, by c.1.0m of massive brown-grey to grey tephric mud that downwardly grades to c.0.3m of massive, bluish green mud and c.0.3m of soft, planar to weakly cross-laminated, grey to bluish grey sands (Plate 9.06). This older wave-cut platform (NT3?), exposed at mean sea level (MSL), comprises Tertiary siltstone and sandstones. Further westwards this older cut surface is not



Plate 9.04: NT2 fossil cliff and NT3 terrace at Q19/198420 looking south along Ngatimaru Road.



Plate 9.05: NT2 terrace cover-beds exposed at Q19/244455 near Section 28. Arrow indicates position of NT2 wave cut surface. Brown-grey tephric mud and laminated bluish-grey micaceous sand of NT3 terrace are preserved beneath unnamed debris avalanche deposit near high tide mark.



Plate 9.06: Highly carbonaceous clay, brown-grey tephric mud, bluish-green mud and laminated bluish-grey micaceous sand overlying the NT3 wave cut surface at Q19/244455 near Section 28.

exposed in coastal cliffs but unpublished exploratory well data (Bechtel 1981) from the Motunui G.T.G plant suggests that this wave cut platform occurs at mean sea level, along this portion of the coast.

In this study, correlation of NT2 terrace with the Rapanui Marine Terrace of Wanganui District is supported by similar coverbed stratigraphy; especially the occurrence on both terraces of the c.90ka loess.

9.4 NT3 TERRACE

As indicated previously the NT3 terrace is bounded on its outer edge by a conspicuous cliff which separates it from the lower NT2 terrace. At its inner edge, the NT3 terrace is bounded by a prominent cliff at c.70m elevation which separates it from the higher NT4 terrace in the east and a surface mapped as Maitahi Lahars (Neall 1979) in the west.

North of the Onaero River, NT3 terrace is c.0.7km wide and immediately south broadens to between 3 and 4.5km near the Waitara River. Further west, NT3 terrace is interpreted to dominate the coastal plain between Brixton and Bell Block. The outer edge of NT3 terrace in this vicinity appears to have been completely buried by the Motunui laharic deposit and Okawa Formation, resulting in little or no surface expression.

The associated coverbeds of NT3 terrace are well exposed along the active cliffs north-east of Bell Block. Here the wave-cut surface occurs below low water mark (LWM). Exposed at the cliff base are well cemented, iron stained, steeply angled cross-bedded

sands with occasional large tree stumps in growth position. The sands are buried beneath two closely spaced laharic units which are separated by 0.60m of woody lignite with prominent tephra inter-beds. The upper laharic unit is separated from Okawa Formation above by c.3.60m of woody lignite and carbonaceous muds with tephra inter-beds. The sequence of tephra is dissimilar in appearance to other known tephra sequences of Egmont source and may relate to activity centred at Pouakai Volcano. No central North Island rhyolitic chrono-horizons have so far been found within the extensively exposed lignitic coverbeds of NT3 terrace.

The NT3 wave-cut surface is rarely exposed further inland but has been recognised in a cliff section adjacent to the Waitara River at Osbornes Property (Q19/187383). Here, a gravel unit above the wave-cut Tertiary platform is closely overlain by c.8m of gyttja containing wood and lignitic lenses which abruptly grades upward to a c.5m thickness of planar to low angled cross-bedded well sorted sands, unconformably overlain by a laharic unit correlating to Motunui laharic deposit.

Conspicuously absent from the NT3 terrace at Osbornes Property is the particularly prominent lahar deposit which at the coast preserves the NT3 wave-cut surface beneath its base. At the same coastal section, the upper surface of this lahar has been truncated by the NT2 marine transgression. Assuming the correct correlation of the NT3 wave-cut surfaces, this prominent lahar deposit appears not to have been channelled down the Waitara River, unlike Motunui laharic deposit and Okawa Formation. Rather it was directed north-east across the NT3 terrace from Pouakai Volcano.

NT3 terrace is here provisionally correlated to the Ngarino Marine Terrace of Wanganui District (Pillans 1981; 1983). This correlation is based on a single wood sample obtained from

lignite closely overlying the NT3 wave cut surface at Paritutu Beach, just west of New Plymouth. This sample was amino acid racemisation dated by Dr B.J. Pillans (R.S.E.S., Victoria University of Wellington) and yielded a D/L ratio similar to that woods obtained from the cover of the Ngarino Terrace in Wanganui (Pillans pers.comm. 1988).

Correlation of NT3 terrace to Ngarino Terrace is also based upon the occurrence of two closely spaced rhyolitic tephras at the base of a prominent cutting near the seaward edge of the next higher surface mapped as Maitahi Lahars (Neall 1979) and their absence within the well exposed coverbeds of NT3 terrace further seaward (Plate 8.22). Their glass chemistry is similar and indistinguishable from the MGR1 and MGR2 tephras in the loess section at Griffins Road Quarry near Marton (see Figure 3.05), which are estimated to be a little younger in age (between 210 and 230ka B.P) than Mt.Curl Tephra. The apparent absence of these tephras on NT3 terrace and their occurrence on the next higher surface, suggests that they were either deposited at the time of the NT3 high sea level event (late- oxygen isotope Stage 7) or in the interval prior to this high sea level event (mid-oxygen isotope Stage 7).

9.5 NT4 TERRACE

The NT4 terrace is bounded on its outer edge by a very prominent cliff which separates it from the lower NT3 terrace. On the other hand, the fossil cliff at its inner edge with the higher NT5 terrace, is more subtle and often difficult to locate. The distribution of NT4 terrace, inferred where indicated, is shown on Map 1. Exposure of NT4 coverbeds and the wave-cut surface is sparse despite extensive dissection.

NT4 terrace in the area west of the Onaero River forms a narrow dissected surface with small remnants. Further westwards NT4 remnants progressively broaden, so that in the area south of Bell Block the terrace widens noticeably and merges with an extensive dissected surface mapped as Maitahi Lahars (Neall 1979). The position of the NT4 cliff and the older NT5 cliff in this vicinity has yet to be identified.

The westward broadening of NT4 terrace appears to relate to the occurrence of Maitahi Lahars (Neall 1979) within its coverbed succession. These lahars appear to have restricted erosion during the subsequent NT3 high sea level event. The apparent absence of the NT4 and NT5 cliffs in the west may relate to burial by Maitahi Lahars.

9.6 NT5 TERRACE

The NT5 terrace in the area east of Mangaoraka Stream, forms a narrow dissected surface with small remnants. In this vicinity the terrace is bounded on its outer edge by a subtle fossil cliff which separates it from the lower NT4 terrace. It is bounded on its inner edge by a more prominent fossil cliff which separates it from the higher Eltham laharic surface. West of Mangaoraka Stream, the NT5 cliff appears absent and has been presumably buried by Maitahi Lahars.

An age of 0.43 +/- 0.07 Ma was obtained from a rhyolitic tephra within the coverbed succession of NT5 terrace at Mountain Road (see Chapter 3 and Plate 3.08). This establishes a minimum age for the NT5 terrace and the Eltham surface.

9.7 Discussion

Five uplifted marine terraces are recognised forming the `constructional' landscape of the North Taranaki coastal plain and provide a c.0.45 Ma record of successive sea level oscillations with moderate to low rates of vertical crustal deformation (Chappell 1975; Pillans 1986). The extent of the NT2, NT3 and NT4 terraces relate to the occurrence of large volume, extensive laharic deposits that have originated from Pouakai and Egmont Volcanoes. Lahars have repeatedly advanced the coastline seaward and restricted coastal erosion during episodes of Quaternary high sea level.

In the past there has been a tendency to correlate the North Taranaki terraces with those of the Wanganui district on the basis of geomorphology, and interprete them in terms of a succession of transgression - regression cycles counting back from an assumed 130kyr terrace. This study, based on cover-bed stratigraphy correlates NT2 terrace with Rapanui Marine Terrace. However, on older North Taranaki terraces, the widespread lack of exposed coverbeds inhibits more definitive correlation to the Wanganui terraces. With the limited chronostratigraphic evidence available, the NT3 and NT4 terraces are here correlated to Ngarino and Brunswick Marine Terraces, respectively. The NT5 terrace may correlate with either Rangitatau or Kaiatea Marine Terraces.

CHAPTER 10

HAZARD ASSESSMENT OF THE NORTH-EASTERN AND CENTRAL LOWER FLANKS OF EGMONT VOLCANO

10.1 Introduction

The climactic May 18 1980 eruption of Mt.St.Helens increased the level of interest in volcanic hazards in New Zealand. In late 1980, a National Civil Defence Planning Committee on Volcanic Hazards was formed and requested reports on the likely areas and types of future eruptions, the risk to public safety and the need for special precautions. An unpublished report concerning potential hazards from future eruptions of Egmont Volcano was submitted to the Committee by Neall in 1981. Extracts of that unpublished report were later included in a volcanic hazard map of Egmont Volcano (Neall 1982) and in reviews of volcanic hazards of the North Island (Dibble and Neall 1984; Dibble et al. 1985).

More recently, the Taranaki United Council (1987) produced a report which used the unpublished hazard report as a basis for commenting on the likely impact and effect of future volcanic activity on regional infrastructure. The implications for civil defence and emergency response contingency plans were also discussed.

Hazard assessment is an essential first stage in the preparation of contingency plans in the event of a volcanic eruption. The only veritable way of assessing volcanic hazards and the risks those hazards pose to Taranaki is based upon the stratigraphic record which provides information about past eruptive activity at Egmont Volcano.

This information is intergrated to illustrate how activity at a given volcano has varied with time and to make justifiable

predictions as to the average periodicity, severity and extent of future eruptions. The risk at that volcano can then be estimated.

In assessing volcanic risk in north-eastern and central Taranaki, it is necessary to designate areas of potential volcanic hazard. These areas of potential volcanic hazard are divided into a number of volcanic hazard zones that demarcate areas of estimated risk from volcanic processes. Hazard zones are constructed with emphasis on minimising loss of life and damage to property and are based on particular types of volcanic hazard and from the known volcanic history. Risk between the delineated zones is gradational and boundaries should not be regarded as precise lines. The hazard zone boundaries are seldom more than rough approximations (Miller et al. 1981) and represent the best estimate of risk based on models developed from past events. The location of these lines have a factual basis, but do not indicate absolute differences, or even large differences of risk from one side to another.

In determining hazard zones based on events known to have occurred, there is difficulty in balancing between predicted range of risk and the amount of risk acceptable to society. For instance, if boundaries based on eruptions were placed far enough from the volcano to rule out any significant risk, much public criticism could be anticipated especially if the predicted event did not take place resulting in public inconvenience and economic loss. If, on the other hand, less conservative boundaries were drawn closer to the volcano, severe criticism could also be expected if a catastrophic event did occur and lives were lost.

On the basis of stratigraphic information obtained from beyond the National Park boundary in north-east and central Taranaki (this study), hazard zones delineated by Neall (1982b) for lahars, pyroclastic flows and tephra are revised. Hazards from

lava flows and pyroclastic projectiles are not discussed in this study because there is no new evidence to suggest they have ever extended beyond the present National Park boundary (c.9.6km from source) and offer no great hazard to life or movable property outside the Park.

10.2 Tephra Hazard

Tephra has been intermittently erupted from Egmont Volcano for the past c.130kyrs B.P. Up until recently it was thought that on average one pumiceous eruption occurred every 500 years (Neall 1972). However the occurrence of at least thirty-five tephras $>10^7$ m^3 erupted between c.3 and c.12 kyrs B.P. suggests that average periodicity for moderate to major sized eruptions may be as frequent as one every c.250 years. Presumably many relatively more tephras of lesser magnitude were erupted and deposited closer to source within the confines of the National Park.

Post-12kyr tephra attains thicknesses of c.5.0m in the vicinity of Mahoe, c.16km south-east from the present summit. In contrast in the vicinity of Inglewood, c.20km north-east from the present summit, the same sequence of tephra is only c.2.40m thick. On the North and South Taranaki coastal plains, the thickness of post-12kyr tephra is significantly less (<1m).

These variations in thickness of tephra surrounding Egmont Volcano appear to be primarily influenced by the prevailing wind pattern. In the advent of future eruptions of Egmont Volcano, the tephra cloud will probably encounter atmospheric zones of varying wind speed, direction and rates of lateral shear. Specific high altitude data is not available for Taranaki so information was collected from Ohakea, 150km to the south-east (Neall 1981). Three dominant wind directions relating to altitude were noted from <3000m, 3000 - 10,400m and 12000 - 16300m. Wind directions and thus likely tephra distribution occurs to the sector between

north-east and south-east for 91% of the time between 12000 - 16300m. For the 3000 - 10400m altitude range, tephra is likely to be carried into the same sector (north-east to south-east) for 73% of the time and below 3000m for 55% of the time.

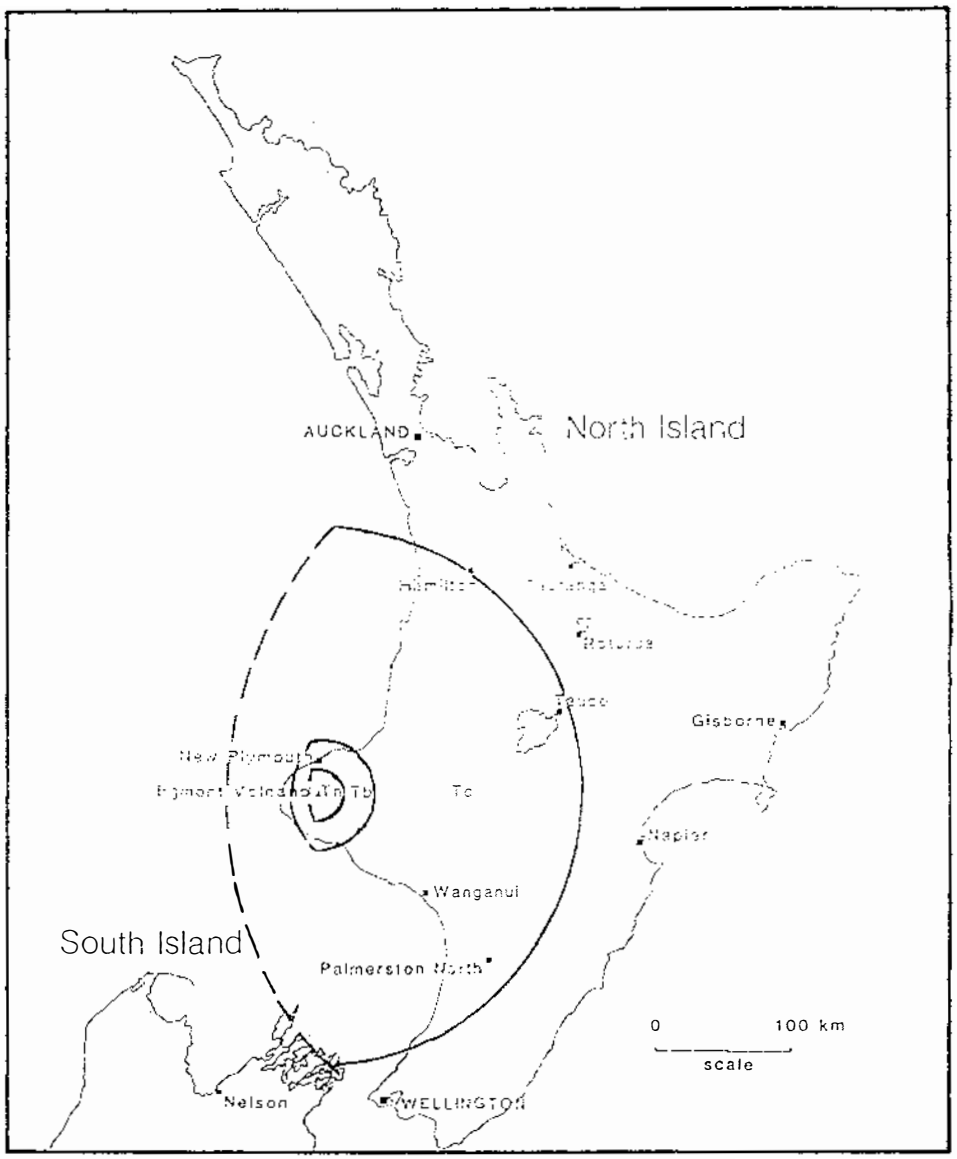
The extent of tephra distribution from past eruptive activity at Egmont Volcano can be demonstrated to be considerable. Macroscopically visible Egmont-source tephras have so far been identified in lake sediments of the Waikato, c.200km to the NNE (Lowe 1987) as well as in the Wanganui district to the south-east (this study). Dispersed mineral grains with Egmont-type chemistry have also been identified in present-day soils of the Manawatu district, c.170km SSE from source (Wallace 1987).

In constructing a hazard map for north-eastern and central Taranaki information on the wind directions and the past distribution of moderate to large magnitude tephra was used. Past eruptives give a likely indication of the magnitude of eruptions one can expect in the future. Three major zones of tephra hazard are recognised in this study and these are, in order of decreasing risk delineated as Zones Ta, Tb and Tc (Figure 10.01).

Zone Ta is bounded where >0.10m thickness of tephra could be expected during a moderate to major eruption (>10^7 m^3). This zone covers an area from NNE to SSE within 24km of the present Egmont summit and includes the communities of Egmont Village, Inglewood, Stratford, Eltham and Kaponga.

Zone Tb is the area where between 0.10m and 0.01m of tephra could be expected during a >107 m3 eruption. It occupies a similar areal extent as Zone Ta, between 24 and 40km from the present Egmont summit. This zone includes the communities of Waitara, Manaia and Hawera.

FIG. 10.01 TEPHRA HAZARD ZONES



Zone Tc is the area where between 0.01 and 0.001m of tephra could be expected during a >107 m3 eruption. This zone covers an area in the sector from NNE to SSE between 40 and c.200km from the present summit. Tephra deposition in this zone will not seriously endanger human life or health but may have significant economic consequences.

10.3 Lahar and Associated Flood Hazards

At least thirteen post-22kyr lahar deposits of varying magnitude have been recognised in north-eastern and central Taranaki. Most lahars extend from Egmont Volcano to the North Taranaki coast after having been channelised within the confines of radial drainage paths. On the lower flanks of Egmont Volcano, many of these lahars were of sufficiently large scale, to overtop the channels and laterally spread in a uncontrolled manner onto the extensive interfluve surfaces of the ring plain.

Lahar formation is very much dependant on pre-disposed conditions, which are most favorable during periods of active volcanism (Neall 1981). Such conditions include heavy rains and high run-off volumes, rapid melting of snow and ice, and lateral transformation from deflating pyroclastic density currents. In future eruptions of Egmont Volcano lahars can be expected to be a major hazard, potentially influencing many catchments on the volcano, simultaneously.

Based on the geologic record over the last c.22kyr an average frequency of lahar occurrence in north-eastern and central Taranaki has been interpreted for each of the outer lahar zones. Three hazard zones are recognised and these are in order of decreasing order of risk, Zones La, Lb and Lc (see Map 2).

Zone La represents the zone of immediate lahar risk. This zone occurs where the greatest frequency of lahars has occurred throughout the last c.22kyrs B.P. and has been repeatedly inundated by lahars in the last c.10kyrs. Over this period the average incidence lahar interval in this zone has ranged from 1 per 1,500 years to 1 per 3,000 years.

Areas of this zone judged to be of highest risk are those within stream and river courses that originate from the upper flanks of Egmont Volcano. In the eastern and north-eastern sectors, there is high density of stream courses with shallow channels. In the south-eastern sector, stream courses are less frequent, with the channels usually entrenched more deeply within the surficial cover-beds. Areas of the south-eastern sector judged to be of highest risk are within the confines of the Kaupokonui, Kapuni and Mangatoki Streams, as well as the Waingongoro and Patea Rivers.

Other areas of high risk in this zone include interfluve areas immediately adjacent to drainage channels in the eastern and north-eastern sectors. In the south-eastern sector inter-fluve areas are of less risk because they are more extensive and elevated.

In Zone La, there are ten instances where radial drainage channels from Egmont Volcano pass very close to urban development. These specifically include the Waiwhakaiho, Waitara and Patea Rivers where they flow through New Plymouth, Waitara and Stratford respectively, and adjacent to the communities of Egmont Village (Mangaoraka Stream), Inglewood (Waiongana and Ngatoro Streams), Lepperton (Waiongana Stream), Midhurst (Te Popo Stream), Eltham (Waingongoro River) and Kaponga (Kaupokonui Stream).

Zone Lb represents the zone of intermediate risk based on the distribution of moderate to large magnitude lahars over the last c.22kyrs B.P. The average lahar incidence interval in this zone is 1 per c.4500 years.

Zone Lc represents the lowest risk lahar zone and would only be affected by most infrequent and large volumed debris avalanches generated by partial or complete collapse of Egmont Volcano. In such an event, debris avalanche deposits could potentially inundate the entire NNE to SSE sector of the volcano as well as, reach the North and South Taranaki coasts. The possibility of an event occurring without prior warning or precursory activity should not be discounted. Large magnitude earthquakes, unrelated to volcanism, generated by either tectonism or sedimentary loading have the potential to destabilise portions of the edifice inducing gravitational collapse.

10.4 Pyroclastic Density Current Hazard

In north-eastern and central Taranaki, prehistoric pyroclastic density current deposits are restricted in distribution to the confines of Egmont National Park. The absence of such deposits from the stratigraphic succession beyond the Park boundary makes it difficult to identify an expected hazard from such a phenomenon. It does not mean, however, that a future event will not exceed any known precedent at that same volcano. For instance the lateral blast deposit of the May 18 Mt.St Helens eruption, extended about three times further from the volcano than the largest known previous blast and devastated an area that is approximately 10 to 15 times larger (Miller et al. 1981). However, on the basis of existing knowledge, the principal danger to life and property from future pyroclastic density current events are likely to be residents and buildings within the

confines of the National Park. If an event were sufficiently large, it could endanger life and property in zone Ta.

10.5 Discussion

Eruptive activity at Egmont Volcano is shown in this study to have been sufficiently frequent for potential hazards to be evaluated based on the former volcanic stratigraphic record. Past behavior of the volcano suggests that, on average, the present dormancy will not exceed a duration of 250 years. Since Egmont Volcano last erupted c.230 years ago, a large eruption could occur within the next one hundred years.

At present there is no method of predicting more precisely when the next eruption of Egmont Volcano will take place. Precursory activity (i.e. increasing seismicity and/or edifice dilation) may give some period of warning, the length of which is largely unknown. There is no guarantee that the critical levels of precursory activity at Egmont Volcano would be similar to that experienced at other volcanoes. At present there is minimal surveillance of Egmont Volcano, restricted to a single, visually recording 10Hz seismograph at North Egmont (3.7km from the present summit) and two tilt levelling stations.

CHAPTER 11
A BIOSTRATIGRAPHIC RECORD OF NORTH-EASTERN AND CENTRAL TARANAKI

11.1 A Late last-glacial - Early post-glacial Vegetation Record

11.1.1 Introduction

A well preserved record of floral changes spanning the last glacial - post-glacial boundary, occurs within a well dated peat section on the lower eastern flanks of Egmont Volcano. The section is exposed in a deep drain parallel to upper Durham Road (**Section** 8 of Appendix 1) beneath a prominent debris flow deposit mapped as **Kahui Formation.** Several andesitic tephras erupted from Egmont Volcano are interstratified within the peat. The peat section was first reported in early 1981 by Mr A.S. Hull (N.Z Geological Survey, D.S.I.R) and briefly described. A radiocarbon date (NZ5289A) of 11,650 +/- 200 years B.P. was obtained from wood in peat 0.5m beneath the basal boundary of the debris flow deposit.

Following this investigation, Dr M. M^{c}Glone (Botany Division, D.S.I.R) then systematically channel sampled the peat for detailed palynological examination in late 1981. Four peat samples were extracted for radiocarbon dating as part of his study. The uppermost sample yielded a date (NZ5409A) of 9,280 +/- 130 years B.P. at approximately 0.25m depth from the upper boundary of the peat, while the lowermost sample established an age (NZ5412A) of 13,150 +/- 200 years B.P. at approximately 2.25m depth.

The significance of this section is threefold. Firstly, several newly defined andesitic tephra marker beds have been correlated to the site where they were found preserved in the peat. The ages

for these tephra markers were then approximately estimated from their position with respect to the four dated peat samples.

Secondly, the site provides a well preserved floral record spanning the last glacial - post-glacial boundary of the north-eastern lower flanks of Egmont Volcano. This record concurs with the record obtained from Eltham swamp on the lower south-east flanks over a similar time interval (McGlone & Neall pers. comm. 1987).

Thirdly, the position of the last glacial - post-glacial boundary (indicated by vegetation changes) in relation to tephra marker beds in the peat, can then be approximately determined within neighbouring non-peat sections using the same markers.

11.1.2 Results

A complete pollen diagram for the section is given in Figure 11.01. The peat section is subdivided into two palynological zones which are informally named Zones A and B. Both zones are sufficiently complex to require subdivision into sub-zones. Estimated ages for the beginning and end of each sub-zone are given in brackets. Sampling intervals were at c.0.1m in the peat. Interpretations of the sub-zones are given below.

Durham A1: 2.50 - 2.00m depth (c.13.3 - 13.0kyr B.P.)
This sub-zone is characterised by moderate levels of Gramineae pollen which make up between 6 and 13% of the total pollen sum. Shrubs are represented at the base of this zone, with Phyllocladus, Halocarpus bidwillii-type, Myrsine, Compositae and Coprosma together constituting up to 67% of the total pollen sum. Towards the top of this sub-zone, shrubs are reduced to less than half of the level prevailing at 2.50m depth. Phyllocladus and Halocarpus bidwillii pollen are not recorded above 2.00m depth.

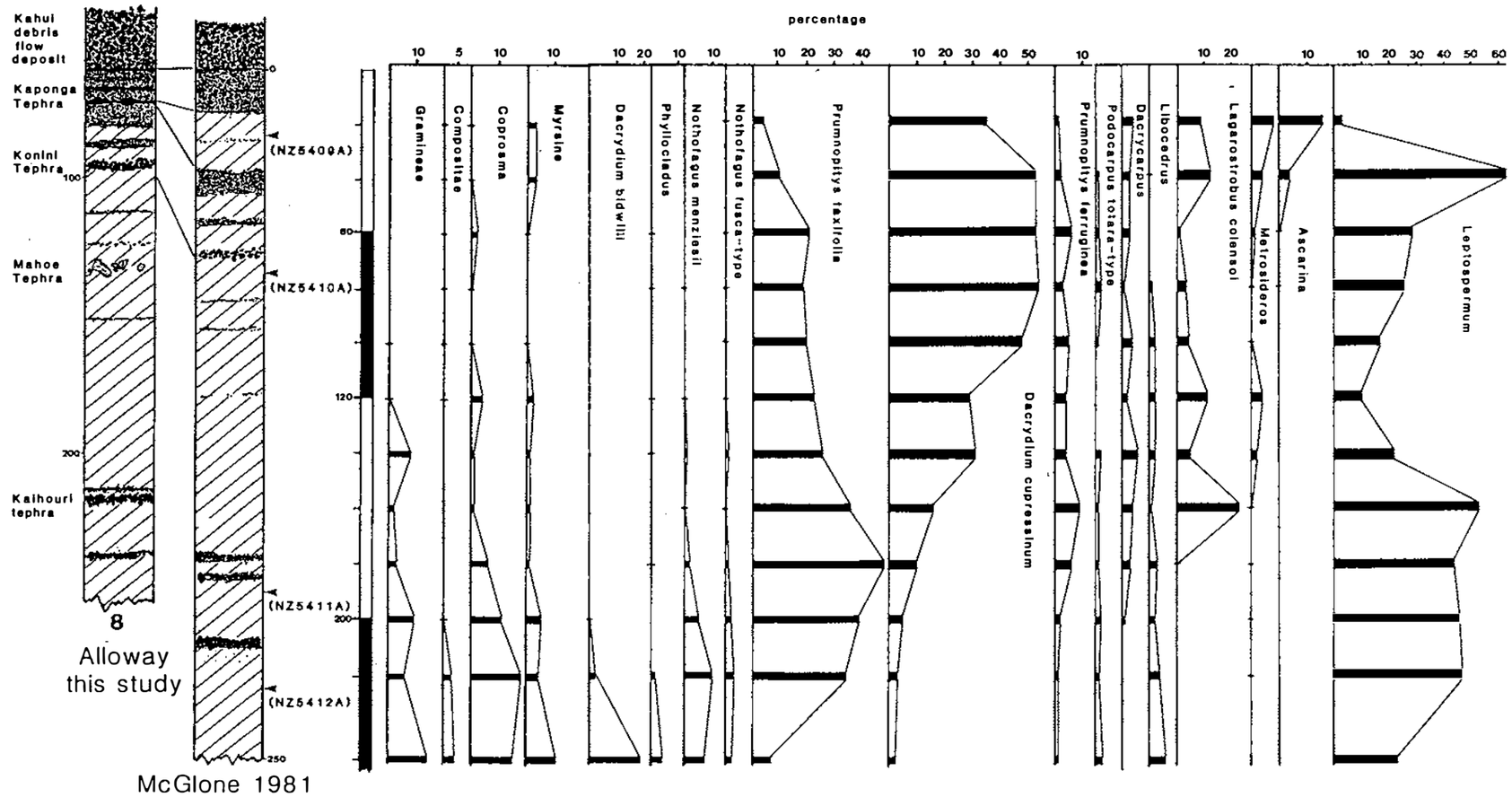


FIG. 11.01 Pollen Diagram: Durham Road

Prumnopitys taxifolia pollen dramatically increases from 7% at the base of this sub-zone to 39% at the top. There are less marked but significant rises in the Dacrydium cupressinum pollen curve from 2% to 9% but Metrosideros pollen shows no change in recorded trace levels.

Nothofagus menziesii pollen, represented by moderate levels (7 - 10%) in the lower portion of this sub-zone, steadily decreases to 4% at 2.00m depth, while there are parallel but less pronounced decreases in the Nothofagus fusca-type and Libocedrus pollen curves. Prumnopitys ferruginea and Podocarpus totara-type are represented throughout by consistently low levels. This sub-zone contains a noticeable component of sand and silt. Leptospermum pollen throughout this sub-zone constitutes approximately 45% of the total pollen sum. Tree fern spores remain at constant levels of 10%.

Durham A2: 2.00 - 1.20m (c.13.0 - 11.5kyr B.P.)
The two uppermost **Kaihouri tephras** occur near the base of this sub-zone between 1.75 and 1.86m depth. A dated (NZ5411A) peat sample obtained from 1.90m depth established an age of 12,900 +/- 200 years B.P. and provides a maximum age for the tephras. Small wood fragments are scattered throughout this sub-zone. Apart from horizons of silty peat at the base of the sub-zone and between 1.4 and 1.2m depth, much of the peat that accumulated in this sub-zone contains little obvious sand and silt in comparison with sub-zone A1.

This sub-zone is characterised by a continuing steady increase of Dacrydium cupressinum pollen to a level of 29% at the top of the sub-zone. Prumnopitys taxifolia, the only other substantial contributor to the arboreal pollen spectra, steadily increases to a peak level of 42% at 1.80m depth, then steadily declines to

23%. Smaller amounts of other tall podocarp tree pollen including Prumnopitys ferruginea, P.totara-type, Dacrycarpus and Lagarostrobus colensoi are consistently recorded. Levels of Metrosideros pollen increase from trace amounts to 4% in the upper half of this sub-zone. Libocedrus continues to occur at consistently low levels. Nothofagus menziesii and Nothofagus fusca-type pollen decline to trace levels, while Coprosma and Myrsine which were previously represented in moderate levels, also drop to very low levels. Levels of Gramineae pollen fluctuate throughout this sub-zone becoming absent in overlying sub-zones.

Tree fern spores and Leptospermum pollen maintain similar levels to those prevailing in sub-zone A1. However, at 1.6m depth there is a significant decrease of Leptospermum to its lowest recorded levels. A converse trend occurs in the tree fern pollen curve which is represented in low levels at 1.6m depth and then steeply increases to a peak level between 1.4 and 1.2m depth. Coinciding with these changes a higher silt component is recorded in the peat between 1.4 and 1.2m depth. This may indicate nearby disturbance caused by the passage of debris flows or alluvial flood deposits.

Durham B1: 1.20 - 0.60m depth (c.11.5 - 10.1kyr B.P.)
At approximately 0.99m depth **Mahoe Tephra** occurs interstratified within the peat. **Konini Tephra** also interstratifies this sub-zone but at 0.70m depth. A dated (NZ5410A) peat sample obtained from 0.75m depth established an age of 10,500 +/- 150 years B.P. and thus provides a maximum age for Konini Tephra.

The pollen spectrum during this interval indicates a podocarp - broadleaf forest was the dominant vegetation type. This is shown by a dramatic rise in D.cupressinum pollen to reach levels exceeding 50% of the total pollen sum and a steadily declining

level of Prumnopitys taxifolia. Smaller amounts of other tall podocarp tree pollen are also indicated. Metrosideros pollen increases throughout the sub-zone to approximately 8% of the total pollen sum. The frequency of Libocedrus pollen in the lower half of this sub-zone is low, dropping to trace amounts in the upper half. Tree fern spores progressively decrease to a steady but higher level than that prevailing in zone A, while Leptospermum rapidly increases.

Durham B2: 0.60 - 0.00m depth (c.10.1 - 9.0kyr B.P.)
Interstratified within this sub-zone are four coarse ash and lapilli beds of **Kaponga Tephra.** A peat sample at approximately 0.25m depth has been dated (NZ5409A) at 9,280 +/-130 years B.P. The upper boundary of this sub-zone is defined by the basal contact of the overlying Kahui debris flow deposit.

This sub-zone is characterised by the first appearance and steady rise of Ascarina and Eugenia pollen and a decline in the levels of D.cupressinum. P.taxifolia present in some quantity dramatically decreases to 4% of the total pollen sum, while Leptospermum pollen levels steadily increase from those prevailing in sub-zone B1. Tree fern spores remain at steady levels, which are notably higher than those levels recorded in sub-zone A1.

11.1.3 Discussion
Sub-zone A1 represents a period when the lower north-eastern and central flanks of Egmont Volcano were occupied by a mosaic of Prumnopitys taxifolia -dominant forest and Leptospermum-dominated shrubland and grassland. Dacrydium cupressinum first appears as a minor constituent of the forest.

During sub-zone A2 Prumnopitys taxifolia - dominant forest steadily increased. As this forest spread, the area of shrubland

and grassland diminished with local extinctions of Phyllocladus and Halocarpus bidwillii. Leptospermum still persists as the dominant shrub vegetation, while D.cupressinum steadily increases.

Sub-zone B1 reflects a time during which the lowland forest achieved a composition similar to that of the present (prior to European arrival in the area). From evidence at this site there was a rapid increase of Dacrydium cupressinum which led to this tall tree becoming the dominant, with a correspondingly large reduction of Prumnopitys taxifolia. Nothofagus menziesii and Nothofagus fusca-type were eliminated from the slopes of Egmont Volcano and surrounding ring plain. Libocedrus, which had been an element in the podocarp-broadleaf forest in the area, became restricted to its present distribution on the upper flanks of Egmont Volcano. In sub-zone B2 Ascarina lucida became a common constituent of the small tree component of the podocarp-broadleaf forest.

On the basis of results obtained from this study it is considered that amelioration of the climate was rapid in the immediate post-glacial period with podocarp-broadleaf forest well established by c.12.9kyrs B.P. This forest was dominated by Prumnopitys taxifolia unlike the Dacrydium cupressinum dominant forest which succeeded it by c.10.5kyrs. This D.cupressinum forest represents a warmer, moister climate (Figure 4.02). The appearance of Ascarina lucida is also an important climatic indicator because it is uncommon or absent in areas where rainfall is low or where drought is prevalent. Ascarina is so sensitive to frost that it does not presently occur in areas of New Zealand which have cold frosty winters (McGlone & Moar 1977; Sakai & Wardle 1978).

Changes in vegetation at this site occurred at about the same time as at Eltham Swamp on the lower south-eastern flanks of

Egmont Volcano (M^{c}Glone & Neall pers. comm. 1987), on the Central North Island Volcanic Plateau (M^{c}Glone & Topping 1977) and elsewhere in New Zealand (i.e. M^{c}Glone & Moar 1977; Lees 1986).

Climatic amelioration identified from floral changes in the peat between the uppermost Kaihouri tephra and Konini Tephra, can be related to neighbouring medial cover-bed sections using these same tephra marker beds. Here, there is a distinct transition in colour and structure between these tephra markers (e.g. **Section 19** of Appendix 1; Plate 4.04) which coincides with the boundary between **S1** (tephric origin) above, and **L1** (combined tephric and aeolian origin), below (Figure 4.02). This observation is supported by differences in total quartz content and quartz accumulation rate across this boundary at this section (see Chapter 6).

Assuming constant accumulation of medial material between the tephra markers, the transition between **S1** and **L1** in the cover-beds of north-eastern and central Taranaki, is here estimated to have an age of c.12kyrs B.P.

11.2 A Last-Interglacial Vegetation Record

11.2.1 Introduction

The Airedale Reef section (**Section 27**) (Q19/178461) is a coastal cliff, c.1.6km north-east of the Waitara River mouth (Plate 8.10). Here are exposed most of the cover-beds of the NT2 uplifted marine terrace (Chappell 1975). The NT2 wave cut surface, however, occurs beneath present sea level and is not exposed.

The site was first sampled by Grant-Taylor (Stevens 1969). A stratigraphic column of the site, produced much later by Grant-Taylor (1978), indicated that stumps of rata-rimu forest in position of growth occurred immediately above a 3m thick laharic breccia deposit (hereafter termed laharic diamicton). Wood from these tree stumps was radiocarbon dated (NZ406) and a minimum age of >43kyrs was established. A further radiocarbon date (NZ407) of 34,200 +/- 1500 years B.P. was obtained from a fine grained peat bed enveloped by weathered andesitic ash c.1.80m above the stumps of rata-rimu forest.

In early 1985, the Airedale Reef Site was visited and described in detail by the writer and Dr M. McGlone of Botany Division, D.S.I.R. The stumps of rata-rimu forest in position of growth were reinterpreted to underlie the laharic diamicton rather than overlie it, as Grant-Taylor had previously indicated.

11.2.2 Stratigraphy

A detailed stratigraphic column of the section exposed at Airedale Reef is presented in Figure 27 of Appendix 1. The base of the exposed section comprises >0.30m of massive, moderately well sorted grey andesitic sands which upwardly grade to c.0.85m of lignite containing wood and at least two unnamed fine

andesitic ashes. At low tide, the lignite with numerous tree stumps in growth position is exposed on an extensive beach platform which gently descends below present sea level (Plate 8.10).

Overlying the lignite in the cliff section is a c.4m thick laharic diamicton which has been mapped as marginal facies of Okawa Formation. Along most of the exposed cliff section, the upper boundary of Okawa Formation is nearly planar. However in part of the cliff section the Formation appears to mantle a pre-existing physiographic depression resulting in the development of a shallow concave basin on its upper surface (Plate 11.01). Within this basin is c.1.6m thick lignite deposit containing wood and preserving units of Epiha Tephra (Section 27B of Figure 11.02; Plate 11.02).

Above this lignitic deposit the remainder of the section comprises c.2.6m of medial beds with proportionately thinner andesitic tephra inter-beds (Plate 11.01). The Central North Island rhyolitic chronohorizon Aokautere Ash has also been identified within this sequence as a 0.01m thick discontinuous inter-bed in L1 at c.1.0m depth below ground surface.

11.2.3 Pollen Analysis

From the lignitic deposit above Okawa Formation eleven samples were obtained for detailed palynological examination by Dr M. McGlone. Four samples were also collected from the lignite underlying Okawa Formation but were not examined in detail. The pollen diagram (Figure 11.02) presented here for the upper lignite is subdivided into three palynological zones which are informally named Zones AR/Ab, AR/B and AR/C. The lower lignite comprises a single zone which is informally named Zone AR/Aa.

The ages of these zones cannot be accurately stated. However, the age of Zone AR/B is estimated at c.95kyrs B.P. This is

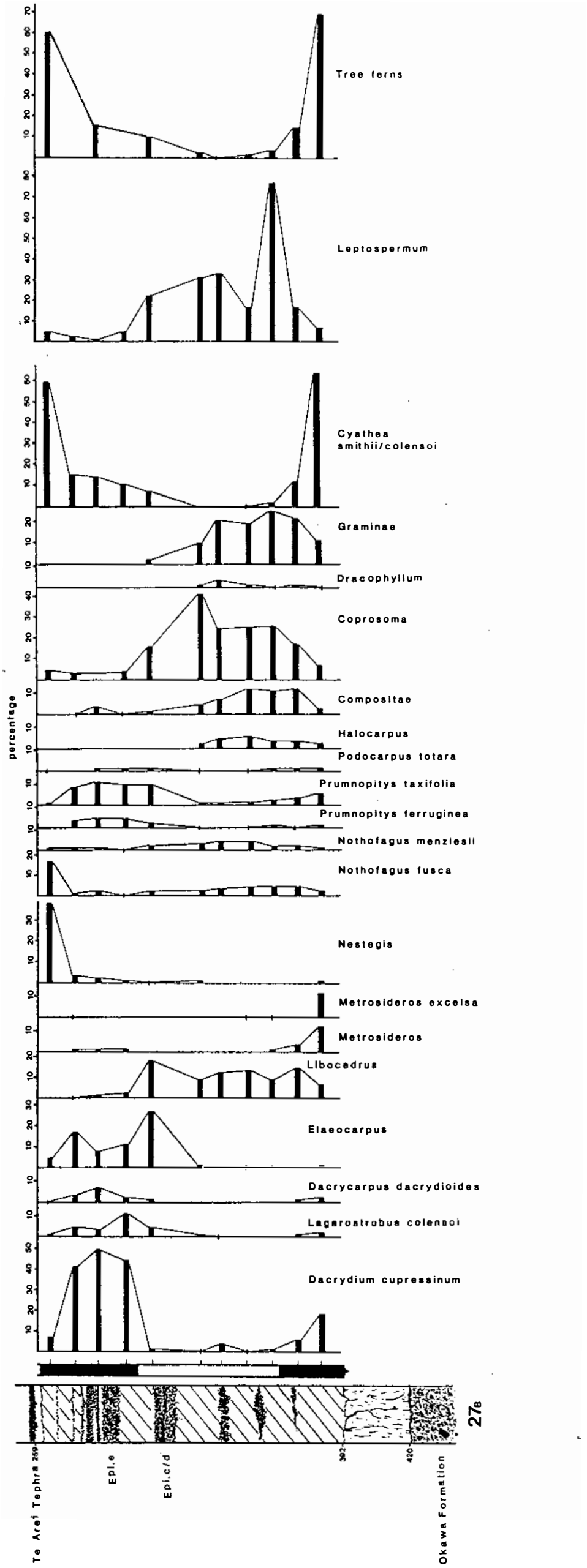


FIG. 11.02 Pollen Diagram : Airedale Reef



Plate 11.01: Woody lignite formed in shallow depression developed on the upper surface of **Okawa Formation** at Airedale Reef (Section 27; Q19/178461). This lignite was sampled for detailed palynological examination.



Plate 11.02: **Epiha Tephra** interbedded within the sampled lignite (Section 27B; Q19/178461). Note **Te Arei Tephra** (indicated by arrow) at the top of the exposed section within clayey material of **L3**.

based on the stratigraphic occurrence of Epi c/d of Epiha Tephra within (i) zone AR/B, (ii) within L4 on the NT2 terrace at Onaero and (iii) within Parao loess on the Rapanui Marine Terrace at Kohi Road in the Wanganui district. Alloway et al.(1988) suggest that L4 was deposited during oxygen isotope sub-stage 5b.

Zone AR/Aa (8.20m - 9.05m)
Pollen characteristic of podocarp-broadleaf forest dominates; especially abundant is Dacrydium cupressinum. There are high pollen levels of a great variety of taxa including Metrosideros, Dacrycarpus dacrydioides, Lagarostrobus colensoi, Prumnopitys ferruginea and Prumnopitys taxifolia (McGlone pers.comm. 1986).

Zone AR/Ab (3.92 - 3.65m)
Dacrydium cupressinum percentages fall from 16% to less than 5%, and there is a corresponding decrease in Metrosideros from 11% to less than 3%. Prumnopitys taxifolia decreases slightly to 3%. Pollen of trees characteristic of podocarp-hardwood forest such as Nestegis, Dacrycarpus dacrydioides, L. colensoi, Podocarpus totara, Prumnopitys ferruginea and Elaeocarpus are all recorded in this zone but in low levels. Ascarina lucida is absent. Cyathea smithii-type and tree fern pollen levels decline rapidly from 62% to 13%. Levels of Gramineae steadily increase from 10% to 20% towards the AR/A - AR/B boundary. Compositae (2% to 10%) and Coprosma (6% to 15%) show similar steady increases towards the upper boundary of the zone. Libocedrus is also recorded.

Zone AR/B (3.65m - 3.04m)
Nearly all the podocarp - hardwood pollen types are severely reduced; most are discontinuously represented by levels of 1 - 2% or less. Prumnopitys taxifolia percentages after remaining low throughout most of Zone AR/B steadily increase to 9% towards the upper part of this zone. Gramineae after an initial rise to 23%,

maintains similar levels before declining to 2% within the upper part of Zone AR/B. Compositae pollen also maintains the level reached at the top of Zone AR/A up to 3.52m depth, then steadily declines to 1% towards the top of this zone. Tree fern and Cyathea smithii/colensoi pollen are markedly less abundant compared to Zone AR/A. Throughout this zone, the percentage of Coprosma fluctuates but maintains moderately high levels (15 - 37%). Halocarpus and Libocedrus pollen also occur throughout this zone in levels higher than in the preceding zone. Dracophyllum pollen was noted at low (<3%) levels.

Zone AR/C (3.04 - 2.62m)
At the beginning of Zone AR/C Dacrydium cupressinum rapidly increases to a maximum of 42% at c.2.85m depth, then declines to 6% at the top of the zone. Lagarostrobus colensoi, Dacrycarpus dacrydioides, Elaeocarpus, Nothofagus menziesii and Prumnopitys ferruginea are consistently recorded throughout this zone. Nothofagus fusca, Nestegis, Metrosideros and Podocarpus totara are also present throughout most of this zone but in lower levels. However, Metrosideros and Podocarpus totara are absent in the uppermost part of this zone, whereas Nothofagus fusca and Nestegis rapidly increases over the same interval.

Coprosma, Compositae and Libocedrus pollen types are severely reduced and drop to levels of 1 - 3% or less. Gramineae and Dracophyllum are absent from the pollen spectra. Cyathea smithii-type, tree fern and Nestegis pollen dramatically increase throughout the zone and achieve unusually high levels at the top of this zone.

11.2.4 Vegetation and Climate

At the time represented by Zone AR/Aa, podocarp-broadleaf forest occupied the North Taranaki coastal plain (McGlone pers.comm. 1986). This coastal forest was extensively inundated by the Okawa lahar. Following this, the bare ground on the upper surface of the Okawa Formation was rapidly colonised. There appears to be the same floristic mixture overlying Okawa Formation as that present underlying the Formation but levels were reduced and the forest apparently now had an open canopy with small areas of grassland and shrubland.

At the Zone AR/Ab - AR/B boundary, the declining abundance of Dacrydium cupressinum and tree ferns in the forest surrounding the site indicates deteriorating climate conditions. This is further supported by the decline of Metrosideros and Prumnopitys taxifolia. Cooling of climate in Zone AR/B is suggested by the slight expansion of Nothofagus menziesii, N.fusca type, Gramineae, Halocarpus, Libocedrus, Coprosma and Compositae. The forest of this zone became similar to that of the late last-glacial (c.12.9 to 13.3kyr B.P.) forests of the area (see Section 11.1; this Chapter).

At the Zone AR/B - AR/C boundary, warming and increasing rainfall is indicated by the initial expansion of Prumnopitys taxifolia, closely followed by a rapid increase in Dacrydium cupressinum and tree ferns. Podocarp - broadleaf forest became more widespread than in Zone AR/Ab. The forest apparently had a closed canopy and grassland/shrubland was probably not common on the North Taranaki coastal plain.

A slight cooling in uppermost Zone AR/C is suggested by an increase in Nothofagus fusca-type pollen. The apparent decline of Dacrydium cupressinum and Prumnopitys taxifolia probably occurs

as a result of dilution by unusually high levels of Nestegis (R.Bussell pers.comm. 1987).

11.2.5 Correlation

The climatic events represented in the Airedale Reef section may be matched with those determined from oxygen isotope stratigraphy in deep sea cores (Shackleton et al. 1983) (see Figure 4.02).

An abundance of Dacrydium cupressinum in Zone AR/A and AR/C suggests two intervals when rainfall was similar to that of the present day. Both intervals post-date the cutting of the NT2 terrace during oxygen isotope sub-stage 5e when rainfall is inferred to have been the same as or greater than the present day and vegetation attained both the distribution and development of present day vegetation (McGlone 1985).

The only other pre-Holocene periods when a similar degree of rainfall and vegetation can be tentatively inferred from the oxygen isotope record are sub-stages 5a and 5c. Pollen zones AR/A and AR/C are considered to represent warm and moist periods during which forest cover was near complete. These zones are tentatively correlated with the Karioi and Otamangakau interstadials of McGlone (1983). The top of Zone AR/C may indicate initial approach to the period of cold conditions during oxygen isotope Stage 4.

Zone AR/B is considered to represent a cool period, where the presence of a grassland-shrubland-forest mosaic suggests that the climate was the equivalent of the last stages of the last-glacial. This zone is tentatively correlated to oxygen isotope sub-stage 5b (Figure 4.02).

The stratigraphic occurrence of Epi.c/d of Epiha Tephra interbedded within Zone AR/B and within L4 on the NT2 terrace at

Onaero and Parao loess on the Rapanui Marine Terrace at Kohi Road in the Wanganui district tends to support correlation of Zone AR/B to cool climate conditions of sub-stage 5b (Figure 4.02).

CHAPTER 12

NEOTECTONICS

The Norfolk and Inglewood Faults are two sub-parallel, north-east trending faults that occur immediately north and south of Inglewood (Map 1). The Norfolk Fault, 5km south of Inglewood, is upthrown to the south-east but no lateral or vertical component of displacement was observed in the post-glacial to late last-glacial cover beds.

The Inglewood Fault approximates to the southern margin of the Eltham Laharic Planeze (Plate 12.01) and can be traced from Kaimiro in the south-west to the Waitara River in the north-east. Further south-west of Kaimiro, the surface trace of the Inglewood Fault is obscured beneath post-glacial volcaniclastics from Egmont Volcano but if extrapolated would extend through the edifice of Egmont Volcano.

The Inglewood Fault is upthrown to the north and north-west, and has both normal and dextral components of displacement which vary along the strike of the fault. The use of tephra and laharic chronohorizons has permitted the age of the most recent displacements on two sections of this fault to be approximately estimated.

Exposed in a farm excavation cut across the Inglewood fault trace at Q19/128275, sub-horizontal debris flow units of Warea Formation and medial material of L1.1 are upthrown c.2.5m to the north-west. On both sides of the fault trace, the S1 medial unit forms a 2.5m thick mantle but at the scarp S1 is clearly overthickened. Despite overthickening, lapilli inter-beds within S1 are generally continuous and remain undisturbed by vertical displacement. This suggests that this portion of the Inglewood

Fault has not been active since deposition of S1 beginning in late last-glacial times.

Another section across the Inglewood Fault was exposed during excavations at Everett Road Quarry, c.7km north-east of Inglewood (Figure 12.02). Here, the surface trace of the fault is not visible but a c.5m wide zone of open, en-echelon fissures cut vertically across sub-horizontal debris and hyperconcentrated flow deposits of Warea Formation was recognised. These fissures form discrete faulted blocks with minor vertical displacements on their uppermost surface. No vertical displacements of mantling medial beds (S1 and uppermost L1) and tephra inter-beds were observed.

Tephric and medial material mantling uppermost Warea Formation from both sections indicate their similar age and suggest differential rates of uplift along the fault.

Along the downthrown side of the Inglewood Fault, near Inglewood Borough, mounds of Okawa Formation are pricipally concentrated within a 2.5km wide belt that extends north-east to just west of the Waitara River. This suggests that at c.100kyrs B.P., the scarp of Inglewood Fault was physiographically prominent enough to constrain the major portion of the Okawa debris avalanche.

The Norfolk and Inglewood Faults are here considered to represent the onshore extension of a complex zone of sub-parallel, north-east trending normal faults that occur offshore within sediments of the Taranaki Basin. This zone, known as the 'Cook-Turi Lineament' (after Knox 1982), is a major structural feature of the Taranaki Basin and relates to differential stress within the continental crust as the dipping Pacific Plate boundary in the north, changes to an inferred vertical plate boundary beneath the South Island (Knox 1982).



Plate 12.01: Aerial Photograph of Inglewood Fault in the vicinity of Bristol Road, north-east of Inglewood Borough. Note hummocky terrain of **Okawa Formation** on the down-thrown (south-east) side of the fault trace.

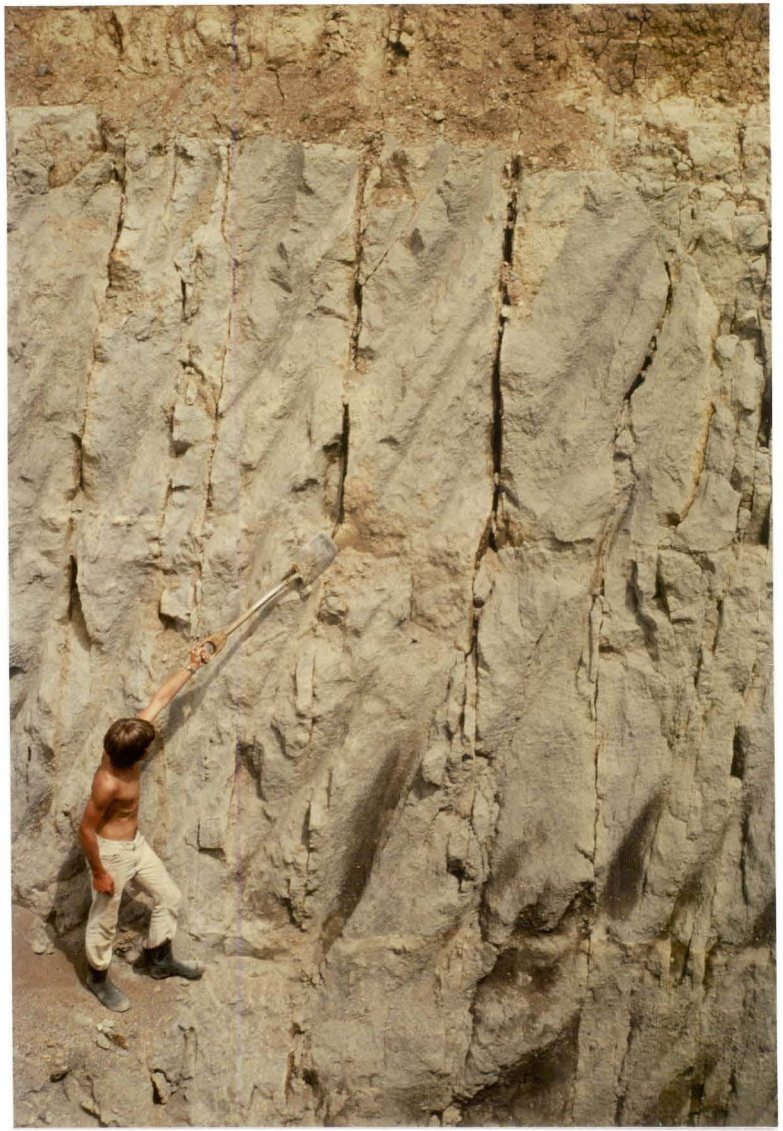


Plate 12.02: Cross-section of Inglewood Fault at Everett Road Quarry at Q19/205299. Here the fault dissects sub-horizontal debris flow deposits of **Warea Formation** and has formed a c.5m wide zone of open vertical en-echelon fissures.

Both the Inglewood and Norfolk Faults can be extrapolated to extend through Egmont Volcano, with activity on the former clearly demonstrated. If further movement were to occur along these faults and a portion of Egmont Volcano was displaced, an edifice collapse could occur without prior warning or precursory volcanic activity. This presents a significant new dimension to the consideration of hazards at Egmont Volcano.

CHAPTER 13

13.0 SUMMARY CONCLUSION

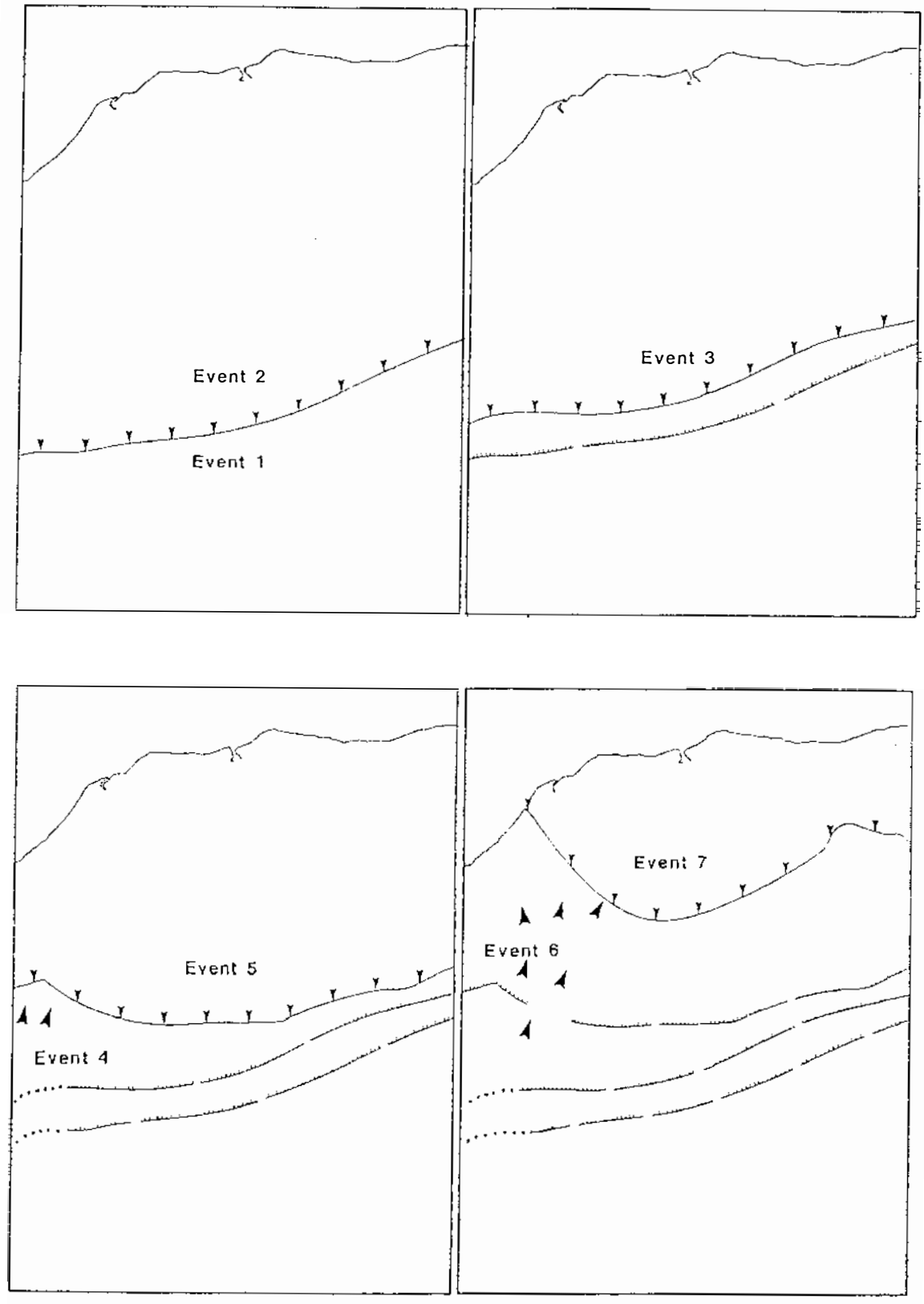
13.1 Lower to mid-Quaternary History of North-eastern Taranaki.

The oldest observable landform remnants in north-eastern Taranaki are prominent, high planar inter-fluves situated to the north of Inglewood, which were previously mapped as Eltham Lahars (Grant-Taylor 1964; Hay 1967). Eltham Lahars are considered to be related to volcanism centred at Kaitake Volcano and were probably deposited around 0.5 myrs B.P. (Event 1 of Figure 13.01). The seaward edge of the Eltham Laharic Surface was subsequently truncated by the NT5 high sea level transgression (Event 2 of Figure 13.01). A minimum age of 0.43 +/- 0.07 myrs B.P. for NT5 terrace is established from a fission-track date of zircons obtained from the Mountain Road tephra occurring within its cover. The NT5 terrace was later truncated during the culmination of the NT4 high sea level transgression (Event 3 of Figure 13.01). NT4 terrace, west of Bell Block, was then extensively inundated by Maitahi Lahars which relate to volcanism centred at Pouakai Volcano (Event 4 of Figure 13.01). The apparent absence of the NT4 and NT5 cliffs in this vicinity almost certainly relates to burial by Maitahi Lahars.

Near New Plymouth, a Maitahi Lahar deposit, is closely overlain by the Smart Road tephras originating from the Central North Island. These rhyolitic tephras are provisionally correlated to MGR1 and MGR2 tephra exposed at Griffin Road Quarry, near Marton, which are considered to be slightly younger (between 210 and 240kyrs B.P.) than the c.240kyr Mt. Curl Tephra. The Smart Road tephras, are therefore useful in establishing an approximate minimum age for Maitahi Lahar deposits on NT4 terrace.

FIG. 13.01 Construction of the North Taranaki Coastal Plain

(Events 1 – 7)



The seaward edge of the surface mapped as Maitahi Lahars by Neall (1979), which grades eastward into NT4 terrace, was then cliffed during the culmination of the NT3 high sea level transgression (Event 5 of Figure 13.01). The conspicuous absence of Smart Road tephras within the cover of this terrace suggests that the culmination of the marine transgression which cut the NT3 wave cut surface must have post-dated the deposition of the tephras. A single amino acid racemisation date of wood obtained from lignite closely overlying the NT3 wave-cut surface yielded a D/L ratio similar to wood samples from the cover of Ngarino Terrace in Wanganui. In the absence of any direct evidence as to the exact timing of this culmination, an age of c.200kyrs B.P. is postulated.

Closely following the emergence of NT3 terrace, several unnamed lahars originating from Pouakai Volcano inundated the terrace between Bell Block and the New Plymouth Airport. One particularly large lahar, containing fragmental rock clasts, was directed north-eastwards across the terrace to as far as Waiau Stream (Event 6 of Figure 13.01). From the distribution of these lahars they appear to have been channelled within an ancestral Waiwhakaiho River catchment which flowed in a north-easterly direction and formerly occupied the northern portion of the present-day Mangaoraka Stream course.

The NT3 terrace was later cliffed during the culmination of the NT2 high sea level event at c.130kyrs B.P. (Event 7 of Figure 13.01). Eastward of Waiau Stream, Tertiary siltstone was wave-cut by the NT2 high sea level event. However, westward of Waiau Stream, the NT2 high sea level cut an unnamed lahar deposit that preserves the NT3 wave cut surface closely beneath its base. During this NT2 high sea level, a prominent soil (S6) was forming upon the surface of older uplifted terraces.

13.2 Upper Quaternary History of North-eastern and Central Taranaki.

Stratigraphic summaries are given in Figures 13.03 and 13.04 as accompaniments to the Upper Quaternary history of north-eastern and central Taranaki.

Following the emergence of NT2 terrace the coastal plain was extensively inundated by the Motunui lahar at c.115kyrs B.P. (Event 8 of Figure 13.02). This event coincided with climatic conditions in Taranaki becoming cooler and drier. Motunui lahar, channelled down the Waitara River valley, laterally spread onto the coastal plain and extended north-eastward to as far as the Onaero River. Except for a small remnant located south-east of Waitara, the lahar mostly inundated and subdued the surface expression of the NT2 fossil cliff. This event probably represents the first evidence of activity centred at Egmont Volcano, however the extent and volume of this laharic event suggests that Egmont Volcano was already a prominent physiographic feature of the Central Taranaki landscape in Upper Quaternary time. Exactly when activity at Egmont Volcano first commenced is presently unknown.

A period of continuous, small scale, tephra emission closely followed deposition of Motunui lahar, with at least forty-five ash and lapilli beds of Ninia tephra recognised. These beds are often preserved within lacustrine sediment and lignites that overlie the Motunui lahar deposit. Occasionally in the soil forming environment these tephras were locally redeposited.

A major collapse of Egmont Volcano, generating the Okawa debris avalanche, occurred during a warm period at c.100kyrs B.P. when the North Taranaki coastal plain was occupied by an extensive podocarp-broadleaf forest. The Okawa debris avalanche laterally

transformed into a mudflow as it channelled down the Waiongana Stream and Manganui/Waitara River catchments. The Okawa debris avalanche extensively inundated the forested coastal plain and contributed to burial of the NT2 fossil cliff to the west of Waitara (Event 9 of Figure 13.02).

A period of intense eruptive activity, depositing Epiha Tephra, marked the beginning of a major reconstruction phase of the volcano following the Okawa cone collapse event. As the cone began to be rebuilt, climatic conditions again became cooler and drier. This change in climate is evident from localised overthickening of tephra indicating aeolian redeposition and the change in coastal vegetation from forest to a forest-shrubland-grassland mosaic.

Epiha Tephra continued to be deposited as climatic conditions became warmer and wetter, and as the podocarp-broadleaf forest recolonised the coastal plain. This warming culminated in a marine transgression which cut the NT1 wave-cut surface and truncated the seaward edge of NT2 terrace at c.80kyrs B.P. (Event 10 of Figure 13.02).

The ensuing period between c.78 and 60kyrs B.P. was characterised by intermittent tephra emission from Egmont Volcano that included Te Arei Tephra as well as, Araheke and Waitui tephras. This period was also characterised by cold and dry climatic conditions as indicated by the addition of an inter-regional aeolian quartz component to the Taranaki cover beds and localised aeolian overthickening of medial material.

The episode following this cold period was characterised by mild climate and reduced activity at Egmont Volcano between c.60 and 48kyrs B.P. It was during this episode that S3 formed. At c.50kyrs B.P. the Rotoehu Tephra derived from the Okataina Volcanic Centre was deposited in uppermost S3.

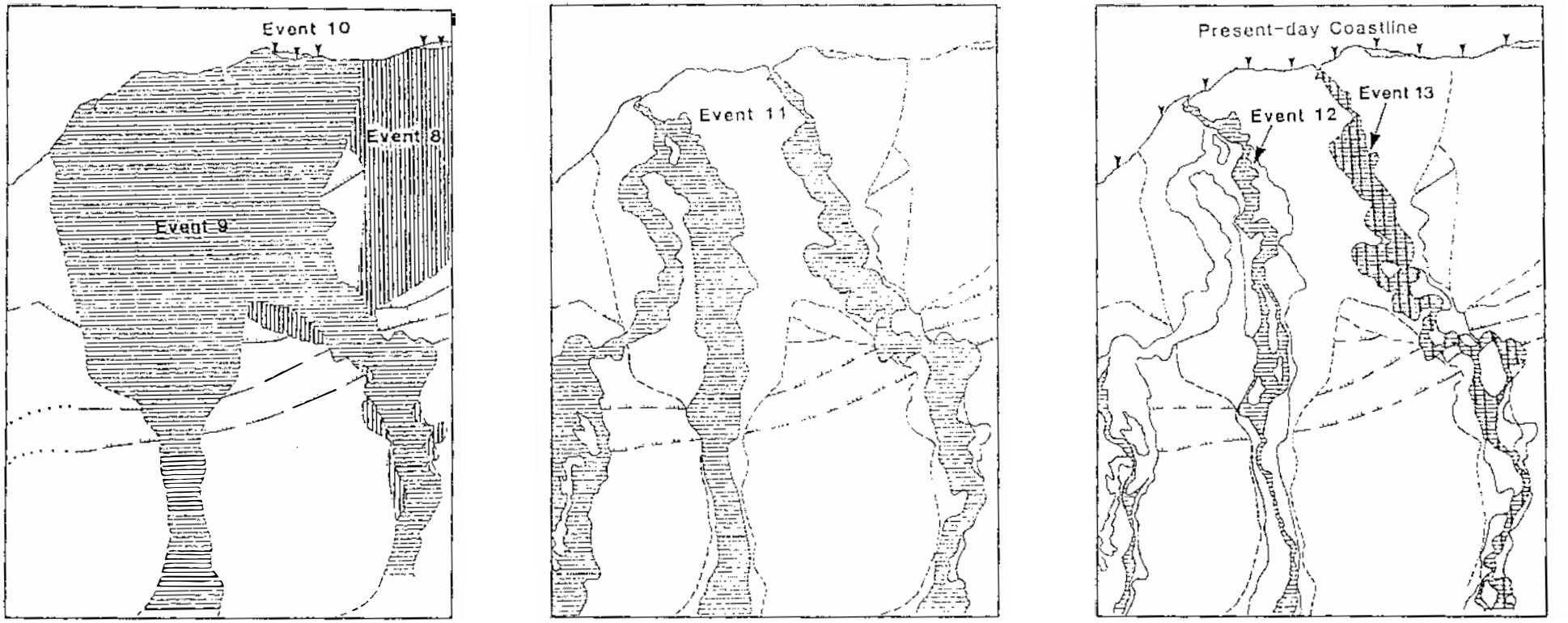


FIG. 13.02 Construction of the North Taranaki Coastal Plain

(Events 8 – 13)

FIG. 13.03 Post-130kyr and Pre-28kyr Stratigraphic Summary

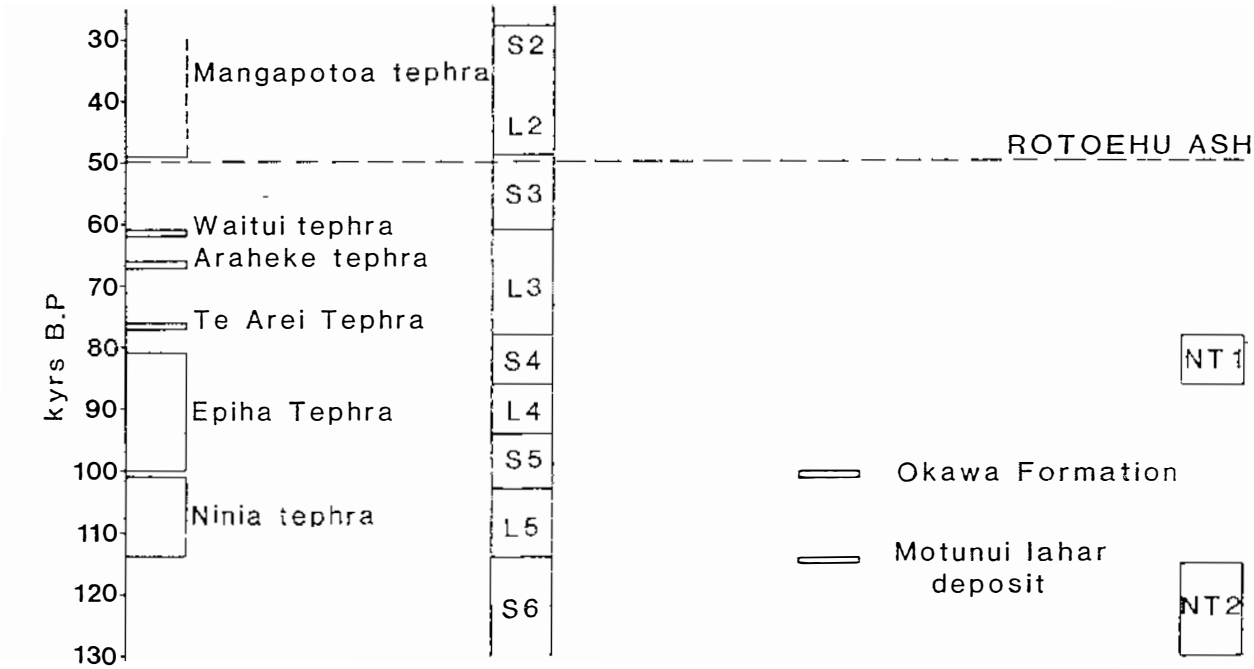
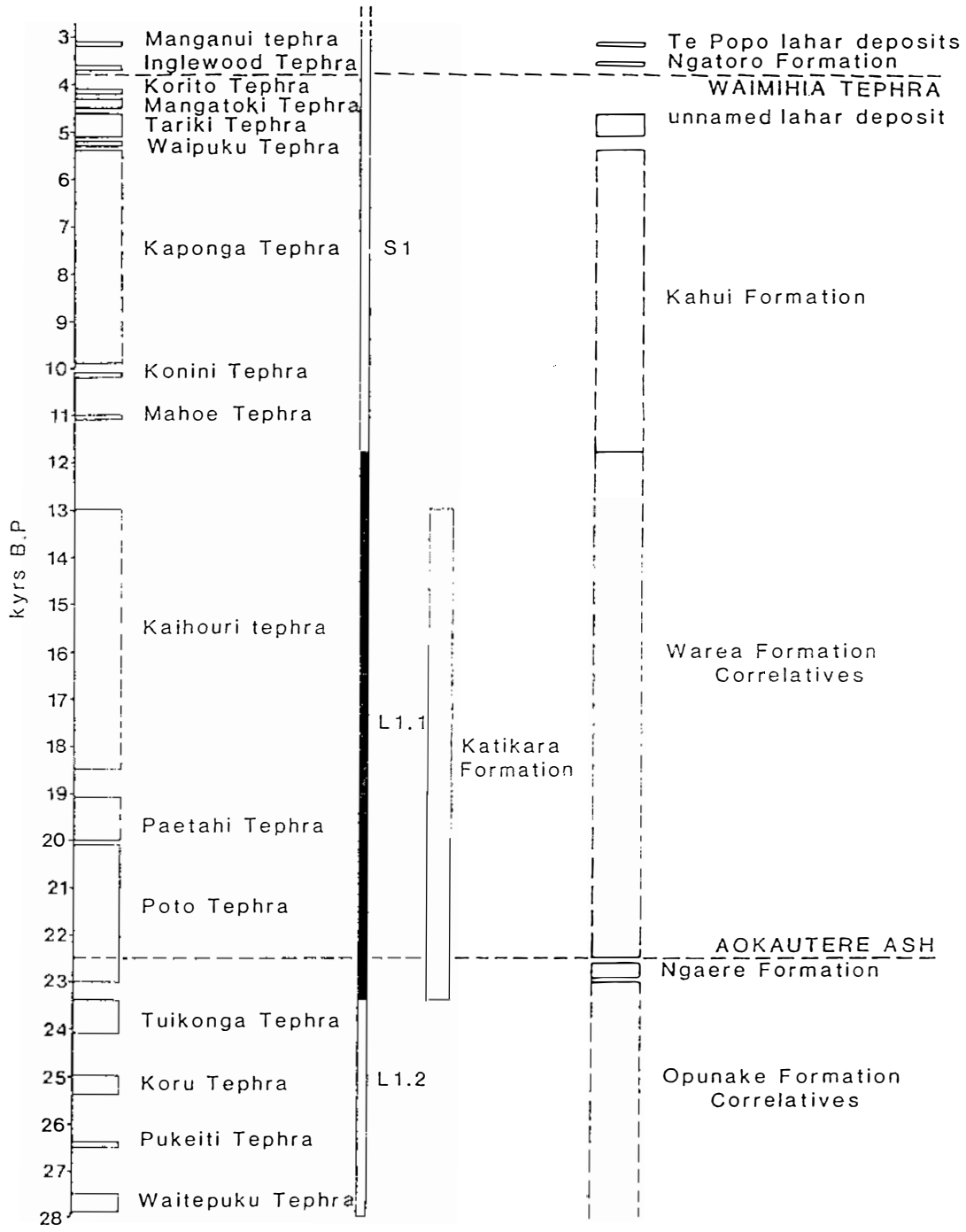


FIG. 13.04 Post-28kyr and Pre-3kyr Stratigraphic Summary



Following the deposition of Rotoehu Tephra in Taranaki, climatic conditions between c.48 and 40kyrs became cooler. Sporadic small magnitude ash and lapilli beds (Mangapotoa tephra) erupted during this period were locally redeposited.

The formation of S2 and the apparent absence of coarse ash and lapilli inter-beds within it, suggests minor volcanic activity centred at Egmont Volcano during a mild climate episode between c.40 and 28kyrs B.P.

At about c.28kyrs B.P. activity at Egmont Volcano intensified with frequent, moderate to large magnitude tephra emissions. This activity resulted in a sequence of thirteen tephras (lower Tuna Tephra Sub-group) being deposited in north-east and central Taranaki. Debris flows (Opunake Formation), also generated from this activity, inundated north-eastern portions of the Egmont ring plain. Larger debris flows spread down the Waiwhakaiho, Mangaoraka and Waiongana catchments to the coastal plain.

Coinciding with this increase in eruptive activity was a steadily increasing influx of inter-regional aeolian quartz to the cover beds. This indicates progressively colder and drier climatic conditions. At c.23kyrs climatic conditions in Taranaki had deteriorated to such an extent that andesitic sand dunes of Katikara Formation started to develop from pedospheric stripping of tephra and from the aeolian redeposition of sub-aerially exposed fluvial deposits within and adjacent to major catchments. Localised erosion and aeolian redeposition of tephric and medial material also commenced on the ring plain about this time.

A tephra eruption, representing a renewed cycle of activity at c.23kyrs B.P., appears to have initiated a partial collapse of

Egmont Volcano and generated a large volume debris avalanche that spread principally east and south-eastwards. The resulting deposit (Ngaere Formation), with a minimum areal extent of 320km^2, is characterised by numerous mounds between Waipuku and Kaponga, and is recognised at the South Taranaki coast and within the Waitara River valley on the North Taranaki coastal plain. Immediately overlying Ngaere Formation is a sequence of thirteen units of Poto Tephra that represent a post-avalanche phase of high frequency eruptive activity and active reconstruction of a lava dome or central cone. The eruptive products originating from this intense activity were principally directed east and south-eastwards and the initial phase of this intense activity was coincident with the deposition of Aokautere Ash erupted from the Taupo Volcanic Centre at c.22.5kyrs B.P.

A subsequent collapse of Egmont Volcano generating another debris avalanche that spread principally westwards, occurred during the latter stages of the post-Ngaere avalanche phase of cone reconstruction (closely following deposition of Aokautere Ash). The resulting deposit (Pungarehu Formation), with a minimum volume of 6km^3 and an areal extent of over 250km^2 is characterised by an extensive area of mounds between Okato and Opunake.

Closely after deposition of Poto Tephra, a renewed cycle of activity between c.20 and 19kyrs resulting in fresh tephra eruptions (Paetahi Tephra) that were principally directed east and south-eastwards. A culmination in the influx of inter-regional aeolian quartz to the region closely coincided with the deposition of Paetahi Tephra.

A period of sporadic eruptions followed, depositing Kaihouri tephra between c.18.5 and 13kyrs B.P. Levels of inter-regional quartz over this time progressively declined indicating climatic

amelioration. At least five debris flows (Warea Formation), generated from activity between c.22.5 and 13kyrs, extensively inundated the north-eastern portion of the Egmont ring plain and spread down the Mangaoraka, Waiongana and Manganui/Waitara catchments onto the North Taranaki coastal plain (Event 11 of Figure 13.02). Some Warea debris flows laterally transformed into hyperconcentrated flows.

As climatic conditions became steadily warmer at c.13kyrs B.P., the ring plain vegetation changed from a forest-shrubland-grassland mosaic to podocarp-broadleaf forest and the influx of inter-regional aeolian quartz was reduced to trace levels. The incidence of localised erosion and redeposition of tephra in central Taranaki also diminished. By c.12kyrs B.P. climatic conditions were warm and moist, and a podocarp-broadleaf forest was now well established on the ring plain.

Sporadic activity between c.12 and 10kyrs resulted in the deposition of Mahoe and Konini Tephra over a large area of central and south-eastern Taranaki at c.11.4 and c.10.1kyrs B.P., respectively. Activity then intensified between 10 and 8kyrs B.P. which resulted in eight units of Kaponga Tephra being deposited over central and south-eastern Taranaki. At least three debris flows (Kahui Formation), also generated from this activity, inundated north-eastern portions of the Egmont ring plain and became principally confined within the channels of the Mangaoraka and Waiongana Streams. One Kahui debris flow confined within the Waiongana catchment extended north to the coast (Event 12 of Figure 13.02).

A period of sporadic activity between c.8 and 5kyrs B.P. followed, which resulted in two units of Kaponga Tephra being deposited over south-eastern Taranaki, and Waipuku Tephra deposited over a wider area of north-eastern and south-eastern

Taranaki. An unnamed debris flow generated from the emission of Waipuku Tephra at c.5.2kyrs B.P., inundated eastern portions of the Egmont ring plain and spread along the channels of Waipuku Stream and its tributaries.

At about c.4.7kyrs B.P. activity briefly intensified with frequent, small to large magnitude tephra emissions. This activity resulted in a sequence of six tephra (Tariki Tephra) being deposited over south-eastern and central Taranaki. This was closely followed by sporadic activity which resulted in two small pumiceous tephra (Mangatoki Tephra) being deposited over south-eastern Taranaki at c.4.4kyrs B.P. Ensuing sporadic large magnitude tephra emission resulted in Korito Tephra at c.4.1kyrs B.P. and Inglewood Tephra at c.3.6kyrs B.P. being widely dispersed over north-eastern and central Taranaki. At least three pyroclastic density currents were also generated during this phase of large magnitude tephra emission but did not extend beyond the confines of the National Park boundary.

The eruption of Inglewood Tephra was closely followed by a laharic event (Ngatoro Formation) which extensively inundated the forested north-eastern and central portions of the ring plain. The lahar reached the North Taranaki coast (Event 13 of Figure 13.02) after it had become confined within the channels of Ngatoro, Waitepuku and Mangamawhete Stream tributaries and the Manganui River.

At about c.3.1kyrs activity at Fanthams Peak began with frequent, small to moderate magnitude tephra emissions. This activity resulted in a sequence of four closely spaced tephra (Manganui tephra) being deposited over central and north-eastern Taranaki. At least two debris flows (Te Popo debris flows), were also generated during this activity at Fanthams Peak. These debris flows extended just outside the National Park boundary on the

eastern lower flanks of Egmont Volcano and were confined within the channels of tributaries between the Manganui River and Waingongoro River.

In north-eastern and central Taranaki, the last definite evidence of activity at Egmont Volcano is represented by dispersed lapilli above Manganui tephra in the topsoil. An eruption at c.2kyrs B.P. from the main vent of Egmont Volcano (Neall and Alloway 1986) resulted in Maketawa tephra being deposited just outside the National Park boundary.

REFERENCES

Adams, R.D.; Ferris, B.G. 1976: A further earthquake at exceptional depth beneath New Zealand (note). New Zealand Journal of Geology and Geophysics 19: 269 - 273.

Adams, R.D.; Ware, D.E. 1977: Sub-crustal earthquakes beneath New Zealand; locations determined with a laterally inhomogeneous velocity model. New Zealand Journal of Geology and Geophysics 20: 59 - 84.

Aitken, J.F.; Campbell, I.B.; Wilde, R.H. 1978: Soils of Stratford County, North Island, New Zealand. New Zealand Soil Survey Report 42.

Alloway, B.V.; Neall, V.E.; Vucetich, C.G. 1988: Localised volcanic loess deposits in north Taranaki, North Island, New Zealand. In Loess - its distribution, geology and soils. Edited by Eden, D.N; Furkert, R.J. A.A.Balkema Publishers, Rotterdam. p.1 - 8.

American Commission on Stratigraphic Nomenclature, 1961: Code of Stratigraphic Nomenclature In Bulletin of the American Association of Petroleum Geologists 45 (5): 645 - 665.

Ando, S.; Yamagishi, H. 1975: Hill topography on the nuee-ardente deposits on the Shikaribetsu volcano. Bulletin of Volcanological Society of Japan 20: 31 - 36.

Aomine, S.; Wada, K. 1962: Differential weathering of pumice resulting in formation of hydrated halloysite. American Mineralogist 47: 1024 - 1048.

Aramaki, S.; Shimozuru, D.;Ossaka, J. 1981: Asama volcano. in S.Aramaki (editor) Symposium Arc Volcanism field excursion guide to Fuji, Asama, Kusatsu-Shirane and Nantai volcanoes, part 2. Volcanological Society of Japan : 23 - 48.

Baumgart, I.L.; 1954: Some ash showers of the Central North Island. New Zealand Journal of Science and Technology B35: 456 - 467.

Bechtel 1981: Investigation for Site Improvement. Gas to Gasoline Plant, Motunui. Unpublished Report held at Taranaki Catchment Commission, Stratford.

Berryman, K. 1985: Climatic implications of Quaternary geology at Mahia Peninsula, East Coast, North Island in the period 133,000 years B.P. to present. In The second symposium of results and discussions concerned with late Quaternary climatic history of Australia, New Zealand and surrounding seas. Proceedings of the second CLIMANZ conference held at Harihari, Westland, New Zealand, February 4-8 1985. Pillans, B.J. (ed). Geology Department, Victoria University of Wellington Publication 31. p. 2 - 4.

Bemmelen, R.W. van. 1949: The geology of Indonesia. General geology of Indonesia and adjacent archipelagoes 1A. The Hague, Government Printing Office, 732 p.

Benny, L.A. 1982: A mineralogical and textural study of Central North Island Tephra, Okareka Ash and its overlying tephric loess deposits. MSc.thesis lodged in the library, Massey University, Palmerston North.

Beverage, J.P.; Culbertson, J.K. 1964: Hyperconcentrations of suspended sediments. Journal of the Hydraulics Division, Proceedings of the American Society of Civil Engineers, 117 - 128.

Birrell, K.S. 1951: Some physical Properties of New Zealand Ash Soils. Proceedings of the 7th Congress of the Royal Society of New Zealand., pp.208 - 216.

Birrell, K.S.; Feildes, M. 1952: Allophane in Volcanic Ash Soils. Journal of Soil Science 3: 156 - 166.

Boellstorff, J.D.; Te Punga, M.T. 1977: Fission track ages and correlation of middle and lower Pleistocene sequences from Nebraska and New Zealand. New Zealand Journal of Geology and Geophysics 20: 47 - 58.

Bossard, L. 1928: Origin of the conical hills in the neighbourhood of Mt. Egmont. New Zealand journal of Science and Technology 10: 119 - 125.

Campbell, I.B. 1971: A weathering sequence of basaltic soils near Dunedin, New Zealand. New Zealand Journal of Science 14: 907 - 924.

-1986: New occurrences and distribution of Kawakawa tephra in South Island, New Zealand. New Zealand Journal of Geology and Geophysics 29: 425 - 437.

Chappell, J. 1964: Quaternary geology of south-west Auckland and North Taranaki. Unpublished Ph.D thesis lodged in the library, University of Auckland.

-1975: Upper Quaternary warping and uplift rates in the Bay of Plenty and West Coast, North Island, New Zealand. New Zealand Journal of Geology and Geophysics 18: 129 - 155.

Christoffel, D.A.; Calhaem, I.M. 1973: Upper mantle viscosity determined from Stokes Law. Nature 243: 51 - 52.

Clarke, E.de C. 1912: The geology of the New Plymouth Subdivision. New Zealand Geological Survey Bulletin n.s.14: 58p.

Cole, J.W.; Kohn, B.P. 1972: Pyroclastic nomenclature in New Zealand (comment). New Zealand Journal of Geology and Geophysics 15: 686 - 692.

Colmet-Daage, F.; Gautheyrou, J.; Gautheyrou, M.; de Kimpe, C.; Fusil, G. 1972: Dispersion et etude des fractions fines de sols a allophane des Antilles et d'Amerique Latin. Part 1 Dispersion, C.A.H., O.R.S.T.O.M Serie Pedologie (France) 10; No.2: 169 - 191.

Cotton, C.A. 1969: Volcanoes as landscape forms (2nd ed.). Hafner, New York, N.Y., 416p.

Crandell, D.R. 1971: Postglacial lahars from Mount Rainier Volcano, Washington. U.S. Geological Survey Professional Paper 677, 73 p.

Crandell, D.R.; Miller, C.D.; Glicken, H.X.; Christiansen, R.L.; Newhall, C.G. 1984: Catastrophic debris avalanche from ancestral Mount Shasta volcano, California. Geology 12: 143 - 146.

Cullen, D.J. 1967: Submarine evidence from New Zealand of a rapid rise in sea level at 11,000 years B.P. Palaeogeography, Palaeoclimatology and Palaeoecology 3: 289 - 298.

De Angelis, M.; Barkov, N.I.; Petrov, V.N. 1987: Nature 325: 318 - 321.

Dibble, R.R.; Neall, V.E. 1984: Volcanic hazards in New Zealand In Natural Hazards in New Zealand. Speden, I.; Crozier, M.J. (eds.) (332 - 374). New Zealand Commission for UNESCO, Wellington 500p.

Dibble, R.R.; Nairn, I.A.; Neall, V.E. 1985: Volcanic hazards of North Island, New Zealand - Overview. Journal of Geodynamics 3: 369 - 396.

Dickson, M.; Fleming, C.A.; Grant-Taylor, T.L. 1974: Ngarino Terrace: An addition to the late Pleistocene standard sequence in the Wanganui - Taranaki District. New Zealand Journal of Geology and Geophysics 17: 789 - 798.

Druce, A.P. 1966: Tree ring dating of recent volcanic ash and lapilli, Mt.Egmont. New Zealand Journal of Botany 4: 3 - 41.

Dunbar, C.O.; Rodgers, J. 1957: Principles of Stratigraphy. J. Wiley, New York. 356p.

Duncan, A.R.; Taylor, S.R. 1968: Trace element analyses of magnetites from andesitic and dacitic lavas from the Bay of Plenty, New Zealand. Contributions to Mineralogy and Petrology 20: 30 - 33.

Ewart, A. 1967: Pyroxene and magnetite phenocrysts from the Taupo Quaternary rhyolitic pumice deposits, New Zealand. Mineralogical Magazine 36 (278): 180 - 194.

Fergusson, G.J.; Rafter, T.A. 1957: New Zealand C14 measurements - 3. New Zealand journal of science and technology B38: 732 - 749.

Fey, M.; Le Roux, J. 1975: Quantitative determination of allophane in soil clays. Proceedings of the International clay conference, Mexico. Applied Publishing, Wilmette, Illinois. pp. 451 - 463.

-1977: Properties and quantitative estimation of poorly crystalline components in sesquioxidic soil clays. Clay and Clay Mineralogy 25: 285 - 294.

Fisher, R.V. 1961: Proposed classification of volcaniclastic sediments and rocks. Geological Society of America Bulletin 72: 1409 - 1414.

Fisher, R.V.; Schmincke, H.-U., 1984: Pyroclastic Rocks. Springer - Verlag, Berlin, 472 p.

Fleming, C.A. 1953: The geology of the Wanganui Subdivision. New Zealand Geological Survey Bulletin 52, 362p.

Franks, A.M. 1984: Soils of Eltham County and the tephrochronology of Central Taranaki. Unpublished Ph.D thesis, lodged in the Library, Massey University, Palmerston North.

Froggatt, P.C. 1981a: Review of Holocene eruptions from Taupo. In Howorth, R. et.al. ed. Proceedings of the tephra workshop. Geology Department, Victoria University of Wellington publication 20: 21 - 28.

-1981b: Karapiti Tephra Formation: a 10,000 years B.P. rhyolitic tephra from Taupo. New Zealand Journal of Geology and Geophysics 24: 95 - 98.

-1983: Toward a comprehensive Upper Quaternary tephra and ignimbrite stratigraphy in New Zealand using electron microprobe analysis of glass shards. Quaternary Research 19: 188 - 200.

Froggatt, P.C.; Nelson, C.S.; Carter, L.; Griggs, G.; Black, K.P. 1986: An exceptionally large late Quaternary eruption from New Zealand. Nature 319: 578 - 582.

Geddes, A.M.; Neall, V.E. 1982: Elucidation of the Stratford Shower In Soil Groups of New Zealand, Part 6, Yellow-Brown Loams. V.E.Neall (Ed); New Zealand Society of Soil Science.

Glicken, H.X. 1986: Rockslide-avalanche of May 18 1980, Mt. St. Helens volcano. Unpublished Ph.D thesis lodged in the library Santa Barbara University of California.

Glicken, H.X.; Voight, B.; Janda, R.J. 1981: Rockslide-debris avalanche of May 18, 1980, Mount St. Helens volcano (abstr.) IAVCEI Symposium Arc Volcanism, Tokyo and Hakone, pp. 109 - 110.

Grange, L.I.; Taylor, N.H. 1933: Report on soil surveys for 1932-33. Department of Scientific and Industrial Research, Annual Report 1932-1933.

Grant-Taylor, T.L. 1964a: Volcanic history of western Taranaki. New Zealand Journal of Geology and Geophysics 7: 78 - 86.

-1964b: Geology of Egmont National Park. pg. 13 - 26 in Scanlan, A.B. (Ed.): Egmont National Park. Handbook of Egmont National Park Board, New Plymouth. p.87.

Grant-Taylor, T.L., Rafter, T.A. 1971: New Zealand radiocarbon measurements - 6. New Zealand Journal of Geology and Geophysics 14: 364 - 402.

Hatherton, T. 1969: The geophysical significance of calc-alkaline andesites in New Zealand. New Zealand Journal of Geology and Geophysics 12: 436 - 459.

-1970: Upper mantle inhomogeneity beneath New Zealand: surface manifestations. Journal of Geophysical Research 73: 269 - 284.

Hay, R.F. 1967: Sheet 7 Taranaki (1st Ed) "Geological Map of New Zealand 1:250,000" N.Z. D.S.I.R, Wellington.

Healy, J. 1964: Stratigraphy and chronology of late Quaternary volcanic ash in Taupo, Rotorua and Gisborne districts. Part 1. New Zealand Geological Survey Bulletin 73: 7 - 42.

Healy, T.R. 1970: Dust from Australia - a reappraisal. Earth Science Journal 4 (2): 106 - 116.

Henderson, J.; Ongley, M. 1923: The geology of the Mokau Subdivision, New Zealand. Geological Survey Bulletin 24: 83pp.

Higashi, T.; Ikeda, H. 1974: Dissolution of Allophane by Acid Oxalate Solution. Clay Science 4: 205 - 212.

Hogg, A.G.; McCraw, J.D. 1983: Late Quaternary tephras of Coromandel Peninsula, North Island, new Zealand: a mixed peralkaline and calcalkaline tephra sequence. New Zealand Journal of Geology and Geophysics 26: 163 - 187.

Howorth, R. 1975: New formations of late Pleistocene tephras from the Okataina Volcanic Centre, New Zealand. New Zealand Journal of Geology and Geophysics 18: 683 - 712.

Howorth, R.; Topping, W.W. 1979: Rhyolitic late Pleistocene tephras to the south and west of Lake Taupo, New Zealand. New Zealand Journal of Geology and Geophysics 22: 759 - 762.

Howorth, R.; Froggatt, P.C.; Robertson, S.M. 1980: Late Quaternary volcanic ash stratigraphy of the Poukawa area, central Hawkes Bay, New Zealand. New Zealand Journal of Geology and Geophysics 23: 487 - 491.

ICOMAND (International Committee on the Classification of Andisols, C/- Soil Bureau, D.S.I.R., Lower Hutt, New Zealand) Circular No.10, 29 February 1988.

Jackson, M.L. 1956: Soil Chemical Analysis - Advanced Course. Published by the author, Department of Soil Science, University of Wisconsin, Madison, Wisconsin.

Janda, R.J.; Scott, K.M.; Nolan, K.M.; Martinson, H.A. 1981: Lahar movement, effect and deposits. In Lipman, P.W. and Mullineaux, D.R., editors, The 1980 eruptions of Mount St. Helens, Washington: U.S. Geological Survey Professional Paper 1250: 461 - 478.

Johnson, P.R.; Beavers, A.H. 1959: A mineralogical characterisation of some loess derived soils in Illinois. Soil Science Society of America Proceedings 23: 143 - 146.

Kaewyana, W. 1980: Late Quaternary alluvial terraces and their cover bed stratigraphy, Eketahuna and Pahiatua districts, New Zealand. Unpublished M.Sc thesis lodged in the library, Victoria University of Wellington.

Katz, H.R. 1974: Offshore petroleum potential in New Zealand. APEA Journal 14: 3 - 13.

Kennedy, N.M. 1987: Third meeting of the Western Pacific Working Group of the INQUA Loess Commission (Ed. Heine, J.C). Tour Guide for International Symposium on Loess 14-21 February 1987, New Zealand. p.71 - 81.

-1988: Late Quaternary loess associated with the Mamaku Plateau, North Island, New Zealand. In Loess - its distribution, geology and soils. Edited by Eden, D.N; Furkert, R.J. A.A.Balkema Publishers, Rotterdam. 245p.

Kirkman, J.H. 1978: Clay mineralogy of New Zealand ash soils and tephras: A silver Jubilee review. New Zealand Soil News 26: 12 -18.

-1980b: Clay mineralogy of a sequence of andesitic tephra beds of Western Taranaki, New Zealand. Clay Minerals 15: 157 - 163.

-1981: Morphology and structure of Halloysite in New Zealand tephras. Clays and Clay Minerals 29: 1 - 9.

-1981a: Some primary mineral to clay mineral transformations in New Zealand tephras and tephra-derived soils. Abstracts, International "Soils with Variable Charge" Conference, Massey University, Palmerston North, New Zealand: 169 - 170.

Kirkman, J.H.; McHardy, W.J. 1980: A comparitive syudy of the morphology, chemical composition and weathering of rhyolitic and andesitic glass. Clay Minerals 15: 165 - 173.

Knox, G.J. 1982: Taranaki Basin, structural style and tectonic setting. New Zealand Journal of Geology and Geophysics 25: 125 - 140.

Kobo, K. 1964: Properties of Volcanic Ash Soils. FAO/UNESCO, World Soil Resources Report 14: 71 - 73.

Kohn, B.P. 1970: Identification of New Zealand tephra layers by emission spectrographic analysis of their titanomagnetites. Lithos 3: 361 - 368.

-1973: Studies of New Zealand Quaternary Pyroclastic Rocks. Unpublished Ph.D. thesis, Victoria University of Wellington Library, Wellington.

Kohn, B.P.; Neall, V.E. 1973: Identification of late Quaternary tephras for dating Taranaki lahar deposits. New Zealand Journal of Geology and Geophysics 16: 781 - 792.

Kuntz, M.A.; Rowley, P.D.; MacLeod, N.S.; Reynold, R.L.; McBroome, L.A.; Kaplan, A.M. ; Lidke, D.J. 1981: Petrography and Particle Size Distribution of Pyroclastic-flow, Ash-cloud, and Surge Deposits In Lipman, P.W. and Mullineaux, D.R., editors, The 1980 eruptions of Mount St. Helens, Washington: U.S. Geological Survey Professional Paper 1250: 525 - 547.

Lees, C.M. 1986: Late Quaternary palynology of the southern Ruahine Range, North Island, New Zealand. New Zealand Journal of Botany 24: 315 - 329.

Lewis, K.B.; Eade, J.V. 1974: Sedimentation in the vicinity of the Maui gas field. New Zealand Oceanographic Institute Oceanographic Summary, 6.

Lowe, D.J. 1987: Studies on late Quaternary tephras in the Waikato and other regions in northern North Island, New Zealand, based on distal deposits in lake sediments and peats. Unpublished D.Phil thesis lodged in the library, University of Waikato, Hamilton.

-1988: Stratigraphy, age, composition, and correlation of Late Quaternary tephras interbedded with organic sediments in Waikato lakes, North Island, New Zealand. New Zealand Journal of Geology and Geophysics 31: 125 - 165.

Lowe, D.J.; Hogg, A.G. 1986: Tephrostratigraphy and chronology of the Kaipo Lagoon, an 11,500 year old montane peat bog in Urewera National Park, New Zealand. Journal of the Royal Society of New Zealand 16: 25 - 41.

Lowe, D.J.; Hogg, A.G.; Green, J.D.; Boubee, J.A.T. 1980: Stratigraphy and chronology of late Quaternary tephras in lake Maratoto, Hamilton, New Zealand. New Zealand Journal of Geology and Geophysics 23: 481 - 485.

MacDonald, G.A. 1972: Volcanoes Prentice-Hall, Englewood Cliffs, N.J., 510p.

Maeda, T.; Takenaka, H.; Warkentin, B.P. 1977: Physical Properties of allophanic soils. Advances in Agronomy 29: 229 - 264.

Marshall, P. 1903: Dust Storms in New Zealand. Nature 68: 223.

Marshall, P.; Kidson, E. 1929: The duststorms of October 1928. New Zealand Journal of Science and Technology 10: 291 - 299.

McBeath, D.M. 1977: Gas condensate fields of the Taranaki basin, New Zealand. New Zealand Journal of Geology and Geophysics 20: 99 - 128.

McGlone, M.S. 1985: Biostratigraphy of the last interglacial-glacial cycle, southern North Island. In The second symposium of results and discussions concerned with late Quaternary climatic history of Australia, New Zealand and surrounding seas. Proceedings of the second CLIMANZ conference held at Harihari, Westland, New Zealand, February 4-8 1985. Pillans, B.J. (ed). Geology Department, Victoria University of Wellington Publication 31. p.17 - 32.

McGlone, M.S; Moar, N.T. 1977: The Ascarina decline and post-glacial climatic change in New Zealand. New Zealand Journal of Botany 15: 485 - 489.

McGlone, M.S; Topping, W.W. 1977: Aranuian (post-glacial) pollen diagrams from the Tongariro region, North Island, New Zealand. New Zealand Journal of Botany 15: 749 - 760.

McGlone, M.S; Howorth, R.; Pullar, W.A. 1984: Late Pleistocene stratigraphy, vegetation and climate of the Bay of Plenty and Gisborne Regions, New Zealand. New Zealand Journal of Geology and Geophysics 27: 327 - 350.

McGlone, M.S.; Neall, V.E.; Clarkson, B.D. 1988: The effect of recent volcanic events and climatic changes on the vegetation of Mt Egmont (Mt Taranaki), New Zealand. New Zealand Journal of Botany 26: 123 - 144.

Miller, C.D.; Mullineaux, D.R.; Crandell, D.R. 1981: In Lipman, P.W. and Mullineaux, D.R., editors, The 1980 eruptions of Mount St. Helens, Washington: U.S. Geological Survey Professional Paper 1250: 789 - 802.

Milne, J.D.G. 1973a: Upper Quaternary geology of the Rangitikei drainage basin, North Island, New Zealand. Unpublished Ph.D thesis lodged in the library, Victoria University of Wellington.

Milne, J.D.G.; Smalley, I.J. 1979: Loess deposits in the southern part of the North Island of New Zealand: an outline stratigraphy. Acta Geologica Academiae Scientiarium Hungaricae 22: 197 - 204.

Mimura, K.; Kawachi, S.; Fijimoto, U.; Taneichi, M.; Hyuga, T.; Ichikawa, S.; Koizumi, M. 1982: Debris avalanche hills and their natural remnant magnetisation - Nirasaki debris avalanche, central Japan. Journal Geological Society of Japan 88: 653 - 663.

Mizuno, Y. 1964: Landforms associated with volcanic debris flows at the foot of Zao volcano. Hirosaki University Faculty Bulletin 13: 23 - 32.

Momose, K.; Kobayashi, K.; Minagawa, K.; Machida, M. 1968: Identification of tephra by means of ferromagnetic minerals in pumice. Bulletin of Earthquake Research Institute 46: 1275 - 1292.

Morgan, P.G.; Gibson, W. 1927: The geology of the Egmont Subdivision, Taranaki. New Zealand Geological Bulletin 29 (n.s.) 92p.

Mokma, D.L.; Syers, J.K.; Jackson, M.L.; Clayton, R.N.; Rex, R.W. 1972: Eolian additions to soils and sediments in the South Pacific area. Journal of Soil Science 23: 147 - 162.

Murai, I. 1961: A study of the textural characteristics of pyroclastic flow deposits in Japan. Bulletin Earthquake Research Institute, Tokyo University 39: 133 - 248.

Nakamura, Y. 1978: Geology and petrology of Bandai and Nekoma volcanoes. Tohoku University Science Report Series 3, 14: 67 - 119.

Neall, V.E. 1972: Tephrochronology and tephrostratigraphy of western Taranaki (N108-109) New Zealand. New Zealand Journal of Geology and Geophysics 15: 507 - 557.

-1975: Climate controlled Tephra redeposition on Pouakai ring plain, Taranaki, new Zealand. New Zealand Journal of Geology and Geophysics 18: 317 - 326.

-1977: Genesis and weathering of Andosols in Taranaki, New Zealand. Soil Science 123 (6): 400 - 408.

-1979: Sheets P19, P20 and P21 New Plymouth, Egmont and Manaia (1st Ed.) "Geological Map of New Zealand 1:50,000". 3 maps and notes (36p). N.Z D.S.I.R., Wellington.

-1982: Landforms of Taranaki and the Wanganui Lowlands In Landforms of New Zealand. Edited by Soons and Selby. Longman Paul Ltd. Auckland, NZ. 392p.

-1982b: Volcanic Hazard Map of Mount Egmont. N.Z. Department of Scientific and Industrial Research, Wellington.

-1982c: Unpublished Report on volcanic hazards of Mt. Egmont. Submitted to National Civil Defence Committee on Volcanic Hazards June 1981, 51pp.

Neall, V.E., Alloway, B.V. 1986: International Volcanological Congress, New Zealand. Tour Guide C3: Quaternary Volcaniclastics and Volcanic Hazards of Taranaki. New Zealand Geological Survey Record 12.

Neall, V.E., Stewart, R.B., Smith, I.E.M. 1986: History and Petrology of the Taranaki Volcanoes. Royal Society of New Zealand bulletin 23: 251 - 263.

Neumann van Padang, M. 1939: Uber die vielen tausend Hugel in westlichen Vorlande des Raoeng-Vulkans (Ostjava). Ing. Ned. Indies 6 (4): 35 - 41.

Newhall, C.G. 1982: A prehistoric debris avalanche from Mt. St. Helens (abstr.). EOS Transactions American Geophysical Union 63: p.1141.

New Zealand Soil Bureau 1968: Soils of New Zealand Part 2. New Zealand Soil Bureau Bulletin 26 (2) D.S.I.R.

Oliver, W.R.B. 1931: An ancient Maori oven on Mount Egmont. Journal of the Polynesian Society 40: 73 - 79.

Pain, C.F. 1975: Some tephra deposits in the south-west Waikato area, North Island, New Zealand. New Zealand Journal of Geology and Geophysics 18: 541 - 550.

Palmer, A.S. 1982b: The stratigraphy and selected properties of loess in Wairarapa, New Zealand. Unpublished Ph.D thesis lodged in the library, Victoria University of Wellington.

Parfitt, R.L.; Hemni, T. 1982: Comparison of an oxalate-extraction method and an infrared spectroscopic method for determining allophane in soil clays. Soil Science Plant Nutrition 28 (2): 183 - 190.

Parfitt, R.L.; Russell, M. Kirkman, J.H. 1982: The clay mineralogy of yellow-brown loam soils. In Neall, V.E. (ed.) Soil Groups of New Zealand. Part 6, Yellow-brown loams. New Zealand Society of Soil Science, Lower Hutt: 48 - 53.

Parfitt, R.L.; Russell, M.; Orbell, G.E. 1983: Weathering sequence of soils from volcanic ash involving allophane and halloysite, New Zealand. Geoderma 29: 41 - 57.

Pierson, T.C. 1985: Initiation and flow behavior of the 1980 Pine Creek and Muddy River lahars, Mount St. Helens, Washington. Geological Society of America Bulletin:

Pierson, T.C.; Scott, K.M. 1985: Downstream dilution of a lahar: Transition from debris flow to hyperconcentrated streamflow. Water Resources Research 21, number 10: 1511 - 1524.

Pillans, B.J. 1981: Upper Quaternary landscape evolution in south Taranaki, New Zealand. Unpublished Ph.D thesis lodged in the Library, Australian National University, Canberra, Australia.

-1983: Upper Quaternary marine terrace chronology and deformation, south Taranaki, New Zealand. Geology 11: 292 - 297.

-1986: A Late Quaternary uplift map for North Island, New Zealand. Royal Society of New Zealand Bulletin 24: 409 - 418.

-1988: Loess chronology in Wanganui Basin, New Zealand. In Loess - its distribution, geology and soils. Edited by Eden, D.N; Furkert, R.J. A.A.Balkema Publishers, Rotterdam: 175 - 193.

Pillans, B.J.; Kohn, B. 1981: A widespread(?) Quaternary marker bed in Taranaki-Wanganui. In Howorth, R. et.al. ed. Proceedings of the tephra workshop. Geology Department, Victoria University of Wellington publication 20: 94 - 104.

Pullar, W.A.; Birrell, K.S.; Heine, J.C. 1973: Named tephras and tephra formations occurring in the Central North Island, with notes on derived soils and buried paleosols. New Zealand Journal of Geology and Geophysics 20: 697 - 717.

Pullar, W.A.; Kohn, B.P.; Cox, J.E. 1977: Air-fall Kaharoa Ash and Taupo Pumice, and sea rafted Loisels Pumice, Taupo Pumice, and Leigh Pumice in northern and eastern parts of the North Island, New Zealand. New Zealand Journal of Geology and Geophysics 20: 697 - 717.

Ruxton, B.P. 1968: Rates of weathering of Quaternary volcanic ash in north-east Papua. Transactions 9th International Congress of Soil Science 4, Paper 38: 367 - 376.

Sarna-Wojcicki, A.M.; Shipley, S.; Waitt, R.B.jun.; Dzurisin, D.; Wood, S.H. 1981: Areal distribution, thickness, mass, volume and grain size of air-fall ash from the six major eruptions of 1980. In Lipman, P.W. and Mullineaux, D.R., editors, The 1980 eruptions of Mount St. Helens, Washington: U.S. Geological Survey Professional Paper 1250: 577 - 600.

Schieferdecker, A.A.G., ed., 1956: Geological nomenclature. Gorinchem, Royal Geological and Mining Society, 521 p.

Schmid, R. 1981: Descriptive nomenclature and classification of pyroclastic deposits and fragments. Recommendations of the IUGS Subcommission on the Systematics of Igneous Rocks. Geology 9: 41 - 43.

Schwertmann, U. 1964: Differenzierung der Eisenoxide des Bodens durch photochemische Extraktion mit saurer Ammoniumoxalate - Losung (in German). Z. Pflanzenern., Dung., Bodenkunde 105: 194 - 202.

Scott, K.M. 1985: Lahars and flow transformations at Mt. St. Helens, Washington, U.S.A., In International Symposium on Erosion, Debris Flow and Disaster Prevention, Tsukuba, Japan, September 3-5, 1985: 209 - 214.

-1988: Origins, Behavior, and Sedimentology of Lahars and Lahar-Runout Flows in the Toutle-Cowlitz River System. U.S. Geological Survey Professional Paper 1447-A. United States Government Printing Office, Washington.

Seward, D. 1976: Tephrostratigraphy of the marine sediments in the Wanganui Basin, New Zealand. New Zealand Journal of Geology and Geophysics 19: 9 - 20.

Shackleton, N.J.; Imbrie, J.; Hall, M.A. 1983: Oxygen and carbon isotope record of East Pacific core V19-30: Implications for the formation of deep water in the late Pleistocene North Atlantic. Earth and Planetary Science Letters 65: 233 - 244.

Siebert, L. 1984: Large volcanic debris avalanches: Characteristics of source areas, deposits, and associated eruptions. Journal of Volcanology and Geothermal Research 22: 163 - 197.

Siebert, L.; Glicken, H.X.; Ui, T. 1987: Volcanic hazards from Bezymianny- and Bandai-type eruptions. Bulletin of Volcanology 49: 435 - 459.

Smith, G.D. 1984: The Andisol Proposal 1978: A preliminary proposal for reclassification of Andepts and Andic Subgroups. New Zealand Soil Bureau Record 96.

Soya, T.; Katsui, Y. 1981: The Zenkoji debris avalanche of Usu volcano, Hokkaido, Japan (abstr.) IAVCEI Symposium Arc Volcanism, Tokyo and Hakone, p.347.

Stewart, R.B.; Neall, V.E.; Pollock, J.A.; Syers, J.K. 1977: Parent material stratigraphy of an Egmont loam profile, Taranaki, New Zealand. Australian Journal of Soil Research 15: 177 - 190.

Stewart, R.B.; Neall, V.E.; Syers, J.K. 1986a: Origin of Quartz in selected soils and sediments, North Island, New Zealand. New Zealand Journal of Geology and Geophysics 29: 147 - 152.

-1986b: Accumulation of aerosolic quartz in an andept chronosequence, North Island, New Zealand. Geoderma 37: 331 - 340.

Sundell, K.A.; Fisher, R.V. 1985: Very coarse grained fragmental rocks: A proposed size classification. Geology 13: 692 - 695.

Taranaki United Council 1987: Future Volcanic Activity in Taranaki: likely impact and effect on Taranaki infrastructure and the implications for civil defence and emergency response contingency plans. A report to the Taranaki United Council and Taranaki Civil Defence Committee, September 1987: pp.129.

Tamm, O. 1932: Uber die Oxalatmethode in der chemischen Bodenanalyse. Medd. Skogsforsoksanst. Stockholm 27 (1).

Taylor, N.H. 1953: The ecological significance of the central North Island ash showers - the soil pattern. Proceedings of the New Zealand Ecological Society 1: 11 - 12.

Taylor, N.H.; et al. 1954: Soils of the North Island of New Zealand (with map of ash showers). New Zealand Soil Bureau Bulletin (n.s.) 5.

Thiede, J. 1979: Wind regimes over the late Quaternary southwest Pacific Ocean. Geology: 259 - 262.

Thorarinsson, S. 1944: Tefrokronologiska studier pa Island. Geografiska Annaler, Stockholm, 217p.

-1974: The terms Tephra and Tephrostratigraphy In World Bibliography and Index of Quaternary Tephrostratigraphy. Edited by J.A. Westgate and C.M. Gold. Department of Geology, University of Alberta, Edmonton, Canada.

Till, R.; Spears, D.A. 1969: The Determination of Quartz in Sedimentary Rocks using an X-ray Diffraction Method. Clays and Clay Minerals 17: pp.323 - 327.

Tonkin, P.J. 1970: The soils of the south-eastern sector of Egmont National Park. Earth Science Journal 4 (1): 36 - 57.

Topping, W.W. 1973: Tephrostratigraphy and chronology of late Quaternary eruptives from the Tongariro Volcanic Centre, New Zealand. New Zealand Journal of Geology and Geophysics 16: 375 - 395.

-1974: A 1480 A.D. Maori oven from Mount Egmont. New Zealand Journal of Science 17: 119 - 122.

Topping, W.W.; Kohn, B.P. 1973: Rhyolitic tephra marker beds in the Tongariro area, New Zealand. New Zealand Journal of Geology and Geophysics 16: 375 - 395.

Trostel, L.J.; Wynne, D.J. 1940: Determination of quartz (free silica) in refractory clays. Journal of American Ceramic Society 23: 18 - 22.

Ui, T. 1983: Volcanic dry avalanche deposits - identification and comparison with non-volcanic debris stream deposits. In S.Aramaki and Kushiro (Editors), Arc Volcanism. Journal of Geothermal Research 18: 135 - 150.

Ui, T.; Kawachi, S.; Neall, V.E. 1986: Fragmentation of Debris avalanche material during flowage - evidence from the Pungarehu Formation, Mount Egmont, New Zealand. Journal of Volcanology and Geothermal Research 27: 255 - 264.

Voight, B.; Glicken, H.; Janda, R.J.; Douglass, P.M. 1981: Catastrophic rockslide avalanche of May 18. In Lipman, P.W. and Mullineaux, D.R., editors, The 1980 eruptions of Mount St. Helens, Washington: U.S. Geological Survey Professional Paper 1250: 347 - 378.

Vucetich, C.G.; Pullar, W.A. 1964: Stratigraphy and chronology of late Quaternary volcanic ash in the Taupo, Rotorua and Gisborne districts. Part 2. New Zealand Geological Survey Bulletin 73: 43 - 78.

-1969: Stratigraphy and chronology of late Pleistocene volcanic ash-beds in central North Island, New Zealand. New Zealand Journal of Geology and Geophysics 12: 784 - 837.

-1973: Holocene tephra formations erupted in the Taupo area, and interbedded tephras from other sources. New Zealand Journal of Geology and Geophysics 16: 745 - 780.

Wada, K. 1977: Allophane and Imogolite. In J.B. Dixon and S.B. Weed (Editors), Minerals in Soil Environments. Soil Science Society of America, Madison, Wisconsin., pp.603 - 638.

-1978: Allophane and Imogolite. In M.M. Mortland and V.C. Farmer (Editors), International Clay Conference 1978. Elsevier, Amsterdam: 537 - 545.

Wada, K.; Hayward, M.E. 1974: Amorphous Clay Constituents of Soils. Advanced Agronomy 26: 211 - 260.

Wada, S.I.; Wada, K. 1977: Density and structure of Allophane. Clay Minerals, 12: 289 - 298.

Wallace, R.C. 1987: Mineralogy of the Tokomaru Silt Loam and the Occurrence of Cristobalite and Tridymite in Selected North Island Soils. Ph.D thesis lodged in the library, Massey University, Palmerston North.

Wellman, H.W. 1962: Holocene of the North Island of New Zealand: a coastal reconnaissance. Transactions of the Royal Society of New Zealand Geology 1: 29 - 99.

Westgate, J.A.; Fulton, R.J. 1975: Tephrostratigraphy of Olympia interglacial sediments in south-central British Columbia, Canada. Canadian Journal of Earth Sciences 12: 489 - 502.

Whitehead, S.J. 1976: Granulometric studies on selected tephra eruptions, North Island, New Zealand. BSc. Honours thesis lodged in the library, Massey University, Palmerston North.

Wilde, R.H. 1979: Stratigraphy and soils of late Quaternary terrace and cover beds in the Wanganui and south Taranaki districts, North Island, New Zealand. Unpublished M.Sc thesis, Victoria University of Wellington.

Wilde, R.H.; Vucetich, C.G. 1988: Aeolian cover beds of marine terraces in the western Wanganui district, North Island, New Zealand. In Loess - its distribution, geology and soils. Edited by Eden, D.N; Furkert, R.J. A.A.Balkema Publishers, Rotterdam: 215 - 233.

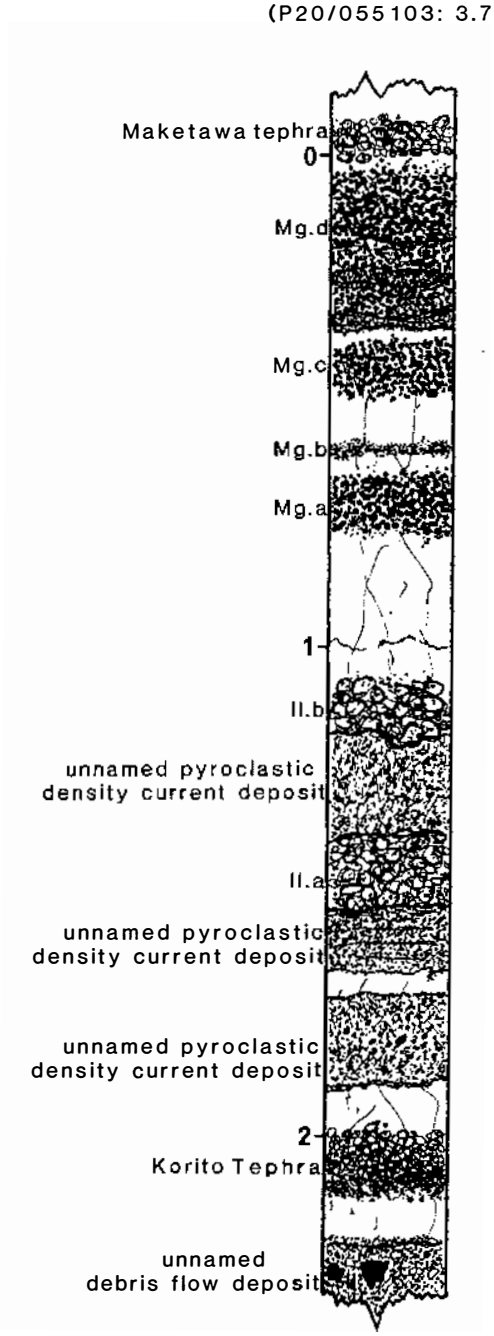
Williams, H.; McBirney, A.R. 1979: Volcanology. Freeman, Cooper and Co., San Francisco, California, 397p.

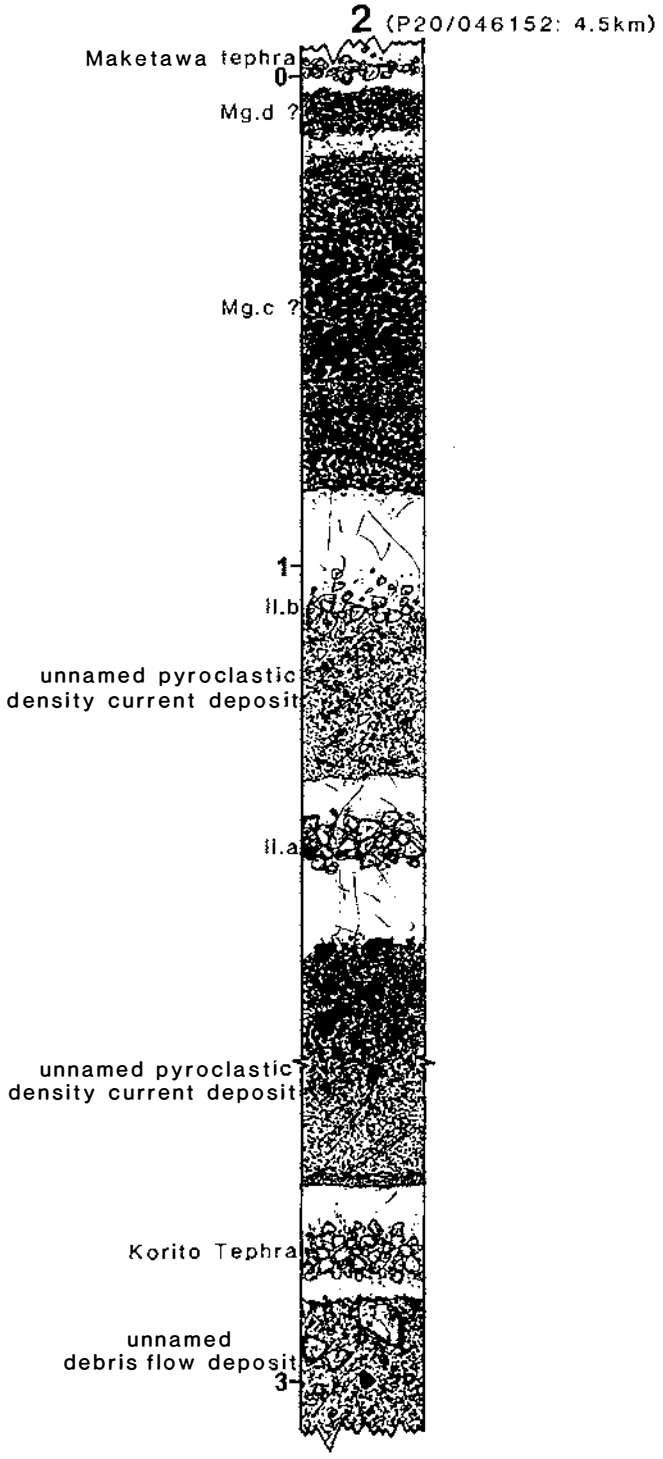
Wilson, C.J.N.; Switsur, V.R.; Ward, A.P. 1988: A new date for the Oruanui Eruption, New Zealand. Geological Magazine 125: 297 - 300.

APPENDIX ONE

1

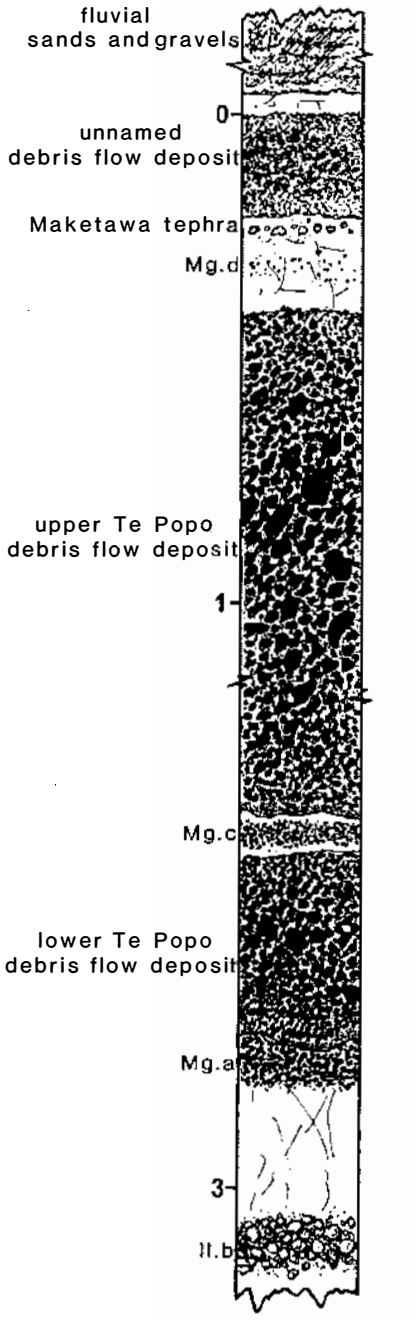
(P20/055103: 3.7km)

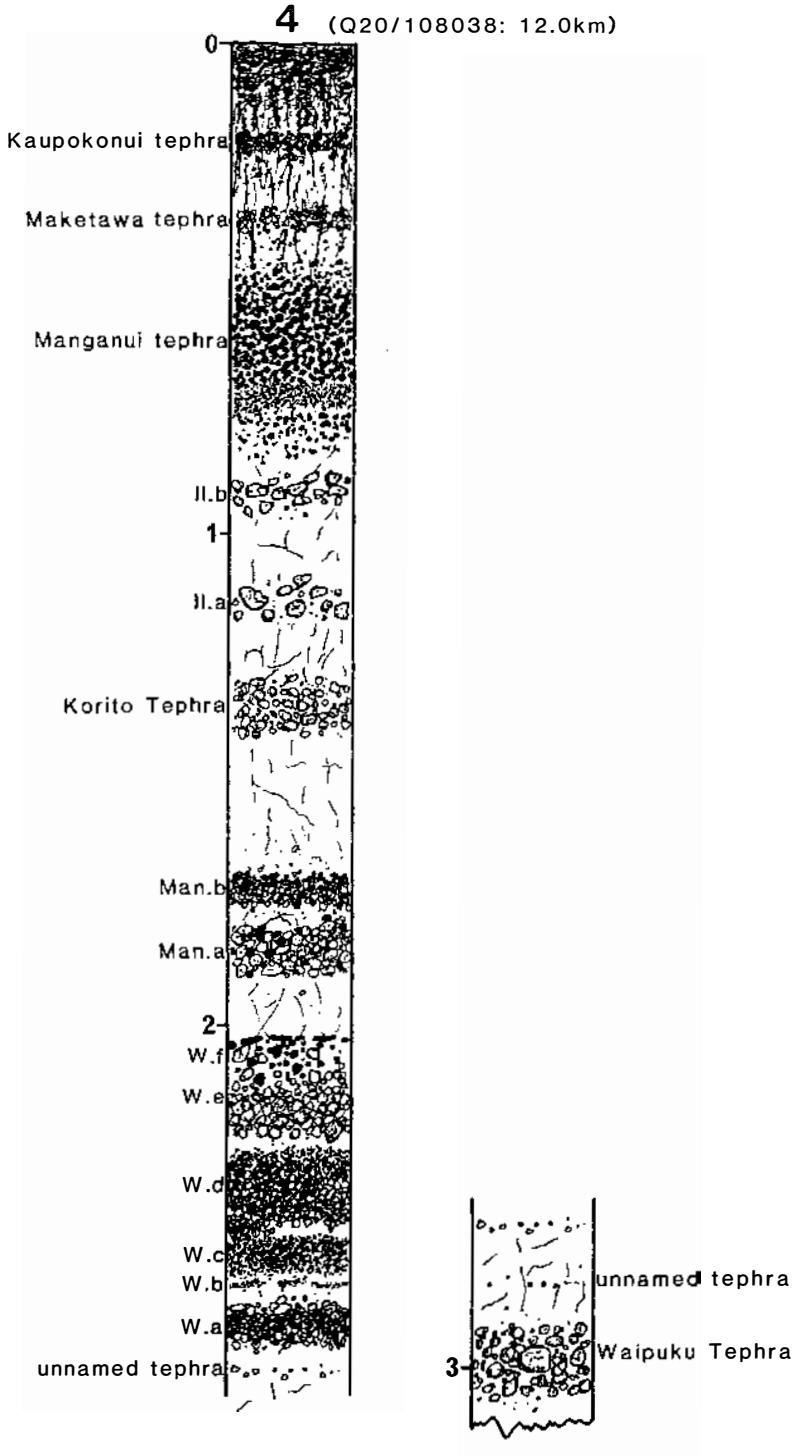



2 (P20/046152: 4.5km)
Maketawa tephra
0
Mg.d ?
Mg.c ?
1
II.b
unnamed pyroclastic
density current deposit
II.a
unnamed pyroclastic
density current deposit
Korito Tephra
unnamed
debris flow deposit
3

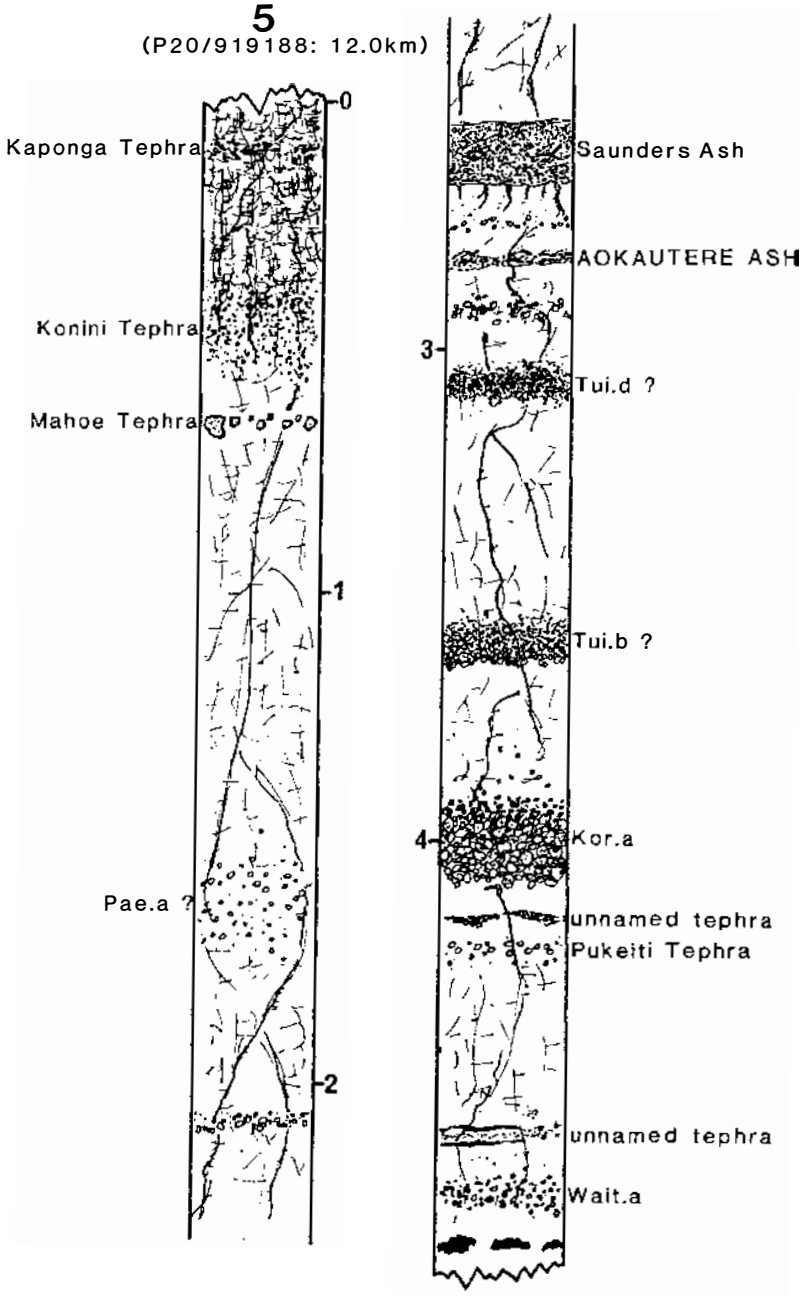
3

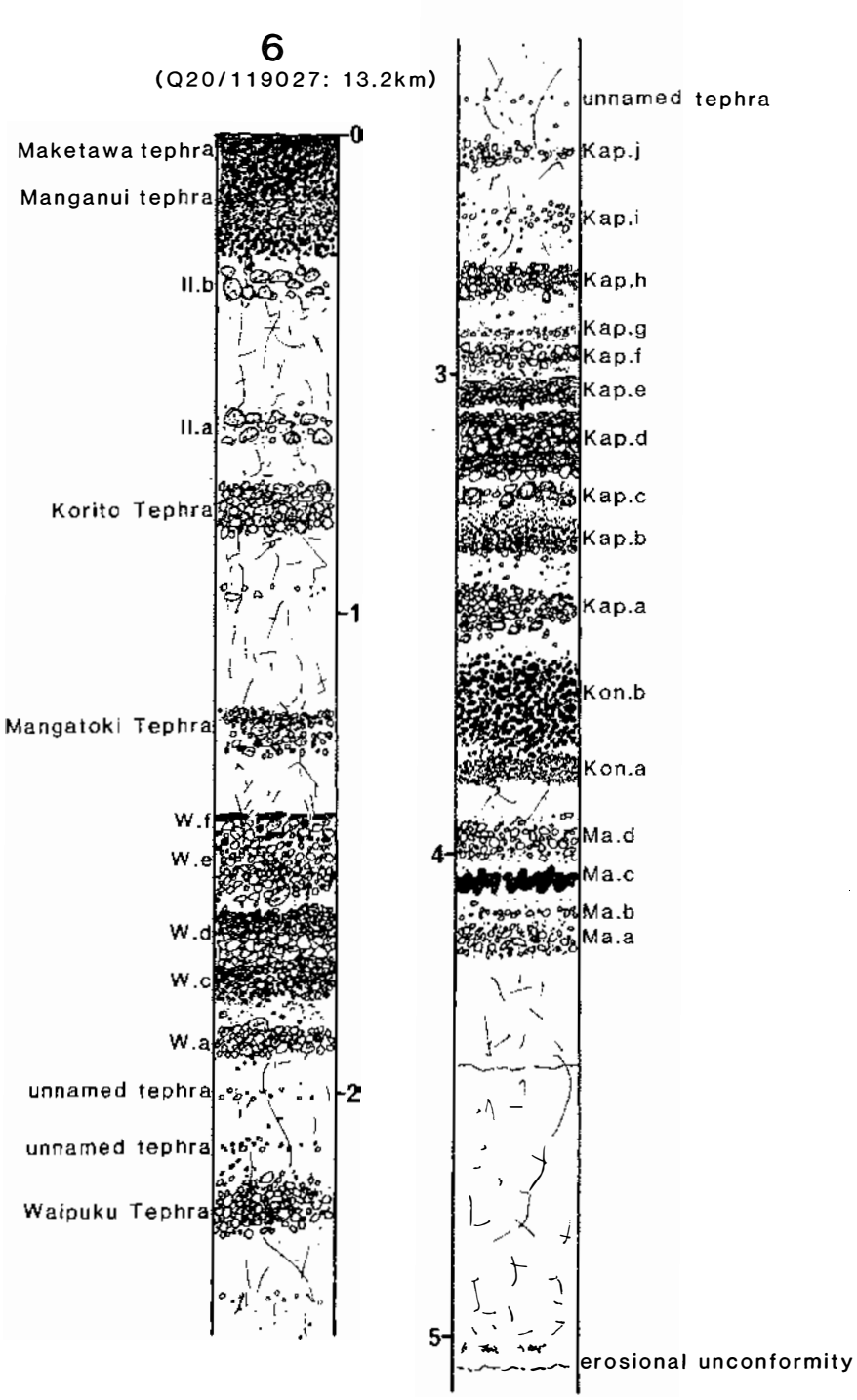
(Q20/129112: 11.2km)



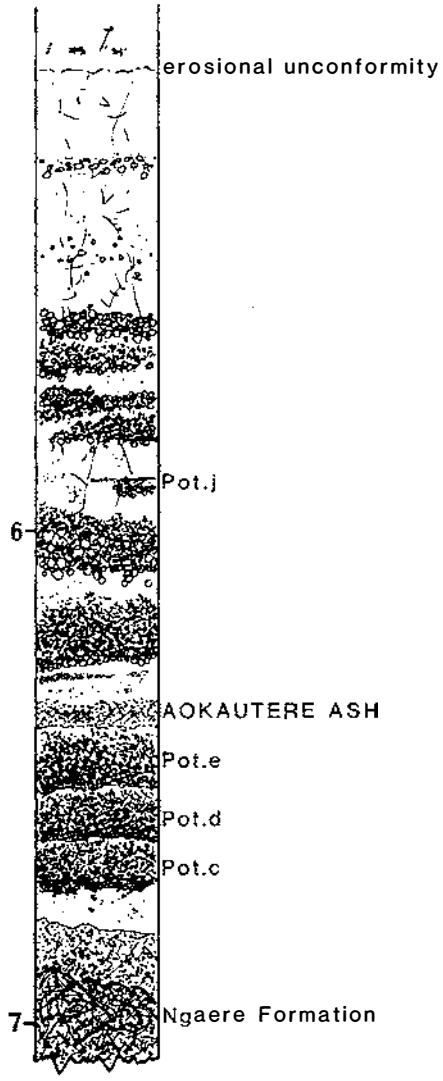

4 (Q20/108038: 12.0km)
0
Kaupokonui tephra
Maketawa tephra
Manganui tephra
II.b
1
II.a
Korito Tephra
Man.b
Man.a
2
W.f
W.e
W.d
W.c
W.b
W.a
unnamed tephra
unnamed tephra
Waipuku Tephra
3

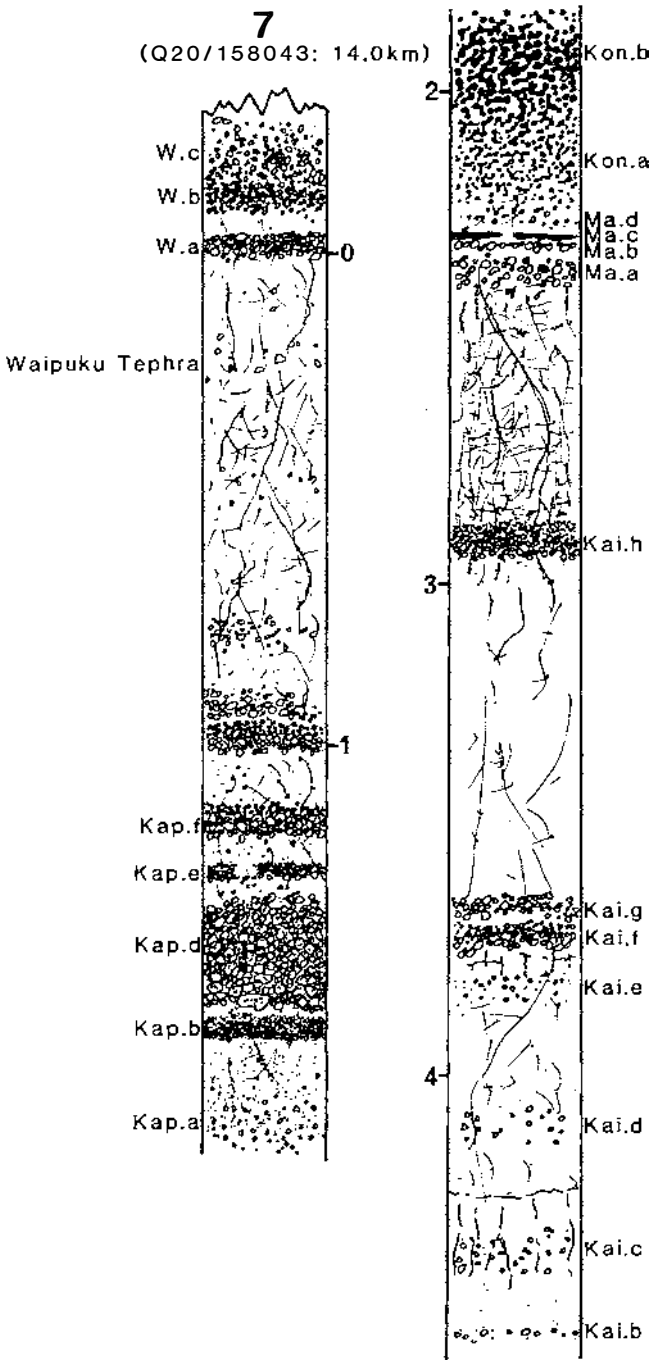
5
(P20/919188: 12.0km)

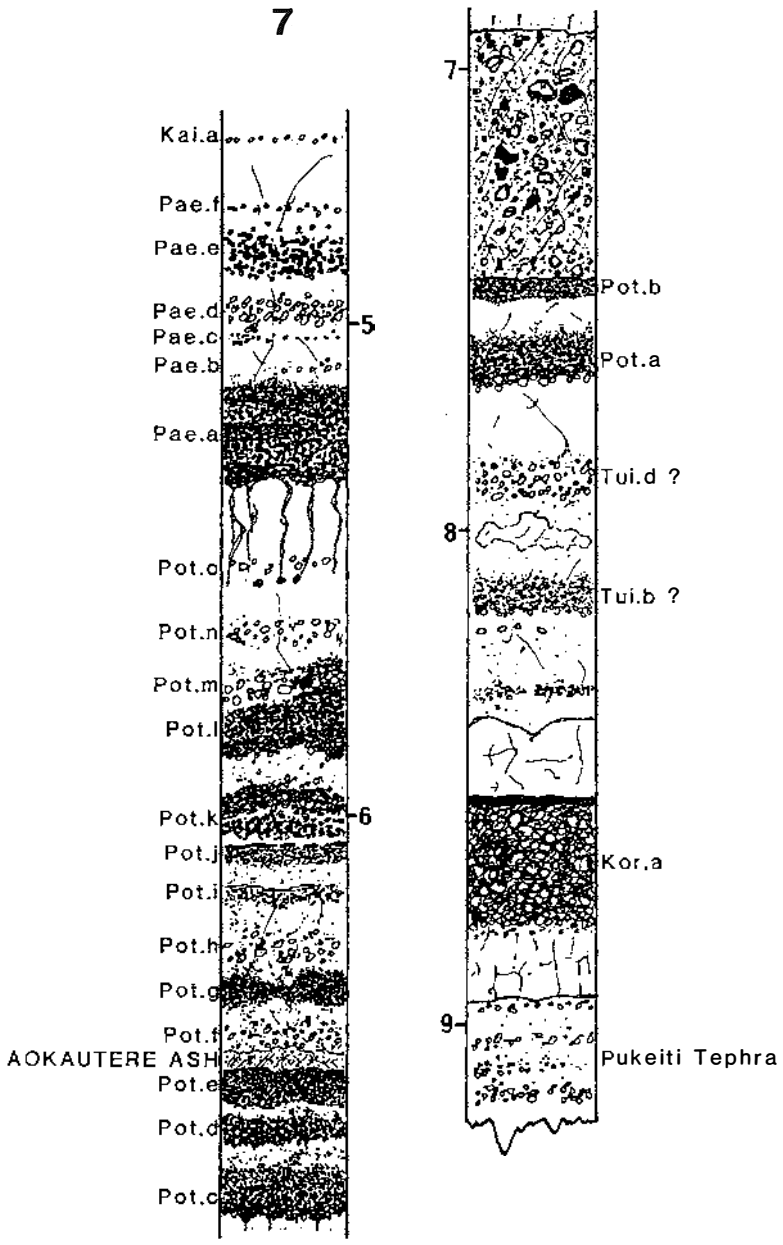



6
(Q20/119027: 13.2km)
Maketawa tephra
Manganui tephra
II.b
II.a
Korito Tephra
Mangatoki Tephra
W.f
W.e
W.d
W.c
W.a
unnamed tephra
unnamed tephra
Waipuku Tephra
0
1
2
3
4
5
unnamed tephra
Kap.j
Kap.i
Kap.h
Kap.g
Kap.f
Kap.e
Kap.d
Kap.c
Kap.b
Kap.a
Kon.b
Kon.a
Ma.d
Ma.c
Ma.b
Ma.a
erosional unconformity

6

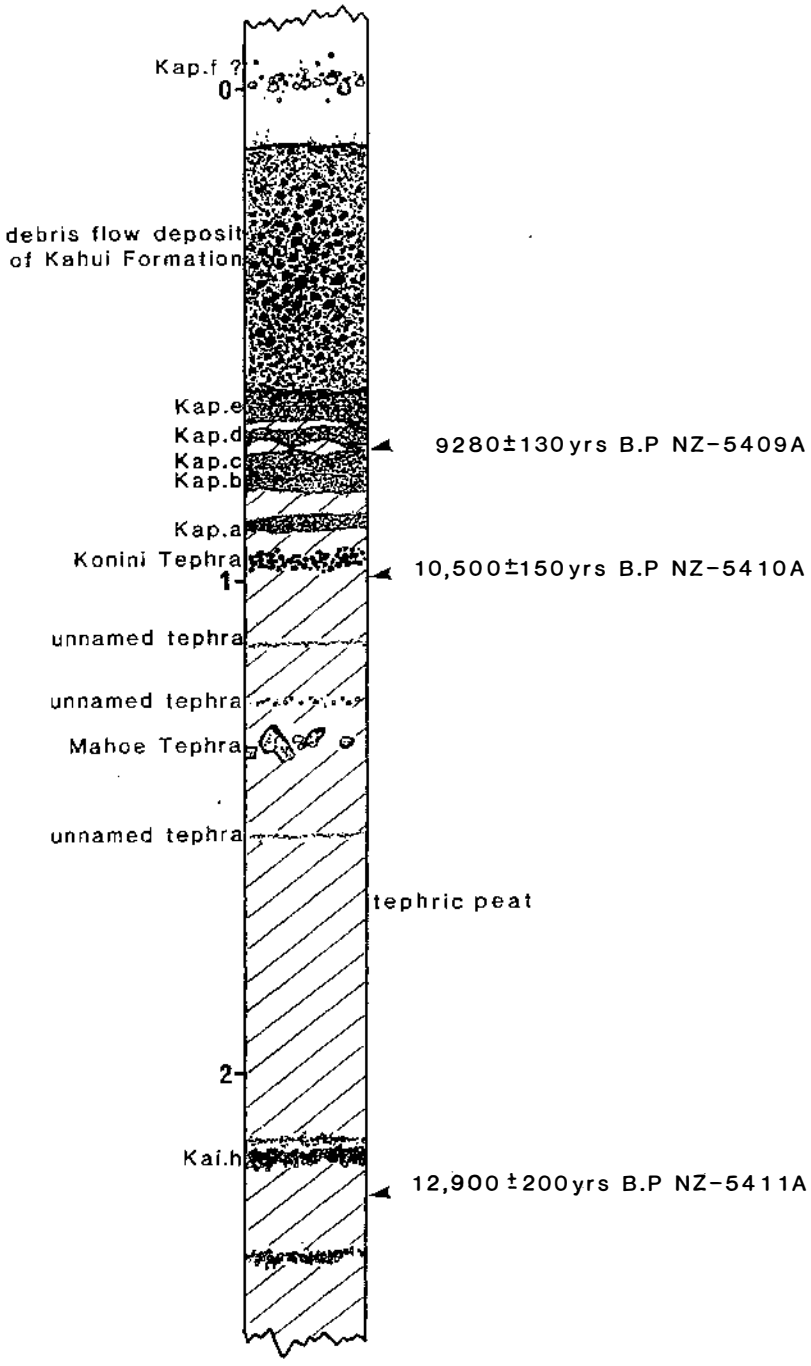

erosional unconformity
Pot.j
6
AOKAUTERE ASH
Pot.e
Pot.d
Pot.c
7
Ngaere Formation

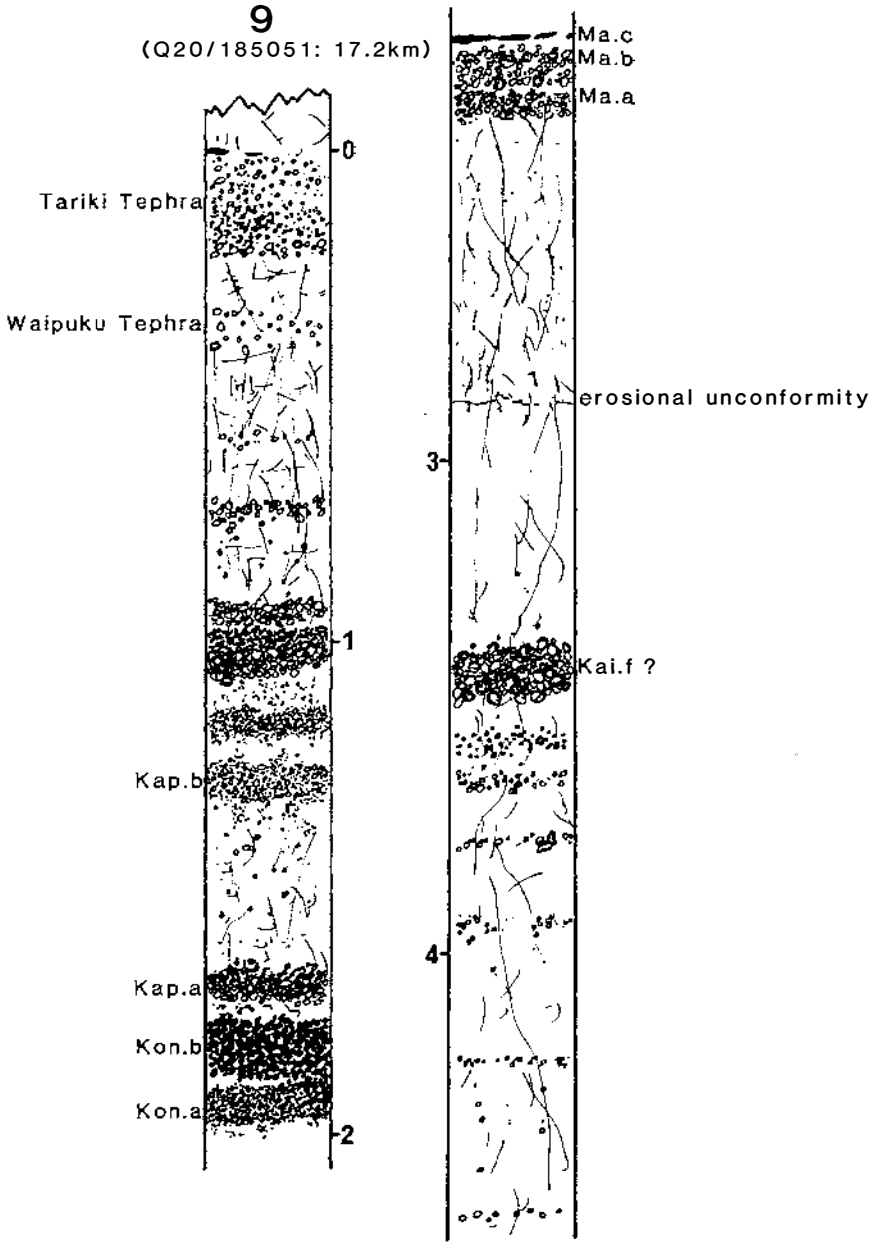

7
(Q20/158043: 14.0km)
W.c
W.b
W.a
0
Waipuku Tephra
1
Kap.f
Kap.e
Kap.d
Kap.b
Kap.a
2
Kon.b
Kon.a
Ma.d
Ma.c
Ma.b
Ma.a
Kai.h
3
Kai.g
Kai.f
Kai.e
4
Kai.d
Kai.c
Kai.b

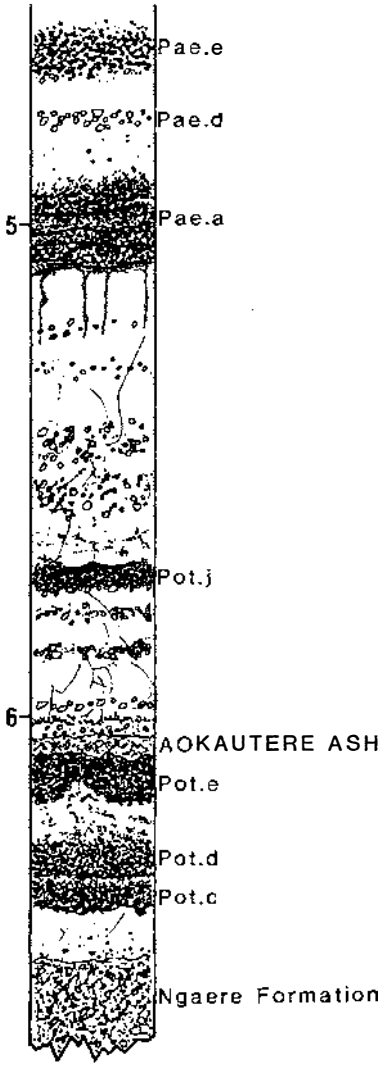

7
Kai.a
Pae.f
Pae.e
Pae.d
Pae.c
Pae.b
Pae.a
5
Pot.o
Pot.n
Pot.m
Pot.l
Pot.k
6
Pot.j
Pot.i
Pot.h
Pot.g
Pot.f
AOKAUTERE ASH
Pot.e
Pot.d
Pot.c
7
Pot.b
Pot.a
Tui.d ?
8
Tui.b ?
Kor.a
9
Pukeiti Tephra

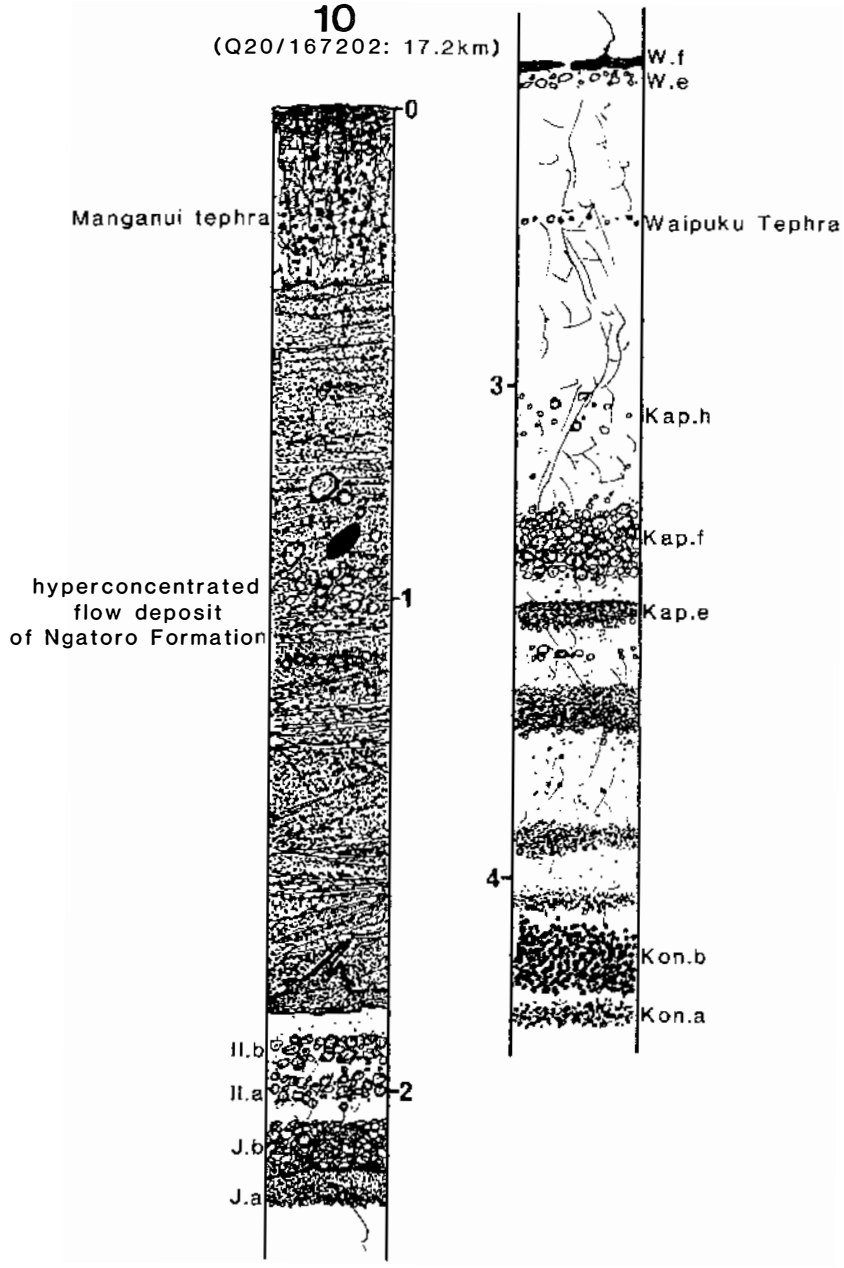
8

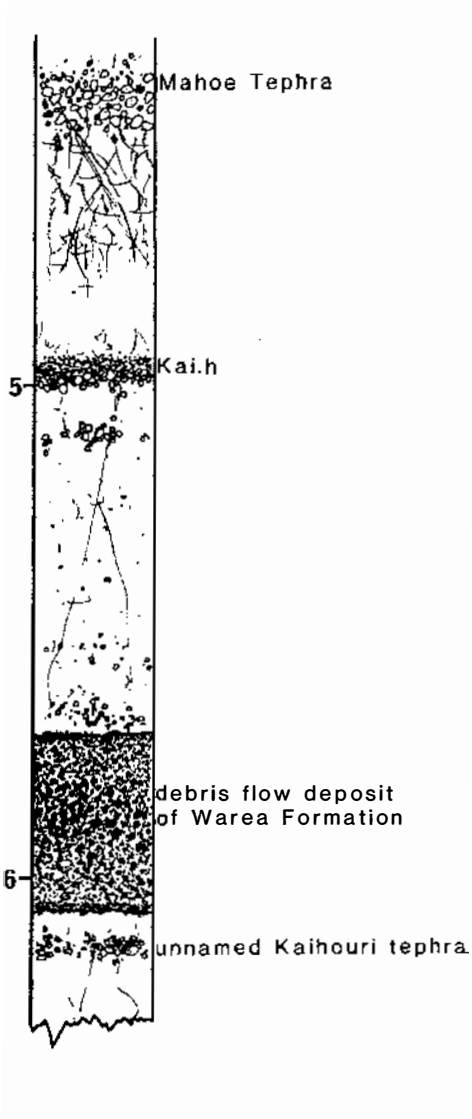
(Q19/144226: 16.0km)

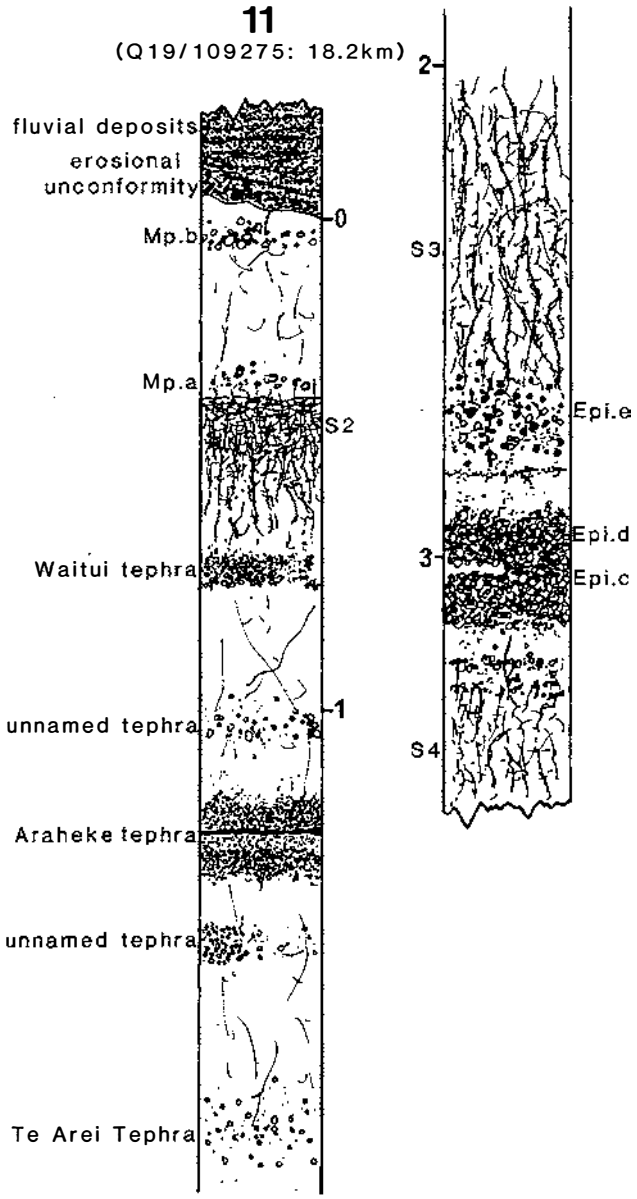


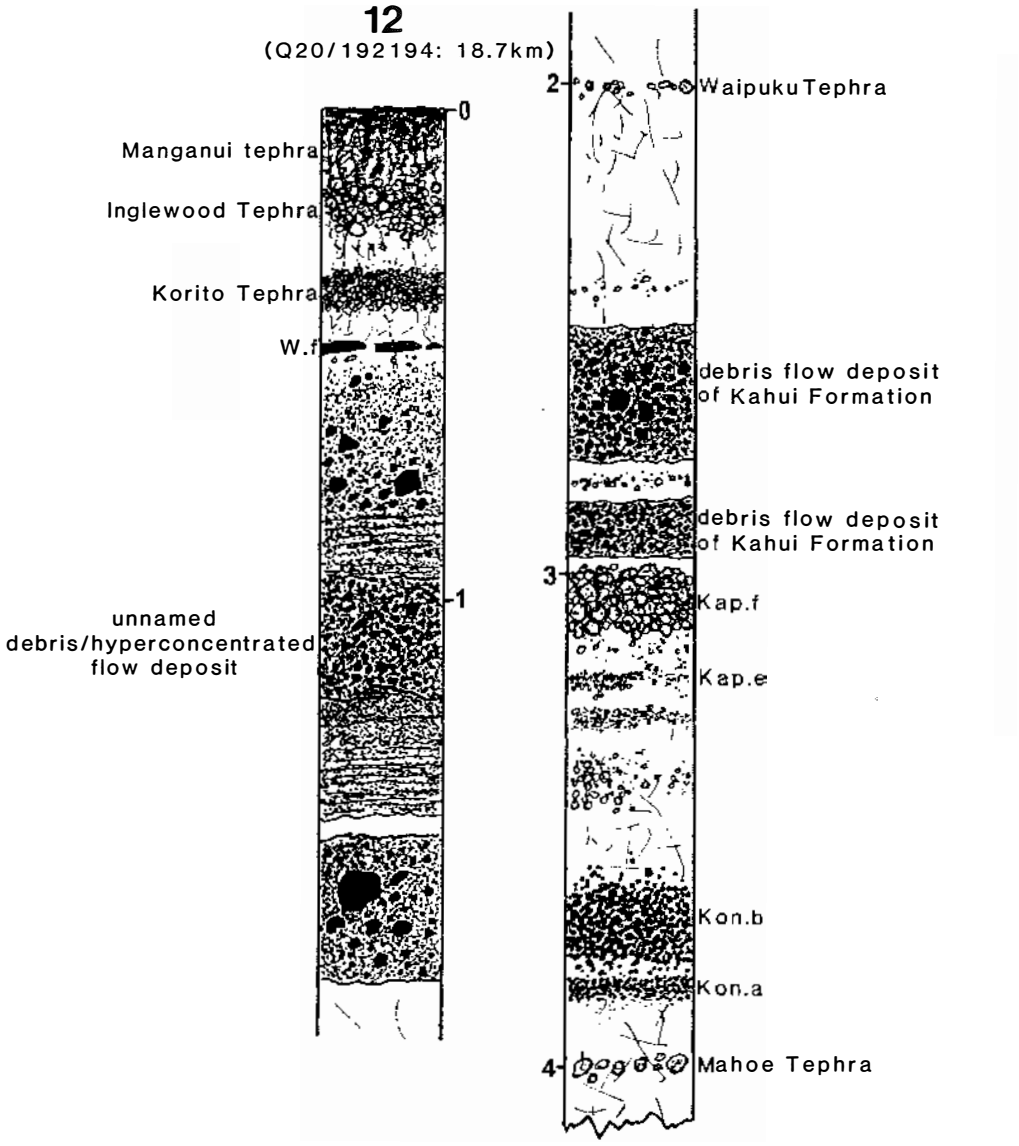

9
(Q20/185051: 17.2km)
Ma.c
Ma.b
Ma.a
0
Tariki Tephra
Waipuku Tephra
1
erosional unconformity
3
Kai.f ?
1
Kap.b
4
Kap.a
Kon.b
Kon.a
2

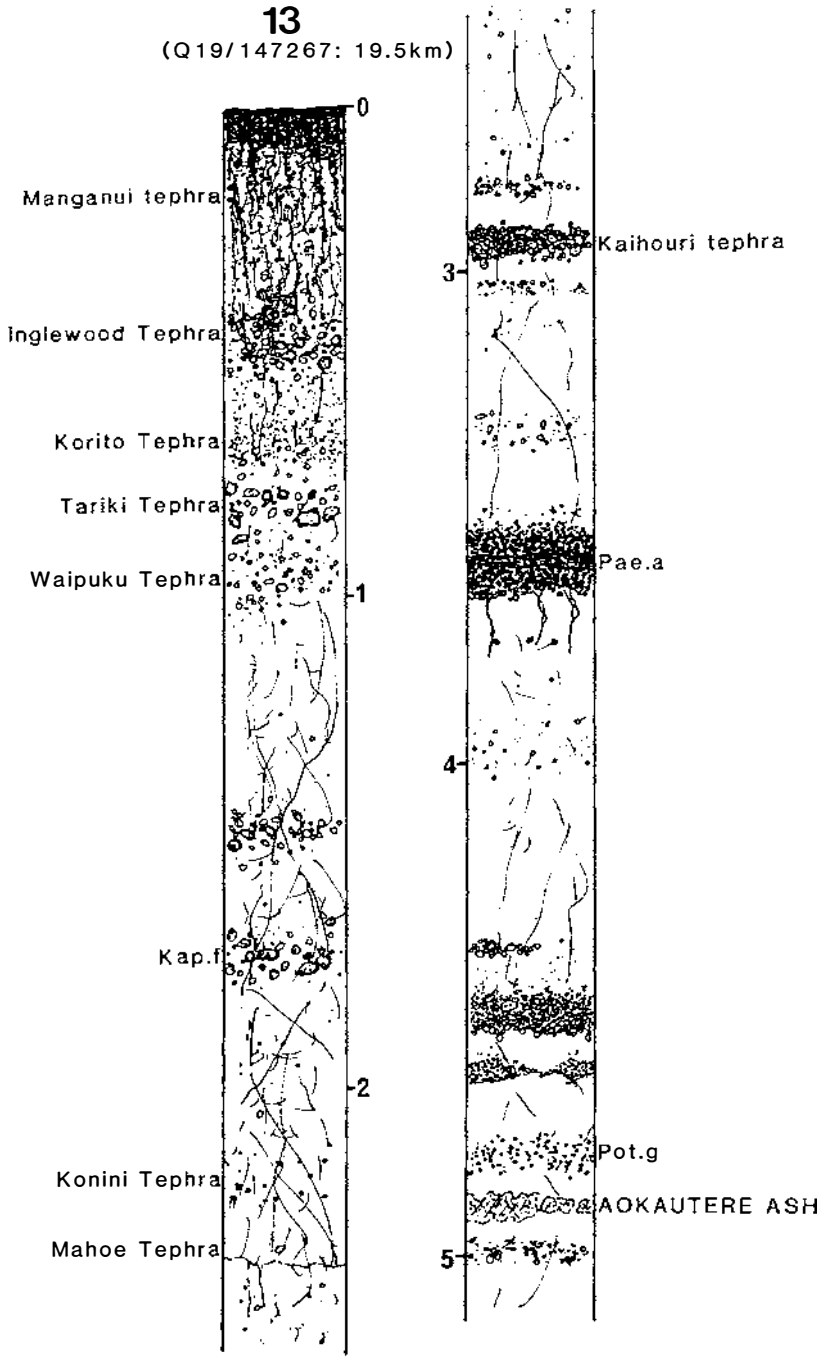

Pae.e
Pae.d
5
Pae.a
Pot.j
6
AOKAUTERE ASH
Pot.e
Pot.d
Pot.c
Ngaere Formation

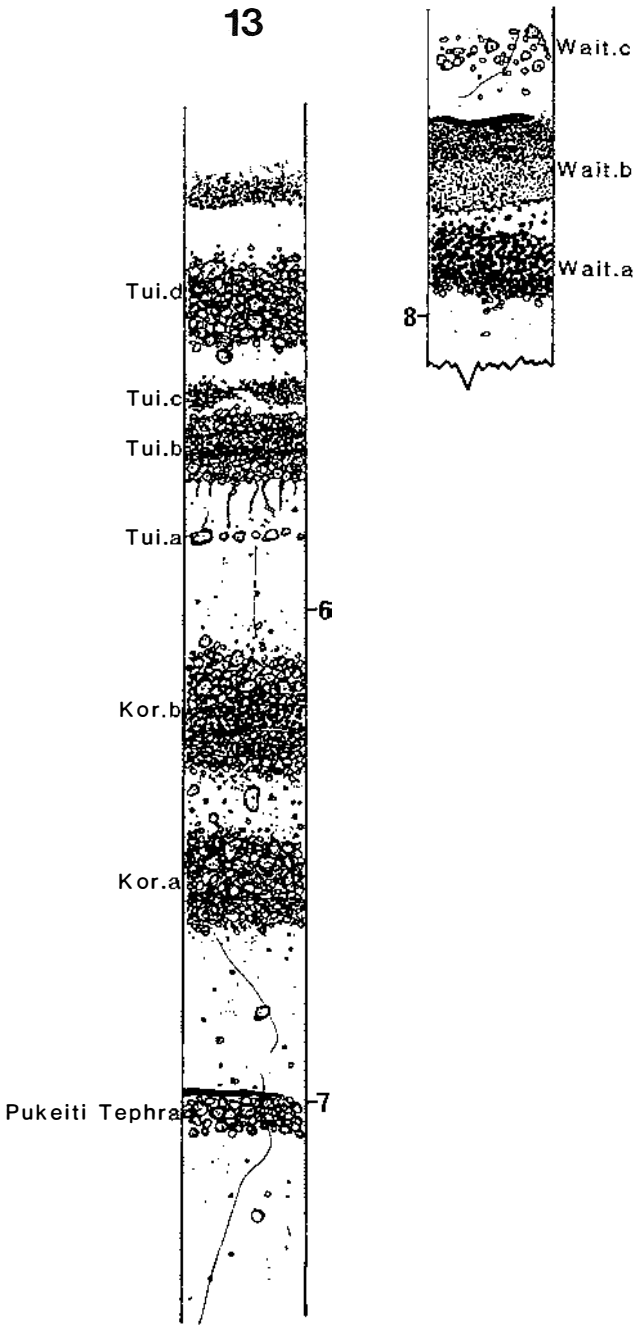

10
(Q20/167202: 17.2km)
W.f
W.e
Waipuku Tephra
Kap.h
Kap.f
Kap.e
Kon.b
Kon.a
Manganui tephra
hyperconcentrated
flow deposit
of Ngatoro Formation
II.b
II.a
J.b
J.a
0
1
2
3
4


Mahoe Tephra
Kai.h
5
debris flow deposit
of Warea Formation
6
unnamed Kaihouri tephra


11
(Q19/109275: 18.2km)
fluvial deposits
erosional unconformity
Mp.b
Mp.a
S2
Waitui tephra
unnamed tephra
Araheke tephra
unnamed tephra
Te Arei Tephra
0
1
2
3
S3
S4
Epi.e
Epi.d
Epi.c

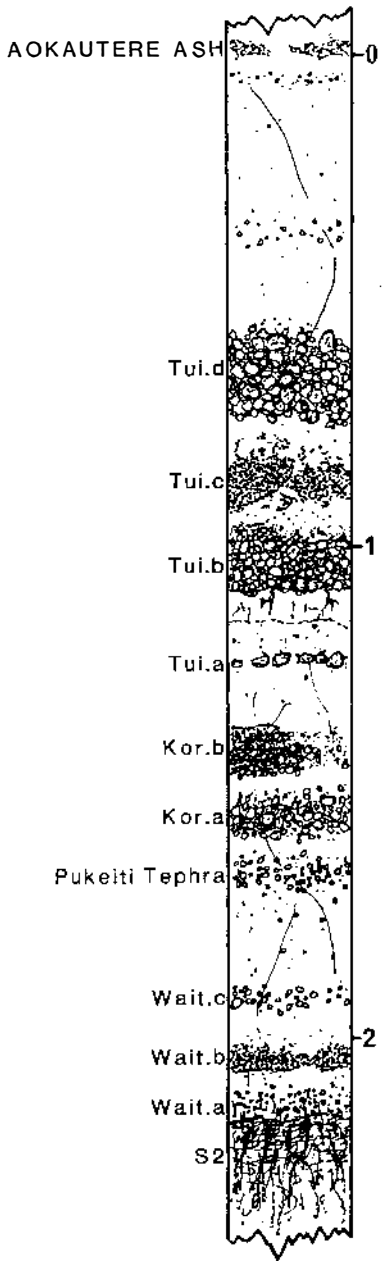

12
(Q20/192194: 18.7km)
0
Manganui tephra
Inglewood Tephra
Korito Tephra
W.f
1
unnamed
debris/hyperconcentrated
flow deposit
2
Waipuku Tephra
debris flow deposit
of Kahui Formation
debris flow deposit
of Kahui Formation
3
Kap.f
Kap.e
Kon.b
Kon.a
4
Mahoe Tephra

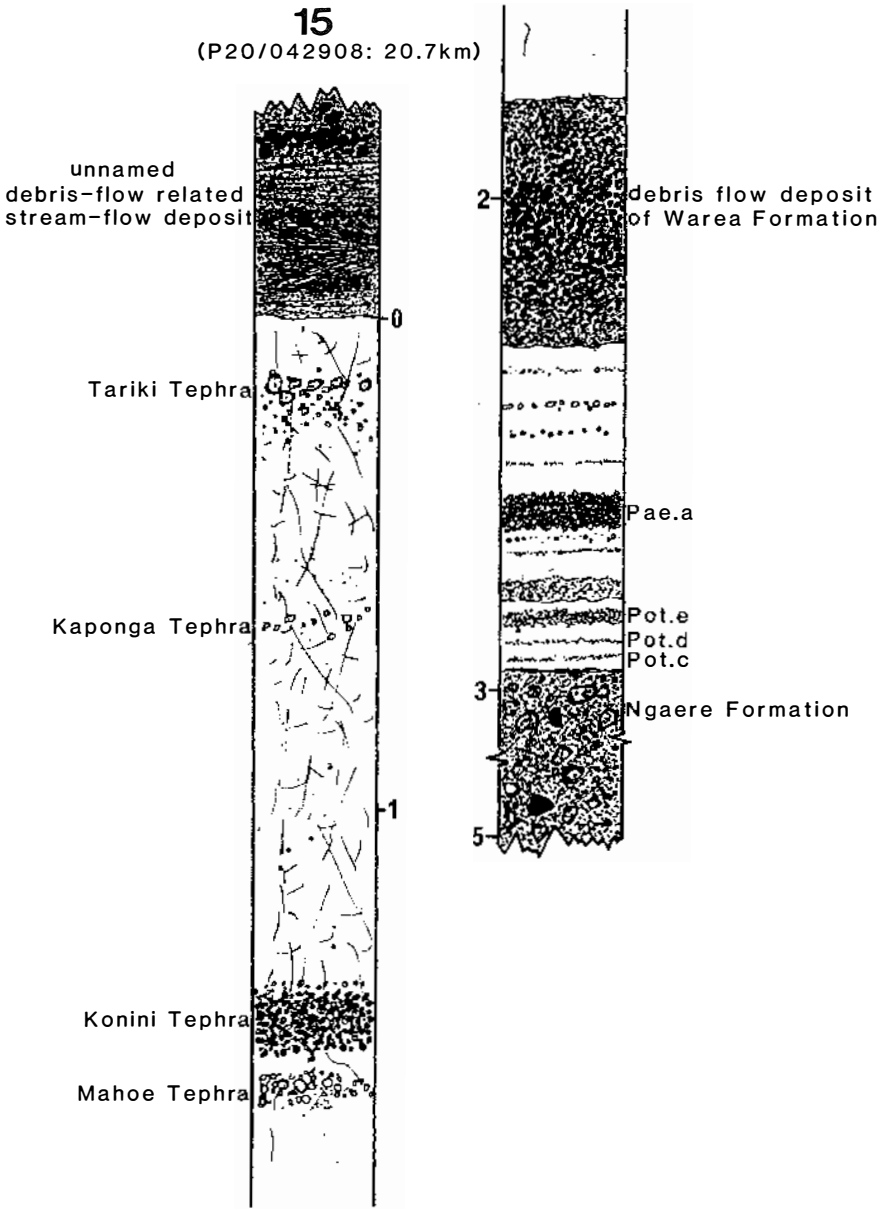

13
(Q19/147267: 19.5km)
0
Manganui tephra
Inglewood Tephra
Korito Tephra
Tariki Tephra
Waipuku Tephra
1
Kap.f
2
Konini Tephra
Mahoe Tephra
3
Kaihouri tephra
Pae.a
4
Pot.g
AOKAUTERE ASH
5


13
Wait.c
Wait.b
Wait.a
8
Tui.d
Tui.c
Tui.b
Tui.a
6
Kor.b
Kor.a
Pukeiti Tephra
7

14

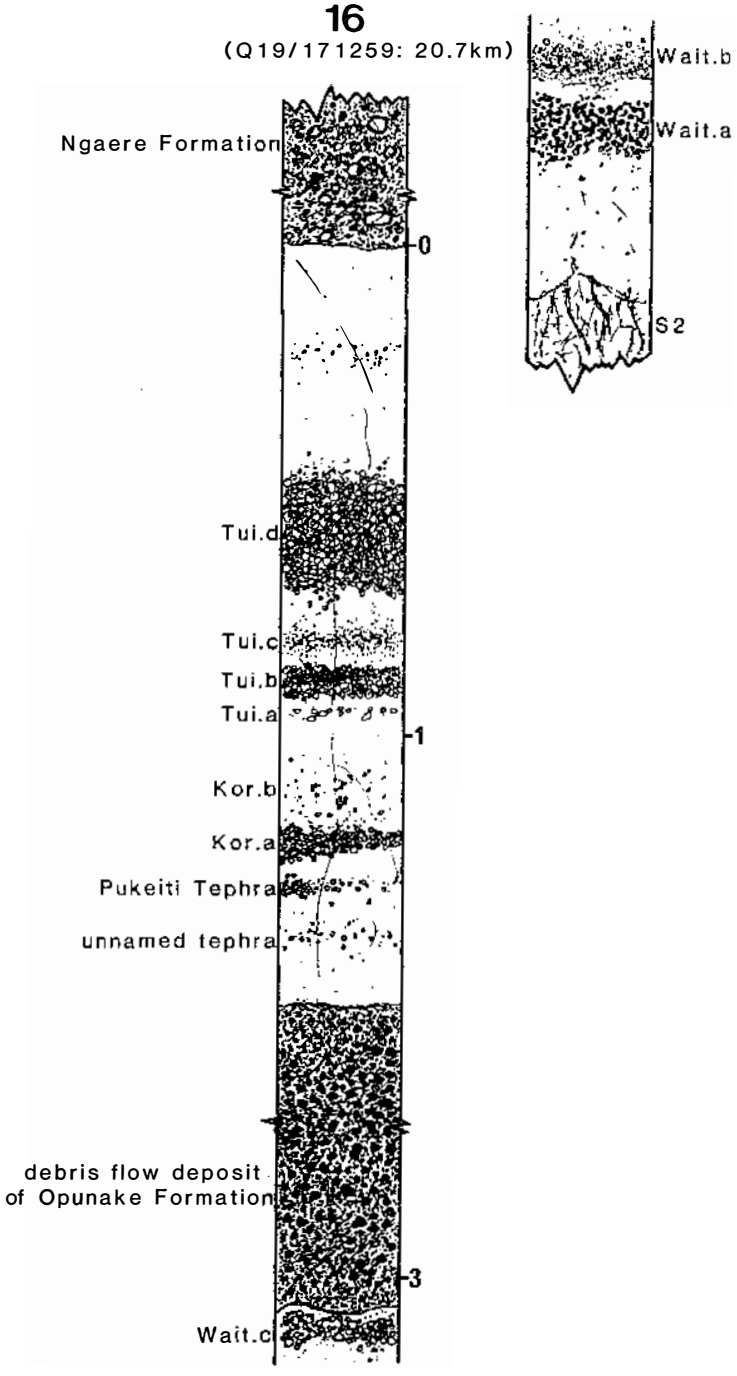
(Q19/149280: 20.5km)

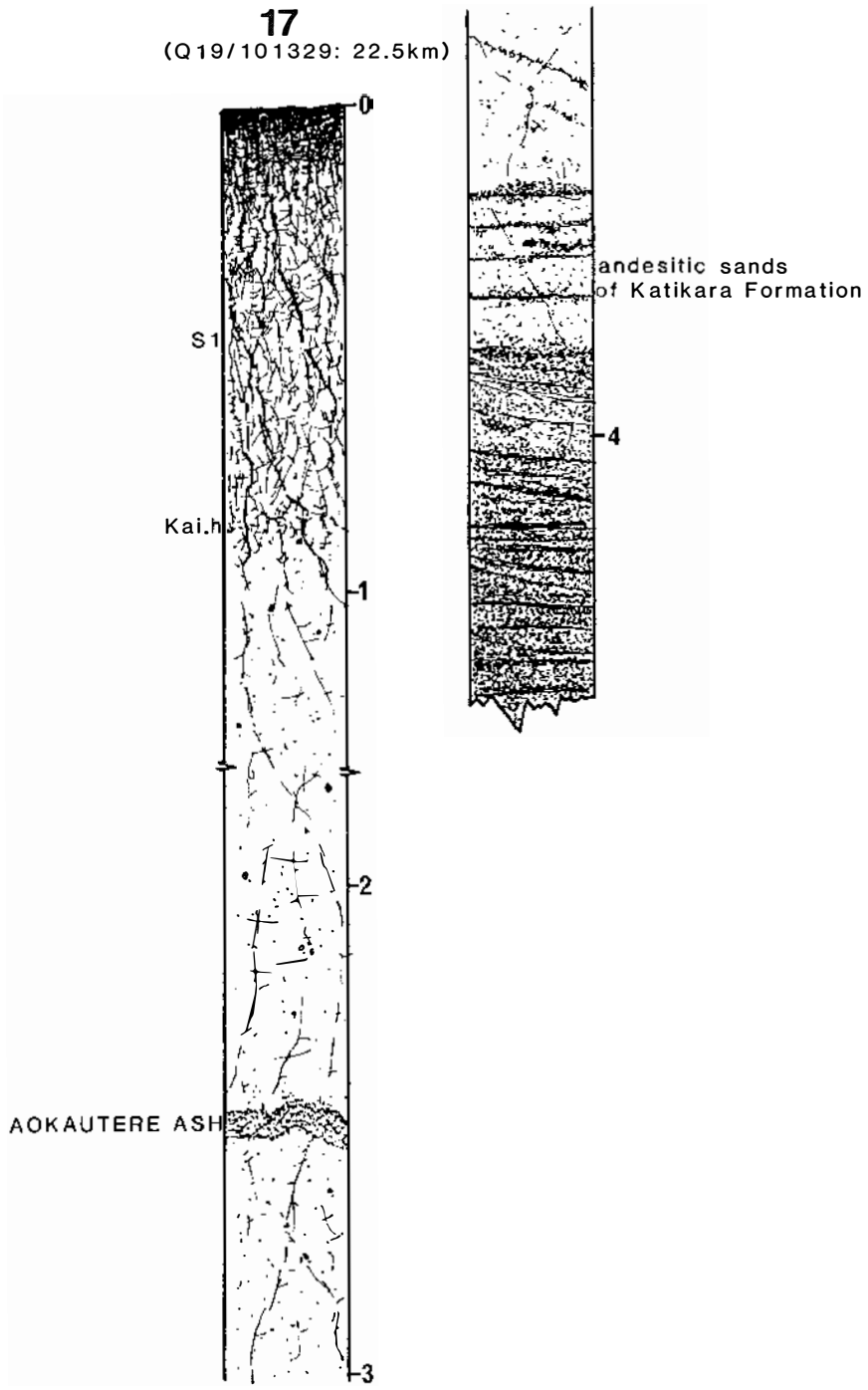


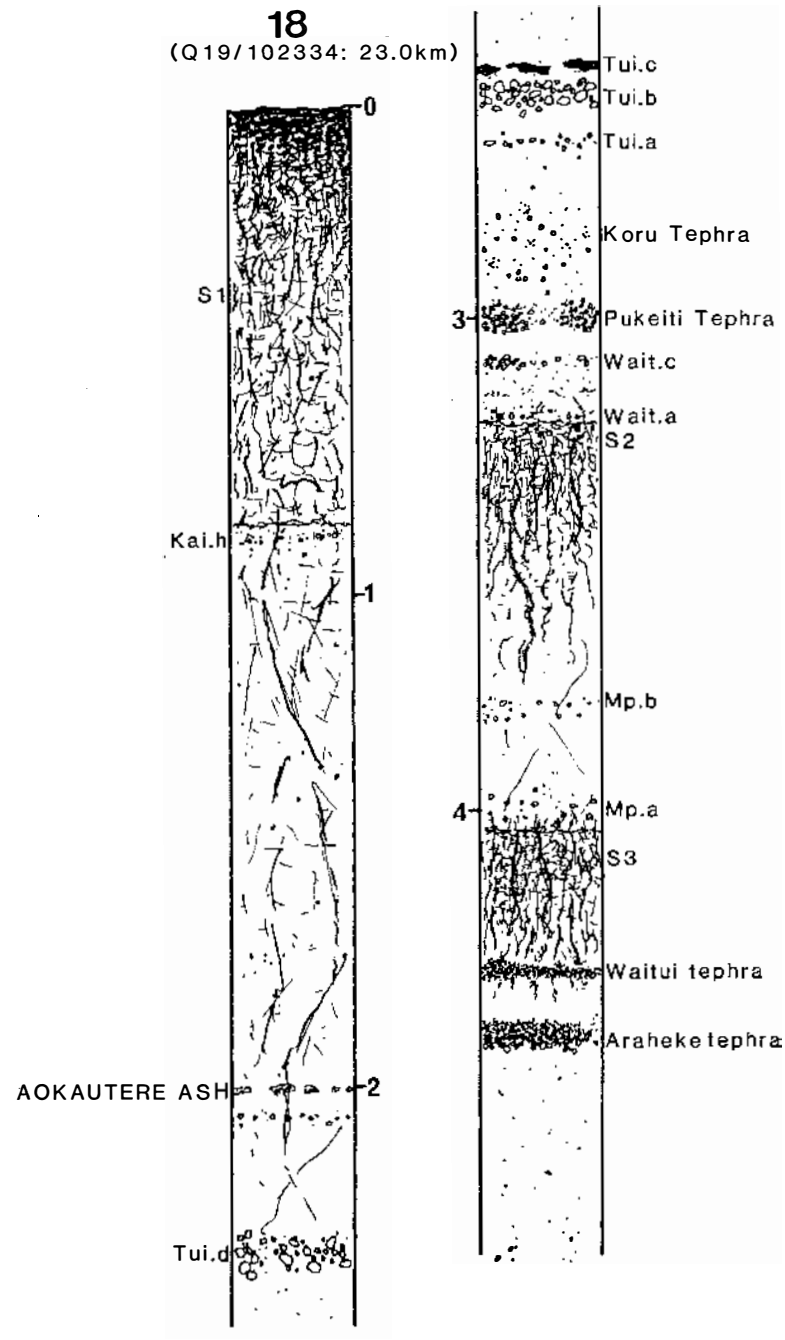

15
(P20/042908: 20.7km)
unnamed
debris-flow related
stream-flow deposit
Tariki Tephra
Kaponga Tephra
Konini Tephra
Mahoe Tephra
0
1
2
3
5
debris flow deposit
of Warea Formation
Pae.a
Pot.e
Pot.d
Pot.c
Ngaere Formation

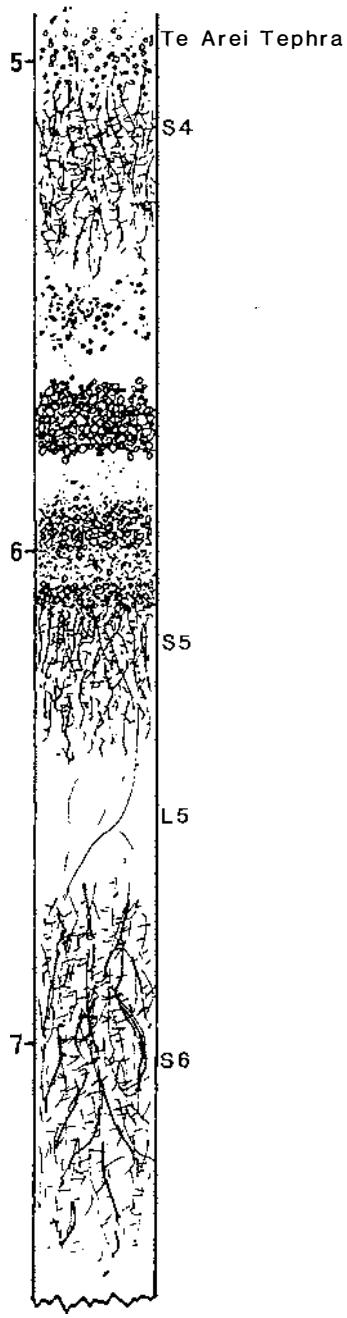
16

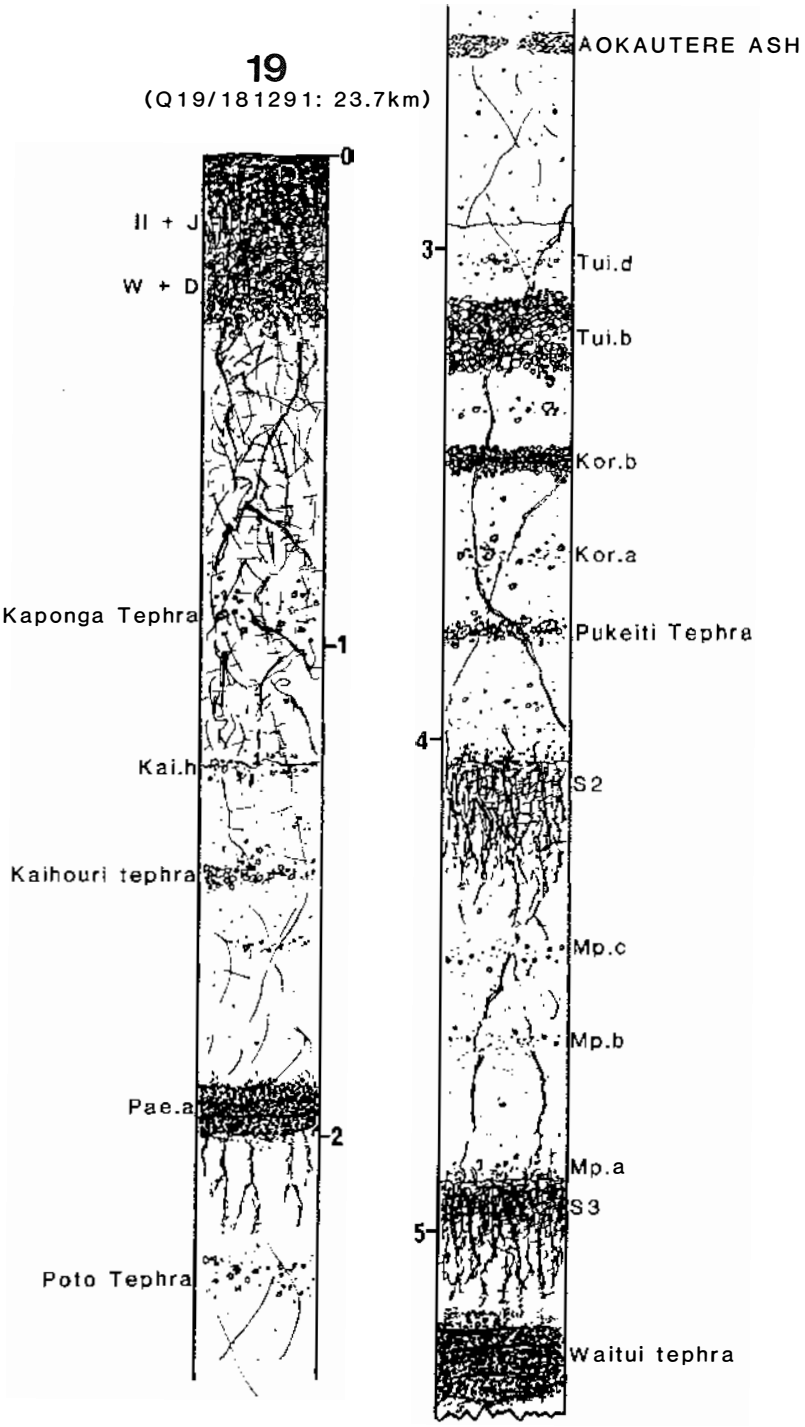
(Q19/171259: 20.7km)




17
(Q19/101329: 22.5km)
0
S1
Kai.h
1
2
AOKAUTERE ASH
3
andesitic sands
of Katikara Formation
4

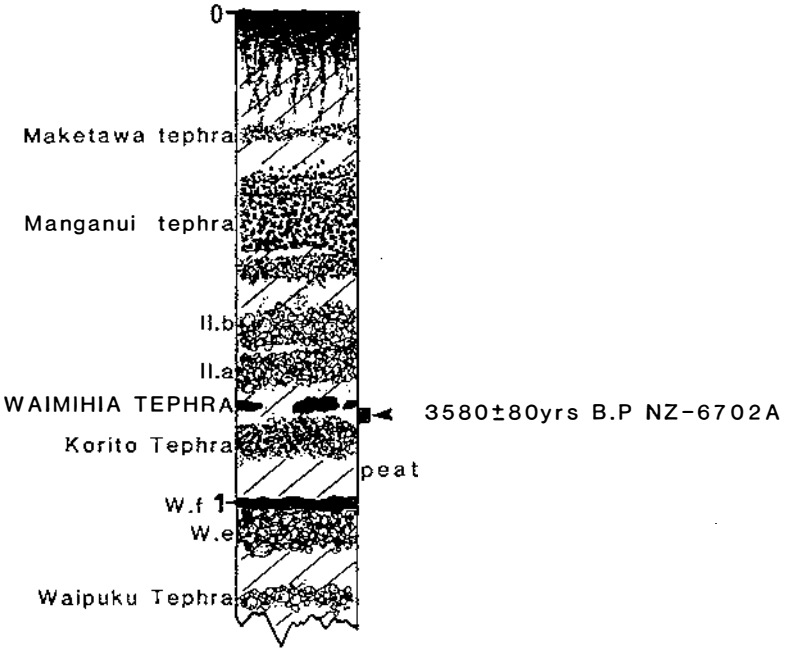

18
(Q19/102334: 23.0km)
0
S1
Kai.h
1
AOKAUTERE ASH
2
Tui.d
Tui.c
Tui.b
Tui.a
Koru Tephra
3
Pukeiti Tephra
Wait.c
Wait.a
S2
Mp.b
4
Mp.a
S3
Waitui tephra
Araheke tephra


Te Arei Tephra
5
S4
6
S5
L5
7
S6


19
(Q19/181291: 23.7km)
AOKAUTERE ASH
0
II + J
W + D
Tui.d
Tui.b
Kor.b
Kor.a
Kaponga Tephra
Pukeiti Tephra
1
Kai.h
S2
Kaihouri tephra
Mp.c
Mp.b
Pae.a
2
Mp.a
S3
Poto Tephra
Waitui tephra
3
4
5

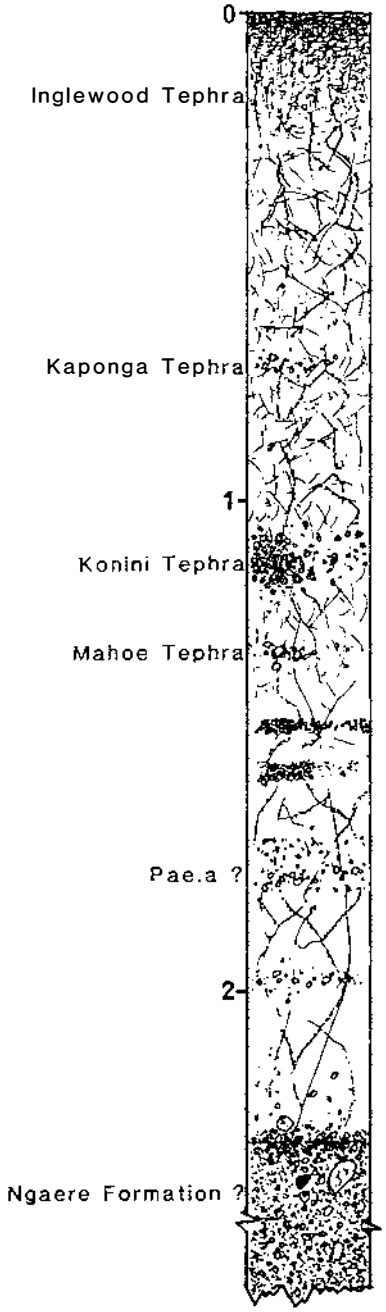
20

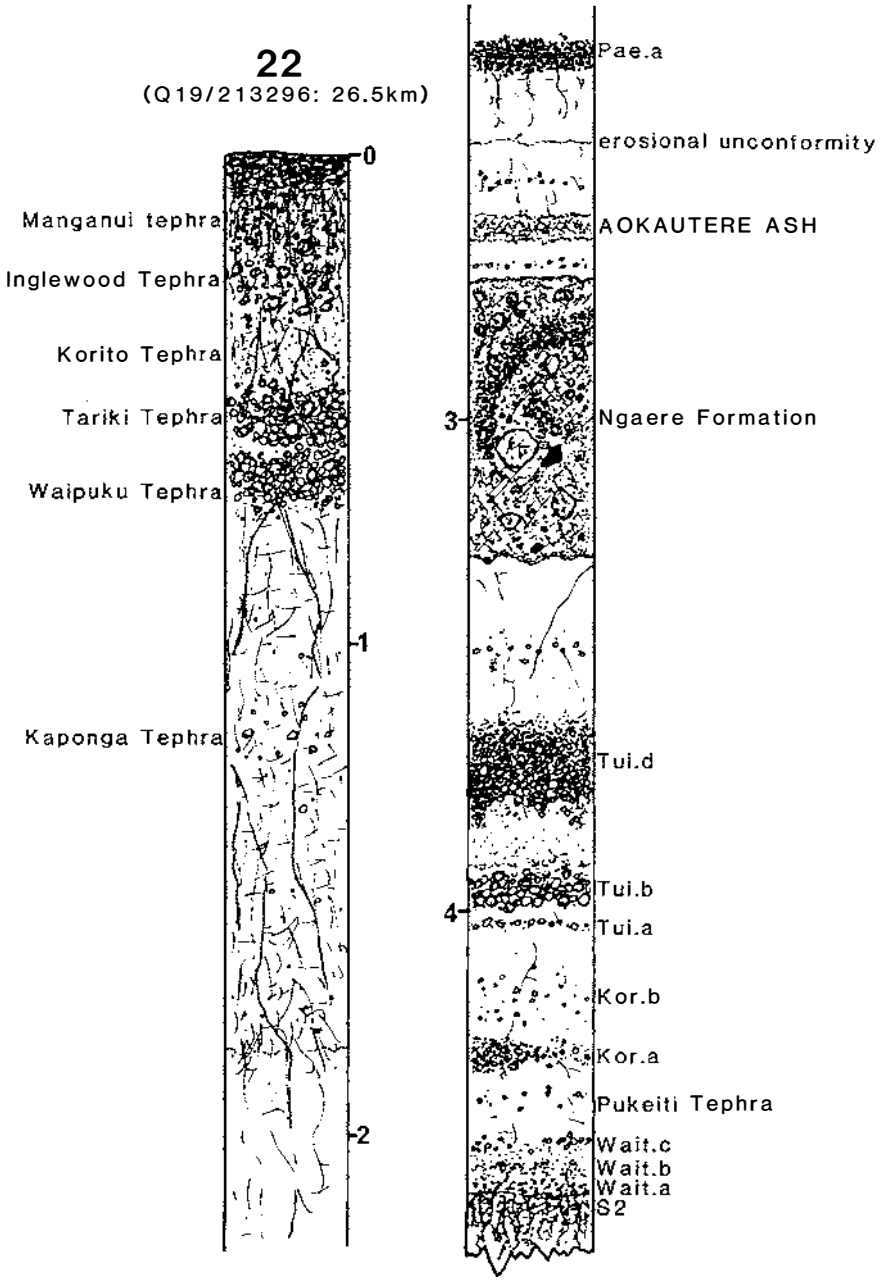
(Q19/216257: 24.0km)

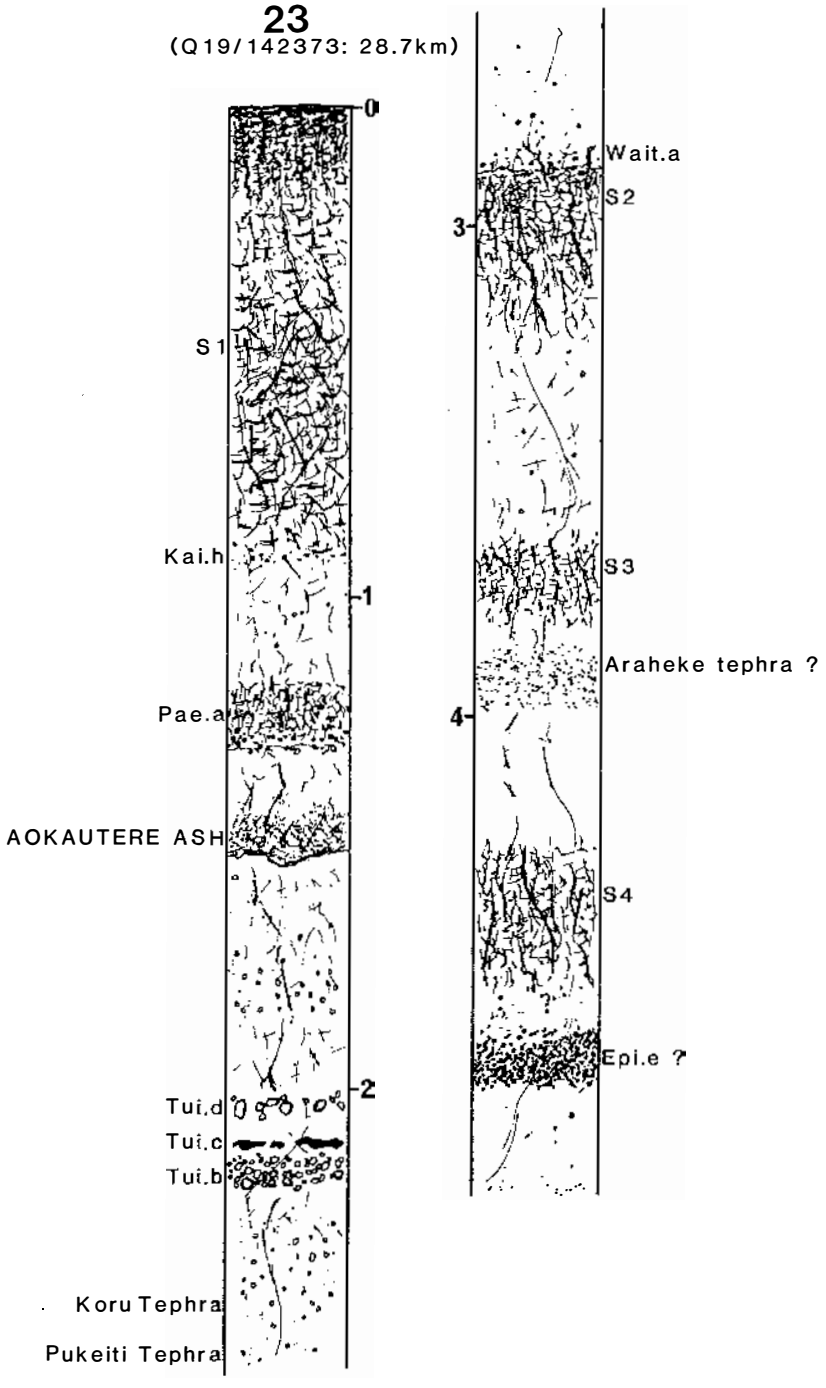


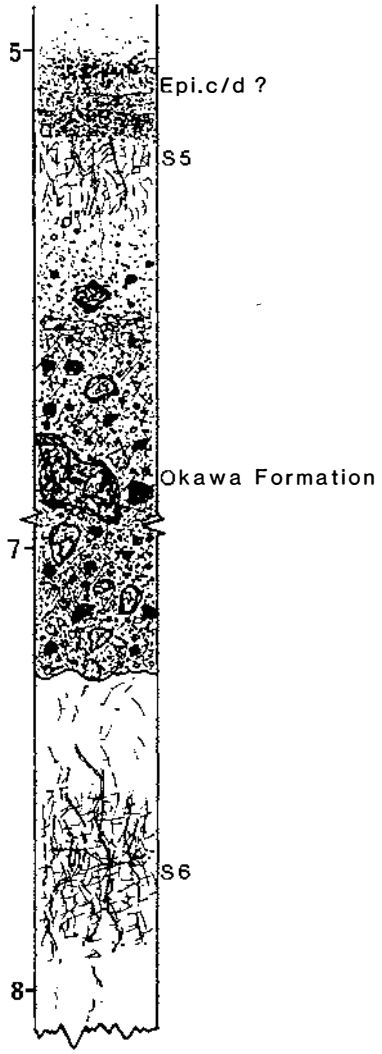
21

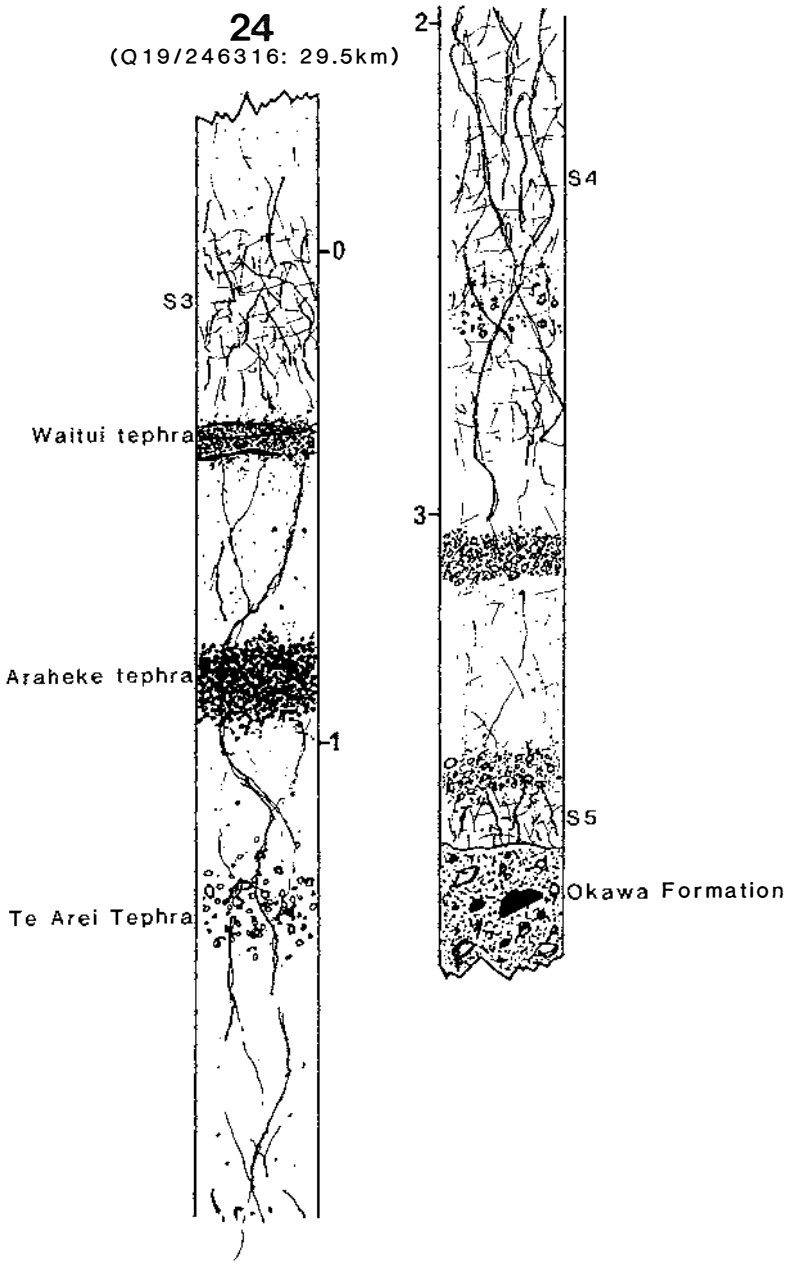
(Q20/272094: 24.7km)



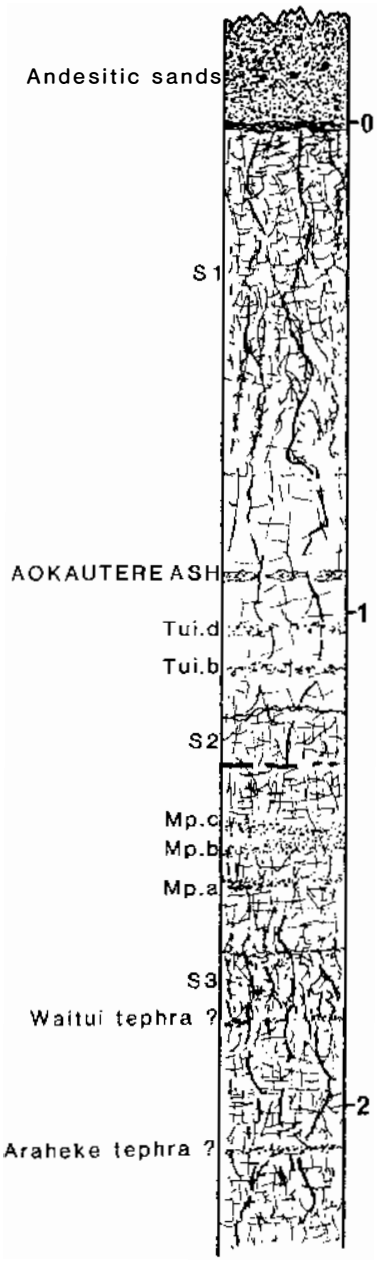

22
(Q19/213296: 26.5km)
0
1
2
3
4
Manganui tephra
Inglewood Tephra
Korito Tephra
Tariki Tephra
Waipuku Tephra
Kaponga Tephra
Pae.a
erosional unconformity
AOKAUTERE ASH
Ngaere Formation
Tui.d
Tui.b
Tui.a
Kor.b
Kor.a
Pukeiti Tephra
Wait.c
Wait.b
Wait.a
S2

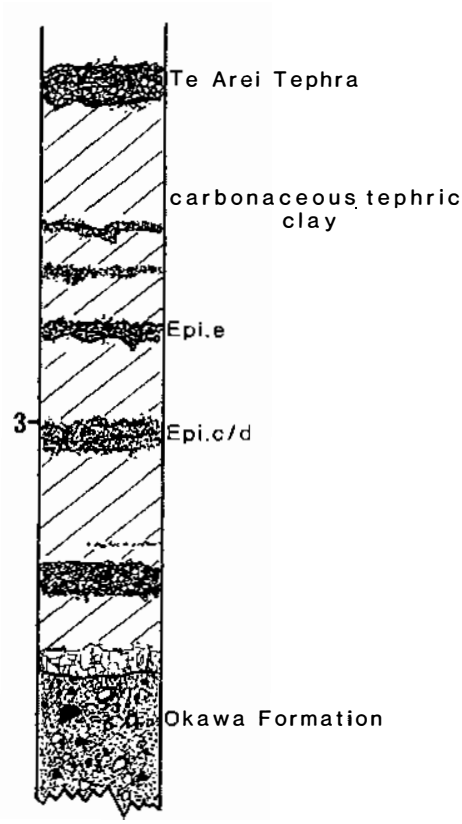

23
(Q19/142373: 28.7km)
0
S1
Kai.h
1
Pae.a
AOKAUTERE ASH
2
Tui.d
Tui.c
Tui.b
Koru Tephra
Pukeiti Tephra
3
Wait.a
S2
S3
Araheke tephra ?
4
S4
Epi.e ?


5
Epi.c/d ?
S5
Okawa Formation
7
S6
8


24
(Q19/246316: 29.5km)
S3
Waitui tephra
Araheke tephra
Te Arei Tephra
0
1
2
3
S4
S5
Okawa Formation

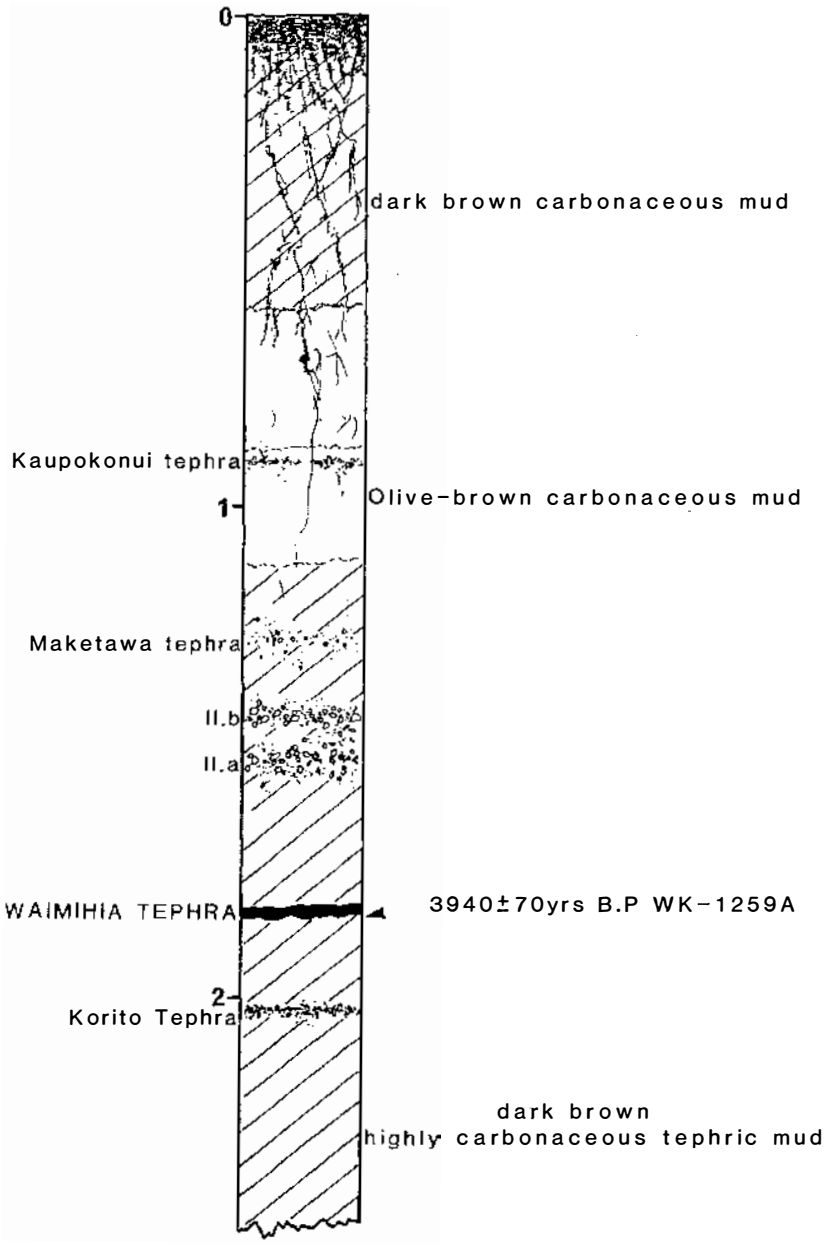
25
(Q19/121445: 34.2

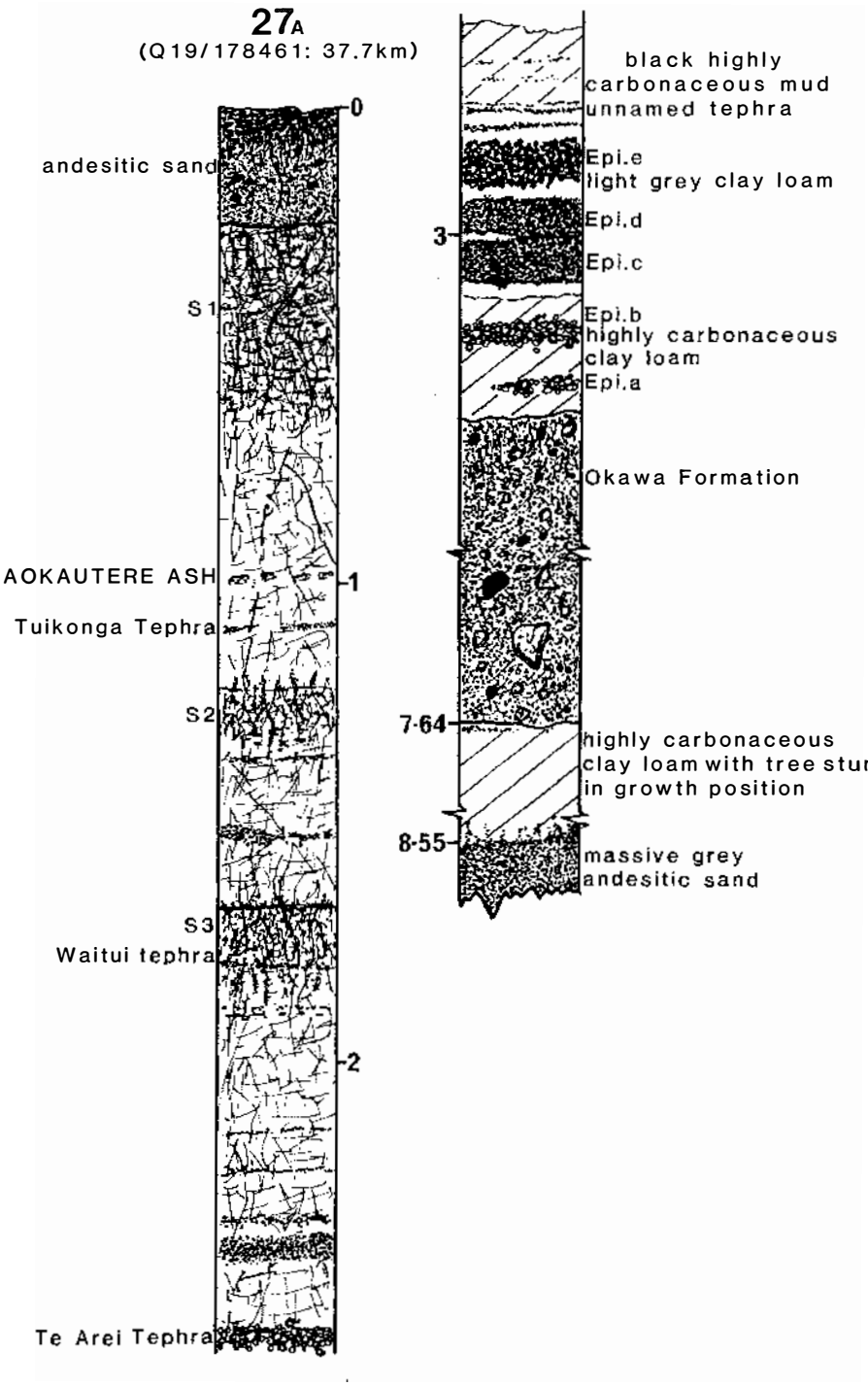


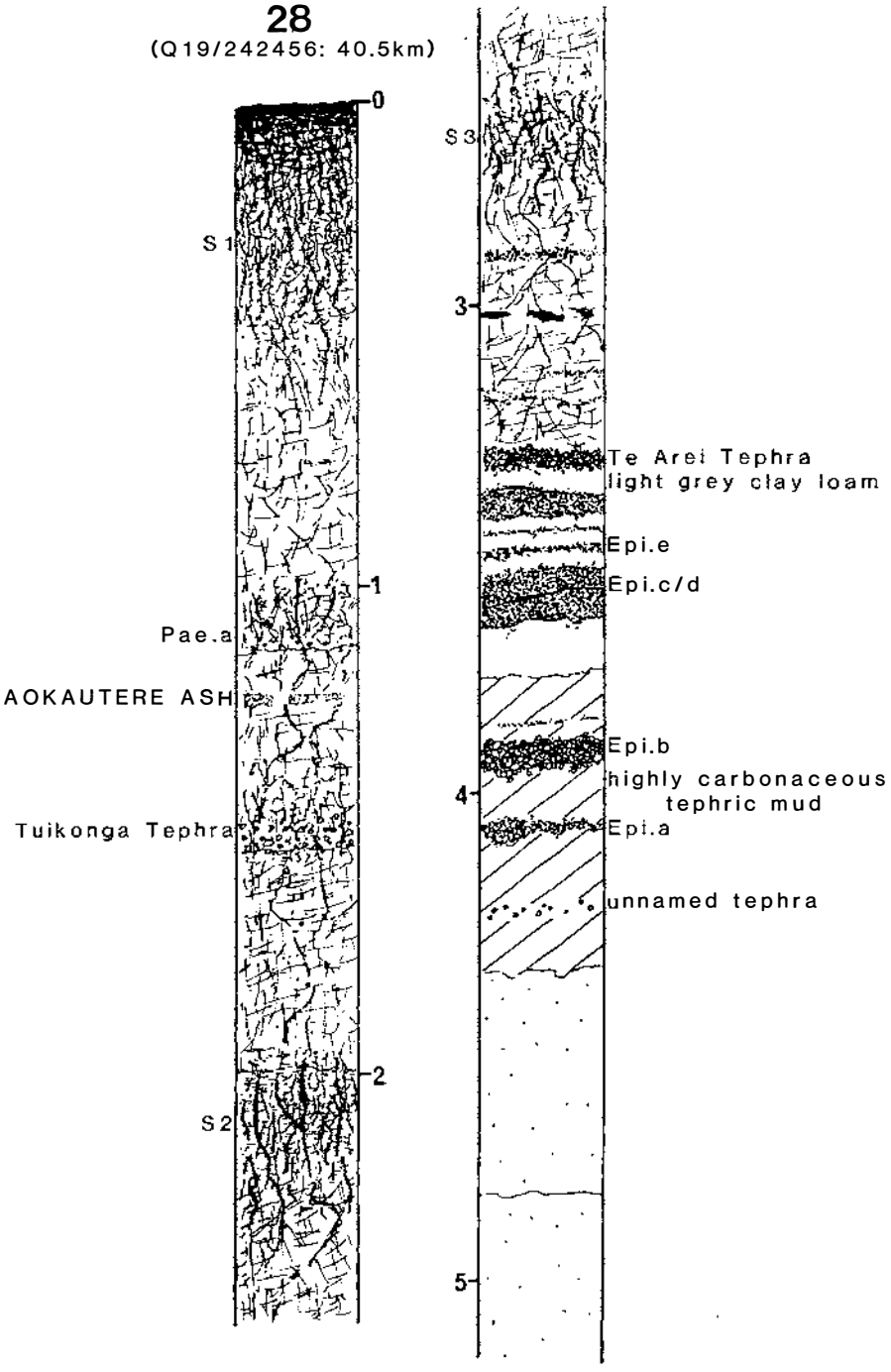


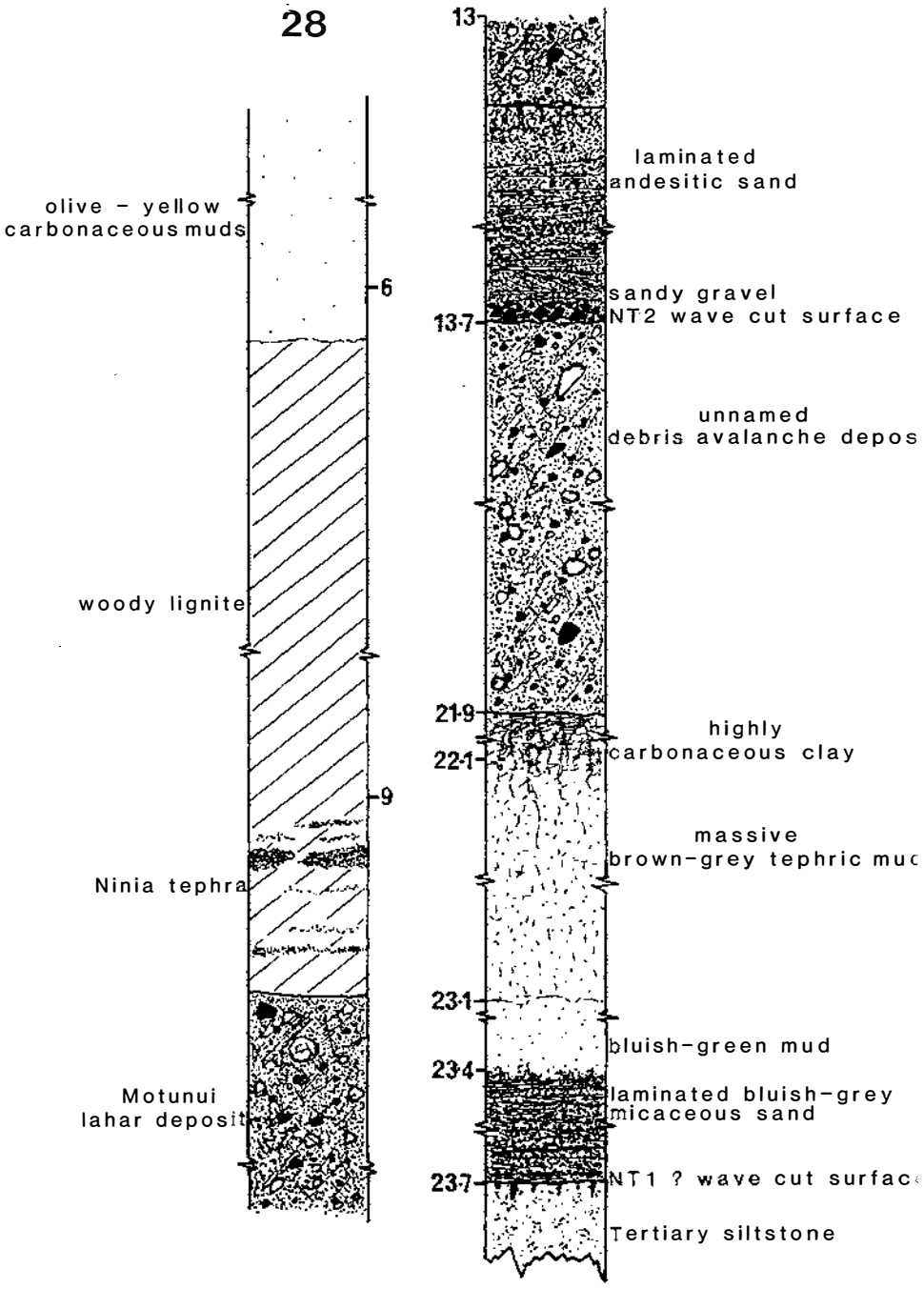
26

(Q20/318926: 33.2km)



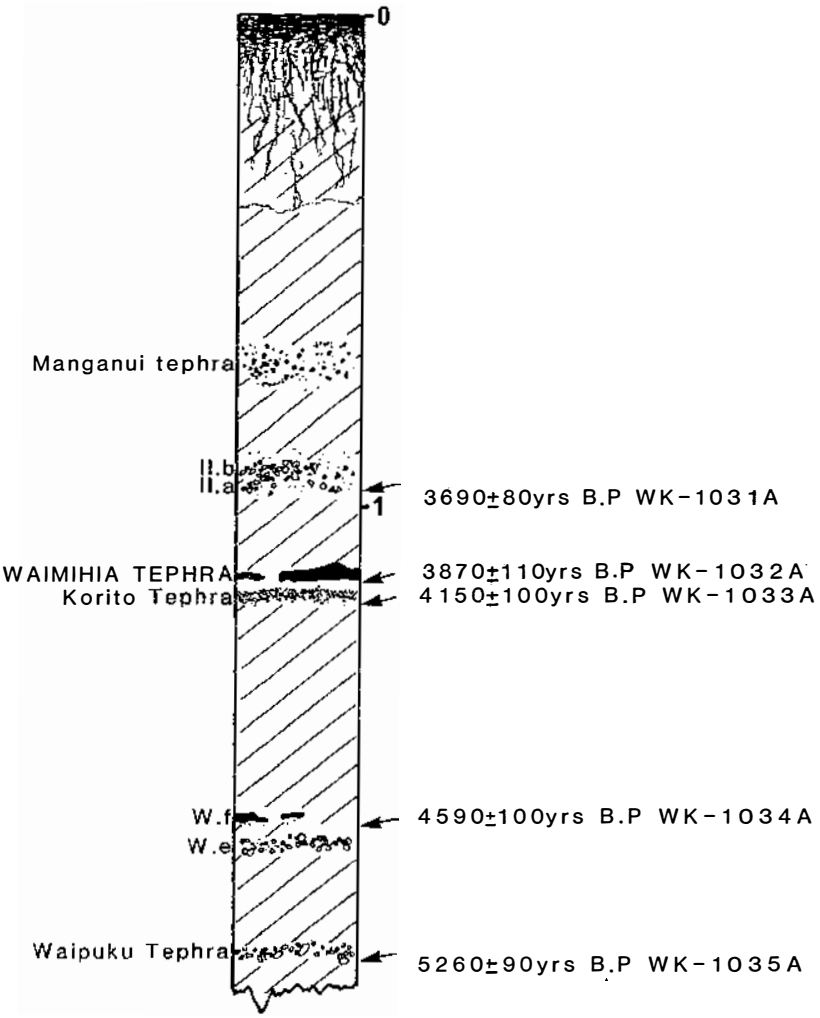

27A
(Q19/178461: 37.7km)
andesitic sand
0
S1
AOKAUTERE ASH
1
Tuikonga Tephra
S2
S3
Waitui tephra
2
Te Arei Tephra
black highly carbonaceous mud
unnamed tephra
Epi.e
light grey clay loam
Epi.d
3
Epi.c
Epi.b
highly carbonaceous clay loam
Epi.a
Okawa Formation
7·64
highly carbonaceous clay loam with tree stump in growth position
8·55
massive grey andesitic sand


28
(Q19/242456: 40.5km)
0
S 1
1
Pae.a
AOKAUTERE ASH
Tuikonga Tephra
2
S 2
S 3
3
Te Arei Tephra
light grey clay loam
Epi.e
Epi.c/d
Epi.b
highly carbonaceous
tephric mud
4
Epi.a
unnamed tephra
5

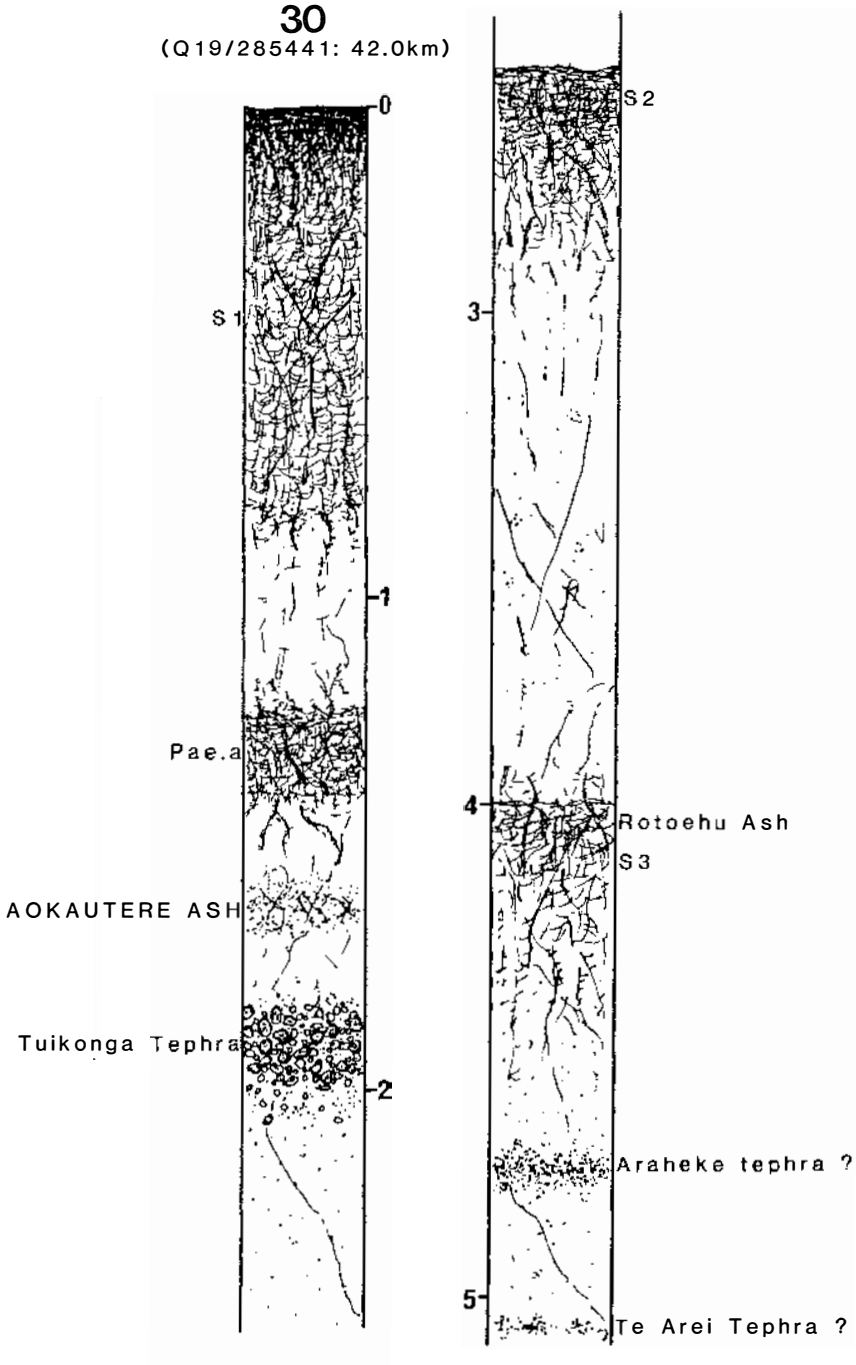

28
olive – yellow
carbonaceous muds
6
woody lignite
9
Ninia tephra
Motunui
lahar deposit
13
laminated
andesitic sand
sandy gravel
13·7
NT2 wave cut surface
unnamed
debris avalanche depos
21·9
highly
22·1
carbonaceous clay
massive
brown–grey tephric muc
23·1
bluish–green mud
23·4
laminated bluish–grey
micaceous sand
23·7
NT1 ? wave cut surfac
Tertiary siltstone

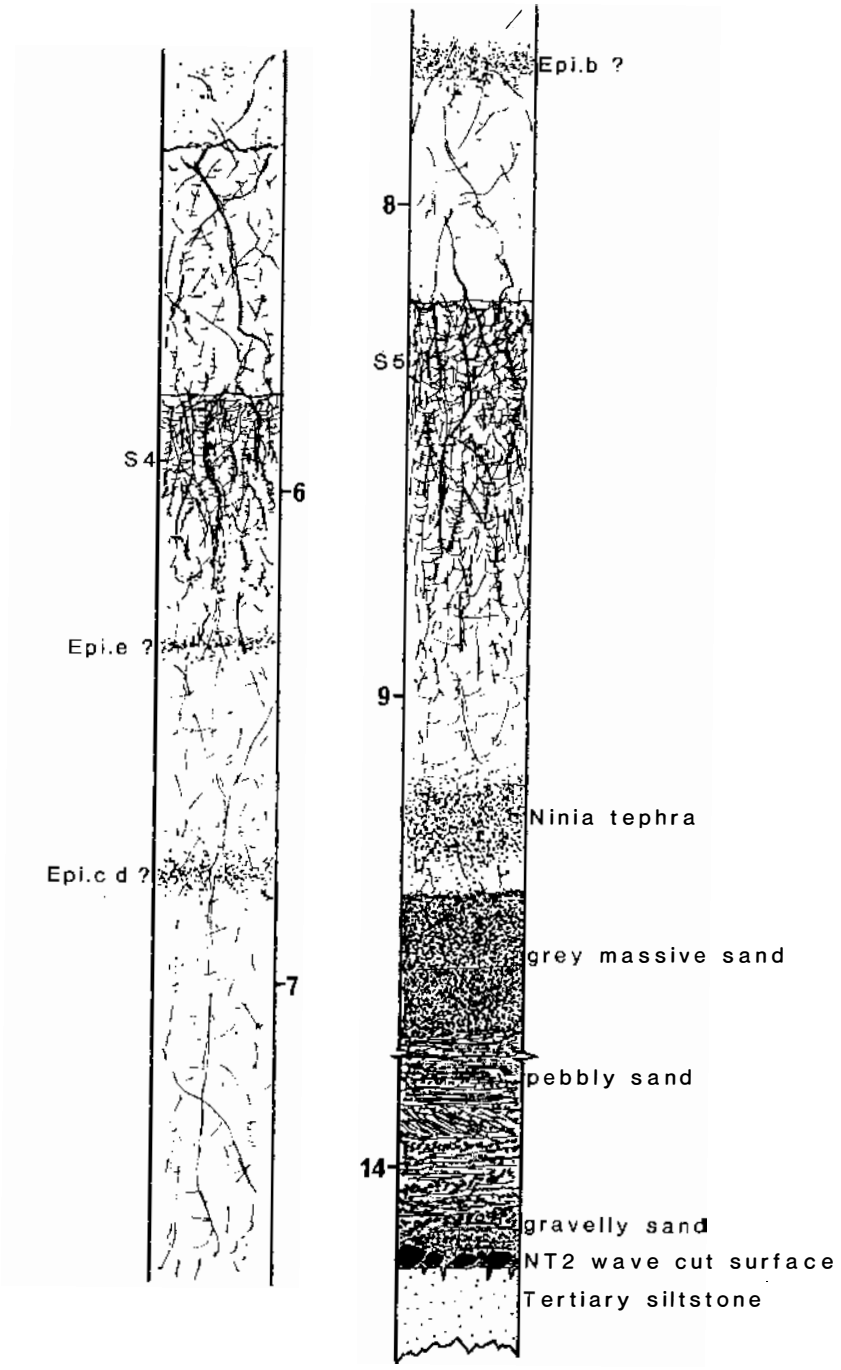
29

(Q19/268448: 41.5km)

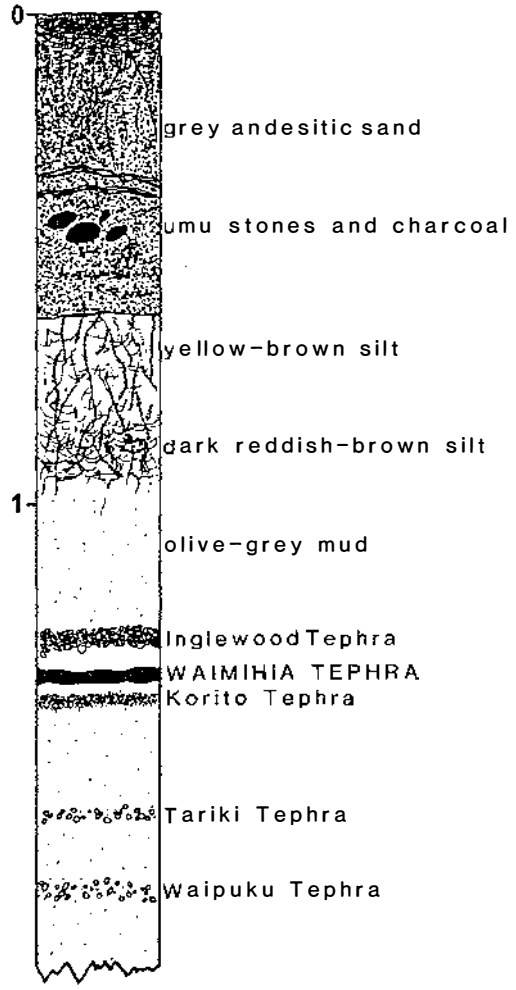


30
(Q19/285441: 42.0km)



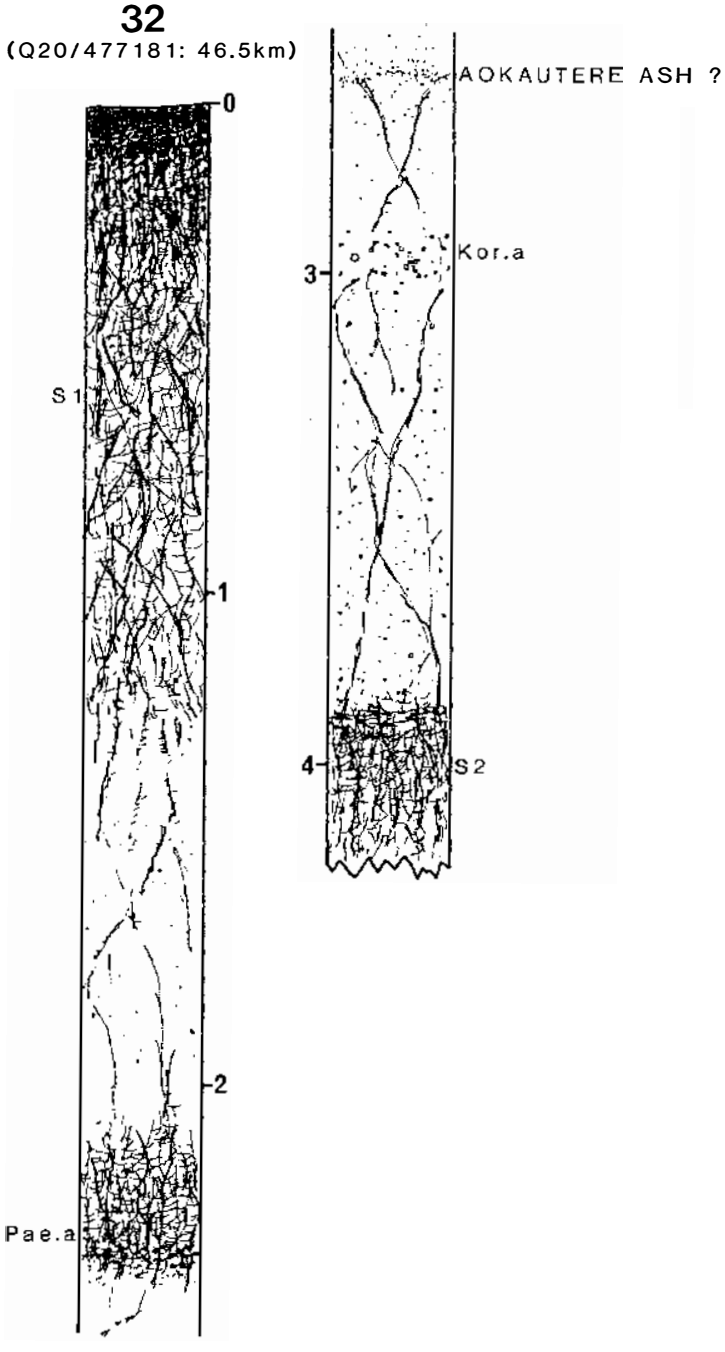

Epi.b ?
8
S5
S4
6
Epi.e ?
9
Ninia tephra
Epi.c d ?
grey massive sand
7
pebbly sand
14
gravelly sand
NT2 wave cut surface
Tertiary siltstone

31
(Q19/282449: 42.7km)

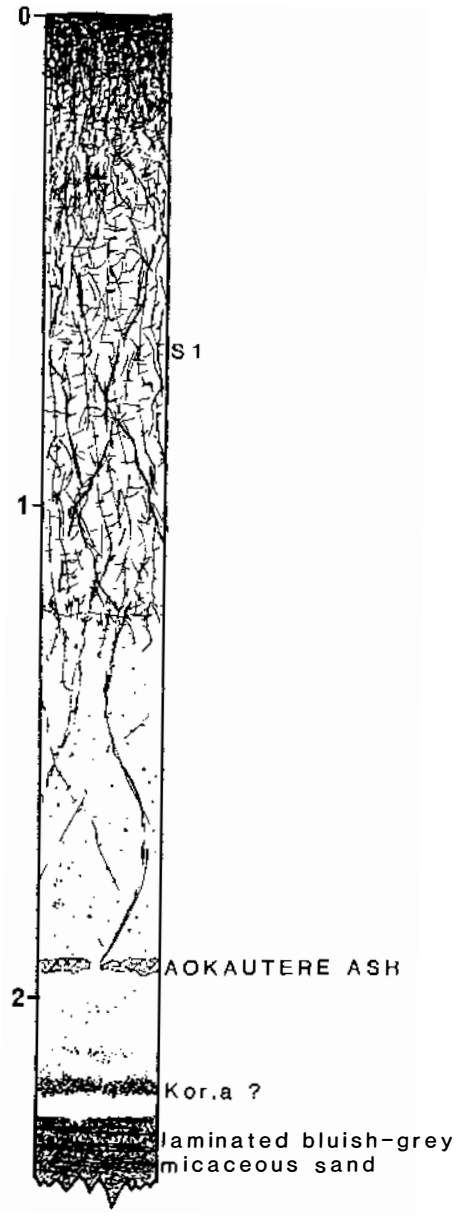


32

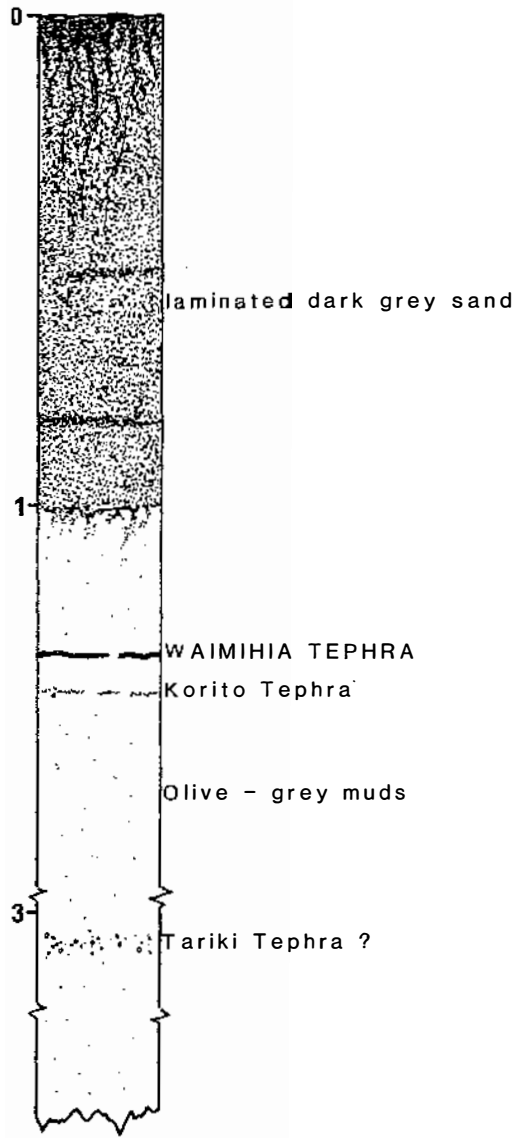
(Q20/477181: 46.5km)

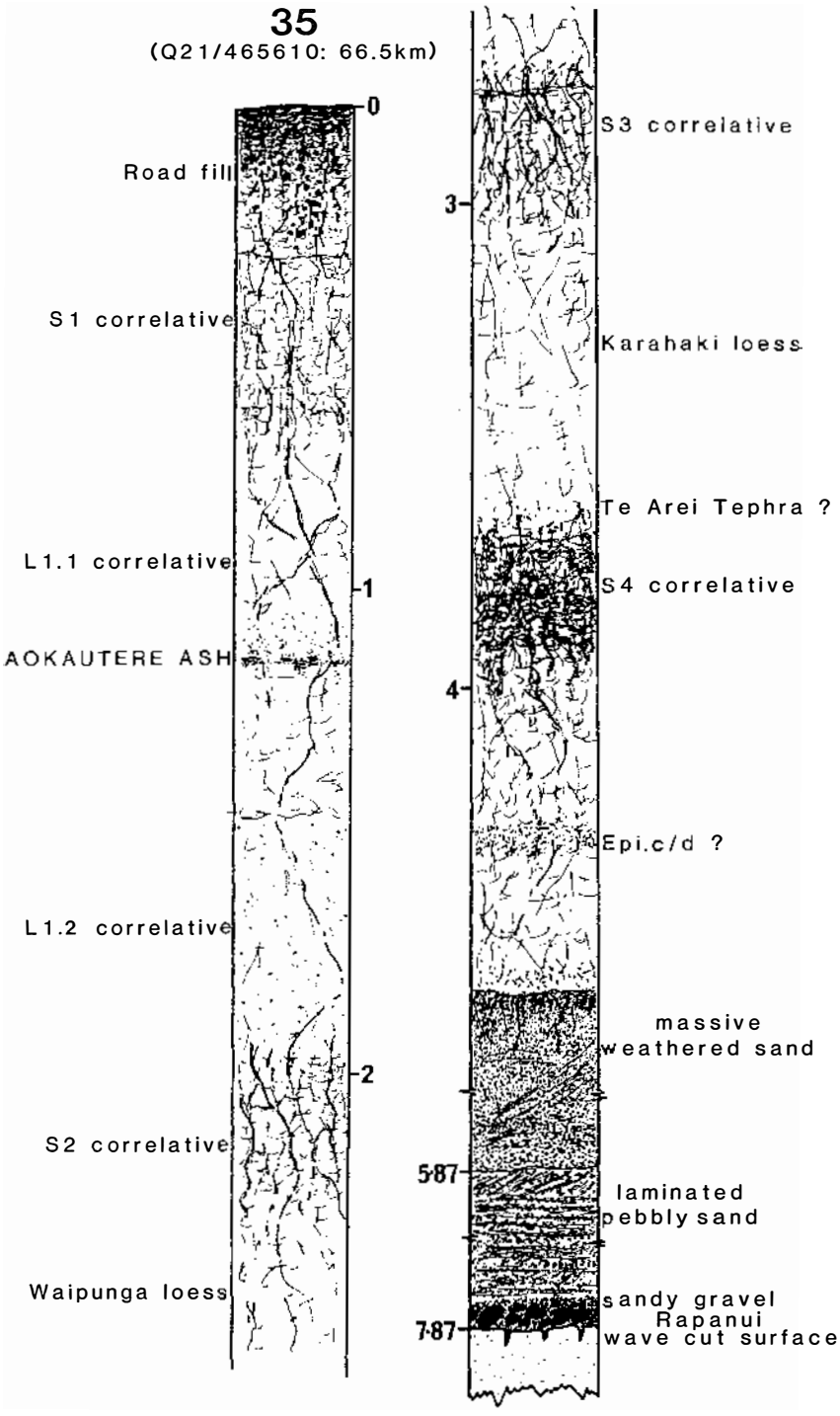


33
(Q20/493133: 47.0km)



34
(N99/026084: 53.0km)




35
(Q21/465610: 66.5km)
0
Road fill
S1 correlative
L1.1 correlative
1
AOKAUTERE ASH
L1.2 correlative
2
S2 correlative
Waipunga loess
3
S3 correlative
Karahaki loess
Te Arei Tephra ?
S4 correlative
4
Epi.c/d ?
massive
weathered sand
5·87
laminated
pebbly sand
sandy gravel
Rapanui
7·87
wave cut surface

APPENDIX TWO

APPENDIX 2.1 Electron Microprobe Data for Rhyolitic Glass Shards from Taranaki:

TEPHRA[a]	SiO_2	Al_2O_3	TiO_2	FeO[b]	MgO	CaO	Na_2O	K_2O	Cl	H_2O[c]
Wm	77.40	12.58	0.20	1.67	0.14	1.31	3.65	3.05	----	2.96
Onaero Beach	77.39	12.77	0.21	1.62	0.13	1.18	3.84	2.86	----	3.15
(Section 29)	77.07	12.59	0.18	1.63	0.20	1.41	3.95	2.96	----	2.05
	77.68	12.48	0.21	1.52	0.14	1.30	3.66	3.00	---	2.23
	77.88	12.50	0.16	1.81	0.17	1.06	3.38	3.05	----	4.48
	77.48	12.49	0.18	1.65	0.16	1.35	3.83	2.86	----	4.26
	77.59	12.65	0.15	1.59	0.14	1.29	3.65	2.92	----	2.55
	76.78	12.63	0.25	3.07	0.16	1.30	2.78	3.04	----	4.54
	78.04	13.05	0.21	1.81	0.18	1.46	2.29	2.95	----	6.21
	76.97	12.82	0.07	1.74	0.13	1.37	3.87	3.03	----	1.62
	77.12	12.53	0.40	1.71	0.19	1.38	3.72	2.96	----	2.06
Wm	77.78	12.11	0.13	1.61	0.17	1.31	3.84	3.05	----	3.59
Kaimata	77.54	12.51	0.15	1.66	0.07	1.28	3.63	3.16	----	1.82
(Section 20)	77.27	12.56	0.21	1.53	0.17	1.39	3.87	3.00	----	3.47
	77.32	12.49	0.35	1.75	0.18	1.28	3.70	2.93	----	3.44
	77.09	12.80	0.23	1.57	0.17	1.35	3.69	3.08	----	1.42
	77.57	12.65	0.18	1.64	0.13	1.24	3.63	2.95	----	1.17
	77.96	12.51	0.23	1.60	0.13	1.28	3.34	2.94	----	2.07
	77.41	12.41	0.12	1.84	0.12	1.33	3.69	3.08	----	1.52
	77.81	12.57	0.21	1.61	0.15	1.22	3.63	2.79	---	1.74
	77.86	12.61	0.25	1.57	0.14	1.08	3.57	2.91	----	1.46
	78.06	12.44	0.19	1.62	0.15	1.10	3.71	2.72	----	1.18
AA	78.79	12.28	0.13	1.13	0.15	0.96	3.27	3.13	0.16	6.12
Onaero	79.56	12.31	0.14	1.25	0.11	1.00	2.24	3.20	0.19	7.09
(Section 30)	78.87	12.39	0.15	1.27	0.11	1.19	2.81	3.02	0.19	6.42
	79.41	12.33	0.16	1.21	0.13	1.13	2.38	3.04	0.21	7.96
	79.11	12.52	0.05	1.33	0.13	1.16	2.28	3.02	0.19	6.33

	79.67	12.28	0.14	0.88	0.14	0.82	2.58	3.30	0.19	7.47
	79.38	12.31	0.13	0.81	0.13	0.83	3.10	3.10	0.20	6.23
Up Smart Rd	78.50	11.97	0.28	1.31	0.05	0.73	3.21	3.95	----	5.04
	79.16	11.82	0.14	1.30	0.12	0.97	2.83	3.66	----	5.40
	78.81	12.03	0.19	1.21	0.07	0.87	3.23	3.59	----	5.30
	78.30	11.82	0.12	1.54	0.21	1.09	3.27	3.67	----	5.07
	78.48	12.24	0.02	1.09	0.10	0.97	3.42	3.69	----	6.20
	78.85	12.05	0.09	1.16	0.06	1.02	3.01	3.75	----	4.60
	78.58	12.00	0.08	1.31	0.11	0.97	3.15	3.81	----	5.01
	77.68	12.29	0.11	1.48	0.16	1.07	3.50	3.71	----	3.88
	77.67	12.50	0.21	1.38	0.13	1.17	3.32	3.62	----	5.28
	79.49	12.18	0.26	1.02	0.07	0.97	2.57	3.43	----	6.22
	77.68	12.48	0.08	1.43	0.11	1.21	3.33	3.68	----	5.52
	78.92	11.64	0.15	1.16	0.07	0.85	3.40	3.80	----	5.26
Lwr Smart Rd	78.54	11.82	0.19	1.30	0.05	0.90	3.26	3.95	----	5.04
	79.17	11.78	0.04	1.08	0.06	0.85	3.12	3.90	----	4.35
	78.86	11.89	0.05	1.33	0.08	0.80	3.06	3.94	----	5.77
	78.84	11.75	0.20	1.21	0.07	0.79	3.36	3.77	----	4.21
	78.62	11.81	0.05	1.35	0.06	0.87	3.55	3.69	----	2.90
	79.19	11.98	0.18	0.57	0.05	0.99	3.45	3.59	----	6.33
	78.53	11.75	0.16	1.24	0.09	0.84	3.52	3.87	----	4.79
	79.41	11.67	0.23	1.08	0.04	0.64	3.12	3.81	----	5.20
	78.96	11.91	0.06	1.09	0.05	0.82	3.33	3.77	----	5.38
	79.45	11.87	0.07	1.22	0.06	0.86	2.54	3.91	----	6.06
	78.69	11.92	0.05	1.38	0.05	0.81	3.41	3.69	----	5.63
	78.82	11.88	0.06	1.30	0.06	0.82	3.35	3.71	----	4.77
Mountain Rd	79.04	11.75	0.13	0.98	0.10	0.89	2.89	4.22	----	5.96
	79.71	11.85	0.16	1.07	0.13	0.76	2.21	4.10	----	8.12
	79.10	11.89	0.15	1.13	0.10	0.84	2.81	3.98	----	5.49
	79.87	12.03	0.13	0.85	0.12	0.80	2.16	4.04	----	6.40
	79.14	11.68	0.16	1.08	0.09	0.80	2.77	4.27	----	6.63
	79.95	11.96	0.12	0.80	0.10	0.82	2.17	4.08	----	7.53

	79.44	12.48	0.11	0.98	0.13	1.18	2.42	3.04	0.22	7.54
	79.69	12.68	0.15	1.09	0.11	1.11	2.04	2.95	0.17	8.26
	79.71	12.34	0.12	1.22	0.12	0.96	2.13	3.20	0.19	7.44
	79.22	12.36	0.10	1.10	0.13	0.94	2.81	3.16	0.18	5.71
	79.35	12.30	0.10	1.11	0.13	1.18	2.71	2.96	0.17	6.01
	79.70	12.42	0.12	1.16	0.12	1.03	2.14	3.11	0.20	8.07
	79.09	12.49	0.16	1.26	0.14	1.11	2.60	3.01	0.14	7.00
	79.62	12.50	0.13	1.16	0.11	1.15	2.00	3.13	0.21	8.83
	79.58	12.24	0.15	1.43	0.10	0.98	2.09	3.26	0.17	8.18
	79.13	12.43	0.10	1.20	0.12	1.02	2.88	2.95	0.17	6.19
AA	77.62	12.41	0.08	1.43	0.14	1.23	3.85	3.04	0.20	5.49
Waitui	77.69	12.48	0.16	1.09	0.11	1.12	3.22	3.96	0.17	4.80
(Section 19)	78.40	12.23	0.14	1.45	0.09	0.99	3.35	3.17	0.19	5.26
	79.04	12.43	0.14	1.08	0.14	0.99	2.83	3.19	0.16	6.91
	79.34	12.45	0.15	1.13	0.11	1.05	2.83	2.77	0.17	6.85
	79.14	12.50	0.16	1.08	0.09	1.15	2.98	2.81	0.11	6.30
	79.34	12.34	0.07	1.06	0.12	1.01	2.70	3.15	0.21	6.56
	79.04	12.31	0.09	1.20	0.10	1.03	2.95	3.10	0.19	5.99
	78.97	12.40	0.11	1.29	0.14	1.18	2.71	3.01	0.19	6.07
	78.65	12.41	0.17	1.26	0.13	1.14	2.99	3.06	0.19	5.92
	79.33	12.47	0.14	1.20	0.11	1.03	2.60	2.93	0.19	6.68
	79.57	12.29	0.13	1.09	0.11	0.96	2.38	3.26	0.20	7.32
	80.01	12.21	0.15	1.13	0.11	0.95	2.04	3.19	0.20	8.28
	79.43	12.54	0.11	1.26	0.14	1.25	2.18	2.89	0.21	7.89
	79.39	12.32	0.13	1.20	0.11	1.13	2.56	2.98	0.17	6.43
Re	79.01	12.41	0.12	0.94	0.13	0.72	3.34	3.14	0.19	5.67
Onaero	79.39	12.44	0.16	0.92	0.14	0.78	2.83	3.18	0.16	6.37
(Section 30)	78.94	12.44	0.18	0.79	0.12	0.93	3.39	3.07	0.15	5.47
	79.25	12.45	0.18	0.89	0.12	0.87	2.93	3.12	0.19	6.95
	79.70	12.41	0.15	0.90	0.14	0.82	2.56	3.17	0.15	7.45
	79.54	12.54	0.13	0.92	0.15	0.90	2.47	3.17	0.17	6.90
	79.71	12.26	0.09	0.83	0.14	0.84	2.89	3.05	0.19	6.91
	79.09	12.32	0.15	0.88	0.17	0.76	3.22	3.26	0.16	5.46
	79.25	12.31	0.14	0.97	0.14	0.84	2.97	3.17	0.21	6.62

Notes:

Wm = Waimihia Tephra, AA = Aokautere Ash and Re = Rotoehu Tephra.

a. Analyses by P.C.Froggatt, R.S.E.S, Victoria University of Wellington.
b. All Fe calculated as FeO.
c. H_2O by difference from 100%.

APPENDIX 2.2 Electron Microprobe Data for Rhyolitic Glass Shards:

TEPHRA[a]	SiO_2	Al_2O_3	TiO_2	FeO[b]	MgO	CaO	Na_2O	K_2O	Cl	H_2O	N[d]
1.Mountain Road	79.47	11.86	0.14	0.98	0.11	0.82	2.50	4.11	----	6.69	6
2.Rangitawa (Omahina Road)	78.03	12.13	0.15	1.03	0.12	0.78	3.35	4.22	0.19	5.86	32
3.Mt.Curl (Mt.Curl)	78.09	12.33	0.14	1.01	0.12	0.79	3.30	4.33	----	4.55	132
4.Lower Smart Rd (New Plymouth rubbish dump)	78.82	11.83	0.11	1.18	0.06	0.83	3.26	3.80	----	5.03	12
5.Upper Smart Rd (New Plymouth rubbish dump)	78.51	12.08	0.14	1.28	0.10	0.99	3.19	3.69	----	5.23	12
6.MGR 1 (Griffin Quarry)	78.10	12.17	0.12	1.17	0.09	0.84	3.72	3.65	0.14	5.03	14
7.MGR 2 (Griffin Quarry)	78.20	12.09	0.10	1.16	0.07	0.80	3.94	3.55	0.08	5.62	16
8.Up. Griffin Rd (Griffin Quarry)	78.10	12.17	0.12	1.17	0.09	0.84	3.72	3.65	0.14	5.03	14
9.Lwr Griffin Rd (Griffin Quarry)	76.76	12.75	0.25	1.27	0.26	1.14	4.11	3.10	0.10	5.60	17

Notes:

a. Analyses 1, 4 and 5 by P.C.Froggatt, R.S.E.S., Victoria University of Wellington. Analyses 2, 6, 7, 8 and 9 from Pillans (1988); analysis 3 from Froggatt et al. (1986). All elements calculated on a water-free basis.
b. All Fe calculated as FeO.
c. H_2O by difference from 100%.
d. Number of analyses upon which mean is calculated for each element.

APPENDIX THREE

APPENDIX 3.1 **WAITUI GRAIN-SIZE AND QUARTZ DATA**

(Expressed as a percentage of Total Sample; <2mm)

	Grain-Size Data								Quartz Data			
	Phi								Phi			
Depth	**0**	**1**	**2**	**3**	**4**	**5**	**0 - 5**	**<5**	**SROCO**	**5**	**<5**	**Total**
0.20 - 0.30	2.93	8.56	22.78	12.15	7.73	5.34	59.51	14.76	25.73	0.03	0.03	0.06
0.30 - 0.40	1.55	4.11	18.32	15.75	9.08	5.49	54.32	15.00	30.68	0.06	0.07	0.13
0.50 - 0.60	1.36	3.10	7.87	8.97	10.27	7.10	38.69	19.58	41.73	0.06	0.25	0.31
0.70 - 0.80	0.54	2.59	7.67	8.24	9.61	7.24	35.92	20.46	43.62	0.06	0.38	0.44
0.80 - 0.90	0.40	2.67	7.93	8.13	8.04	5.29	32.47	17.67	49.86	0.01	0.23	0.24
0.90 - 1.00	0.40	2.78	8.40	7.61	7.59	4.64	31.44	15.50	53.06	0.06	0.24	0.30
1.00 - 1.05	1.36	5.46	7.04	6.87	6.23	3.50	30.47	13.45	56.08	0.05	0.32	0.37
1.05 - 1.10	1.77	6.44	7.10	6.39	5.64	2.92	30.27	14.47	55.26	0.07	0.12	0.19
1.10 - 1.15	2.35	8.41	8.47	7.14	6.26	3.20	35.84	14.70	49.46	0.06	0.47	0.53
1.15 - 1.20	3.44	9.57	8.29	6.67	5.37	3.01	36.36	13.21	50.43	0.05	0.18	0.23
1.20 - 1.25	3.88	12.18	9.07	7.07	5.87	3.41	41.48	14.81	47.71	0.05	0.48	0.55
1.25 - 1.30	4.83	14.08	8.18	6.32	5.23	3.11	41.76	13.53	44.71	0.09	0.34	0.43
1.30 - 1.35	5.34	13.66	8.77	7.43	6.14	3.91	40.64	14.84	44.52	0.15	0.72	0.87
1.35 - 1.40	8.92	9.62	8.47	7.43	5.47	3.01	42.92	16.44	40.64	0.07	0.39	0.46
1.40 - 1.45	7.81	10.53	8.71	8.00	6.14	4.24	45.43	17.19	37.38	0.35	1.52	1.87
1.45 - 1.50	9.16	12.58	9.05	7.80	5.77	3.87	48.24	18.23	33.53	0.41	1.42	1.83
1.50 - 1.55	3.20	10.70	9.94	7.95	6.28	4.43	42.50	21.20	36.30	0.55	2.10	2.65
1.55 - 1.60	1.83	10.25	9.46	8.20	6.17	5.26	41.17	21.86	36.97	0.82	2.79	3.61
1.60 - 1.65	3.09	11.59	9.77	7.88	5.79	4.97	43.09	22.75	34.16	0.97	2.55	3.52
1.60 - 1.70	1.64	6.99	8.10	6.50	5.81	6.20	35.26	28.71	36.03	1.44	4.97	6.41
1.70 - 1.75	2.09	5.46	7.01	5.23	5.47	4.68	29.94	27.68	42.38	1.50	5.47	6.97
1.75 - 1.80	1.47	6.26	7.15	5.65	6.04	7.33	33.92	27.58	38.50	1.69	5.65	7.34
1.80 - 1.85	4.15	7.72	7.99	3.36	5.92	6.43	35.57	25.77	38.66	1.43	4.07	5.50
1.85 - 1.90	7.12	7.76	7.47	6.27	6.59	6.50	41.73	21.16	37.11	0.95	2.86	3.81
1.90 - 2.00	9.38	17.51	9.94	6.05	7.33	4.05	54.25	12.69	33.06	0.02	0.30	0.32
2.00 - 2.05	4.19	8.47	7.97	5.02	6.08	5.91	37.65	22.24	40.11	0.84	2.59	3.43

2.05 - 2.10	0.85	3.85	5.24	4.63	5.87	6.31	26.77	26.52	46.71	1.12	4.26	5.38
2.10 - 2.15	0.73	4.26	5.81	5.10	5.65	5.70	27.25	27.16	45.59	0.97	4.09	5.06
2.15 - 2.20	0.88	5.20	6.74	5.01	5.05	4.77	27.65	25.17	47.18	0.81	4.05	4.86
2.20 - 2.25	1.07	5.96	8.52	5.88	5.72	4.93	32.09	21.90	46.01	0.71	2.49	3.20
2.25 - 2.30	1.62	7.55	8.71	6.31	5.84	4.85	34.89	20.85	44.26	0.59	2.34	2.93
2.30 - 2.35	1.61	9.07	8.45	6.44	5.52	4.23	35.32	18.86	45.82	0.51	1.73	1.24
2.35 - 2.40	0.96	6.19	8.00	6.15	5.56	4.23	31.09	20.05	48.86	0.43	3.03	3.46
2.40 - 2.45	0.56	4.97	8.51	5.56	6.13	5.17	30.91	19.79	49.30	0.85	2.07	2.92
2.45 - 2.50	0.64	2.96	6.33	5.19	5.63	4.86	25.61	19.57	54.82	0.56	2.47	3.03
2.50 - 2.55	1.10	3.92	7.43	6.43	6.55	5.76	31.19	19.94	48.87	0.63	2.06	2.69
2.55 - 2.60	0.18	1.28	7.92	12.50	10.40	10.37	42.67	20.38	36.95	0.38	1.92	2.30
2.60 - 2.65	0.91	3.04	7.54	8.04	7.04	5.19	31.77	21.68	46.55	0.43	1.76	2.19
2.65 - 2.70	2.12	1.98	5.62	6.63	6.53	4.77	27.65	21.69	50.66	0.40	2.19	2.59
2.70 - 2.75	1.14	3.35	5.61	6.19	6.32	5.05	27.66	23.37	48.97	0.52	1.78	2.30
2.75 - 2.80	0.26	2.87	5.20	5.31	6.31	4.38	24.13	21.87	54.02	0.45	2.74	3.19
2.80 - 2.85	0.43	3.82	6.90	6.27	6.53	4.92	28.87	23.56	47.57	0.68	2.13	2.81
2.85 - 2.90	1.29	4.55	7.17	6.29	5.84	4.68	29.84	22.00	48.16	0.57	2.29	2.86
2.90 - 2.95	2.12	6.65	8.78	7.38	6.31	4.14	35.39	22.25	42.36	0.35	1.31	1.66
2.95 - 3.00	6.96	7.82	8.70	7.44	6.60	3.13	40.65	20.85	38.50	0.30	1.64	1.94
3.00 - 3.05	7.72	9.69	8.85	6.92	6.03	3.71	42.92	20.66	36.42	0.24	0.92	1.16
3.05 - 3.10	7.63	7.03	7.00	6.27	5.91	4.02	37.87	17.39	44.74	0.32	1.05	1.37
3.10 - 3.25	51.64	29.16	0.03	0.02	0.02	0.01	80.21	5.46	14.33	0.00	0.02	0.02
3.25 - 3.30	6.88	9.48	8.41	6.83	5.96	4.19	41.77	15.32	42.91	0.19	0.58	0.77
3.30 - 3.35	4.49	10.58	9.67	7.77	6.38	3.85	42.73	16.68	40.59	0.10	0.46	0.56
3.35 - 3.40	4.14	7.77	9.96	12.39	7.81	4.66	46.72	16.28	37.00	0.07	0.31	0.38
3.40 - 3.45	7.11	15.13	11.27	7.13	4.22	1.96	46.81	15.55	37.64	0.00	0.08	0.08
3.45 - 3.50	6.03	9.61	10.67	9.24	6.77	4.69	47.03	15.92	37.05	0.05	0.62	0.67
3.50 - 3.55	7.71	10.18	10.75	8.85	6.86	4.08	48.43	16.92	34.65	0.05	0.18	0.23
3.55 - 3.60	6.29	11.46	10.31	8.66	6.81	4.76	48.13	15.65	36.22	0.05	0.35	0.37
3.60 - 3.65	9.05	13.37	10.85	7.86	6.51	4.33	51.99	15.58	32.43	0.04	0.11	0.15
3.65 - 3.70	5.14	11.84	12.65	9.57	7.39	4.17	50.78	15.60	33.62	0.04	0.27	0.31
3.70 - 3.75	9.98	13.86	11.30	7.61	6.19	4.24	53.02	14.91	32.07	0.04	0.30	0.34
3.75 - 3.80	5.18	12.40	17.20	12.84	7.93	3.16	58.73	0.08	41.19	0.02	0.03	0.05
3.80 - 3.85	4.78	7.99	10.17	9.82	7.93	5.06	45.76	16.55	37.69	0.09	0.48	0.57
3.85 - 3.90	5.01	5.43	8.88	10.52	7.97	5.35	43.17	16.53	40.30	0.11	0.37	0.48
3.90 - 3.95	4.74	4.99	8.50	10.44	7.80	5.28	41.76	16.91	41.33	0.08	0.60	0.68
3.95 - 4.00	3.59	4.98	9.65	11.14	7.60	5.00	41.96	16.92	41.12	0.06	0.41	0.47
4.00 - 4.05	3.08	4.02	10.32	12.06	7.86	4.97	42.32	16.59	41.09	0.13	0.58	0.71

4.05 - 4.10	2.98	3.91	9.08	10.38	7.89	5.36	39.60	14.51	45.89	0.09	0.45	0.54
4.10 - 4.15	2.40	4.93	7.39	8.18	8.63	6.32	37.85	15.77	46.38	0.09	0.74	0.83
4.15 - 4.20	2.14	5.44	6.98	6.12	5.81	4.58	31.08	16.08	52.84	0.09	0.62	0.71
4.20 - 4.25	3.58	6.38	8.72	7.67	6.81	3.91	37.07	16.17	46.76	0.03	0.67	0.70
4.25 - 4.30	3.81	8.67	10.32	7.99	6.50	3.41	40.72	16.82	42.46	0.05	0.30	0.35
4.30 - 4.35	2.36	8.63	11.39	7.82	6.46	3.82	40.49	14.85	44.66	0.05	0.38	0.43
4.35 - 4.40	3.15	8.80	12.47	7.78	6.29	3.33	41.82	15.13	43.05	0.01	0.28	0.29
4.40 - 4.45	3.59	9.61	12.38	9.58	6.79	3.79	45.75	18.69	35.56	0.06	0.23	0.29
4.45 - 4.50	4.16	8.93	10.95	10.10	7.68	4.51	46.34	17.58	36.08	0.03	0.23	0.26
4.50 - 4.55	4.35	9.38	9.88	10.34	7.22	4.04	45.23	15.88	38.89	0.04	0.10	0.14
4.55 - 4.60	2.89	8.23	9.28	10.27	8.41	4.49	43.57	16.24	40.19	0.06	0.17	0.23
4.60 - 4.65	4.08	12.50	12.34	9.50	6.54	3.81	48.78	16.30	34.92	0.03	0.00	0.03
4.65 - 4.70	3.02	12.07	11.99	9.14	7.50	4.43	48.80	16.84	34.36	0.06	0.14	0.20
4.70 - 4.75	1.64	11.19	11.79	8.28	6.56	4.62	44.09	14.94	40.97	0.06	0.22	0.28
4.75 - 4.80	0.74	6.66	11.54	9.86	7.85	4.38	41.03	16.83	42.14	0.03	0.29	0.32
4.80 - 4.85	0.65	5.41	10.91	9.14	6.67	4.69	37.48	15.40	47.12	0.03	0.29	0.32
4.85 - 4.90	0.80	4.77	10.06	9.53	7.21	4.73	37.11	14.11	48.78	0.05	0.32	0.37
4.90 - 4.95	0.99	6.81	12.52	8.95	6.78	4.33	40.41	16.01	43.58	0.06	0.16	0.24
4.95 - 5.00	1.06	5.07	9.09	7.13	6.79	5.00	34.15	15.97	49.88	0.06	0.60	0.66
5.00 - 5.05	0.72	5.67	7.67	8.19	6.71	4.49	33.45	16.22	50.33	0.06	0.68	0.74
5.05 - 5.10	1.60	6.59	7.44	6.86	6.42	4.71	33.62	16.39	49.99	0.11	0.88	0.99
5.10 - 5.15	2.69	6.54	7.81	6.59	5.67	3.56	32.86	15.78	51.36	0.06	0.67	0.73
5.15 - 5.20	3.67	9.48	8.85	6.75	5.92	3.98	38.66	15.96	45.38	0.08	0.50	0.58
5.20 - 5.25	5.04	12.27	8.38	5.89	5.09	3.28	39.96	15.33	44.71	0.08	0.56	0.64
5.25 - 5.30	8.88	18.08	8.45	5.02	4.65	2.92	48.01	15.66	36.33	0.05	0.18	0.23
5.35 - 5.40	11.13	19.04	7.87	4.98	4.65	3.04	50.72	14.46	34.82	0.02	0.14	0.16

APPENDIX 3.2 **ONAERO GRAIN-SIZE AND QUARTZ DATA**

(Expressed as a Percentage of Total Sample; <2mm)

	Grain-Size Data									Quartz Data		
	Phi									Phi		
Depth	0	1	2	3	4	5	0 - 5	<5	SROCO	5	<5	Total
0.20 - 0.30	1.88	3.77	10.08	10.69	7.39	4.36	38.12	15.11	46.77	0.00	0.61	0.61
0.30 - 0.40	0.93	2.71	8.75	9.15	7.15	3.79	33.08	16.27	50.65	0.14	0.74	0.92
0.40 - 0.50	0.20	1.96	6.76	8.16	6.46	3.85	27.40	17.46	55.14	0.19	0.82	1.01
0.50 - 0.60	0.20	2.23	6.10	6.95	5.50	3.10	24.09	18.19	57.72	0.18	1.39	1.56
0.60 - 0.70	0.07	2.11	5.75	6.35	5.49	3.36	23.12	19.72	57.16	0.36	2.12	2.48
0.70 - 0.80	0.07	3.37	6.81	6.22	5.41	3.48	25.37	19.11	55.52	0.49	1.95	2.44
0.80 - 0.90	0.35	4.86	8.42	6.99	5.31	3.78	29.71	21.79	48.50	0.54	3.94	4.47
0.90 - 1.00	0.23	3.80	8.02	7.09	5.58	4.19	28.93	23.00	48.07	1.03	5.07	6.10
1.00 - 1.10	0.00	1.44	7.47	7.36	5.91	5.37	27.56	22.67	49.77	1.51	4.79	6.30
1.10 - 1.20	0.00	1.55	7.56	6.18	5.15	5.03	25.49	24.29	50.22	1.25	6.22	7.47
1.20 - 1.30	0.24	1.13	6.09	5.60	4.84	4.59	22.52	25.82	51.66	1.27	6.79	8.06
1.30 - 1.40	0.13	1.15	6.30	6.59	5.09	3.96	23.23	20.56	56.21	0.94	4.35	5.29
1.40 - 1.50	0.19	1.53	9.22	8.33	6.58	4.91	30.77	20.37	48.46	0.67	3.32	3.98
1.50 - 1.60	0.15	1.61	7.03	8.46	7.23	5.96	30.45	20.61	49.94	0.69	3.19	3.88
1.60 - 1.70	0.57	1.58	5.69	8.86	8.36	6.94	32.01	22.00	45.99	0.70	3.30	4.00
1.70 - 1.80	3.47	3.66	5.59	6.63	6.54	4.29	30.19	19.42	50.39	0.65	2.80	3.45
1.80 - 1.90	8.47	7.29	7.51	7.22	6.09	3.40	40.02	17.59	42.39	0.33	1.89	2.22
1.90 - 2.00	10.06	7.73	7.36	6.63	6.02	3.46	41.26	16.50	42.24	0.17	1.15	1.32
2.00 - 2.10	10.21	9.05	9.01	6.77	5.65	3.31	44.00	16.08	39.92	0.09	0.67	0.75
2.10 - 2.20	2.16	8.85	11.46	7.97	6.33	4.00	40.78	17.45	41.77	0.07	0.63	0.70
2.20 - 2.30	1.82	7.92	11.80	9.47	7.26	4.33	42.60	17.05	40.35	0.04	0.71	0.75
2.30 - 2.40	1.05	5.66	9.06	9.90	7.76	4.13	37.59	17.54	44.87	0.11	1.11	1.21
2.40 - 2.50	0.68	3.91	8.05	8.99	7.03	4.27	32.94	16.35	50.71	0.12	1.32	1.43
2.50 - 2.60	0.43	3.67	8.98	8.62	6.60	3.61	31.93	16.32	51.75	0.12	1.01	1.13
2.60 - 2.70	0.27	2.48	8.32	7.96	5.80	3.30	28.14	17.01	54.85	0.10	0.73	0.83

2.70 - 2.80	0.26	2.84	9.84	8.63	6.17	3.75	31.50	16.46	52.04	0.11	0.86	0.97
2.80 - 2.90	0.08	2.22	8.37	8.18	5.67	3.32	27.85	16.71	55.44	0.08	0.83	0.91
2.90 - 3.00	0.14	1.97	8.39	7.73	5.42	3.18	26.83	14.80	58.37	0.11	1.02	1.13
3.00 - 3.10	0.22	2.75	10.27	8.35	5.69	3.24	30.54	15.41	54.05	0.21	1.06	1.27
3.10 - 3.20	0.29	3.01	9.61	7.25	4.89	2.66	27.72	14.71	57.57	0.09	0.86	0.95
3.20 - 3.30	0.38	4.10	11.09	7.50	5.17	3.08	31.34	16.23	52.43	0.12	0.96	1.09
3.30 - 3.40	0.56	4.83	12.74	7.82	5.18	2.95	34.10	15.47	50.43	0.12	0.77	0.89
3.40 - 3.50	0.36	3.93	12.07	7.82	5.50	3.10	32.78	16.40	50.82	0.11	0.68	0.79
3.50 - 3.60	0.45	3.88	11.61	8.08	5.99	3.47	33.49	16.11	50.40	0.11	0.80	0.91
3.60 - 3.70	0.46	3.97	10.21	8.01	5.93	3.62	32.20	15.44	52.36	0.16	1.10	1.26
3.70 - 3.80	0.35	3.98	10.50	7.73	5.60	3.44	31.58	16.27	52.15	0.15	0.86	1.01
3.80 - 3.90	0.29	4.51	12.36	7.24	4.96	2.77	32.15	16.00	51.85	0.09	0.79	0.86
3.90 - 4.00	0.47	4.13	9.76	7.53	5.82	3.43	31.15	16.48	52.37	0.16	1.16	1.32
4.00 - 4.10	0.55	4.61	11.45	9.51	6.92	4.02	37.07	19.20	43.73	0.27	1.11	1.38
4.10 - 4.20	1.06	5.12	8.95	7.35	6.07	3.41	31.97	17.44	50.59	0.23	1.22	1.45
4.20 - 4.30	1.82	6.24	6.64	5.88	5.17	3.16	28.92	17.79	53.29	0.20	1.36	1.56
4.30 - 4.40	1.80	8.14	6.84	6.07	5.15	2.86	30.87	16.12	53.01	0.18	1.41	1.59
4.40 - 4.50	3.23	9.83	7.38	6.22	5.09	2.73	34.48	16.94	48.58	0.18	0.92	1.10
4.50 - 4.60	2.80	10.35	7.80	6.55	5.65	2.91	36.06	18.75	45.19	0.14	0.52	0.66
4.60 - 4.70	2.81	11.01	8.75	7.26	5.44	2.67	37.96	15.15	46.89	0.08	0.94	1.02
4.70 - 4.80	2.79	12.86	10.68	7.26	5.27	2.71	41.58	14.95	43.47	0.04	0.37	0.41
4.80 - 4.90	1.53	10.15	11.20	7.04	5.24	2.61	37.77	15.08	47.15	0.03	0.51	0.54
4.90 - 5.00	2.14	7.92	11.63	7.10	5.56	2.93	37.30	14.34	48.36	0.08	0.80	0.88
5.00 - 5.10	1.46	7.45	12.49	7.40	6.07	3.44	38.32	15.04	46.64	0.12	0.73	0.85
5.10 - 5.20	1.03	3.81	10.89	7.69	6.56	3.75	33.74	17.07	49.19	0.21	1.10	1.31
5.20 - 5.30	1.37	2.44	8.48	7.83	6.94	4.13	31.21	19.89	48.90	0.41	2.04	2.45
5.30 - 5.40	0.63	2.03	7.66	7.84	7.19	4.69	30.05	20.61	49.34	0.51	2.64	3.15
5.40 - 5.50	0.40	2.42	6.51	7.04	6.63	4.80	27.81	22.57	49.62	0.71	3.58	4.29
5.50 - 5.60	0.45	2.48	7.20	7.84	6.78	4.60	29.36	21.33	49.31	0.57	2.83	3.40
5.60 - 5.70	0.26	1.74	6.72	7.64	6.28	3.97	26.61	20.11	53.28	0.38	2.06	2.44
5.70 - 5.80	0.17	2.11	7.76	8.21	6.13	3.64	28.04	18.76	53.20	0.29	1.66	1.95
5.80 - 5.90	0.38	3.05	10.06	8.99	5.75	2.76	30.99	16.41	52.60	0.09	0.82	0.91
5.90 - 6.00	0.35	3.33	10.63	7.79	5.17	2.51	29.80	15.50	54.70	0.09	0.47	0.56
6.00 - 6.10	0.53	4.52	12.10	7.96	5.00	2.46	32.58	16.03	51.39	0.04	0.22	0.26
6.10 - 6.20	0.59	4.83	11.91	8.28	5.26	2.55	33.44	16.29	50.27	0.05	0.37	0.42
6.20 - 6.30	0.40	3.98	11.13	8.00	5.28	2.60	31.40	15.71	52.89	0.06	0.43	0.49
6.30 - 6.40	0.43	3.30	10.72	7.47	5.56	2.99	30.47	15.36	54.23	0.06	0.30	0.36
6.40 - 6.50	0.00	3.11	11.38	6.96	5.05	2.75	29.26	14.70	56.04	0.03	0.11	0.14

6.50 - 6.60	0.30	4.41	12.70	7.02	4.83	2.22	31.49	15.06	53.45	0.04	0.14	0.18
6.60 - 6.70	0.21	5.30	15.03	7.79	5.06	2.47	35.87	15.85	48.28	0.04	0.10	0.14
6.70 - 6.80	0.12	4.47	12.06	7.87	4.99	2.44	31.95	14.85	53.20	0.02	0.19	0.21
6.80 - 6.90	0.29	3.57	8.55	7.54	4.86	2.41	27.22	14.21	58.57	0.03	0.15	0.18
6.90 - 7.00	0.18	3.42	7.90	8.60	4.98	2.46	27.55	15.37	57.08	0.03	0.31	0.33
7.00 - 7.10	0.59	2.91	8.68	9.35	5.13	2.37	29.03	14.89	56.08	0.05	0.42	0.47
7.10 - 7.20	0.58	2.90	9.29	10.74	5.37	2.61	31.49	14.75	53.76	0.06	0.42	0.48
7.20 - 7.30	0.82	3.47	10.32	11.64	5.55	2.98	34.78	15.74	49.48	0.04	0.42	0.46
7.30 - 7.40	1.54	5.28	11.51	10.40	5.36	2.85	36.95	15.59	47.46	0.08	0.36	0.44
7.40 - 7.50	2.70	6.33	12.99	8.50	6.21	3.19	39.92	17.18	42.90	0.06	0.20	0.26
7.50 - 7.60	2.72	7.32	10.63	8.79	6.15	3.27	38.89	17.75	43.36	0.09	0.48	0.57
7.60 - 7.70	0.80	4.49	10.11	8.96	6.92	3.90	35.19	15.14	49.67	0.14	0.39	0.53
7.70 - 7.80	0.62	2.73	10.24	9.22	6.43	3.51	32.77	16.25	50.98	0.08	0.68	0.76
7.80 - 7.90	0.39	2.72	10.06	9.24	5.98	3.10	31.50	16.16	52.34	0.14	0.45	0.59
7.90 - 8.00	0.27	3.01	12.06	11.35	5.98	2.95	35.63	14.98	49.39	0.12	0.27	0.39
8.00 - 8.10	0.26	2.90	10.31	10.71	5.73	2.71	32.63	15.41	51.96	0.10	0.28	0.38
8.10 - 8.20	0.27	2.14	8.05	9.57	5.07	2.41	27.52	13.89	58.59	0.07	0.20	0.27
8.20 - 8.30	0.57	3.44	8.35	8.59	4.93	2.48	28.38	13.22	58.40	0.05	0.29	0.34
8.30 - 8.40	0.54	3.99	8.21	8.07	5.13	2.60	28.55	13.73	58.05	0.06	0.35	0.41
8.40 - 8.50	0.41	3.93	6.81	7.25	5.09	2.52	26.02	15.36	58.62	0.06	0.12	0.18
8.50 - 8.60	0.24	3.21	7.89	7.53	5.27	2.66	26.82	14.24	58.94	0.07	0.20	0.27
8.60 - 8.70	0.16	3.36	7.85	7.73	5.37	2.56	27.05	14.36	58.59	0.07	0.53	0.60
8.70 - 8.80	0.25	3.71	9.05	7.99	5.19	2.63	28.84	14.99	56.17	0.07	0.47	0.54
8.80 - 8.90	0.41	3.92	9.61	7.55	4.85	2.75	29.10	15.49	55.41	0.11	0.57	0.68
8.90 - 9.00	0.50	3.81	8.13	7.19	4.53	2.53	26.69	16.44	56.87	0.11	0.60	0.71
9.00 - 9.10	1.08	5.82	9.81	7.74	4.44	2.53	31.54	16.10	52.36	0.11	0.26	0.57
9.10 - 9.20	1.08	5.00	10.10	8.29	4.89	2.69	32.06	16.80	51.14	0.09	0.36	0.45
9.20 - 9.30	1.94	8.68	9.08	7.84	4.85	2.92	35.32	16.11	48.57	0.10	0.34	0.44
9.30 - 9.40	2.43	10.39	12.64	9.90	5.03	2.71	43.11	14.42	42.47	0.10	0.36	0.46
9.40 - 9.50	1.05	6.80	28.97	17.04	5.02	1.98	60.86	15.44	23.70	0.05	0.04	0.09
9.50 - 9.60	0.18	6.24	39.58	20.25	4.63	1.54	72.42	11.99	15.59	0.01	0.06	0.07

APPENDIX 3.3 15-BAR WATER CONTENTS OF A) Selected Samples from S1 and L1.1 at Waitui, and B) the upper c.2.60m of the Onaero Section.

	15-bar H_2O field moist sample (%)	15-bar H_2O air dried sample (%)		% decrease of fresh 15-bar H_2O
A) WAITUI				
S1				
0.70 - 0.80m	80	29	52	64
0.80 - 0.90m	89	32	57	68
0.90 - 1.00m	93	33	60	65
L1.1				
2.45 - 2.55m	82	42	41	49
2.60 - 2.70m	81	45	36	45
2.70 - 2.80m	96	45	50	53
B) ONAERO				
S1				
0.40 - 0.50m	82	34	48	58
0.50 - 0.60m	90	33	57	63
0.60 - 0.70m	93	33	60	64
0.70 - 0.80m	83	30	53	64
0.80 - 0.90m	75	29	46	61

L1.1

0.90 - 1.00m	73	32	41	56
1.00 - 1.10m	69	35	34	49
1.10 - 1.20m	70	36	34	48
1.20 - 1.30m	85	30	55	65
1.30 - 1.40m	91	33	58	64
1.40 - 1.50m	68	41	27	40
1.50 - 1.60m	63	42	21	33
1.60 - 1.70m	65	41	24	37
1.70 - 1.80m	72	39	33	46
1.80 - 1.90m	67	38	29	43

L1.2

1.90 - 2.00m	63	42	21	33
2.00 - 2.10m	58	53	05	09
2.10 - 2.20m	58	48	10	17
2.20 - 2.30m	58	47	11	19
2.30 - 2.40m	69	50	19	27

S2

2.40 - 2.50m	86	41	45	52
2.50 - 2.60m	77	42	35	45

APPENDIX 3.4 CHEMICAL ANALYSES OF SELECTED SAMPLES (Air dry; <2mm) FROM WAITUI (SECTION 19) AND ONAERO (SECTION 30).

	Pyrophosphate Extraction		Acid-oxalate Extraction		
	Fe %	Al	Fe	Al	Si
Waitui					
S1 0.90 - 1.00m	0.03	0.32	1.65	7.80	3.70
L1.1 2.70 - 2.80m	0.03	0.42	1.65	7.55	4.65
Onaero					
S1 0.60 - 0.70m	0.02	0.31	2.20	8.95	4.25
L1.1 1.70 - 1.80m	0.02	0.28	0.86	6.75	3.90

Al/Si ratio = $Al_o - Al_p / Si_o$

Waitui
S1 7.80 - 0.32/ 3.70 = 2.02
L1.1 7.55 - 0.42/ 4.65 = 1.53

Onaero
S1 8.95 - 0.31/ 4.25 = 2.03
L1.1 6.75 - 0.28/ 3.90 = 1.65